Plastic Shrinkage Cracking in Hot Weather Conditions

by

Mohammed Abdul Waris

A Thesis Presented to the

FACULTY OF THE COLLEGE OF GRADUATE STUDIES

KING FAHD UNIVERSITY OF PETROLEUM & MINERALS

DHAHRAN, SAUDI ARABIA

In Partial Fulfillment of the
Requirements for the Degree of

MASTER OF SCIENCE

In

CIVIL ENGINEERING

April, 1996

Plastic Shrinkage Cracking in Hot Weather Conditions

BY

Mohammed Abdul Waris

A Thesis Presented to the

FACULTY OF THE COLLEGE OF GRADUATE STUDIES

KING FAHD UNIVERSITY OF PETROLEUM & MINERALS

DHAHRAN, SAUDI ARABIA

In Partial Fulfillment of the
Requirements for the Degree of

MASTER OF SCIENCE

In

Civil Engineering

April 1996


بسم الله الرحمن الرحيم

PLASTIC SHRINKAGE CRACKING IN HOT WEATHER CONDITIONS

Mohammed Abdul Waris

MS Thesis

KING FAHD UNIVERSITY OF
PETROLEUM AND MINERALS

April, 1996

KING FAHD UNIVERSITY OF PETROLEUM AND MINERALS
DHAHRAN, SAUDI ARABIA
COLLEGE OF GRADUATE STUDIES

This thesis, written by

Mohammed Abdul Waris

under the direction of his Thesis Advisor, and approved by his Thesis committee, has been presented to and accepted by the Dean, College of Graduate Studies, in partial fulfillment of the requirements for the degree of

MASTER OF SCIENCE IN CIVIL ENGINEERING (STRUCTURES)

Thesis Committee

Dr. Abdullah A. Almusallam (Chairman)

Dr. Ahmed S. Al-Gahtani (Co-Chairman)

Dr. Fahd H. Dakhil (Member)

Dr. M. Maslehuddin (Member)

Dr. Omar S. B. Al-Amoudi (Member)

Dr. Al-Farabi Sharief
Department Chairman

Dr. Ala H. Al-Rabeh
Dean, College of Graduate Studies

Date : 22-6-96

123

Dedicated as a humble tribute to

my beloved mother

whose prayers, sacrifice, inspiration and love

led to this accomplishment

and to

the loving memory of my father

ACKNOWLEDGEMENT

First and foremost, all praise and thanks to Allah, *subhanahu-wa-ta-Aala*, the Almighty, Who gave me the opportunity, strength, determination and patience to complete this work successfully. I seek His mercy, favor, and forgiveness, and peace and prayers be upon his Prophet. Acknowledgements are due to King Fahd University of Petroleum & Minerals for having given me an opportunity to pursue my graduate study here, for providing research facilities and financial assistance to me during the course of the MS program.

I am extremely thankful and deeply indebted to my thesis committee chairman, Dr. Abdullah A. Almusallam for his invaluable help and advice. I acknowledge him for his untiring efforts, constant encouragement, unlimited support, concern, patience, guidance and valuable time during all the stages of this work and above all for having complete faith in me.

I wish to express my sincere appreciation and gratitude to my thesis committee co-chairman Dr. Ahmed S. Al-Gahtani for his cooperation in arranging the construction of the humidity chamber and procuring the necassary equipment from within and outside the Kingdom without delay. I am grateful to my committee members Dr. F. Dakhil and Dr. O. S. B. Al-Amoudi for their interest, constructive criticism and personal understanding. I acknowledge them for their useful and valuable comments and suggestions.

My special thanks to my thesis committee member, Dr. M. Maslehuddin for his constant help throughout the course of this investigation. I am greatly indebted to him for his untiring efforts and patience in reviewing and organizing this report at various stages of its preparation. I acknowledge him for his valuable time, patience, guidance and critical review of the thesis during all stages of this work. The credit for the good part of this thesis goes to him. Working with him was indeed a learning experience.

I am also thankful to the department chairman, Dr. Alfarabi M. Sharif and other faculty members for their cooperation, throughout the duration of my stay in KFUPM.

I sincerely appreciate the help and guidance provide by late Professor Rasheeduzzafar and my dear friend late Mr. Ashrafuddin, whose untimely deaths had a great impact on me, may Allah forgive their sins and grant them a place in Paradise.

I express my sincere appreciation and thanks to Mr. Mukarram and Mr. Ibrahim Asi for their help throughout this work. Thanks to Omar, Nahash, Hasan Zakariya, Abdulappa, Tolentino, Essa, Farooq, Abu-Jaffar, Abdullah and other staff of the civil engineering laboratories for their help during various stages of this work. I would also like to the thank the secretaries of the CE dept., Mr. Mumtaz, Mr. Olly and Mr. Effren for their help throughout my stay in KFUPM. I would also like to express my thanks to Mr. Younus of the workshop for fabricating the molds

used for the experiment. I am also thankful to the help rendered by Maintenance and AC Plant Department, specially Mr. Sameer, Mr. Dawood, Mr. Sidro, Mr. Toledo, Mr. Raol and Mr. Dias for the construction of the humidity chamber. I also appreciate the help rendered by the Research Institute personnel in various stages of the experimental work. Special thanks to my friends Ibrahim, Sharfuddin, Mujeeb, Imran, and undergraduate students Abdur Rahman and Abdullah for their help during the casting of the specimens.

I also express my thanks to my friends Ilias, Asad, Abbas, Qureshi, Lashari and Hadi for making my stay at KFUPM a memorable one. A word of appreciation is also due to many of my friends and the Hyderabadi community whose moral support and patronage provided an impetus for the completion of this work.

Finally, without the emotional and moral support, prayers, sacrifices, love, patience, encoragement and understanding of my mother, brothers, sisters, other family members, in-laws and specially my wife, the completion of this work would not have been a possibility. This work is dedicated to my mother for taking pains to fulfill my personal and academic pursuits and shaping my personality and to the loving memory of my father whose dream was to see me reach the pinnacle of my academic career.

Contents

123

List of Tables

List of Figures

ABSTRACT

Name: Mohammed Abdul Waris

Title: Plastic Shrinkage Cracking in Hot Weather Conditions
Major Field: Civil Engineering (Structures)
Date of Degree: April 1996

Deterioration of concrete structures, due to the hot climatic conditions, is one of the major problems in the Arabian Gulf countries. The hot-weather affects both the fresh and hardened properties of concrete. One of the drawbacks of hot-weather, which has not been adequately studied is the cracking due to plastic shrinkage. The cracks so formed become the focal point of the ingress of harmful elements in to the concrete matrix. This research was conducted to investigate the effect of environmental conditions and mix proportions on plastic shrinkage cracking in concrete. The effect of relative humidity, wind velocity, ambient temperature, cement content, water cement ratio and cement type on the water evaporation, plastic shrinkage cracking, bleeding, shrinkage strains, compressive strength and microstructure was evaluated.

Results of this research indicated that ACI 305 graphical method can only be used to determine the rate of evaporation and cannot provide any indication with regard to plastic shrinkage cracking. Cracking was observed at much lower rates of evaporation than that recommended by ACI 305. Water evaporation and plastic shrinkage cracking increased with an increase in the wind velocity, ambient temperature, cement content, water cement ratio and addition of blended cements. A decrease in the relative humidity had a similar effect. Bleeding increased with cement content as well as water cement ratio. Exposure conditions at the time of casting influenced the properties of hardened concrete. There exists a qualitative relationship between bleeding, water evaporation and plastic shrinkage cracking. However, the total cracked area increased almost linearly with the rate of evaporation. The results also show that lean and stiff mixes crack earlier than rich and plastic mixes, but cracking in the latter was much more than the former. The data also indicate that the technological benefit of using blended cements can be utilized only when adequate measures to control plastic shrinkage cracking are assured.

MASTER OF SCIENCE DEGREE
KING FAHD UNIVERSITY OF PETROLEUM AND MINERALS
Dhahran, Saudi Arabia

ملخص رسالة البحث

الإسم : محمد عبدالوارث

العنوان : تشققات الإنكماش اللدن في الظروف البيئية الحارة.

التخصص : هندسة مدنية (إنشاءات).

تاريخ الدرجة : إبريل ١٩٩٦ م.

يعتبر تدهور المنشآت الخرسانية في دول الخليج العربي (نتيجة لإرتفاع درجات الحرارة) من أهم المشاكل التي تواجه هذه الصناعة حيث يؤثر الطقس الحار على كل من خواص الخرسانة الحديثة الصب والخرسانة المتصلبة. وإحدى عيوب خرسانة الطقس الحار هي عدم وجود الدراسات التي تختص بدراسة التشققات الناتجة عن الإنكماش اللدن. وتمثل هذه التشققات فتحات لدخول المواد الضارة إلى داخل الخرسانة. وتم في هذا البحث دراسة تأثير الظروف المناخية وخواص الخلطات الخرسانية على تشققات الإنكماش اللدن. وتم تحليل تأثير نسبة الرطوبة، سرعة الرياح، درجة الحرارة، كمية الأسمنت، نسبة الماء إلى الأسمنت وكذلك نوعية الأسمنت على تبخر الماء، تشققات الإنكماش اللدن، نزف الماء، الشد الإنكماشي، وقوة الضغط والتركيب الجزئي للمكونات.

وقد دلت نتائج الدراسة على صلاحية طريقة الرسوم البيانية (ACI 305) لتقرير معدل التبخر فقط وعدم تمكن هذه الطريقة من إعطاء أي دلائل عن تشققات الإنكماش اللدن. وتمت ملاحظة وجود التشققات على مستويات تبخر أقل بكثير من المستويات المحددة من قبل مواصفات (ACI 305) . وقد لوحظ أيضاً زيادة نسبة التبخر وتشققات الإنكماش اللدن مع زيادة سرعة الرياح، درجات الحرارة السائدة، نسبة الأسمنت، نسبة الماء إلى الأسمنت وإضافة الأسمنت المخلوط. ونتج عن إنخفاض نسبة الرطوبة نفس النتائج السابقة. وزاد النزف مع زيادة كمية الأسمنت ونسبة الماء للأسمنت. وأثرت الظروف المناخية المصاحبة لعملية الصب على خواص الخرسانة المتصلبة ولوحظ وجود علاقة نوعية بين نزف الماء وتبخره وتشققات الإنكماش اللدن. وبالرغم من ذلك فقد زادت مساحة الكمية المتشققة زيادة خطية مع نسبة التبخر. كما بينت النتائج تعرض الخلطات التي تحتوي على كمية قليلة من الأسمنت والناشفة إلى التشققات في فترة أسرع من الخلطات الغنية واللدنة، ولكن زادت كمية التشققات في الخلطات الغنية واللدنة عن تلك في الخلطات التي تحتوي على كمية قليلة من الأسمنت والناشفة. كما دلت النتائج على وجوب دراسة الفوائد التقنية الناتجة عن إستخدام الأسمنت المخلوط وتقرير إستخدام تلك المواد إذا كانت هناك مقاييس للتحكم بتشققات الإنكماش اللدن.

درجة ماجستير في العلوم الهندسية

جامعة الملك فهد للبترول والمعادن

الظهران، المملكة العربية السعودية

Chapter 1

INTRODUCTION

1.1 CONCRETE DURABILITY IN THE ARABIAN GULF

Concrete has been extensively used in the construction of the infrastructure necessary for the development of mankind. Its potential has been fully exploited by the construction industry and research has been conducted to make it stronger and more economical. Though research and development efforts were totally diverted towards the production of energy-efficient and high-strength cements, the durability performance of such cements due to the resulting changes in the physico-chemical characteristics was not properly addressed. It was assumed that concrete produced by mixing of cement, aggregate and water can withstand all the weather and ex-

posure conditions. Concrete was thought to be a maintenance-free material until durability problems were reported from various parts of the world. While the deterioration of highway structures in North America and Europe is attributed to the use of deicer salts, the deterioration of concrete structures in the Arabian Gulf is caused by the cumulative effect of severe climatic and geomorphic conditions in conjunction with incorrect material specifications and defective construction practices. The ever-growing demand for the infrastructure, in this region, has resulted in an unprecedented construction activity in the last two decades. Within Saudi Arabia, the construction activity is mostly concentrated in the central and coastal parts, which are characterized by hot climatic conditions. It has been observed through a growing number of case histories that within a short span of time, various defects ranging from unsightly blemishes to serious failures have occurred in many types of concrete structures in this region. Studies [1, 2] have indicated that the problem of concrete durability in arid and semi-arid regions, such as many parts of Saudi Arabia and other Gulf and Middle East countries, is due to three main reasons :

(a) severe climatic and geomorphic conditions,

(b) low quality of construction materials,

(c) unskilled labor, lack of proper supervision, inadequate specifications and design and construction practices which do not commensurate with local conditions.

The magnitude of concrete deterioration problem in the hot weather conditions of the Arabian Gulf region, presented in a study conducted at King Fahd University of Petroleum and Minerals (KFUPM) [3], indicated that the climatic conditions of this region, characterized by high temperature and humidity and large fluctuations in the diurnal and seasonal temperature and humidity, adversely affect the performance of concrete. The temperature can vary by as much as 20 °C during a typical summer day and the relative humidity ranges from 40 to 100% over 24 hours. These sudden and continuous variations in temperature and humidity initiate ever present cycles of expansion/contraction and hydration/dehydration which cause damage due to thermal and mechanical stresses. The damage due to these stresses is reflected by microcracking and enhanced permeability, which results in a tremendous increase in the diffusion of aggressive species, such as chloride, oxygen and carbondioxide, towards the steel-concrete interface.

The other factor which contributes to the poor durability performance of concrete in this region, is the quality of local aggregates. Most of the coarse aggregates available in this region is crushed limestone which is marginal, porous, absorptive, relatively soft and excessively dusty on crushing. The aeolian dune and coastal sand form the main source of fine aggregate. These sands are extremely fine-grained and have narrow grading. Nearly all the material passes No. 30 sieve. The fineness modulus is less than 1.3 and lies outside the ASTM C 33 grading limits and is finer than zone 4 of BS 882 [4]. The excessive fineness of sand and its narrow grading

leads to a gap-graded particle size distribution in the combined grading in nearly all the mixes made using local materials. The sand is mainly of carbonate origin, fine, poorly graded and contaminated with chloride and sulfate salts. Furthermore, the fine and the coarse aggregates are characterized by excessive dust content. Dust and excessive fines cause high water demand resulting in lower strength and greater shrinkage of concrete. Dust also forms a fine interstitial coating between the aggregate and the cement paste thereby weakening the bond at the aggregate-paste interface. This transition zone, being the weakest link of concrete composite, may further lower the concrete strength and quality [5].

The severe environmental conditions of the Arabian Gulf form a conducive environment for the cracking of concrete due to plastic and drying shrinkage. These deterioration processes are further aided by the sharp temperature gradients on the surfaces and the inner portions of the concrete. The changes in the diurnal and seasonal temperatures cause continuous expansion and contraction cycles which may lead to the cracking of concrete. These expansion-contraction cycles become all the more damaging due to the movements of the aggregate material and hardened cement paste setting up tensile stresses beyond the tensile capacity of concrete resulting in microcracking. Limestone, the predominantly used aggregate in this region, has a coefficient of thermal expansion of 1 x 10^{-6}/°C. The coefficient of expansion for hardened cement paste is much higher (usually between 10 x 10^{-6} and 20 x 10^{-6}/°C). With the fall in temperature, tensile and compressive stresses are setup

in the cement paste and the aggregates, respectively. With a rise in temperature, the stresses are not exactly reversed but tensile stresses are setup at the aggregate-paste interface tending to cause interface bond failure and significant microcracking around the transition zone. It has been shown by Hsu [6] that a volume change of 0.3% is enough to generate tensile stresses of the order of 800 psi at the aggregate-paste interface. Slate and Matheus [7] have determined volume changes of cement paste and concrete from the time of casting to an age of 7 days. Their results show that volume changes even larger that 0.3% occur during setting and hardening of concrete. The authors [7], on the basis of a simple mathematical model, have inferred that tensile stresses of more than 250 psi for every 10 °C fall in temperature are set up in the concrete.

The climatic and geomorphic factors may combine to accelerate the deterioration processes. In most areas, groundwater table is relatively high and close to the ground surface. The capillary rise of moisture and frequent flooding in conjunction with the high evaporation rate leaves a heavy crust of salt in the upper few feet of the soil. This leaves the soil, groundwater and atmosphere heavily contaminated with chloride and sulfate salts [3]. Concrete construction in the coastal areas of the Arabian Gulf is continually exposed to ground and atmosphere contaminated with salts. Aided by capillary action and high humidity conditions, the salt-contaminated groundwater and the salt-laden airborne moisture and dew find an easy ingress into the concrete matrix. Further, the salts also pollute the mix water and the

aggregates thereby increasing the total salt content of concrete. In the coastal areas of the Arabian Gulf, sulfates and chlorides occur at several horizons in the geological formations. Numerous salt domes in this region constitute "built-in" sources of salt contamination especially when they are located in the zones of groundwater circulations [8]. Other sources of salt are the numerous sabkhas which constitute natural evaporating pans saturated with brines and generate chloride, sulfate and carbonate minerals on their surface crusts. These salts are wind blown and have been found to heavily contaminate dune sands up to a distance of 40 kms from the shore.

The use of incorrect material specifications and defective construction practices is the other cause for the premature deterioration of concrete. It may not be out of place to mention that to meet the growing demand for infrastructure, specifications borrowed from other parts of the world were injudiciously used. In the aggressive environmental conditions of the Arabian Gulf, the predominant modes of concrete deterioration are :

(1) corrosion of reinforcement,

(2) sulfate attack,

(3) salt weathering, and

(4) cracking due to thermal gradients and plastic and drying shrinkage.

While reinforcement corrosion is the predominant mode of deterioration, failure due to other causes is not common. It is also possible that one mode of deterioration may form the basis for the initiation of other types of failure. For example, cracking of concrete due to plastic shrinkage cracking may facilitate reinforcement corrosion.

It should be noted that corrosion of reinforcing steel, which is the most prevalent durability problem in the Arabian Gulf region [3, 9, 10, 11], is highly dependent on the permeability of concrete. Dense and impermeable concrete with no cracks, therefore, considerably reduces the ingress of the deleterious agents, like oxygen and moisture, thereby inhibiting reinforcement corrosion. Further, the variation in the daily and seasonal temperature and humidity in the local environment may propagate and widen the initial plastic shrinkage cracks in concrete which lead to a reduction in strength and long-term durability.

1.2 NEED FOR THIS RESEARCH

According to the review of the literature presented in Chapter 2, there is a predominant concern for the formation of plastic shrinkage cracks in the hot and arid environments, data are scarce on the cumulative effect of concrete mix design and environmental conditions on their formation. Since plastic shrinkage cracking is related to the rate of bleeding and evaporation, it should be influenced by both concrete composition and the environmental conditions. Therefore, Menzel's formula

used for predicting the occurrence of plastic shrinkage cracking and recommended by the ACI Committee 305, cannot be used for calculating the evaporation rate and predicting the formation of plastic shrinkage cracking. This concern has been lately voiced by several researchers [12, 13, 14]

Further, the cement composition has undergone several changes principally resulting in a finer cement and its effect on the rate of bleeding is also of concern. The influence of supplementary cementing materials, fiber reinforcement and chemical admixtures on plastic shrinkage cracking under the environmental conditions of the Arabian Gulf needs also to be investigated.

While research to date has been concentrated on evaluating the effect of environmental conditions on evaporation rate, no research has been conducted to assess the effect of plastic shrinkage cracking on the microstructure of the hardened concrete and its influence on strength and durability.

Therefore, there is a need to evaluate the interactive effect of concrete mix design, using proportions normally used in the field, chemical and mineral admixtures, and the environmental conditions on the rate of evaporation and plastic shrinkage cracking.

1.3 RESEARCH OBJECTIVES

The objectives of this research were to evaluate the interactive effect of concrete mix design and environmental conditions on the rate of bleeding, evaporation of surface water and plastic shrinkage cracking in the fresh concrete, and microstructure in the hardened concrete. The specific objectives were:

1. to fabricate controlled temperature and humidity chamber for evaluating the effect of hot weather conditions on the properties of fresh concrete,
2. to evaluate the cumulative effect of environmental conditions and concrete composition on bleeding and evaporation of water and quantify plastic shrinkage cracking,
3. to study the plastic shrinkage cracking in blended cements under hot and humid environments, and
4. to ascertain the effect of plastic shrinkage cracking on the microstructure of hardened concrete.

Chapter 2

LITERATURE REVIEW

2.1 EFFECT OF HOT WEATHER ON PROPERTIES OF CONCRETE

"Hot countries" is a rather general term applicable to regions of relatively high air temperature with both low and high relative humidities, high or low precipitation, various degrees of solar radiation and prevailing wind velocities. In the ACI Manual of concrete construction [15], it is defined as "any combination of high temperature, low relative humidity, and wind velocity tending to impair the quality of fresh and hardened concrete". Most parts of Saudi Arabia are included in the typical environment that is classified as hot weather. In these regions summer temperatures are frequently in excess of 40 °C. Direct solar radiation on hardened concrete surfaces

may raise the temperature to as high as 70 °C on a typical summer day in these regions [16]. Humidity is very low in the central parts and varies from very low to high in the coastal areas within a short span of time. Data on relative humidity and temperature, based on 20 years, is presented in Figures 2.1, 2.2 and 2.3 for Riyadh, Dhahran and Jeddah areas, respectively [17] to provide an indication of the hot weather conditions of these regions.

Hot weather creates many problems in the preparation, placing, compaction and curing of concrete [18, 19, 20, 21, 22, 23, 24, 25, 26, 27]. The possible adverse effects of hot weather conditions on concrete quality are:

(a) Rapid evaporation of mixing water, resulting in a rapid slump loss,

(b) Reduced ultimate concrete strength due to:

  (i) an increase in the quantity of mixing water as a result of enhanced water demand,

  (ii) insufficient curing at high temperature,

  (iii) non-uniform precipitation of the products of hydration between cement grains due to comparatively rapid hydration, and

  (iv) microcracking as a result of strain incompatibility due to different expansions of concrete constituents,

(c) Reduction in setting time of cement which creates problems in handling and

finishing,

(d) Thermal cracking and increased plastic shrinkage cracking,

(e) Reduced durability due to an increase in the mixing water and cracking,

(f) Formation of cold joints,

(g) Increased difficulty in controlling entrained air content, and

(h) Increased permeability.

Specifications for concreting in hot weather conditions usually identify a temperature limit at the time of its placement. According to ACI 305 [28], a maximum concrete temperature of 90 °F (32 °C) is recommended as an upper limit for the production of good quality concrete. To achieve this limit, the following precautions [28, 29, 30, 31, 22] are recommended:

(i) placement of concrete at lower temperatures of the day, such as late afternoon, evening or night. If concreting is to be done at higher temperatures the following measures may be adopted:

  (a) keep aggregates cool by shading them or spraying water over them, and

  (b) use cold water for mixing and if necessary use ice as part of the mixing water,

(ii) use of water reducing and retarding admixtures,

(iii) mixing time to be minimized,

(iv) delivery of concrete to be done in a minimum time,

(v) shortest possible time for placement, compaction and finishing of concrete, and

(vi) proper curing of concrete by keeping it moist to avoid evaporation of mix water.

The most important adverse effect of hot weather conditions on fresh concrete is plastic shrinkage cracking. These cracks, which usually appear a few hours after casting, are caused by evaporation of water from the concrete surface. Shrinkage of fresh concrete is affected both by the rate of evaporation and its rheological properties. The former, depends on the properties of cement, mix proportions, concrete temperature, exposure conditions, rate of hydration and time [32].

Since this study is related to plastic shrinkage cracking in concrete, the subsequent literature review is devoted to evaluate the effect of environmental factors and concrete composition on this aspect.

2.2 PLASTIC SHRINKAGE CRACKING

Cracks are sometimes observed on fresh concrete and mortar exposed to hot and dry climatic conditions. Although these cracks may also develop at normal temper-

atures, this phenomenon is frequently associated with concreting under hot weather conditions, particularly at elevated temperatures [33, 34, 35]. These cracks are known as **plastic shrinkage cracks** and normally take one or more of the forms [36]:

(a) Diagonal cracks at approximately 45 °C to the edges of the slab being 0.2 to 2 m apart.

(b) A very large random map pattern.

(c) Following the pattern of reinforcement or other physical aspects, such as change of section.

Plastic shrinkage cracks are almost straight, without any definite pattern, their length ranging from a few centimeters to meters. Needless to say that unless the cracks are quite shallow and narrow, they weaken the structure of concrete, permit penetration of moisture, and render the reinforcement vulnerable to corrosion.

These cracks, which occur mostly in horizontal surfaces, usually develop as the water sheen disappears from the surface of concrete. The time required for the formation of these cracks is influenced by the ambient temperature, relative humidity, wind velocity, concrete temperature and the bleeding characteristics of concrete. At the stage of their formation, the surface of the concrete has attained some initial rigidity; however, it cannot accommodate the rapid volume change due to shrinkage. After concrete is placed, the aggregate and cement paste start to settle and water

rises or bleeds to the surface. The rate at which this water reaches the surface and the total quantity that accumulates depend on the depth of concrete, materials used, mix proportions, and temperature of concrete. The rate and duration of bleeding influence the time at which the rate of evaporation of water from the surface exceeds the rate at which bleeding water rises to the surface. Even relatively small changes in the temperature and atmospheric conditions may have a pronounced effect on the rate of evaporation, especially if they occur simultaneously and supplement each other. Even though the air may be cool and in a saturated condition, i.e. at 100% relative humidity, there can be a significant evaporation of water from the surface of concrete if its temperature is higher than that of the air. Thus, it is possible to have plastic shrinkage cracking in concrete in cold, damp weather. Plastic shrinkage cracks are not usually progressive. They develop before concrete hardens and retain their original shape and are difficult to close once they have occurred. Such cracks may be focal points for other forms of deterioration, since they allow moisture and oxygen to penetrate concrete, and may impair its performance. These types of cracks may compromise the serviceability, durability, or aesthetics of a concrete structure, and are therefore of economic significance to the concrete construction industry. Such cracks may occur even when standard precautions have been taken to prevent their formation and cause serious damage resulting in expensive repairs. The importance of this property has been recognized and research in recent years has attempted to advance an understanding of the mechanisms of plastic shrinkage

cracking and to determine appropriate methods for its prevention.

According to the ACI Committee 305 [28], the principal cause of plastic shrinkage cracking in portland cement concrete is the excessive rapid rate of evaporation of the water from the surface of concrete and the inability or lack of bleed water to replace the evaporating surface water. Above a certain limit, a high rate of evaporation will decrease the consistency and may cause plastic shrinkage cracking and even a stoppage of the hydration of cement. Plastic shrinkage cracks appear when the water evaporates from freshly placed concrete faster than the concrete can bleed water to the surface, particularly when the ambient conditions are such that the rate of evaporation of water exceeds 0.2 lb./ft^2/h. This value of rate of evaporation can be obtained from the graph (Figure 2.4) given by ACI 305 based on Menzel's formula as given below:

$$W = 0.44(e_o - e_s)(0.253 + 0.096V)$$

where,

W = evaporation rate in $lb/hr/ft^2$ of surface;

e_o = pressure of saturated vapor, psi, at the temperature of concrete surface;

e_s = vapor pressure of surrounding air, psi (a function of its temperature and relative humidity); and

V = wind velocity, mph, over the concrete surface.

This formula is adapted from Dalton's law which states that the rate of evaporation is a function of the differences in the vapor pressures at the water surface and the atmosphere.

The following conditions, either singly or collectively, increase the rate of evaporation and the potential for plastic shrinkage cracks [21]:

1. high concrete temperature,
2. low relative humidity,
3. high wind velocity, and
4. high ambient temperature.

2.2.1 Effect of Environmental Conditions on Plastic Shrinkage

As discussed earlier, high concrete temperature, high air temperature, high wind velocity and low humidity, or combinations thereof, cause rapid evaporation which significantly increases the likelihood of plastic shrinkage cracking. It is believed that plastic shrinkage cracking is likely to occur when the rate of evaporation exceeds the rate at which the bleeding water rises to the surface of the freshly placed concrete and the tensile stress produced by shrinkage and rigidity, exceeds the tensile strength of the fresh mortar or concrete.

Hot and dry environment has a pronounced effect on plastic shrinkage cracking in fresh mortar and concrete. When evaporation takes place while the mortar or concrete is still plastic and the walls of the water channels collapse, a reduction in the w/c ratio of the concrete surface is attained and the mortar or concrete is densified due to shrinkage. If this shrinkage crosses certain limits it may cause plastic shrinkage cracking [37, 38, 39, 40, 41, 42, 43, 44]. Further, rapid evaporation has a predominant effect on plastic shrinkage cracking. However, it is not a direct function of water loss or evaporation rate and that semi-plastic mortar does not crack under high evaporation conditions when compared to plastic and wet mortars. Therefore, prevention of evaporation immediately after casting reduces early drying and cracking.

The action of capillary pressure in fresh concrete is assumed to be the principal cause of plastic shrinkage. Wittman [12] presented characteristic results to verify the essential statements of this hypothesis and dealt with the influence of water-cement ratio on plastic shrinkage in great detail. The results indicated that plastic shrinkage leads to highest contraction of fresh concrete with a w/c ratio in the range of 0.5 to 0.6. He stated that addition of admixtures decreases plastic shrinkage cracking and if serious cracking is avoided, plastic shrinkage has a compacting effect and it leads to improved mechanical behavior of the hardened concrete. The results also indicated that plastic shrinkage is originated by the capillary action and can thus be avoided by keeping the surface of fresh concrete wet.

Kral and Gebauer [45] investigated cracking of concrete slabs in the first 24 hours and later they were placed in a wind tunnel using varying air humidity and wind velocity, as well as different concrete mix compositions. The relationship between evaporation of water, shrinkage cracking at early ages and properties of concrete were discussed on the basis of the experimental results. They concluded that shrinkage cracking at early ages occurs only if several unfavorable atmospheric conditions coincide resulting in high evaporation rates during the critical period between 2 and 4 hours after mixing and placing. They further indicated that shrinkage cracking of concrete can be avoided by employing mix proportions which reduce evaporation during this critical period of time, and protection and curing afterwards are required only for the purpose of hydration and strength development.

The effect of different environmental conditions on the rate and amount of water evaporation from fresh mortar and concrete surfaces was investigated by Berhane [13]. The variables studied were air temperature, wind speed, relative humidity, type of cement and water content. He concluded that the measured water loss in a hot-humid environment is considerably lower than that in a hot-dry climate. However, the rise in temperature caused by the negligible cooling effect of evaporation in concrete in hot and humid climate may have its own drawback. Because of the negligible evaporation and the cooling effect in a hot and humid climate, the temperature of the mortar or concrete will rise above the already high ambient temperature. This rise in temperature adversely affects the hydration products and properties of

mortar and concrete cast in and exposed to a hot and humid climate. It was noted that in hot-dry climate the maximum rate of evaporation was attained 1.5 hours after casting, whereas in hot-humid climate the maximum rate was reached after 4 to 6 hours. It was also observed that the water loss in hot and dry climate was about 7 1/2 times than that lost in hot-humid environment. These results point out the limitations of Menzel's formula [28] for estimating the evaporation rate at any stage of fresh mortar or concrete. It was shown that cracking is possible for an evaporation rate as low as 0.1 lb./ft^2/hr.

Gebler [21] indicated that the water vapor will diffuse from higher to lower vapor pressures as these pressures tend to equalize. As the vapor moves away from the concrete surface, water evaporates to maintain a constant pressure. Therefore, concrete can experience substantial evaporation of mixing water to the surrounding air even at 100% relative humidity.

Cebeci et al. [46] indicated that the evaporation of water is not only affected by air temperature, air velocity and relative humidity but also by the surface temperature, geometry of the system and flow conditions. They criticized the conclusions given by Berhane [13] regarding the validity of Menzel's equation. They compared the results obtained by Menzel and Berhane with those obtained by heat and mass transfer relationship for constant drying rate and that between heat transfer and mass velocity of air for similar environmental conditions. They are of the opinion that the initial temperature of the specimen should not be indiscriminately used

for estimating later evaporation rates from fresh mortar or concrete. They concluded that a valid criticism of Menzel's formula or a convincing recommendation of other methods should be based on a consideration of all the factors affecting the evaporation of water from fresh mortar and concrete.

The evaporation rate formulas can be applied only when the surface is completely covered by water. This fact is not usually taken into account and is not mentioned anywhere in the Standard Practice for Curing Concrete (ACI 308) nor in any other ACI and PCI publications. The equations presented by the authors [46] have not yet been tried in concrete technology. The use of superplasticizers and low water cement ratios nowadays seldom allows the concrete surface to be completely covered by water, hence using the graph based on Menzel's equation is not feasible.

Hasanain et. al. [14] reported a study conducted in the hot weather of western Saudi Arabia on a number of specimens. The results indicated that, besides water components, the time of casting, difference of concrete and air temperatures, and moisture conditions of concrete surface influence the rate of evaporation of water from freshly placed concrete surfaces. Based on the results of that study, the authors suggested specifications for hot weather concreting and discussed the limitations of the graphical method used for estimating the rate of evaporation suggested by Menzel.

2.2.2 Influence of Mix Proportions on Plastic Shrinkage

The cause of plastic shrinkage cracks in fresh concrete may be attributed to its mix design and material properties in addition to the environmental conditions [38, 39, 40, 41, 47, 48, 49]. This is because the mix design affects the magnitude of the volumetric change, rate of hydration and the development of tensile strength. Furthermore, the relationship between the decrease in volume of concrete and the released water varies considerably with age.

Plastic shrinkage cracking of concrete can be reduced by employing mix proportions which produce bleed water to compensate for evaporation during the early stages. It has also been observed that mixes with higher volume of paste possess an increased tendency to crack. Plastic shrinkage in mortar and concrete is generally observed to decrease with the increase in volume fraction of aggregates [41, 50, 51, 52].

Shaeles and Hover [53] investigated plastic shrinkage cracking in mortar panels, simulating cracking in concrete slabs using the procedure developed by Kraai [54]. The focus of this particular study was to investigate the influence of mix proportions and construction operations on the development of plastic shrinkage cracking in test specimens cast under controlled environmental conditions. They concluded that for the specific conditions of the testing program, the incidence of plastic shrinkage cracking increased with the paste volume fraction. It was also observed that the

orientation and severity of the cracks were influenced more strongly by the direction and speed of strike off operations than all other variables studied. They linked the crack orientation to the screeding operation by stating that either the action of screeding tears the surface of the concrete or imposes tensile stresses on the surface that later add to shrinkage stresses that cause the cracks to form in a preferred direction. They believed that some threshold evaporation rate is necessary to initiate cracking, and for the tests conducted, no direct correlation between the severity of the cracking and the rate of evaporation was noted. Turton [55] discussed the results put forward by Shaeles and Hover [53] and appreciated the inclusion of influence of construction operations by the authors.

2.2.3 Mechanism of Plastic Shrinkage Cracking in Concrete

Many researchers [12, 56] have put forward their hypotheses regarding the mechanisms of plastic shrinkage cracking. Wittman [12] stated that the action of capillary pressure in fresh concrete is the principal cause of plastic shrinkage. His results also indicated that plastic shrinkage cracks are originated by the capillary action and can thus be avoided by keeping the surface of fresh concrete wet. Cohen et. al. [56] studied the mechanism of plastic shrinkage cracking in portland cement and portland cement-silica fume paste and mortar specimens. According to them, plas-

tic shrinkage in paste specimens is primarily related to the development of tensile capillary pressure during drying. The higher the surface area of silica fume particles, the higher is the tensile capillary pressure, and consequently, the more vulnerable the system would be to plastic shrinkage cracking. In the mortar specimens, plastic shrinkage was controlled by both capillary pressure in the paste and presence of fine aggregate particles. These particles serve to reduce cracking by: (a) arresting cracks, and (b) refining the size and distribution of capillary pores. According to the authors [56], the charts developed by the Portland Cement Association (PCA) [28] to calculate the rate of evaporation cannot predict the occurrence of plastic shrinkage cracks. They also demonstrated the importance of surface area of cement and silica fume particles on the mechanism of plastic shrinkage cracking. The capillary pressure developed during drying can lead to plastic shrinkage cracking. According to them, the time at which the water sheen disappears from the surface of the paste specimens is critical. Under conditions conducive to plastic shrinkage cracking, an earlier disappearance of the sheen, and prior to setting of the cement paste, would result in a more severe cracking because the paste has not had the time to set and develop sufficient tensile strength to resist the capillary tensile pressure. A delay in the time of disappearance of the sheen would mean less cracking, especially if the paste sets and starts to gain strength.

2.2.4 Influence of Material Properties on Plastic Shrinkage

The elevated temperature is known to increase the rate of cement hydration, thus accelerating the setting of concrete. The degree of acceleration, however, depends on the cement composition. Therefore, cement which gives the lowest heat of hydration is normally preferred, particularly in mass concreting. Of the several factors which influence the magnitude of shrinkage, the important ones are sulfur trioxide (SO_3), tricalcium aluminate (C_3A), and alkali (Na_2O and K_2O) content of the cement [57]. SO_3 is normally added to cement in the form of gypsum, during the grinding of the clinker, to control the time of set. The lower shrinkage characteristics of cement pastes are associated with lower C_3A/SO_3 ratio and lower Na_2O and K_2O contents [57]. To control plastic shrinkage cracking, Type IV (low heat) or Type II (moderate heat) cement is usually specified rather than Type I, which is a high heat cement. The cement fineness also affects the rate at which heat is liberated during the hydration process without influencing the ultimate heat. The finer the cement, the higher the strength at early ages.

The maximum size of aggregate used also has a significant influence on shrinkage, as it provides an internal restraint which reduces the potential contraction of the paste [58]. It is the stiffness or modulus of elasticity of the aggregate which influences its ability to restrain shrinkage [58]. In addition to the compressibility of an aggregate, which influences the shrinkage of concrete, the aggregate itself may

exhibit a high contraction upon drying. In general, the use of an aggregate of high absorption and low modulus of elasticity will produce high shrinkage concrete [59].

2.2.5 Plastic Shrinkage Cracking of Fiber Reinforced Concrete

To reduce the possibility of shrinkage cracks, fibers are normally introduced in the concrete mix to resist the tensile drying stresses [60, 61, 62, 63, 64, 65]. Swamy and Stavides [66] indicated that addition of steel fiber reduced the shrinkage cracks by up to 20%, while others [67, 68] reported a reduction of 10%. However, the reduction in cracks was found to be dependent on the type and volume of the fibers [66, 67, 68, 69]. Other studies, conducted under severe field curing conditions, indicated that addition of steel fibers may increase the concrete shrinkage at its surface due to the uneven distribution of fibers [70].

2.2.6 Plastic Shrinkage of Blended Cements

The advantage of using blended cements containing fly ash, blast furnace slag, silica fume and natural pozzolans to improve the ultimate strength and durability of concrete is well known [71, 72, 73, 74, 75, 76] These blending materials usually develop cementitious properties at a slower rate compared with OPC which they replaced. Therefore, they require more curing period. The general belief is that the

blended cements will perform worse than OPC with respect to shrinkage, but this aspect needs to be investigated [71]. The effect of curing at a high temperature, 45°C, on the strength of some natural pozzolonic material indicated a reduction in the overall strength for pozzolans rich with alumina composition [75]. Therefore, caution should be taken when such materials are used in hot-arid environments [75]. Fly ash and granulated blast furnace slag cements are recommended in hot climate for the production of durable concrete [76]. According to Cohen et. al. [56], the higher surface area of silica fume particles increases the tensile capillary pressure, and consequently, makes the concrete more vulnerable to plastic shrinkage cracking.

2.2.7 Effect of Chemical Admixtures on Plastic Shrinkage

Chemical admixtures are usually used to improve the properties of fresh concrete. These chemicals affect the plastic shrinkage by influencing the mixing water requirement and time of setting. Water reducing admixtures are expected to reduce shrinkage as they reduce the volume of mix water, while the use of retarding admixtures increases the shrinkage due to the delaying effect on setting time [40, 77].

It was observed that the quantity of plasticizer (water-reducing admixture) is increased at higher temperature casting [78]. In high temperature environments, the rate of slump loss is increased even when plasticizers are used [78]. It was shown that superplasticizers (high range water reducers) reduce the capillary pore water pressure resulting in lower plastic shrinkage. The effect, however, depends on the

proportion and type of superplasticizer used. [79]

2.2.8 Effect of Plastic Shrinkage Cracking on Concrete Durability

Concrete must be designed to ensure satisfactory durability, particularly under hot weather conditions. This is so because evaporation of water from fresh concrete has both positive and negative effects on the properties of concrete. The negative effects are slump loss, plastic shrinkage cracking, deficiency in strength at later stages etc. The positive effects are densification of fresh concrete, which lowers the water cement ratio thereby increasing the strength, bringing down drying shrinkage and creep, improving the water tightness and upgrading its durability. But precautions are to be taken in order to attain the optimum positive influences of evaporation of water from fresh concrete. To attain such advantages, studies should be conducted by exposing fresh concrete to different hot climates for different periods in order to pinpoint optimum exposure times which will give best results. [80]

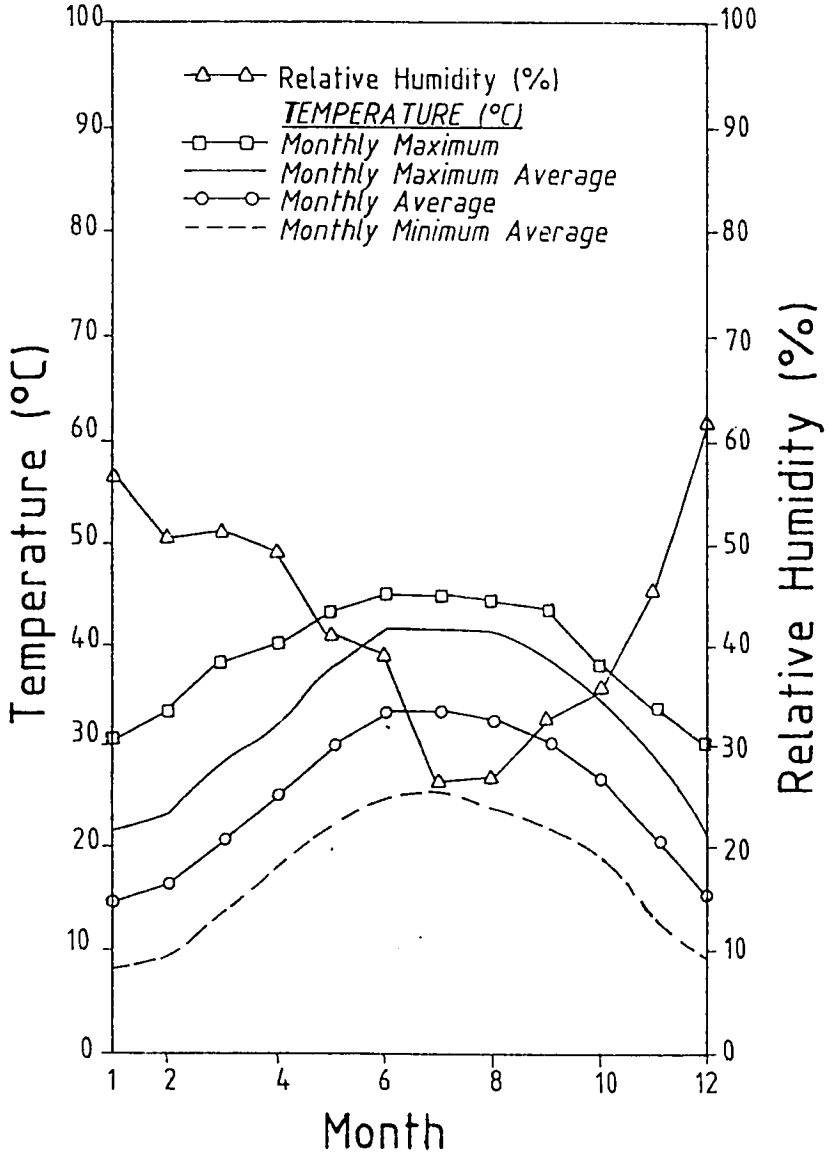

Figure 2.1: Climate of Riyadh

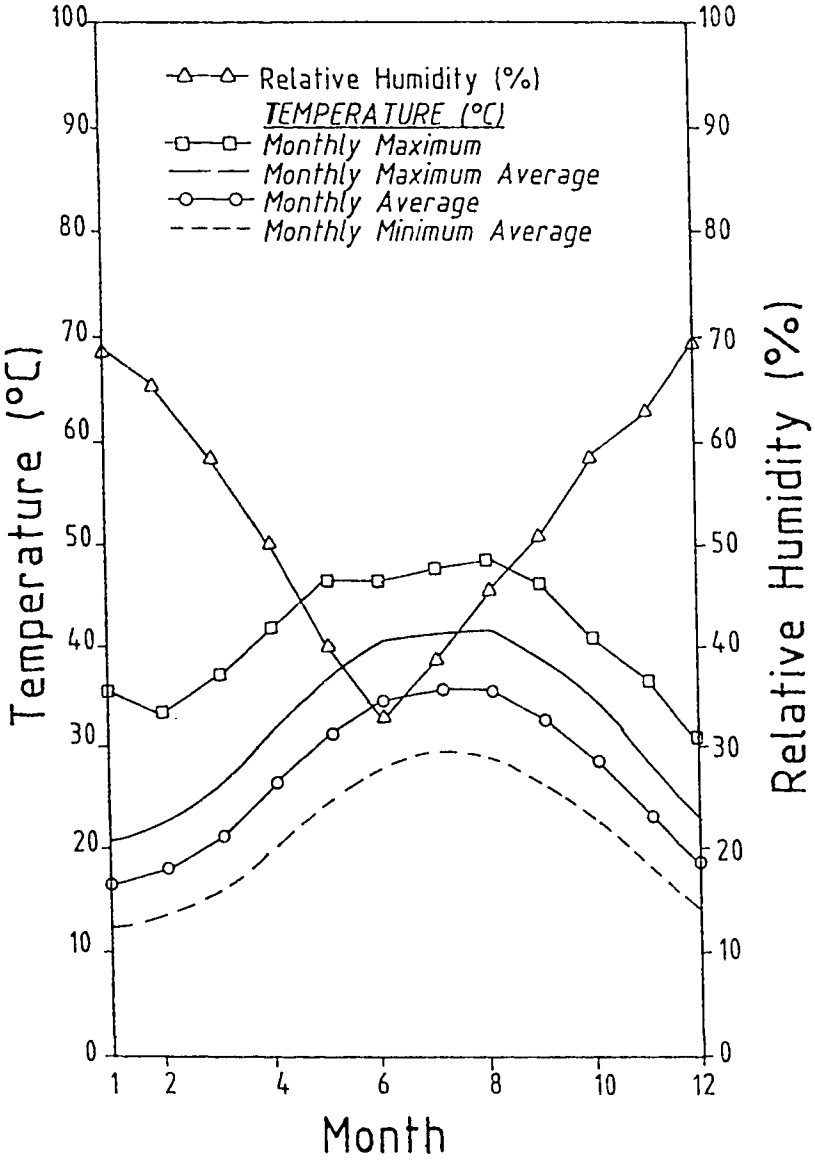

Figure 2.2: Climate of Dhahran

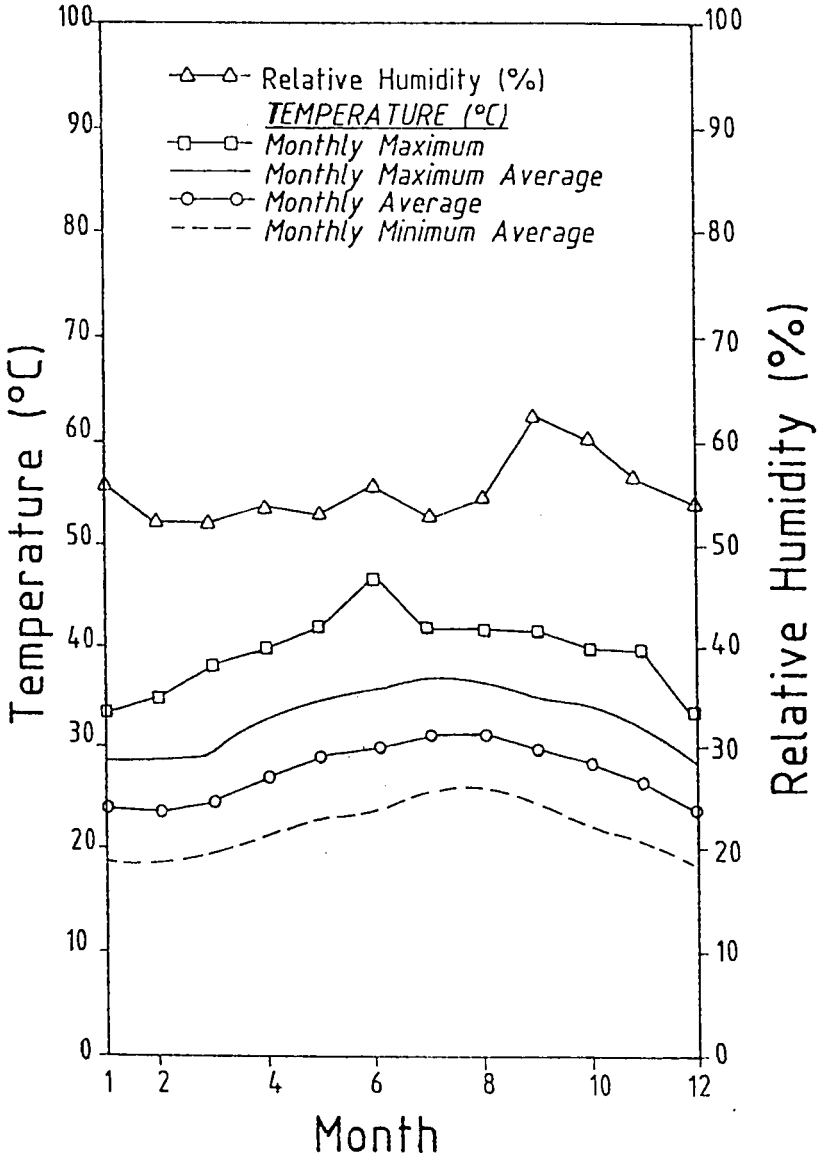

Figure 2.3: Climate of Jeddah

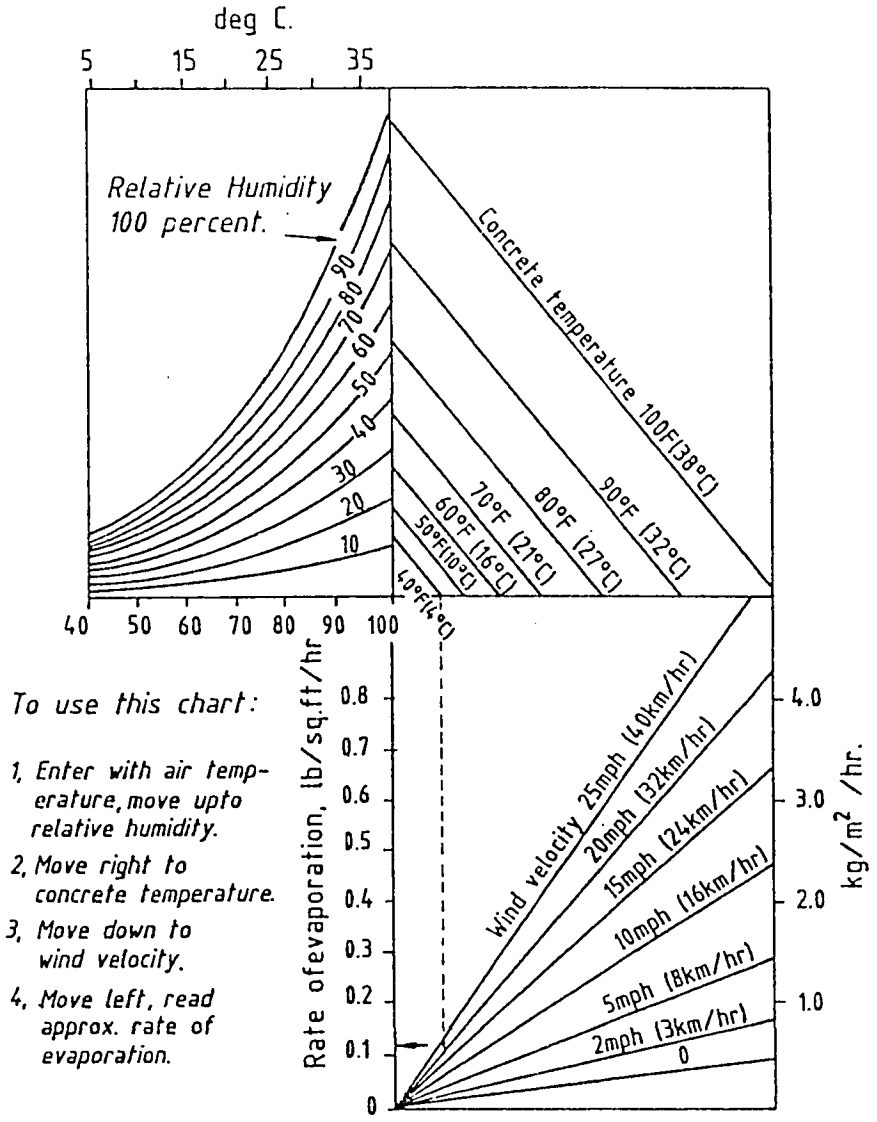

Figure 2.4: Effect of Ambient Conditions on Rate of Water Evaporation

Chapter 3

METHODOLOGY OF RESEARCH

This research work is basically concerned with plastic shrinkage cracking of fresh concrete at different weather conditions. The effects of temperature, humidity and wind velocity on plastic shrinkage cracking, rate of water evaporation, concrete temperature, crack length, time of cracking and cracking intensity were evaluated. The exposure conditions for the experimental program were selected after studying the weather data of the Eastern Province of Saudi Arabia for the last 20 years. The experimental program was broadly divided into five series. In Series I, the effect of wind velocity and relative humidity at a constant high temperature on plastic shrinkage cracking in concrete, with varying mix proportions, was studied. In Series II, the effect of varying ambient temperature, at a constant relative humidity, on

plastic shrinkage cracking in concrete, with different mix proportions, was evaluated. In Series III, plastic shrinkage cracking in blended cement concrete was investigated. In this series, plastic shrinkage cracking in concrete mixes made with different proportions of blending materials was studied under two environmental conditions. This was followed by exposing selected blended cement concrete specimens to different environmental conditions. In Series IV, big specimens, with a single concrete composition, were subjected to varying climatic conditions. In this series, plastic shrinkage strain, compressive strength development and microstructure were also evaluated. In Series V, the bleeding characteristics of all the mixes used in this investigation were studied. The exposure conditions for Series I to IV concrete specimens are summarized in Tables 3.1 to 3.4. The mix constituents for Series I and II specimens are given in Table 3.5 and for Series III in Table 3.6. The experimental details for Series IV specimens are given in Table 3.7. The experimental variables for Series I to IV specimens are shown in Figures 3.1 to 3.4.

3.1 MATERIALS

3.1.1 Coarse Aggregate

The coarse aggregate used in this investigation was brought from Abu-Hadriya. The specific gravity of the crushed limestone coarse aggregate was 2.46. Absorption tests were conducted on the aggregate in accordance with the ASTM C 128. The

absorption capacity of the aggregate is required for determining the total amount of water to be used in each mix. The absorption of the coarse aggregate used in this investigation was 3%. Two gradings of the coarse aggregate were taken, one for the small specimens and the other for the big specimens. In the small specimens, the maximum size of the coarse aggregate was 3/16 " and in the big specimens it was taken as 1/2 ". The grading of the coarse aggregate was chosen so that it falls within the grading limits of ASTM C 33. The adopted grading and the corresponding ASTM limits are shown in Tables 3.8 and 3.9 and Figures 3.5 and 3.6.

3.1.2 Fine Aggregate

Dune sand was used as fine aggregate. It had an absorption of 0.23% and a specific gravity of 2.54.

3.1.3 Cement

The cement used in preparing the specimens was ASTM Type V. Its chemical composition is shown in Table 3.10.

3.1.4 Other Materials

Silica fume, fly ash and blast furnace slag were used in Series III concrete specimens. The chemical and physical analyses of these materials are given in Tables 3.11 to 3.15.

All the concrete mixes were designed for a workability of 50-75 mm slump. Suitable dosage of Conplast 430 superplasticizer was used to obtain the desired workability. This was achieved after carrying out a number of trial mixes with different dosages of superplasticizer, as shown in Table 3.16.

3.2 MIX DESIGN

The mix design variables are shown in Figures 3.1 to 3.4 and Tables 3.1 to 3.6.

3.3 CURING CONDITIONS

The test specimens were exposed immediately after casting to the desired environmental conditions as stated earlier.

3.4 EXPERIMENTAL PROCEDURE

The experimental procedure was based on the methodology developed by Kraai [54] for evaluating the effect of fibers in reducing shrinkage cracking in concrete slabs. The specimens were cast in a chamber with controlled temperature and humidity which was fabricated at KFUPM Workshop, based on the design adopted by King and Timusk [81]. The controlled temperature and humidity chamber is shown in Figures 3.7 and 3.8. The required temperature was maintained using electric heaters

shown in Figure 3.9 and a temperature controller shown in Figure 3.10. In addition, the chamber was provided with a blower, as shown in Figures 3.11 and 3.12, to generate high speed winds. Another important feature was that the humidity was controlled through the commercial humidifier shown in Figures 3.13, 3.14 and 3.15 and the dehumidifier system shown in Figure 3.16 and not by water and other salt solutions as recommended by King and Timusk [81]. The humidity was measured by the humidity dial gauge shown in Figure 3.17.

The big specimens measured 36" x 36" x 2" while the small specimens were 18" x 18" x 3/4" in size. The thickness of the slabs was selected to represent the surface area to volume ratio of a typical concrete slab. Aluminum and Plexiglass forms were used to cast the specimens. These forms are not only durable, but also prohibit absorption of moisture from the mix. This improves the uniformity of conditions among all the tests, increases bleeding, forces a one-dimensional water movement and provides a worst case scenario for plastic shrinkage cracking, by simulating the casting of a slab over a plastic vapor barrier, as recommended by Campbell et. al. [82]. These molds were rigid and therefore protected fresh concrete from being disturbed during handling, weighing and photographing. The molds are shown in Figure 3.18.

The blower was placed such that it covers the whole slab area uniformly. Direction of air movement was parallel to the plane of the surface. Typical experimental setup is shown in Figures 3.19 and 3.20. The wind velocity was measured using a

digital anemometer shown in Figure 3.21.

Temperature, relative humidity and wind speed were controlled to simulate hot weather conditions. In the small specimens, the concrete temperature was measured at three locations, namely, top, middle and bottom. In the big specimens, the concrete temperature was measured at five locations each at a distance of 1/2" through the specimen's thickness by a digital thermometer shown in 3.22. In the small specimens, loss of water, as affected by concrete temperature, air temperature, relative humidity, and wind velocity, was determined by the precision electrical balance shown in Figure 3.23. In the big specimens, loss of water was not determined, but two additional small specimens of 12" x 12" x 2" were cast alongside the large specimens and water loss in them was determined. To measure plastic shrinkage, four studs were placed at the sides of the big specimens to which LVDTs were attached as shown in Figure 3.24, which were connected to a data logger shown in Figure 3.25. The shrinkage displacement readings were recorded every 30 minutes. The specimens were kept under permanent observation for 6 hours. The small specimens were discarded immediately after the completion of the experiment, but the big specimens were cured for 28 days. The specimens were covered by wet burlap followed by a plastic sheet to prevent evaporation of water, as shown in Figure 3.26. After 28 days of curing pulse velocity readings were taken. The instrument used for this purpose is depicted in Figure 3.27. Representative cores, shown in Figure 3.28, were taken using the coring machine shown in Figure 3.29. These cores were

tested for compression on the Universal Compression Testing machine shown in Figure 3.30. The microstructure was evaluated by Mercury intrusion porosismetry technique.

3.5 PREPARATION OF SPECIMENS

3.5.1 Preparation of Materials

All the materials were proportioned by weight to give the required ratios of water to cement (W/C), total aggregate to cement (TA/C) and coarse aggregate to fine aggregate (CA/FA). The aggregates were washed and dried to remove dust and fines. The aggregate was sieved and later mixed to obtain the desired gradings.

3.5.2 Mixing Process

The concrete constituents were mixed in an electrically operated concrete mixer of 0.17 m^3 capacity. The mixing was done in accordance with ASTM C 192. Materials were put into the mixer in the following sequence. First the coarse aggregate was placed in the mixer. A part of the mixing water was added to the coarse aggregate and mixing was started. After a few revolutions, cement, sand and some of the mixing water were added and mixing continued for two minutes. Thereafter, the remaining water was added and mixing continued for 5 minutes. The concrete was then discharged from the mixer into a tray and remixed using hand trowels.

Temperature of the concrete was measured by placing a digital thermometer in the mix. Ambient air temperature was also recorded during the time of concreting. The concrete was then poured in the molds which were already covered with plastic sheets to prevent water leakage. The concrete was vibrated on a vibrating table and levelled by a straight edge without sideways or swaying motion.

3.6 MONITORING AND DATA ANALYSIS

3.6.1 Water Evaporation

The water evaporation was expressed as percentage of the water evaporated and the rate of evaporation. The percentage of water evaporated was expressed as the ratio of water evaporated to the total water added to the mix. The rate of water evaporation was evaluated by recording the change in weight using a digital balance of 0.01 gram sensitivity.

3.6.2 Plastic Shrinkage Cracking

The effect of environmental conditions and concrete mix variables on plastic shrinkage cracking was evaluated through visual inspection by monitoring the time of cracking and the development of cracks. Both the length and average width of the cracks were recorded and expressed as total crack area to distinguish between the hairline cracks and open cracks. The visual survey was conducted at regular in-

tervals to record the surface conditions and plastic shrinkage cracks. During the test, and at regular time intervals, photographs were taken to record the surface conditions and plastic shrinkage cracks. Typical patterns of plastic shrinkage cracks are shown in Figures 3.31 through 3.36.

3.6.3 Bleeding

In Series V, the bleeding water was measured in accordance with ASTM C 232 Method A. In this test, the concrete was cast in the bleeding bucket shown in Figure 3.37 and completely covered by a plastic sheet. The bleeding water was sucked by a pipette at 10 minute intervals during the first 40 minutes and then at an interval of 30 minutes till the cessation of bleeding. The bleeding water was transferred in beakers and weighed. Then the beakers were decanted on a hot plate till the water evaporated. The beakers were reweighed to determine the weight of water evaporated.

3.6.4 Plastic Shrinkage Strain

Plastic shrinkage strain was measured by embedding studs placed at four sides of each specimen. The movement of these studs was monitored using LVDTs connected to a data acquisition system for a period of 24 hours.

3.6.5 Strength Development

The effect of hot weather casting on the strength development was evaluated by taking cores after 28 days of curing. Three cores, 50 mm in diameter were taken from each slab. The cores were retrieved using a coring machine fitted with a diamond tipped core barrel. The coring machine was fixed on the concrete slab in order to prevent its movement, and the water was supplied continuously during the coring process. The cores were drilled vertically through the thickness of the slab. Each core was of 50 x 63.5 mm dimensions. The compressive strength was determined according to ASTM C 39.

3.6.6 Microstructure

The development of microstructure and microcracks in concrete cast under varying temperature, humidity and wind conditions was investigated using the ultrasonic pulse velocity technique and the mercury intrusion porosimetry, respectively.

3.6.6.1 Ultrasonic Pulse Velocity

The ultrasonic pulse velocity technique is based on measuring the time of travel of an ultrasonic pulse through the concrete. The indirect method was used to determine the pulse velocity according to ASTM C 597-83. Lines were drawn in both directions, 100 mm apart on the surface of the slab. Readings were taken at each

cross-section of the lines. Lubricating grease was applied at the junction of the concrete and the transducers to provide a good coupling and avoid air gaps. In this method a transmitting transducer of 88 KHz was fixed on one intersection which propagated ultrasonic pulses through the concrete to be received by the receiving transducer at the next grid point. The time taken by the pulse to travel 100 mm was noted from a digital display. The path length was divided by the transit time to obtain the pulse velocity.

3.6.6.2 Mercury Intrusion Porosimetry

Mercury intrusion porosimetry is used to study the pore size distribution. In mercury intrusion porosimetry, mercury, a non-wetting liquid is forced into the pores of the material at a high pressure. Pore size and volume quantification are accomplished by submerging the sample under a confined quantity of mercury and then increasing the pressure of the mercury hydraulically. As the applied pressure is increased the radius of the pores which can be filled with mercury decreases and consequently the total amount of mercury increases. The data obtained gives the pore volume distribution directly and with the aid of pore physical model, the pore size distribution can be ascertained.

In this study, the pore size distribution of the selected samples was carried out using Carlo Elba Model 2000 high pressure mercury intrusion porosimeter. According to Wash Burn equation of capillary suction or depression, the radius of the

cylindrical pore which will be reached by a pressure p is given by

$$r_1 = 2r\cos(\theta)/p$$

where r is the surface tension, θ is the contact angle. If r and θ are constant for a certain material, then r is inversely proportional to p. In this study a value of r equal to 480 dynes and θ equal to 141.3° was used. Then r (μm) = 750/p MPa. This means that pore sizes of 3.75 μm to 7500 μm can be detected.

Representative concrete specimen, approximately 1 gram, was used for pore size distribution. The pressure in the pressure vessel was increased from 0.1 to 200 Mpa slowly. The slow increase of pressure prevented the mercury from heating up during the test. The measurements of the pressure and the introduced volume of mercury were recorded and used to draw the pore volume against the radius.

45

Table 3.1: Exposure Conditions Adopted for Series I Concrete Specimens

Exposure	Air Temperature (°C)	Relative Humidity (%)	Wind Velocity (kmph)
Hot and Dry	45	25	0
Hot and Normal	45	50	0
Hot and Humid	45	95	0
Hot-Dry and Breezy	45	25	15
Hot-Normal and Breezy	45	50	15
Hot-Dry and Windy	45	25	25
Hot-Normal and Windy	45	50	25

Table 3.2: Exposure Conditions Adopted for Series II Concrete Specimens

Exposure	Air Temperature (°C)	Relative Humidity (%)	Wind Velocity (kmph)
Cool	25	50	0
Mild	35	50	0
Hot	45	50	0
Very Hot	55	50	0

Table 3.3: Exposure Conditions Adopted for Series III Concrete Specimens

Exposure	Air Temperature (°C)	Relative Humidity (%)	Wind Velocity (kmph)
Hot and Dry	45	25	0
Hot and Humid	45	95	0
Cool and Dry	25	25	0
Hot and Normal	45	50	0
Hot, Dry and Windy	45	25	15

Table 3.4: Exposure Conditions Adopted for Series IV Concrete Specimens

Exposure	Air Temperature (°C)	Relative Humidity (%)	Wind Velocity (kmph)
Cool and Normal	30	50	0
Cool, Dry and Windy	30	25	15
Cool and Humid	30	95	0
Hot and Normal	45	50	0
Hot, Dry and Windy	45	25	15
Hot and Humid	45	95	0

Table 3.5: Mix Proportions for Series I and Series II Concrete Specimens

Designation	Cement Content (kg/m^3)	Water Cement Ratio	Mix Proportion by Weight
Lean Stiff (Mix #1)	300	0.40	1:2.2:4.4
Lean Semi-plastic (Mix #2)	300	0.50	1:2.1:4.2
Lean Plastic (Mix #3)	300	0.65	1:2.0:4.0
Medium Stiff (Mix #4)	350	0.40	1:1.8:3.6
Medium Semi-plastic (Mix #5)	350	0.50	1:1.7:3.4
Medium Plastic (Mix #6)	350	0.65	1:1.6:3.2
Rich Semi-plastic (Mix #7)	400	0.40	1:1.5:3.0
Rich Plastic (Mix #8)	400	0.50	1:1.4:2.8
Rich Flowing (Mix #9)	400	0.65	1:1.3:2.6

Table 3.6: Mix Proportions for Series III Concrete Specimens

Mix Designation	Cementitious Material Content (kg/m^3)	Water Cementitious Materials Ratio	Pozzolanic Material
Control	350	0.40	None
SF1	350	0.40	5% Silica Fume
SF2	350	0.40	10% Silica Fume
SF3	350	0.40	15% Silica Fume
FA1	350	0.40	20% Fly Ash
FA2	350	0.40	30% Fly Ash
FA2	350	0.40	40% Fly Ash
BFS1	350	0.40	50% Blast Furnace Slag
BFS2	350	0.40	60% Blast Furnace Slag
BFS3	350	0.40	70% Blast Furnace Slag

Table 3.7: Slab Designations for Series IV Concrete Specimens

Designation	Environmental Conditions
Slab #1	Temp. 45 °C; Humidity 25 %; Wind 15 kmph
Slab #2	Temp. 45 °C; Humidity 50 %; Wind 0 kmph
Slab #3	Temp. 45 °C; Humidity 95 %; Wind 0 kmph
Slab #4	Temp. 30 °C; Humidity 25 %; Wind 15 kmph
Slab #5	Temp. 30 °C; Humidity 50 %; Wind 0 kmph
Slab #6	Temp. 30 °C; Humidity 95 %; Wind 0 kmph

Table 3.8: Grading of Coarse Aggregates Used in Series I, II and III Concrete Mixes

Sieve Opening (mm)	ASTM C 33	Percent Passing Limits
12.5	100	100
9.5	85 - 100	100
4.75	10 - 30	60
2.4	0 - 10	20
1.2	0 - 5	5
0.6	0	0

Table 3.9: Grading of Coarse Aggregates Used in Series IV Concrete Mixes

Sieve Opening (mm)	ASTM C 33	Percent Passing Limits
19	100	100
12.5	90 - 100	90
9.5	40 - 70	50
4.75	0 - 15	5
2.4	0 - 5	0

Table 3.10: Chemical Analysis of Type V Cement

Constituent	Weight, %
Loss on Ignition	0.80
SiO_2	22.20
Al_2O_3	3.48
Fe_2O_3	3.88
CaO	65.05
MgO	2.20
SO_3	1.85
K_2O	0.28
Na_2O	0.15
C_3S	62.0
C_2S	17.0
C_3A	2.7
C_4AF	11.8

Table 3.11: Chemical Analysis of Silica Fume

Constituent	Weight, %
H_2O	0.9
L.O.I. 950 gr. C	2.71
SiO (undissolved)	0.10
tot. C	0.59
tot. S	0.11
SiO_2	92.7
Fe	0.29
Al	0.27
Ca	0.32
Mg	0.92
K	0.99
Na	0.31
Mn	0.013
Ni	0.001
Cu	0.001
Zn	0.01
P	0.025

Table 3.12: Physical Characteristics of Silica Fume

Physical Analysis	Result
Reflection (color)	23.0
Sieve Analysis	0.5
Specific Surface Area m^2/g	16.2
pII fresh	8.6
pH 72 h	8.4

Table 3.13: Chemical and Physical Properties of Fly Ash

Constituent	Weight, %
SiO_2	52.30
Al_2O_3	23.40
Fe_2O_3	4.20
SO_3	0.64
CaO	12.5
Moisture Content	0.14
Loss on Ignition	0.26
Physical Properties	**Result**
Retained on 325 Sieve	23.8
Pozzolonic Activity Index	100
Water Requirement	94
Autoclave Expansion	0.02
Specific Gravity	2.24

Table 3.14: Grain Size Distribution of Blast Furnace Slag (Type A)

Sieve Size Opening μm	Percent Passing
128	100.0
96	100.0
64	97.0
48	94.0
32	81.7
24	69.5
16	54.3
8	33.8
6	27.2
4	21.1
3	16.3
2	12.1
1.5	7.9
1	6.4

Table 3.15: Chemical Analysis of Blast Furnace Slag

Constituent	Weight, %
FeO	0.49
CaO	36.63
MgO	11.27
SiO_2	31.51
Al_2O_3	17.23
TiO_2	0.96
MnO	0.44
K_2O	0.62
S	1.14

Table 3.16: Dosage of Superplasticizer Used

Mix	Dosage of Superplasticizer, % of Cement
Series I and II	
Lean Stiff	5.0
Lean Semi-plastic	1.7
Lean Fluid	0.0
Medium Stiff	2.0
Medium Semi-plastic	1.1
Medium Fluid	0.0
Rich Semi-plastic	1.2
Rich Plastic	0.0
Rich Fluid	0.0
Series III	
Control Mix	2.0
Silica Fume Mixes	2.4
Fly Ash Mixes	1.8
Blast Furnace Slag	1.6
Series IV	1.0

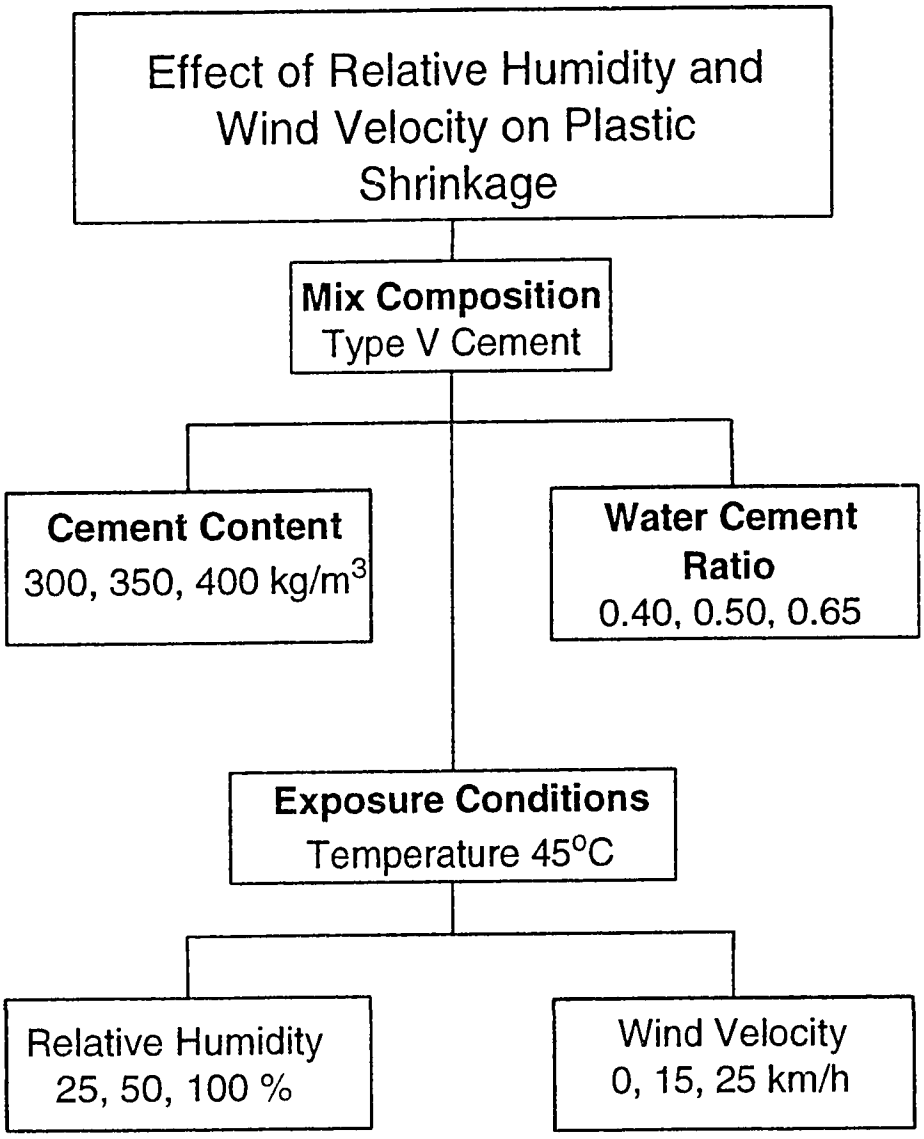

Figure 3.1: Mixture and Exposure Variables for Series I Experiments

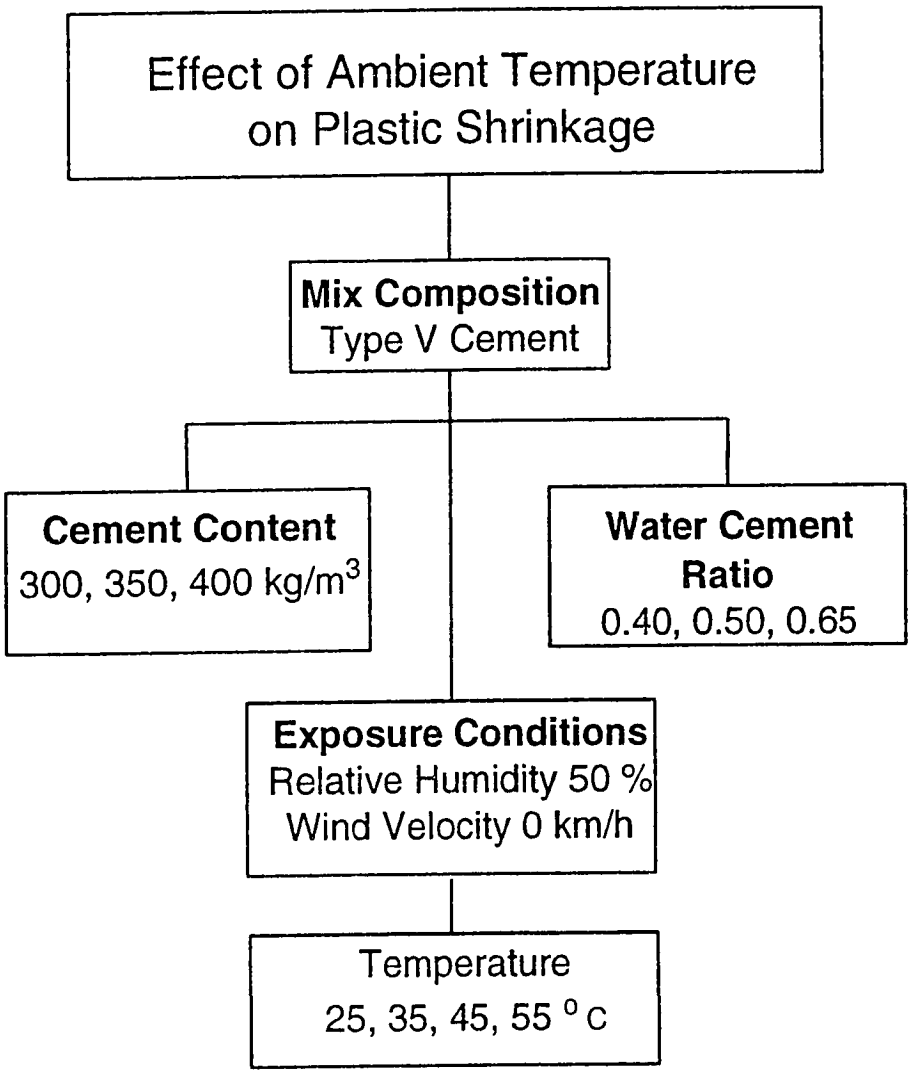

Figure 3.2: Mixture and Exposure Variables for Series II Experiments

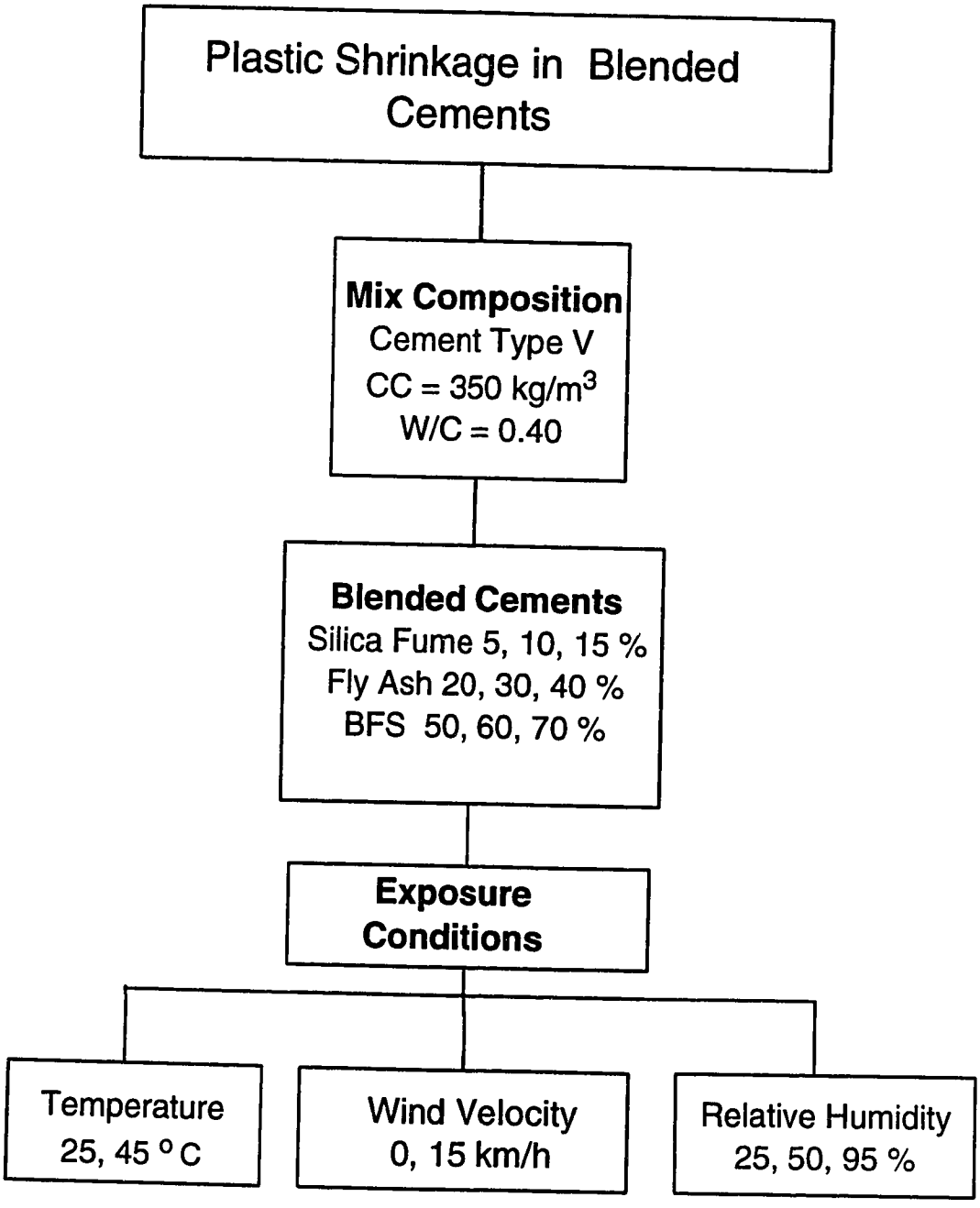

Figure 3.3: Blended Cements and Exposure Variables for Series III Experiments

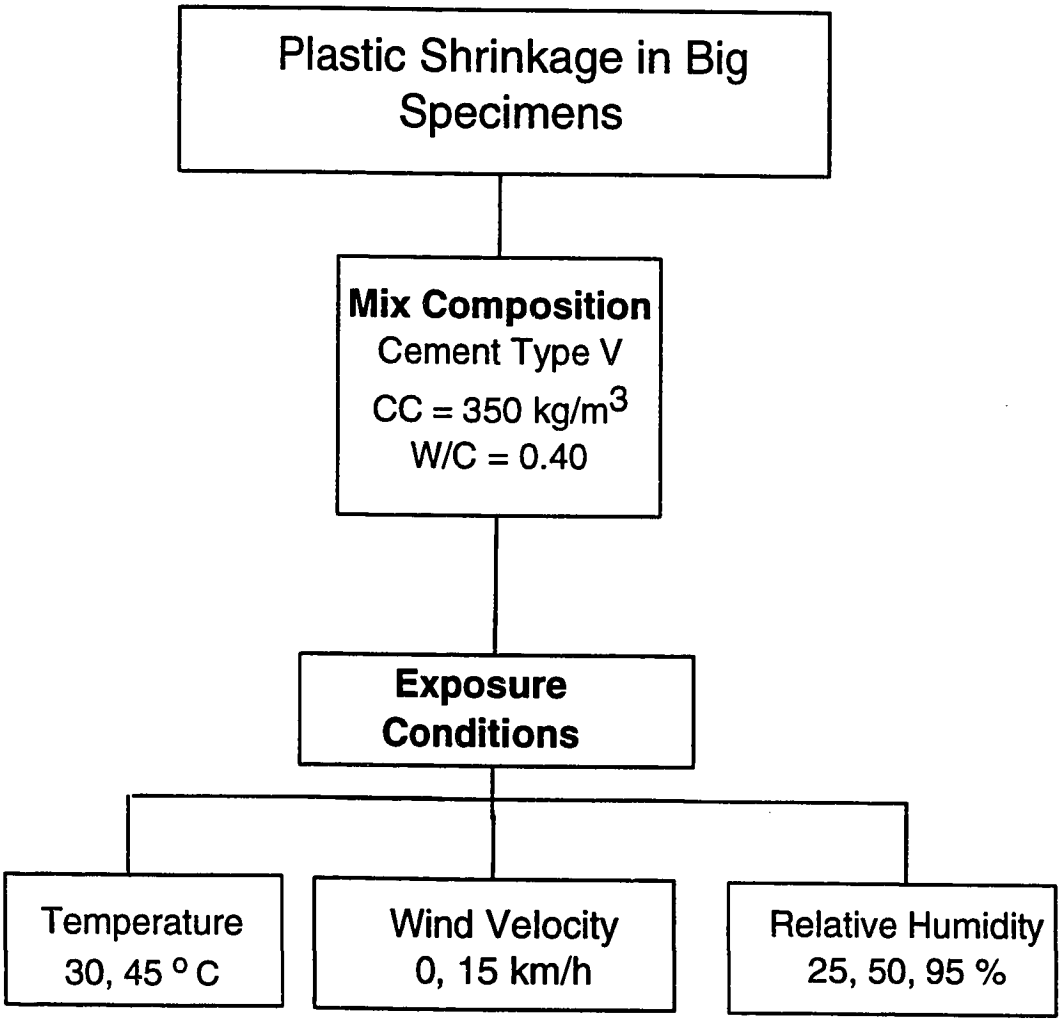

Figure 3.4: Exposure Variables for Series IV Experiments

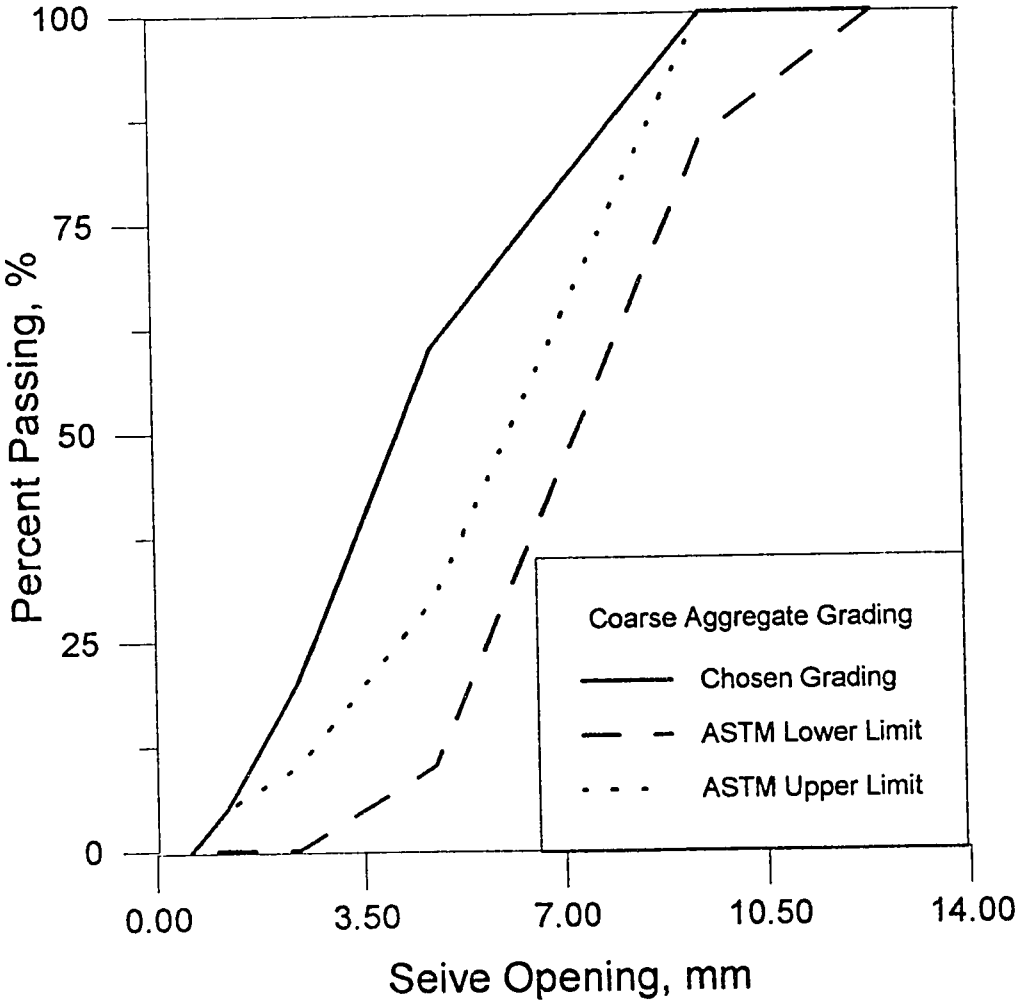

Figure 3.5: Grading of Coarse Aggregate used in Series I to III Concrete Mixtures

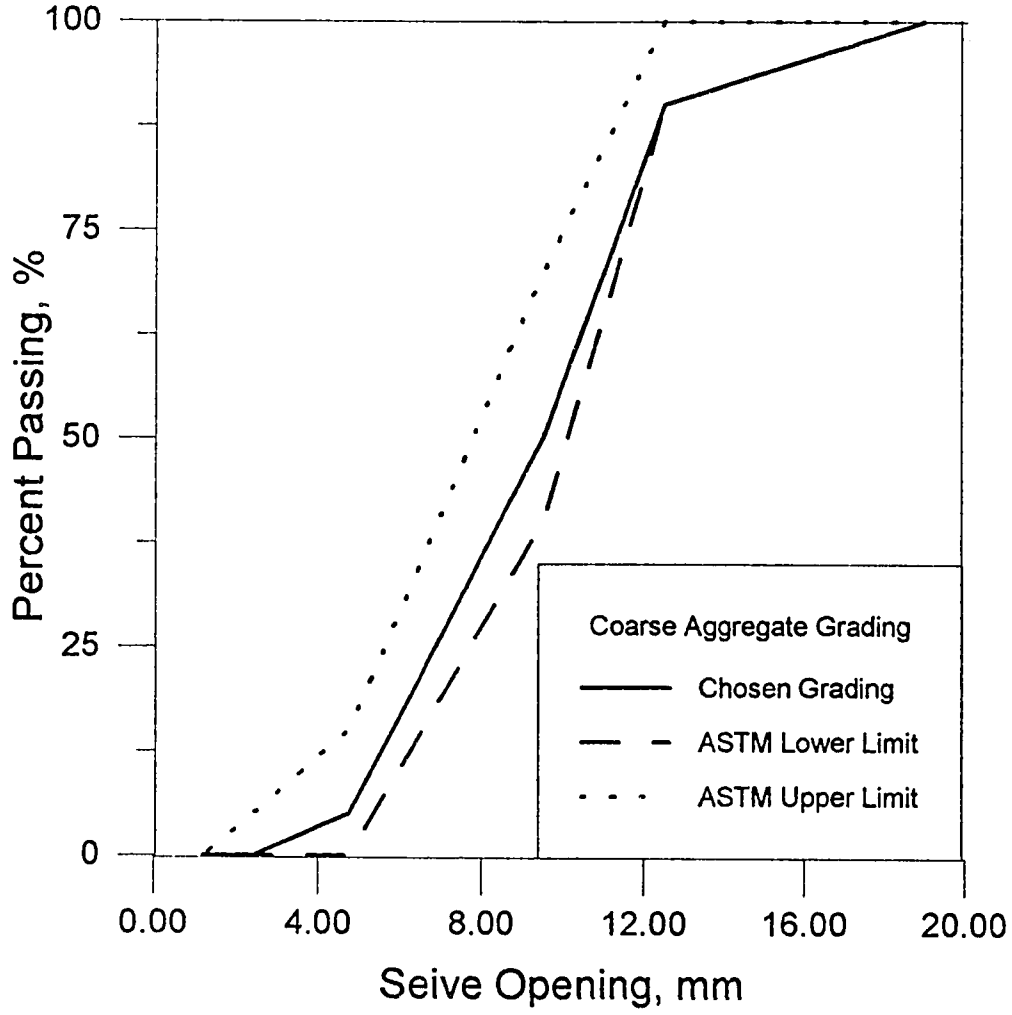

Figure 3.6: Grading of Coarse Aggregate used in Series IV Concrete Mixtures

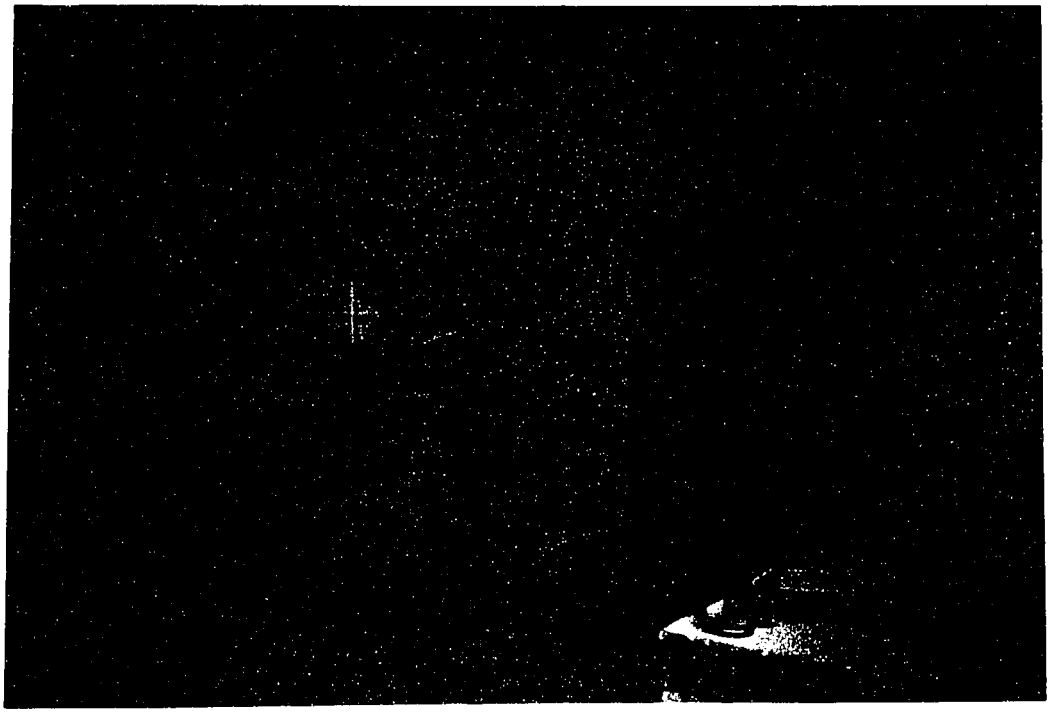

Figure 3.7: Controlled Temperature and Humidity Chamber(Side View)

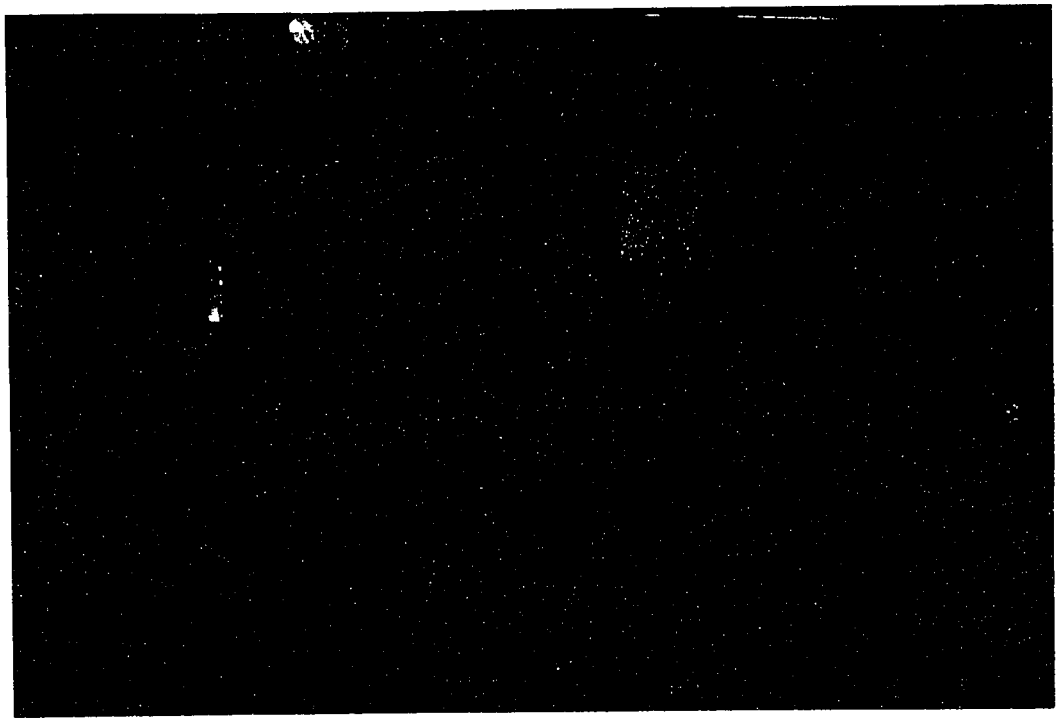

Figure 3.8: Controlled Temperature and Humidity Chamber(Back View)

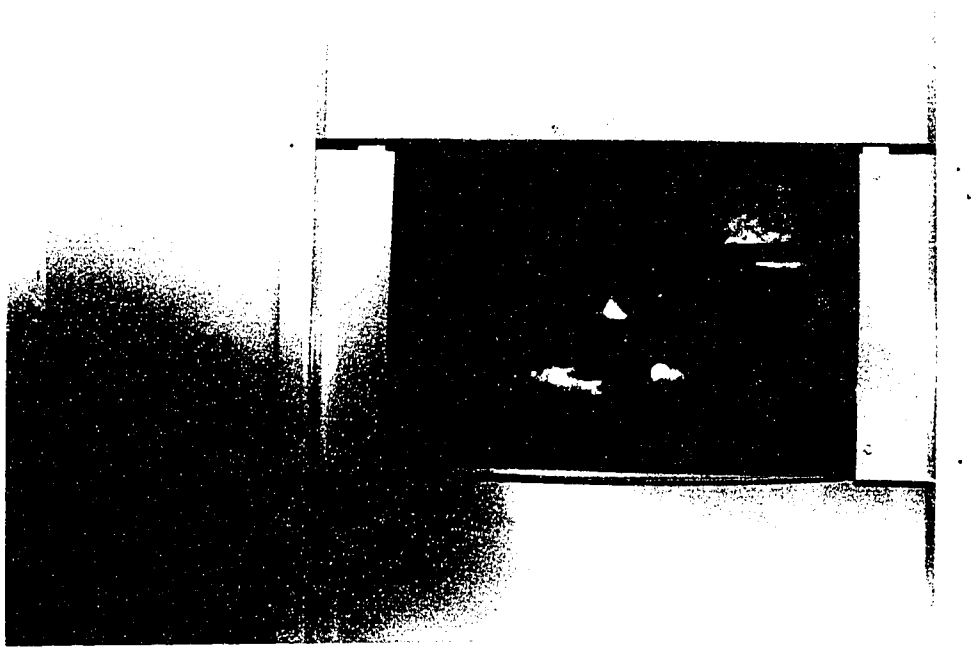

Figure 3.9: Electric Heaters

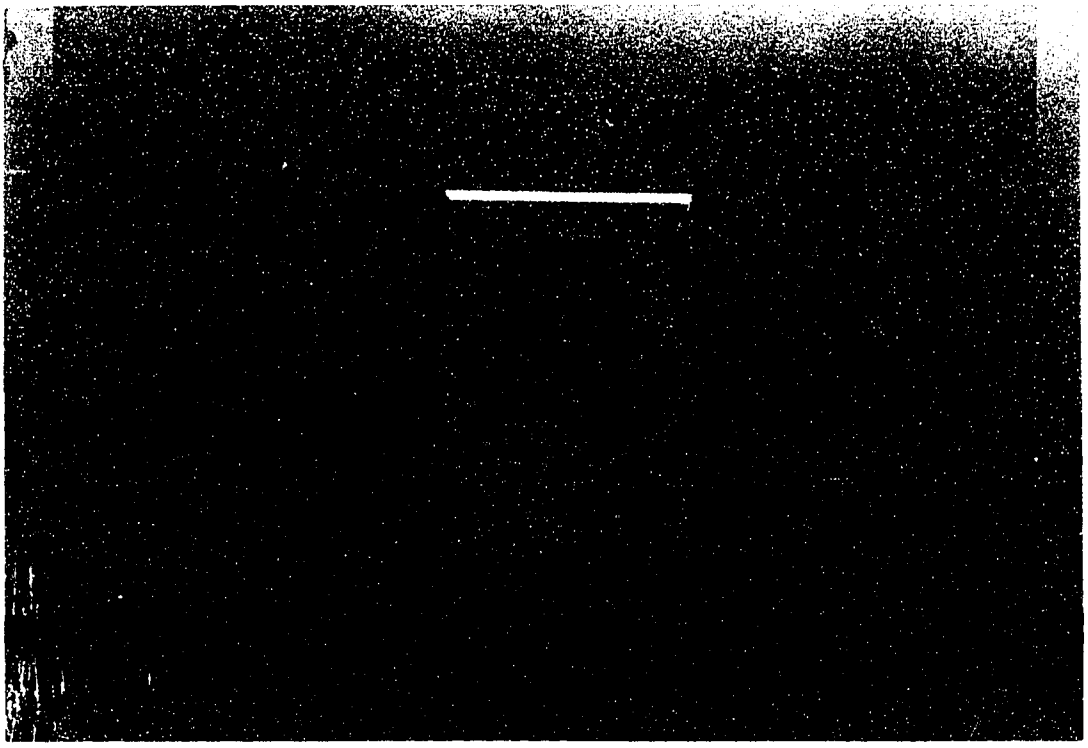

Figure 3.10: Temperature Controller

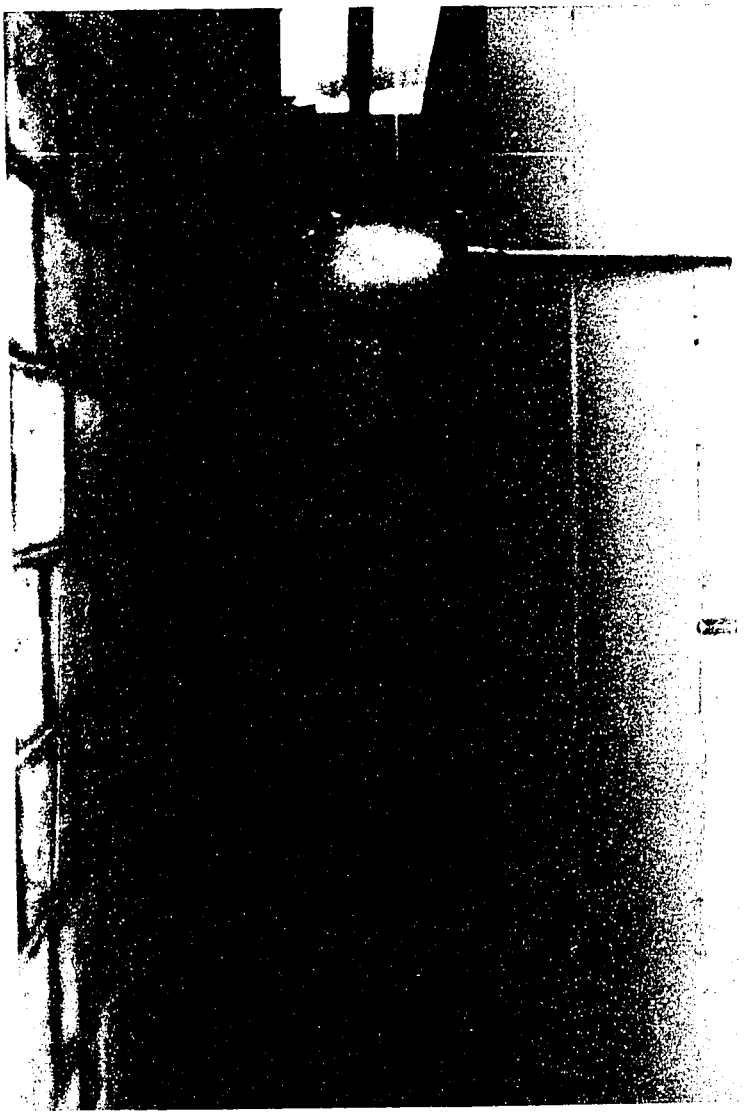

Figure 3.11: High Speed Wind Blower (Exterior View)

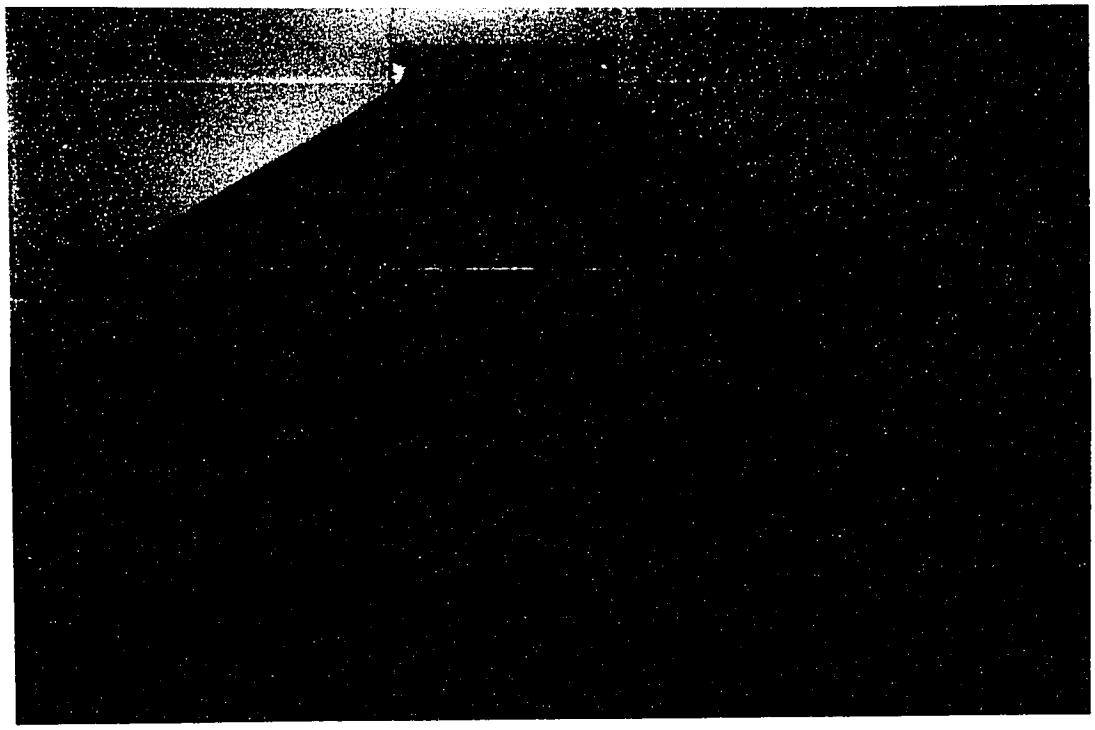

Figure 3.12: High Speed Wind Blower (Interior View)

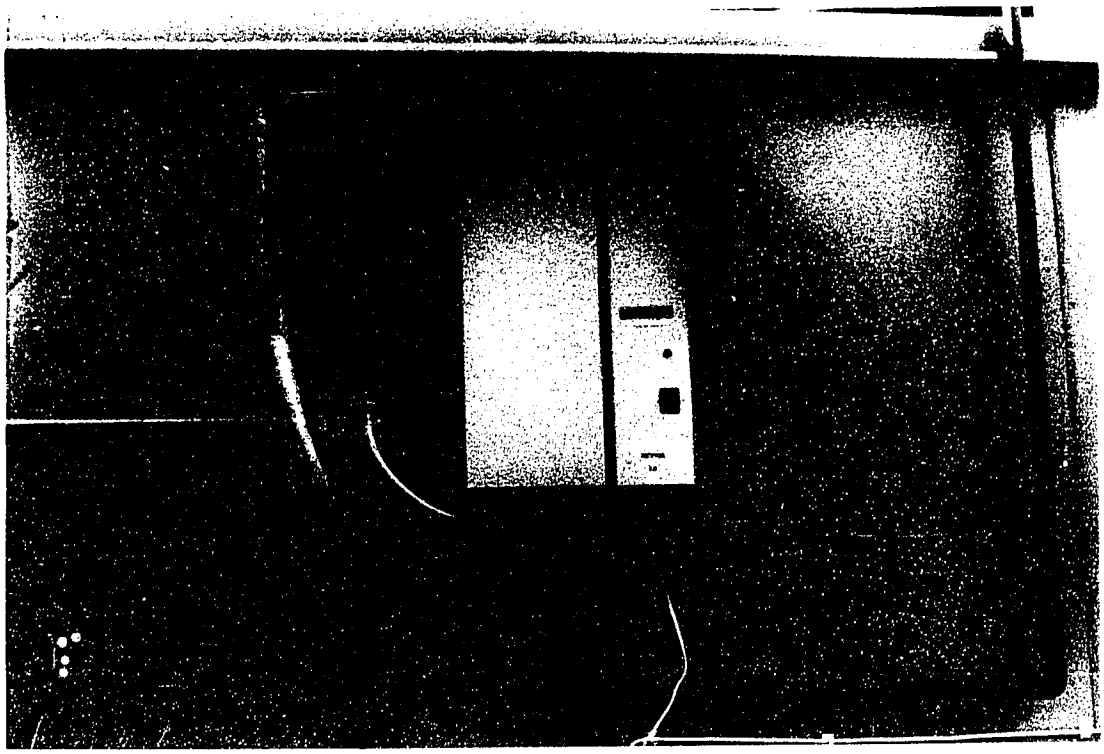

Figure 3.13: Humidifier

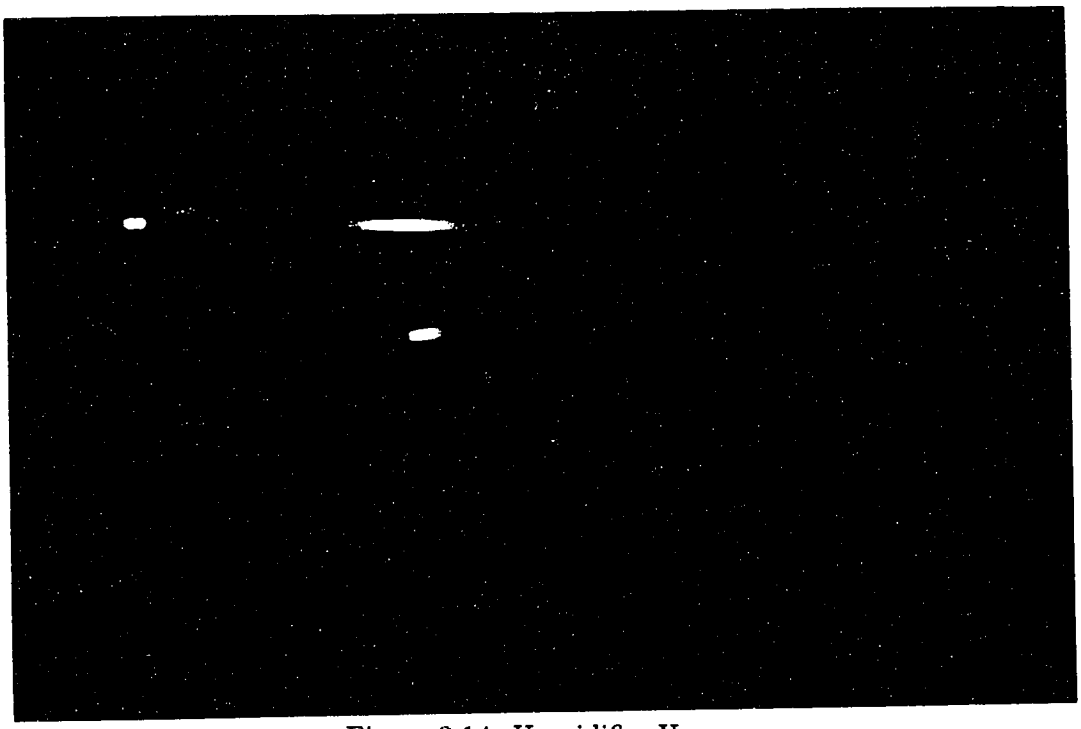

Figure 3.14: Humidifier Hose

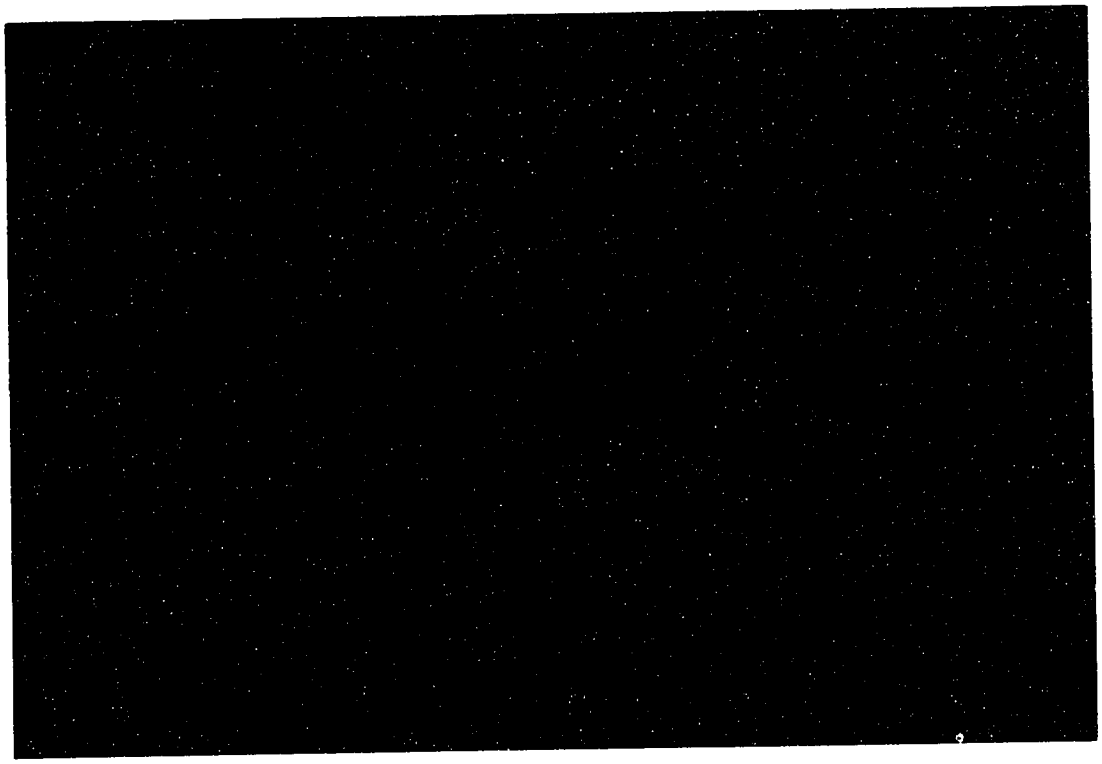

Figure 3.15: Humidifier Controller

Figure 3.16: Dehumidifier

Figure 3.17: Humidity Dial Guage

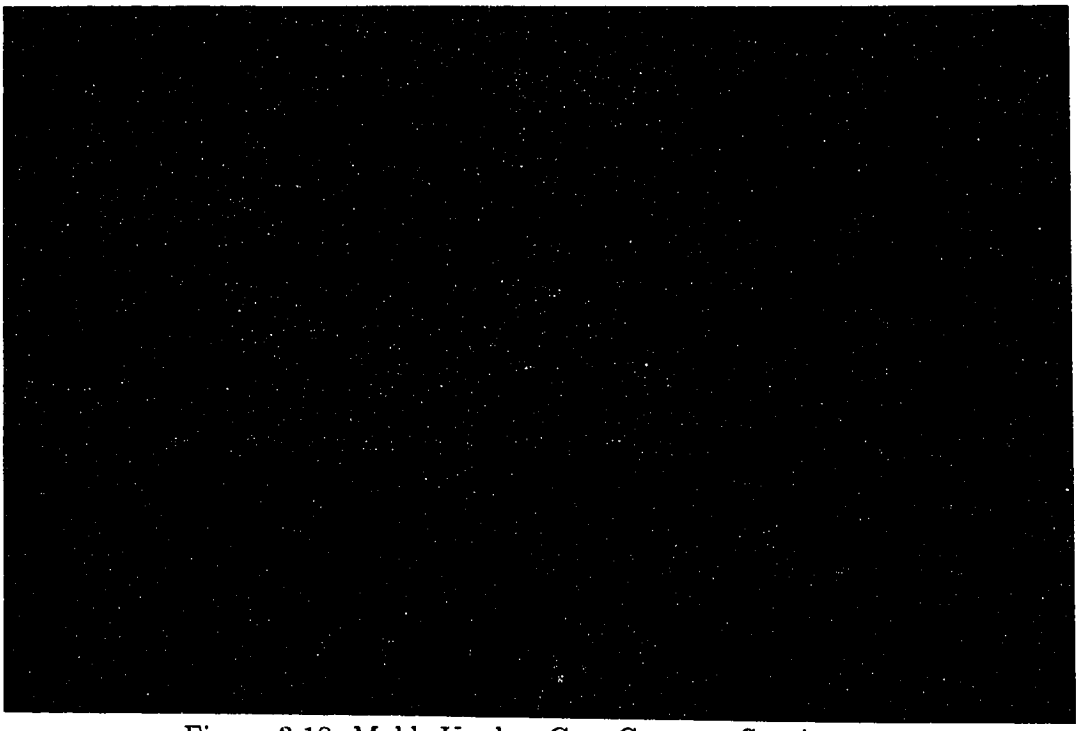

Figure 3.18: Molds Used to Cast Concrete Specimens

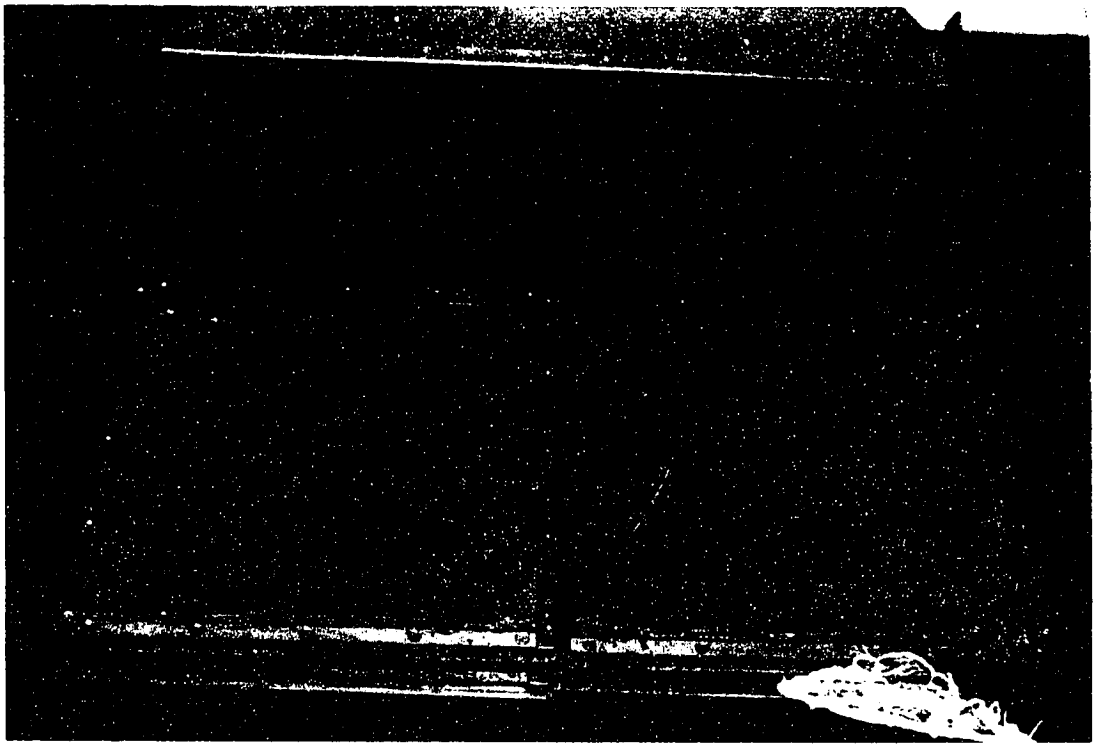

Figure 3.19: Experimental Setup (Small Specimens)

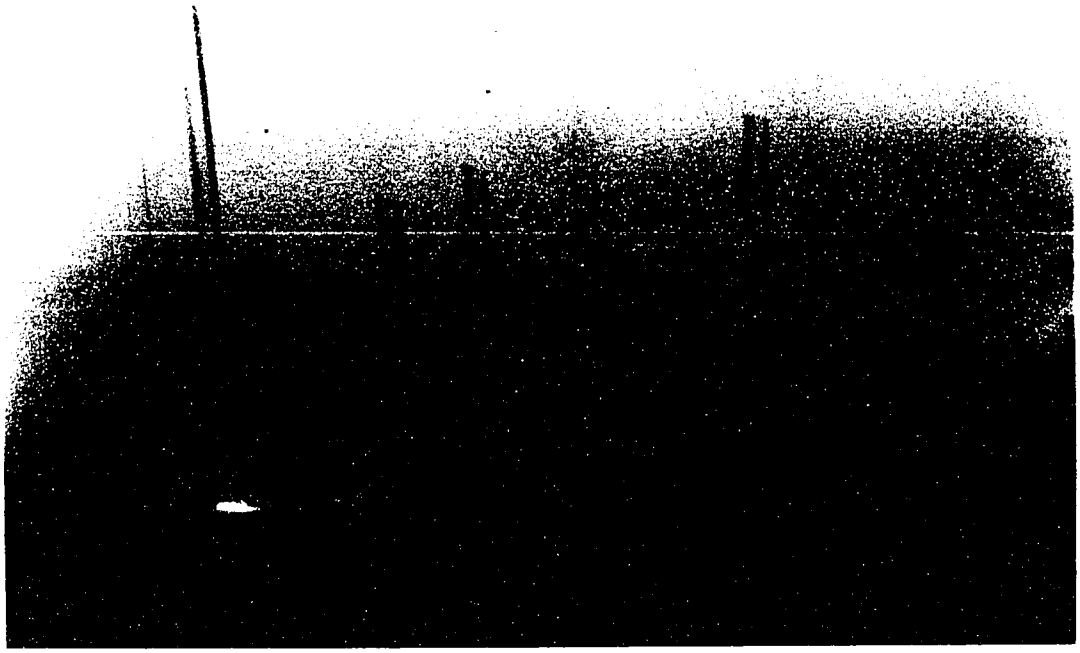

Figure 3.20: Experimental Setup (Big Specimens)

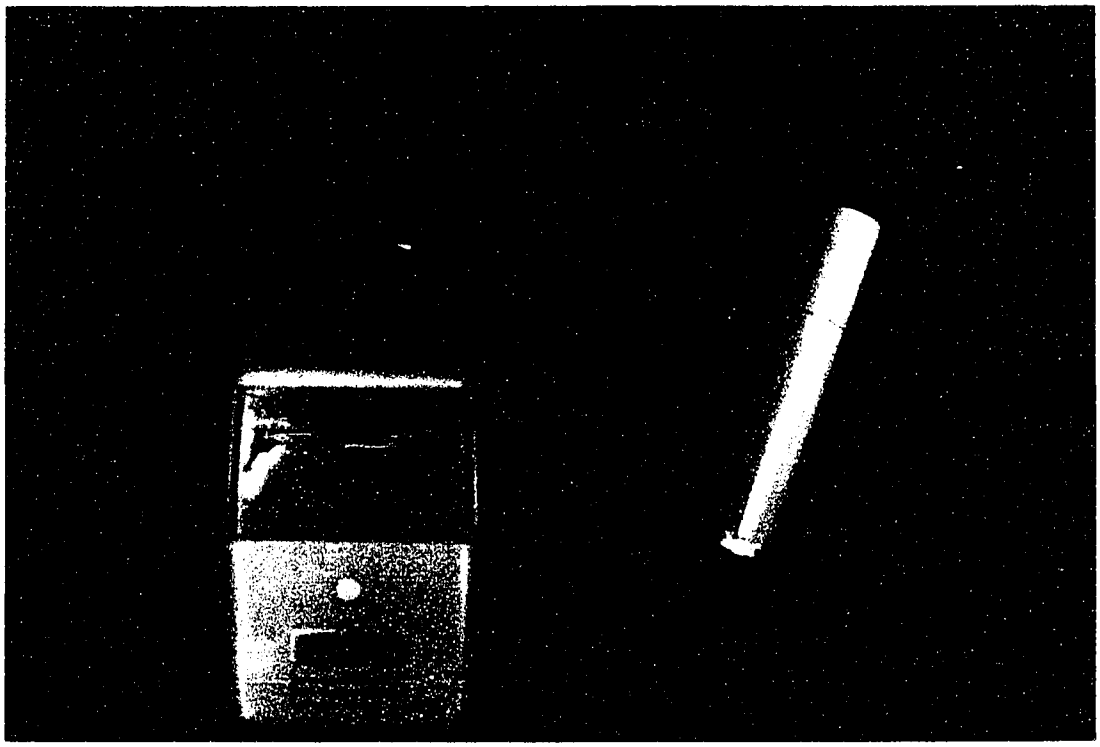

Figure 3.21: Digital Anemometer

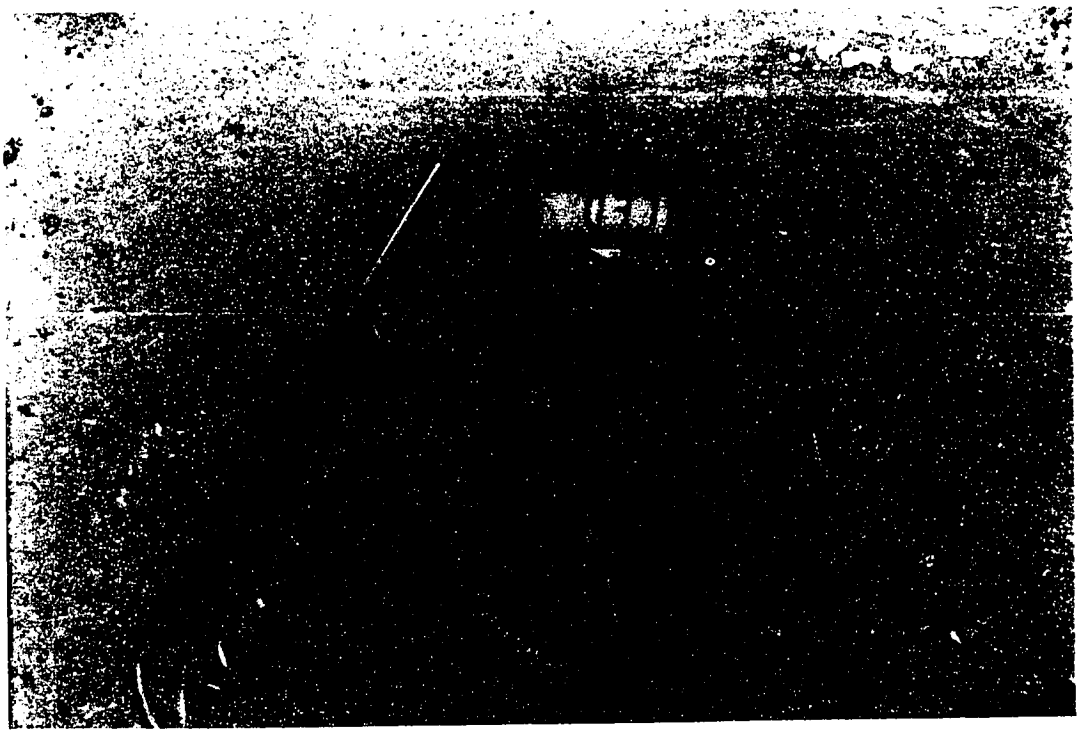

Figure 3.22: Digital Thermometer

Figure 3.23: Precision Electric Balance

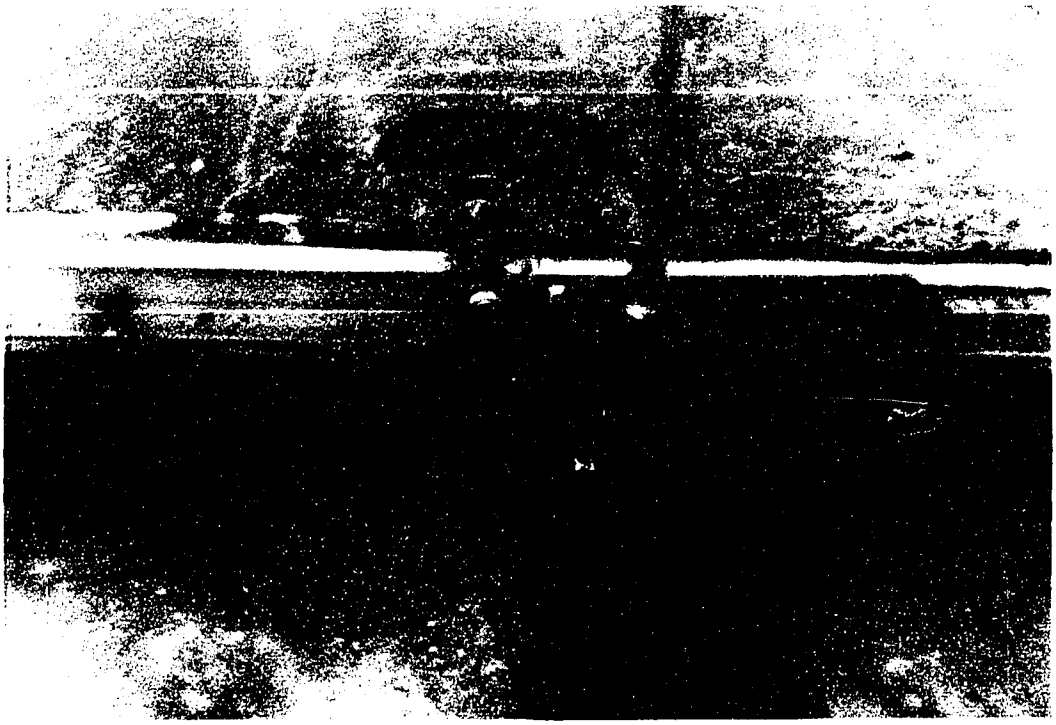

Figure 3.24: Attachment of LVDT to the Concrete Specimen

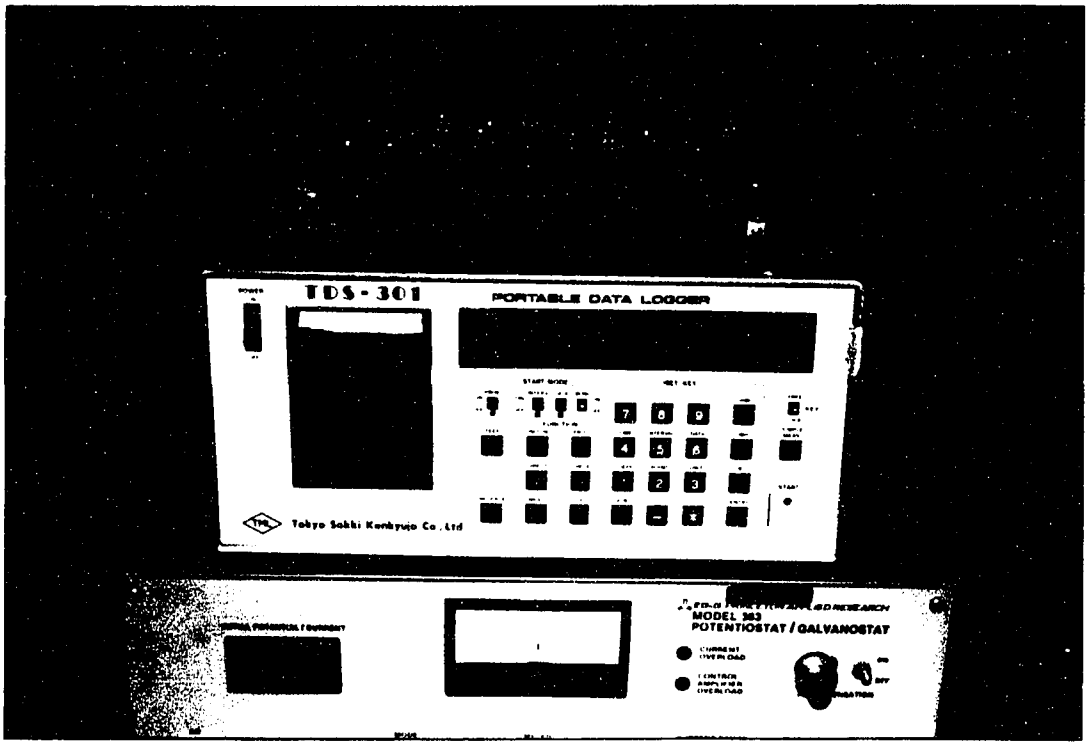

Figure 3.25: Datalogger

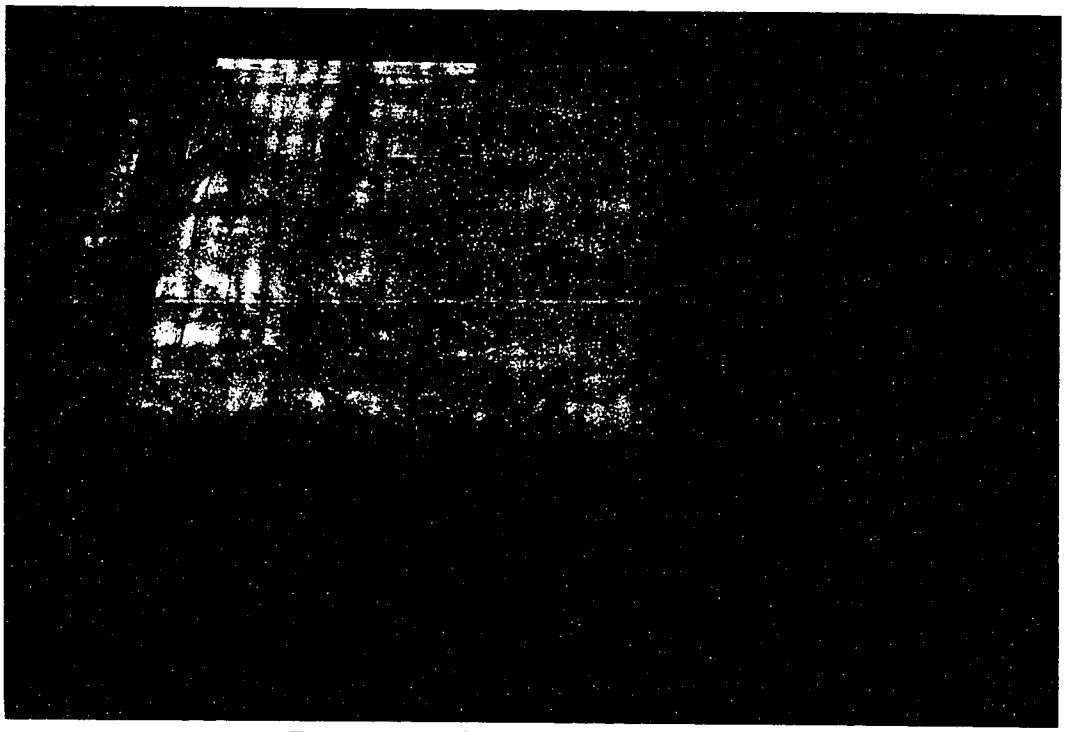

Figure 3.26: Curing of the Specimens

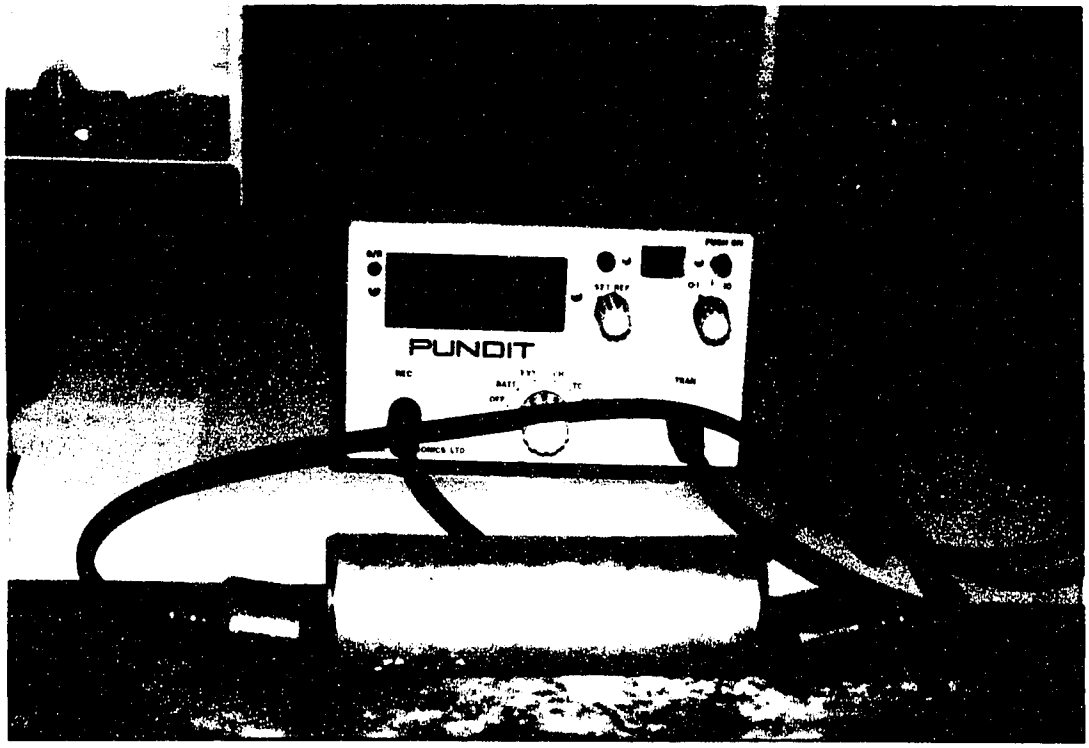

Figure 3.27: Instrument for Measuring Pulse Velocity

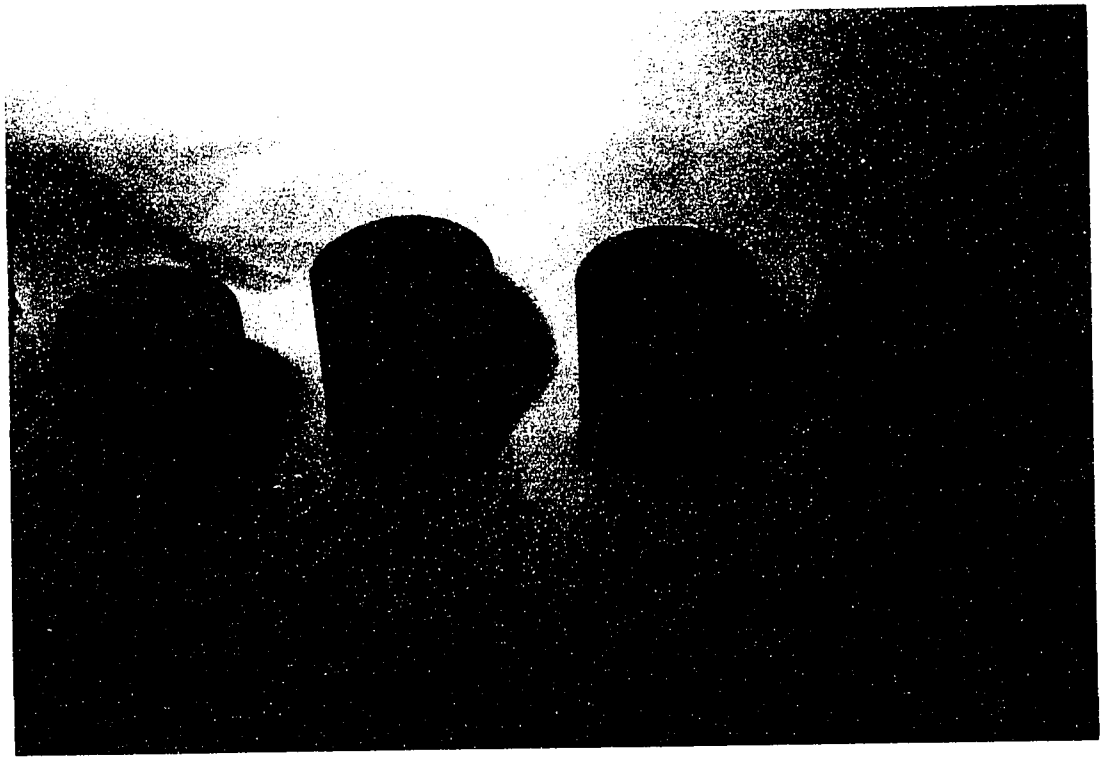

Figure 3.28: Representative Cores taken from the Slabs

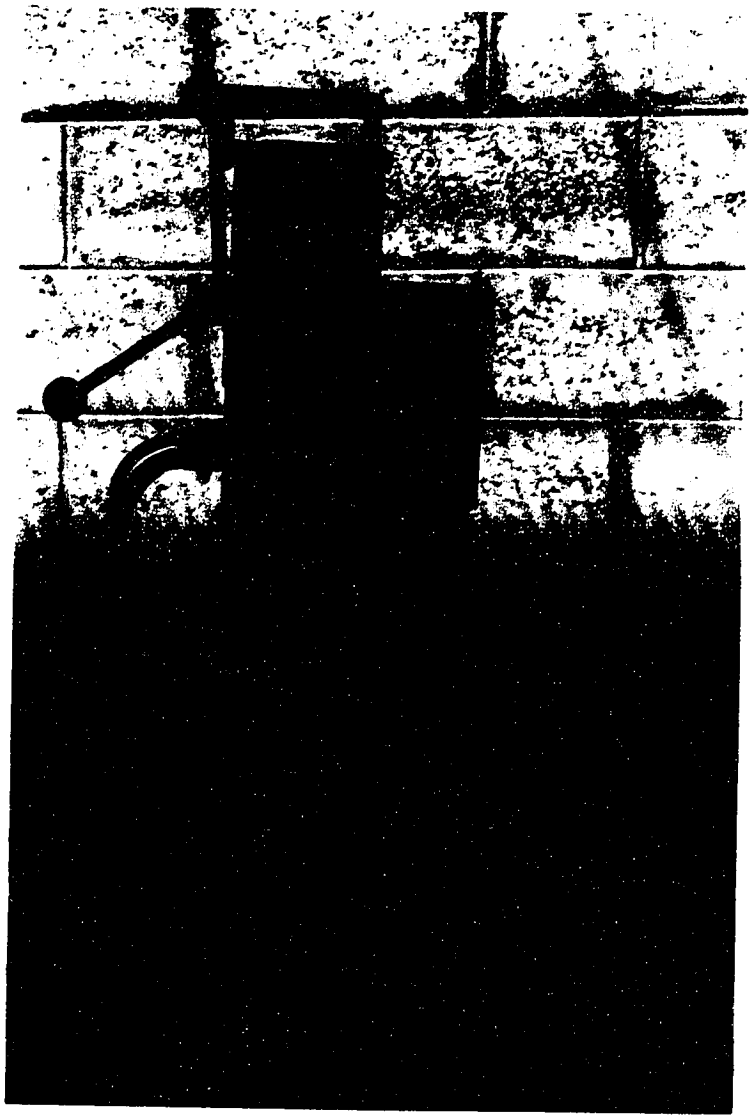

Figure 3.29: Coring Machine

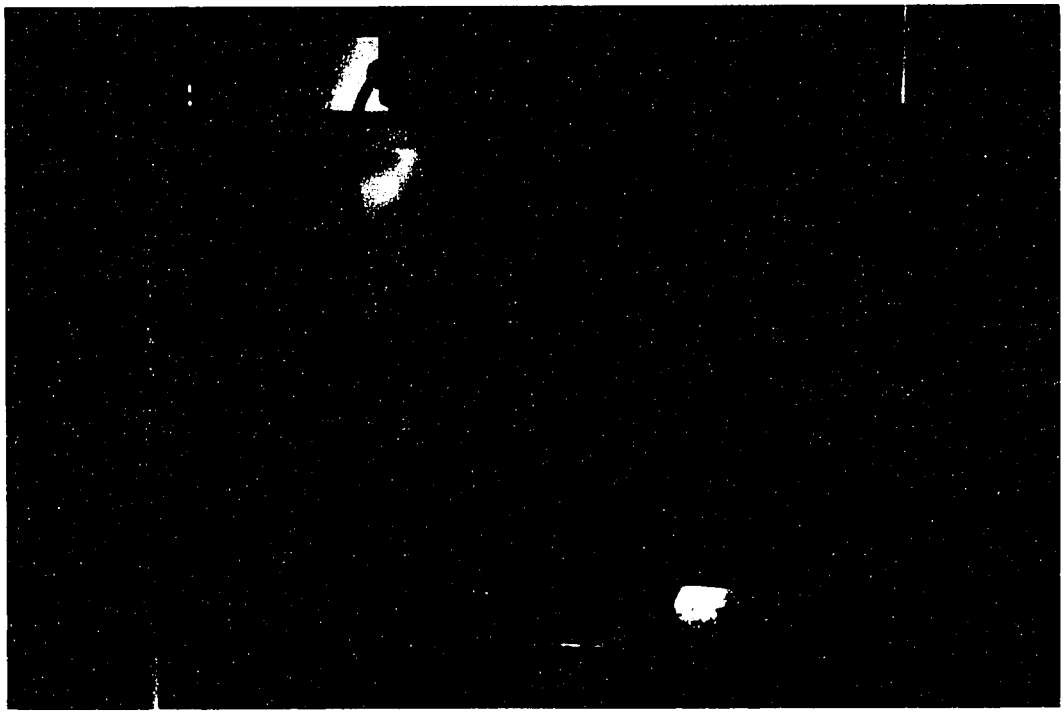

Figure 3.30: Compression Testing Machine

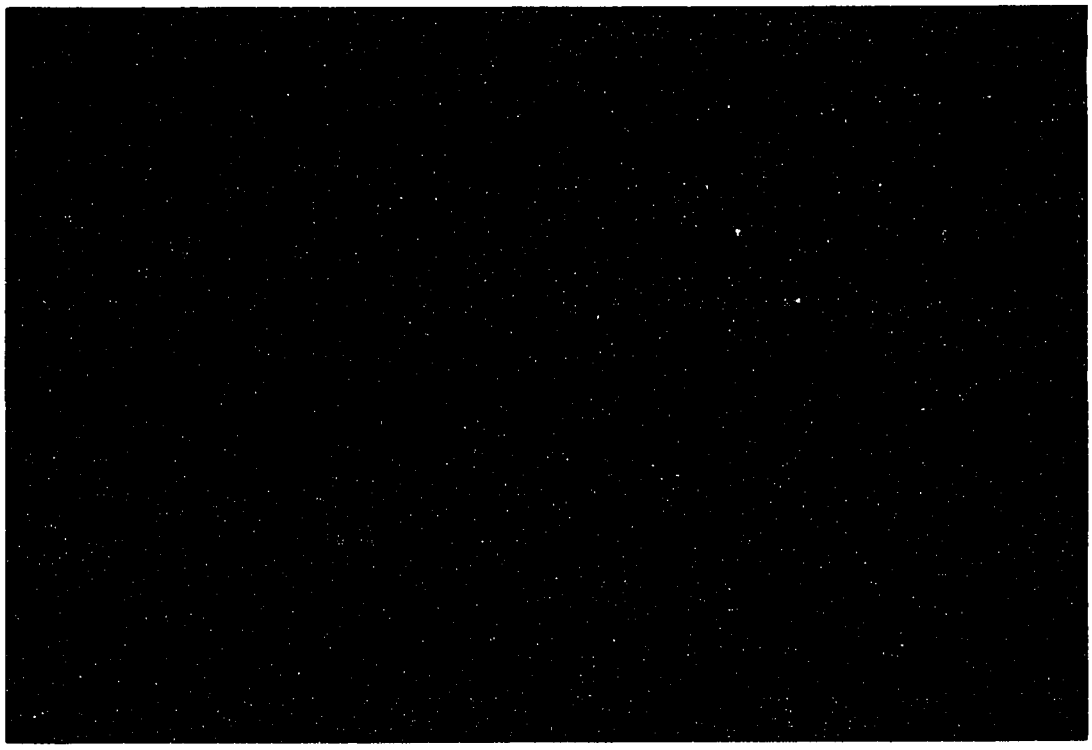

Figure 3.31: Typical Patterns of Plastic Shrinkage Cracks

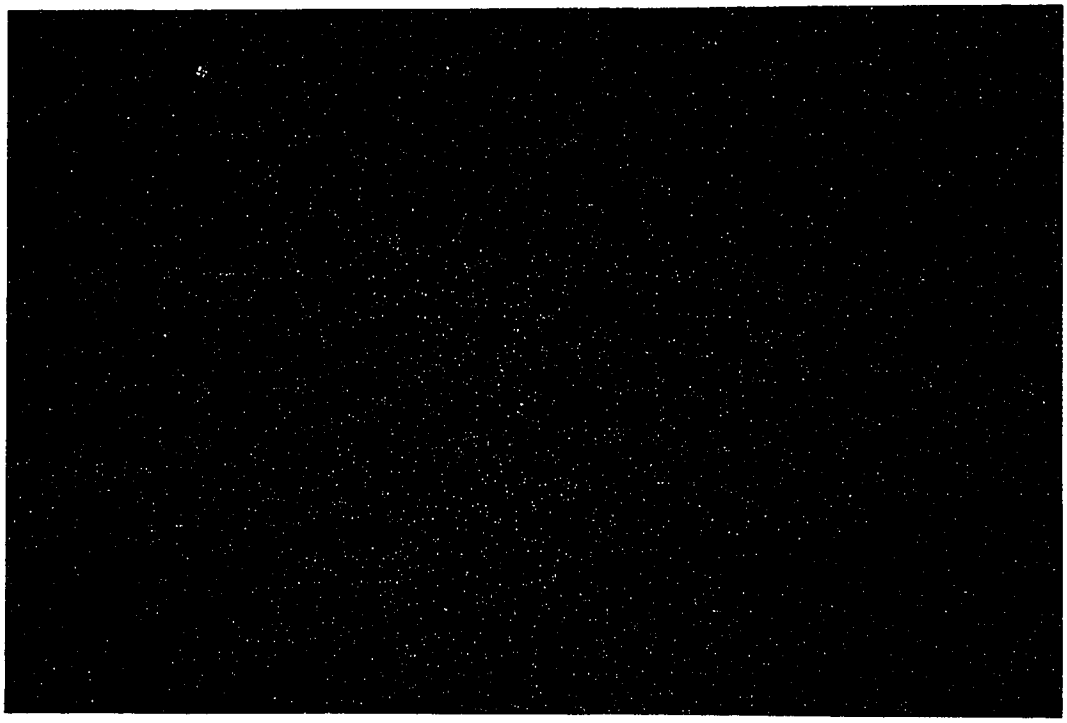

Figure 3.32: Typical Patterns of Plastic Shrinkage Cracks

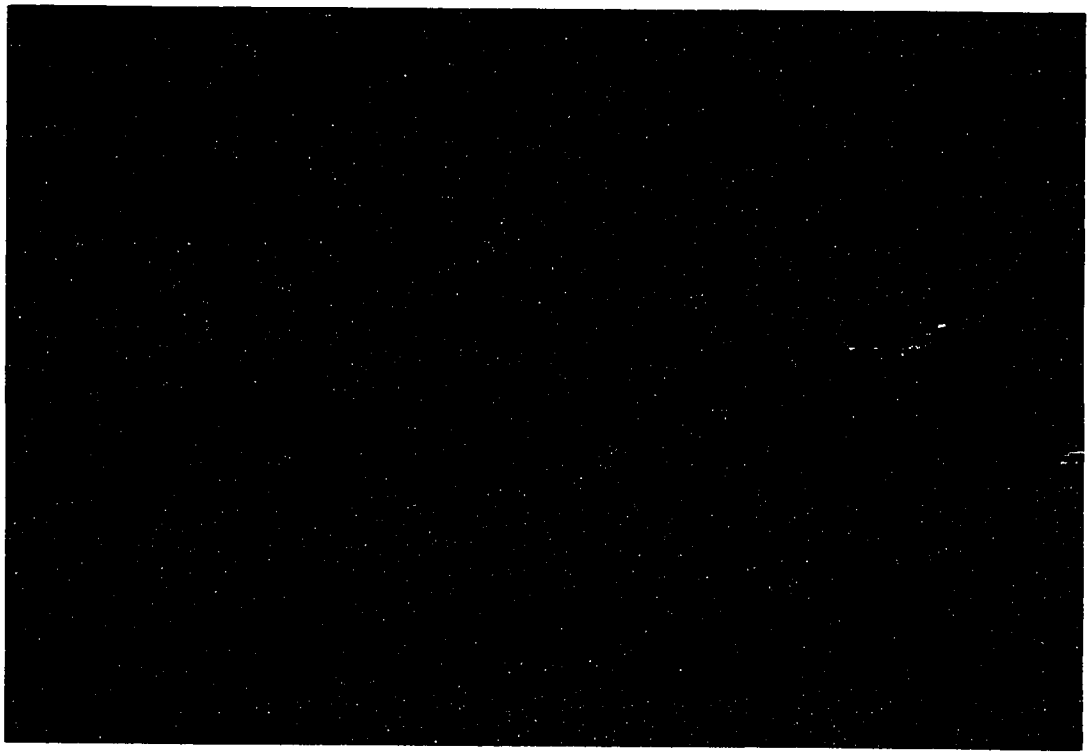

Figure 3.33: Typical Patterns of Plastic Shrinkage Cracks

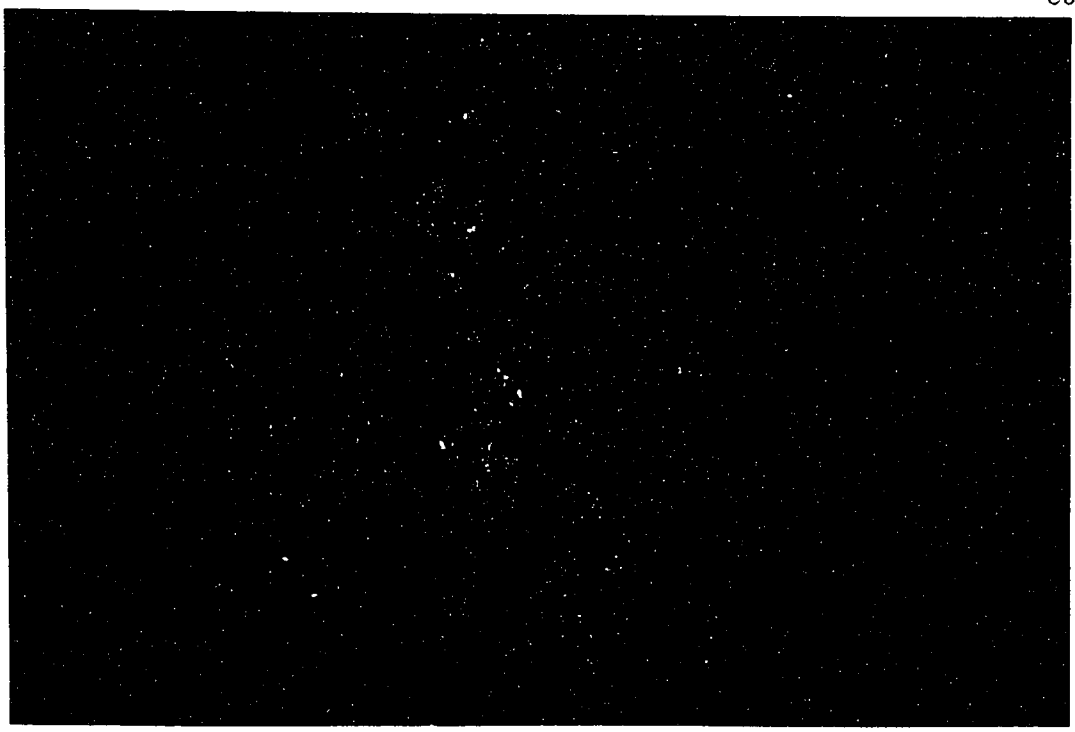

Figure 3.34: Typical Patterns of Plastic Shrinkage Cracks

Figure 3.35: Typical Patterns of Plastic Shrinkage Cracks

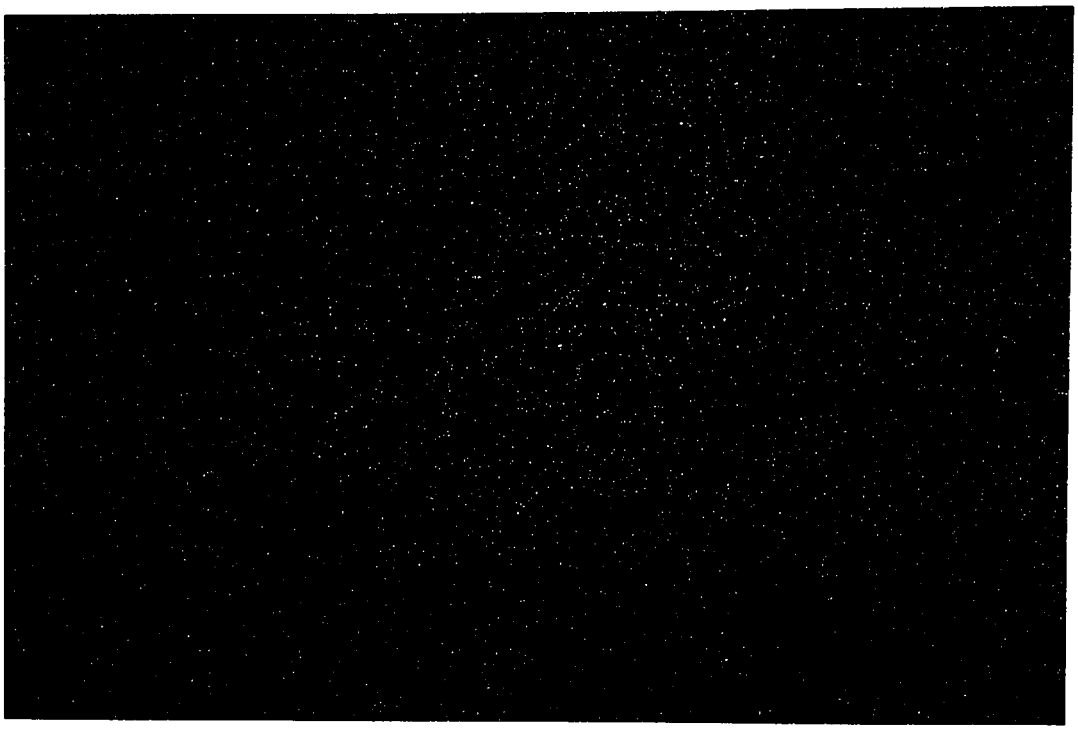

Figure 3.36: Typical Patterns of Plastic Shrinkage Cracks

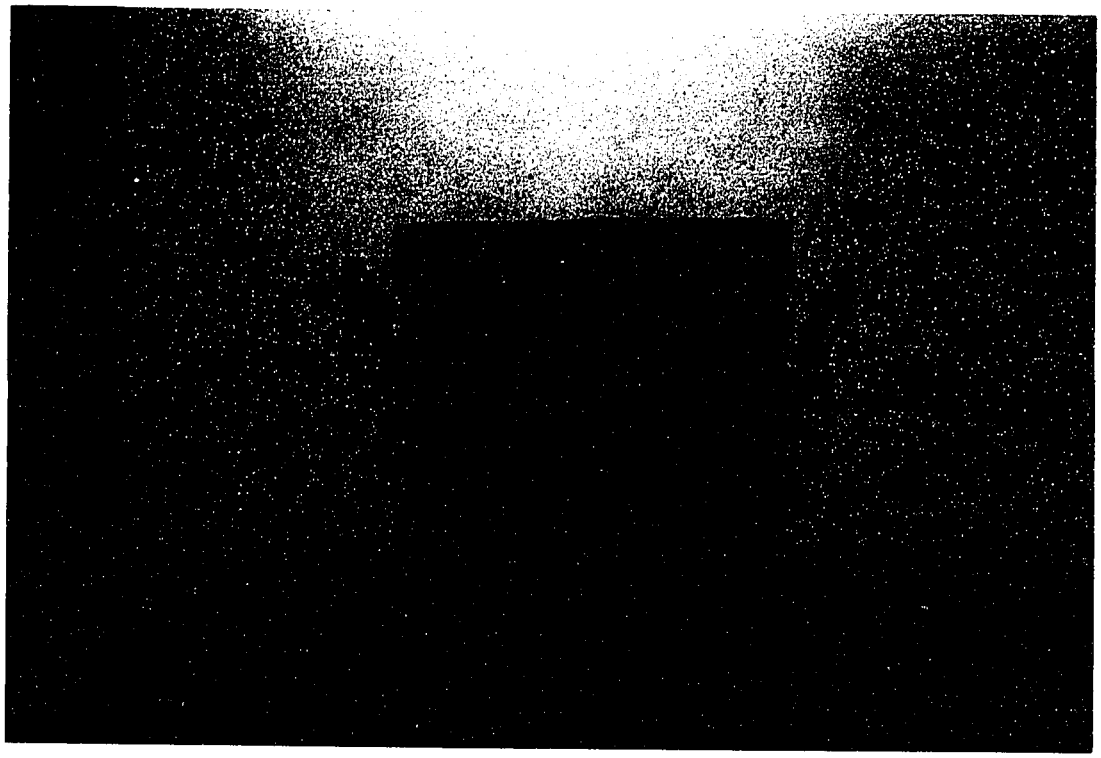

Figure 3.37: Bleeding Bucket

Chapter 4

RESULTS AND DISCUSSION

Based on the experimental results for all the five series mentioned in Chapter 3, the results are divided primarily in to water evaporation and plastic shrinkage cracking, followed by other secondary parameters studied.

4.1 WATER EVAPORATION

The effect of environmental conditions on water evaporation was calculated as percentage of water evaporated and the average rate of evaporation.

4.1.1 Quantity of Water Evaporated

Figures 4.1 through 4.7 show the effect of mix proportions on the quantity of water evaporated in the concrete specimens exposed to different environmental conditions.

Figure 4.1 shows the effect of mix proportions on the percentage of water evaporated in the concrete specimens exposed to a RH of 25 % and ambient temperature of 45 °C. The percentage of water evaporated increased linearly with the cement content. It, however, decreased with increasing water-cement ratio. The percentage of water evaporated was affected more by the water-cement ratio than the cement content. In the specimens prepared with a cement content of 300 kg/m^3 and a water-cement ratio of 0.40, the water evaporated was nearly 42 %. However, it increased to 44 % in the specimens with a cement content of 400 kg/m^3 and a water-cement ratio of 0.40. The percentage water evaporated, however, decreased to 35 % when the water-cement ratio was increased to 0.65 with the cement content remaining the same at 300 kg/m^3. A similar trend was observed in the specimens exposed to other environmental conditions, as shown in Figures 4.2, 4.4, 4.5, 4.6 and 4.7. In the specimens exposed to a RH of 95 % and temperature of 45 °C (Figure 4.3), the percentage of water evaporated increased both with the water-cement ratio and the cement content.

The increase in the percentage water evaporated with an increase in cement content in a concrete mix with a constant water-cement ratio may be attributed to the following reasons :

(i) the increase in capillary pressure due to the increase in specific surface area of the cement with an increase in the cement content, and

(ii) a reduction in the volume of the aggregates.

The decrease in the quantity of water evaporated, with an increase in the water-cement ratio, in a concrete mix with a constant cement content, may be attributed to an increase in the free water left in the concrete mix when compared to the total water added in the mix.

Figure 4.8 summarizes the effect of relative humidity and wind velocity on the percentage of water evaporated in a typical concrete mix prepared with a cement content of 350 kg/m^3 and a water-cement ratio of 0.40 and exposed to an ambient temperature of 45 °C. These data indicate that the relative humidity significantly affects the percentage of water evaporated when there is no wind. The percentage of water evaporated was 45 % when the RH was 25 %, and it was 30 and 2.5 % when the RH was 50 and 95 %, respectively. In windy conditions, the relative humidity has an insignificant effect on the water evaporation. The percentage of water evaporated was nearly the same when the RH was 25 and 50 % and the wind velocity was 15 and 25 kmph. In the specimens exposed to a RH of 50 %, the percentage of water evaporated was 30 and 53 %, when the wind velocity was 0 and 25 kmph, respectively.

The decrease in the quantity of water evaporated with an increase in the relative humidity may be attributed to an increase in the water vapor in the atmosphere. However, in the windy conditions , the presence of water vapor in the atmosphere has a negligible effect on evaporation compared to the force of the wind.

Figures 4.9 through 4.11 show the effect of ambient temperature and water-cement ratio on the quantity of water evaporated in the concrete specimens made with cement contents in the range of 300 to 400 kg/m^3.

Figure 4.9 shows the effect of ambient temperature and water-cement ratio on the percentage water evaporated in concrete mixes prepared with a cement content of 300 kg/m^3 and exposed to a RH of 50 %. The percentage of water evaporated increased almost linearly with the exposure temperature. It, however, decreased with increasing water-cement ratio. In the concrete mix, with a water-cement ratio of 0.40 and exposed to 25 °C, the percentage of water evaporated was nearly 23 % and it increased to 30 % when the temperature was increased to 55 °C. But it decreased to 15 % when the water-cement ratio was increased to 0.65, the temperature being 25 °C. A similar trend was observed in the concrete specimens with cement contents of 350 kg/m^3 (Figure 4.10) and 400 kg/m^3 (Figure 4.11).

The increase in the percentage water evaporated with an increase in the ambient temperature may be attributed to the difference in the concrete and ambient temperatures.

The most efficient concrete mixes for various exposure conditions based on the quantity of water evaporated are shown in Table 4.1. As seen from these data, the most efficient concrete mix based on the percentage of water loss is a lean plastic mix having a cement content of 300 kg/m^3 and a water-cement ratio 0.65 in nearly all the conditions, except in hot-humid environment in which a lean stiff mix with

a cement content of 300 kg/m^3 and a water-cement ratio of 0.40 is efficient.

Figures 4.12 through 4.14 show the quantity of water evaporated in blended cement concrete specimens exposed to a temperature of 45 °C and RH of 25 and 95%.

Figure 4.12 shows the effect of relative humidity on the percentage water evaporated in the blast furnace slag (BFS) cement concrete specimens. For comparison purposes the water evaporated in the plain Type V cement concrete mixes is also plotted in this figure. The BFS cement concrete mixes contained 50, 60 and 70 % BFS. In the specimens exposed to a RH of 25 %, the percentage water evaporated was more or less similar in the plain and BFS cements. However, in the concrete mixes exposed to a RH of 95 %, the quantity of water evaporated increased with the BFS content. The quantity of water evaporated in the plain cement concrete exposed to 95 % RH was 5 %, while it was 10, 11 and 12 %, respectively, in the BFS cement concretes with 50, 60 and 70 % BFS, respectively.

Figure 4.13 depicts the effect of relative humidity on the percentage of water evaporated in the fly ash and plain cement concrete specimens. The fly ash cement concrete specimens contained 20, 30 and 40 % fly ash, used as replacements of cement by weight. In the specimens exposed to a RH of 25 % the percentage water evaporated was nearly the same in all the mixes, however in the specimens exposed to a RH of 95 %, the water evaporated increased with increasing fly ash content. The water evaporated was in the range of 40 to 43 % in the specimens exposed to

a RH of 25 %. In the specimens exposed to a RH of 95 %, the water evaporated in the plain cement concrete specimen was nearly 2 % and increased to nearly 17 % in the 30 % fly ash cement concrete specimens.

Figure 4.14 shows the effect of relative humidity on the water evaporated in the silica fume and plain cement concrete specimens. The silica fume cement concrete specimens contained 5, 10 and 15 % silica fume. Again, the water evaporated in the specimens exposed to a RH of 25 % was nearly the same in all the mixes irrespective of the silica fume content. The quantity of water evaporated in the specimens exposed to a RH of 95 % increased with increasing silica fume content. In the specimens exposed to a RH of 25 % the percentage water evaporated remained nearly the same at 42 %. However, in the specimens exposed to a RH of 95 %, the percentage water evaporated in the plain cement concrete specimens, was 2 % and it increased to 17 % in the 15 % silica fume concrete specimens. The quantity of water evaporated decreased by nearly 30 % when the RH increased from 25 % to 95 % in almost all the cement concrete mixes.

From the data in Figures 4.12 through 4.14 it can be inferred that, when the relative humidity is low, the beneficial effect of blended cements is negligible. The increase in the quantity of water evaporated in the blended cements may be attributed to an increase in the capillary pressure due to an increase in the specific surface area of these cementitious materials.

Figures 4.15 through 4.17 show the effect of different exposure conditions on the

quantity of water evaporated in the blended cement concrete specimens.

Figure 4.15 shows the water evaporated in the plain and blended cement concrete specimens exposed to relative humidities of 25 and 50 %. The quantity of water evaporated in the specimens exposed to a RH of 25 % was nearly the same in all the specimens. In the specimens exposed to a RH of 50 %, the quantity of water evaporated was slightly less in the plain cement concrete specimens than in the blended cement concrete specimens. These data also indicate that blended cements are more prone to plastic shrinkage, in the hot-humid environment, compared to plain cements.

The effect of temperature on the water evaporated in the plain and blended cement concrete specimens, exposed to a RH of 25 %, is shown in Figure 4.16. The quantity of water evaporated decreased with an increase in the exposure temperature, in both plain and blended cement concrete specimens. The quantity of water evaporated decreased by nearly 4-8 % in all the mixes for a temperature decrease from 45 to 35 °C. However, the water evaporated was in the range of 40 to 50 % in all the concrete mixes.

Figure 4.17 shows the effect of wind velocity on the quantity of water evaporated in the plain and blended cement concrete specimens, exposed to a RH of 25 % and a temperature of 45 °C. The quantity of water evaporated increased with increasing wind velocity in all the concrete mixes. While the quantity of water evaporated increased by only 2-4 % in all the mixes, it increased by 8 % in the fly ash cement

concrete specimens. The quantity of water evaporated was in the range of 40 to 50 % in all the concrete mixes.

Figure 4.18 shows the effect of various exposure conditions on the quantity of water evaporated in the big concrete specimens. These concrete mixes were made with a cement content of 350 kg/m^3 and a water-cement ratio of 0.40. The quantity of water evaporated increased with increasing temperature. Maximum evaporation was noted in the concrete specimens exposed to a wind velocity of 15 kmph and a RH of 25 %, this being in the range of 35 to 50 %. The quantity of water evaporated decreased when there was no wind. In the concrete specimens exposed to a RH of 50 % and no wind, the quantity of water evaporated was in the range of 25 to 30 %, while it was approximately 5 % in the specimens exposed to a RH of 95 %.

4.1.2 Rate of Evaporation

Figures 4.19 through 4.25 show the effect of varying mix proportions and exposure conditions on the rate of water evaporation.

Figure 4.19 shows the effect of cement content and water-cement ratio on the rate of water evaporation in the concrete specimens exposed to a RH of 25 % and temperature of 45 °C. The rate of evaporation increased with the cement content and water-cement ratio. The rate of evaporation was nearly the same in the concrete mixes with cement contents of 300 and 350 kg/m^3 and water-cement ratio of 0.40 and 0.50. In the concrete specimens made with a cement content of 300 kg/m^3 and

a water-cement ratio of 0.40 the rate of evaporation was nearly 0.36 kg/m^2.h and it increased to 0.4 kg/m^2.h when the cement content was increased to 400 kg/m^3. However, the rate of evaporation increased to 0.4 kg/m^2.h when the water-cement ratio was increased to 0.65 with the cement content remaining, at 300 kg/m^3. A similar trend was observed in the specimens exposed to other environmental conditions, as shown in Figures 4.20 through 4.25.

Figure 4.26 summarizes the effect of relative humidity and wind velocity on the rate of water evaporation in the concrete specimens made with a cement content of 350 kg/m^3 and a water-cement ratio of 0.40 and exposed to an ambient temperature of 45 °C. The rate of water evaporation decreased with increasing relative humidity when there was no wind. The rate of water evaporation was 0.38, 0.27 and 0.02 kg/m^2.h when the RH was 25, 50 and 95 %, respectively. In windy conditions, the role of relative humidity was insignificant, the rate of water evaporation being nearly the same for wind velocities of 15 and 25 kmph. In the specimens exposed to a RH of 25 %, the rate of water evaporation was 0.27 and 0.43 kg/m^2.h for no wind and a wind velocity of 25 kmph, respectively.

Figures 4.27 through 4.29 show the effect of ambient temperature and water-cement ratio on the rate of water evaporation.

Figure 4.27 shows the effect of ambient temperature and water-cement ratio on the rate of water evaporation in the concrete specimens made with a cement content of 300 kg/m^3 and exposed to a RH of 50 %. The rate of evaporation increased with

increasing temperature and water-cement ratio. The rate of water evaporation was affected more by the ambient temperature than the water-cement ratio. In the concrete mixes made with a water-cement ratio of 0.40 and exposed to 25 °C, the rate of water evaporation was 0.17 kg/m^2.h and increased to 0.24 kg/m^2.h when the exposure temperature was increased to 55 °C. However, the rate of evaporation increased from 0.17 to 0.19 kg/m^2.h when the water-cement ratio was increased from 0.40 to 0.65 in the specimens exposed to 25 °C. A similar trend was observed in the concrete mixes made with a cement content of 350 kg/m^3 (Figure 4.28) and 400 kg/m^3 (Figure 4.29).

Table 4.2 compares the rate of evaporation calculated from ACI 305 graphical method and the data developed in this study. Comparison was made only for those conditions which are covered by the ACI graphical method i.e a maximum ambient temperature of 37.5 °C. The rate of evaporation given in the Table is for a cement content of 350 kg/m^3 and a water-cement ratio of 0.40 for all the conditions. However for ambient temperature of 25 and 35 °C with a RH of 50 %, the rate of evaporation is given in a range. This range is due to the variation in the quantity of cement content and water-cement ratio. From this observation, the effect of mix proportions on the rate of evaporation can be clearly seen. The data in Table 4.2 indicates that the rate of evaporation is nearly the same for the following exposure conditions :

(i) 25 °C, RH 50 %,

(ii) 35 °C, RH 50 %, and

(iii) 35 °C, RH 25 %.

However, when the ambient temperature is 30 °C, RH 25 % and the wind velocity is 15 kmph the experimental value was nearly half that obtained from graphical method proposed by ACI. When the ambient temperature is 30 °C and the RH is 95 %, the experimental value was nearly double the value obtained using the ACI graphical method. Moreover, the ACI 305 states that precautions for plastic shrinkage cracking should be taken only when the rate of evaporation exceeds 1 $kg/m^2.h$. However, cracking was observed in all the concrete specimens except in those exposed to an ambient temperature of 25 °C and a RH of 50 %, even though the rate of evaporation was less than 1 $kg/m^2.h$.

The efficient concrete mixes for various exposure conditions based on the average rate of evaporation are shown in Table 4.3. The most efficient mix, based on average rate of evaporation, is a lean stiff mix with a cement content of 300 kg/m^3 and a water-cement ratio of 0.40 in all the conditions. Although from durability point of view, a mix having a cement content greater or equal to 350 kg/m^3 and a water-cement equal to 0.45 is recommended, the results of this investigation show a much leaner and stiffer mix should be adopted to avoid plastic shrinkage cracking.

Figures 4.30 through 4.32 show the rate of water evaporation in the blended cement concrete specimens.

Figure 4.30 shows the effect of relative humidity on the rate of water evaporation in the BFS cement concrete specimens. These specimens were made with a cementitious material content of 350 kg/m^3, a water-cementitious material ratio of 0.40 and exposed to an ambient temperature of 45 °C. In the specimens exposed to a RH of 25 %, the rate of evaporation increased with the quantum of BFS. A similar trend was noted in the specimens exposed to a RH of 95 %. In the plain cement concrete specimens, exposed to a RH of 25 %, the rate of water evaporation was nearly 0.38 kg/m^2.h and increased to 0.45 kg/m^2.h in the 70 % BFS cement concrete specimens. The rate of water evaporation in the specimens exposed to a RH of 95 % was less than those exposed to a RH of 25 %. This reduction being 0.3 kg/m^2.h.

Figure 4.31 shows the effect of relative humidity on the rate of water evaporation in the fly ash cement concrete specimens. In the specimens exposed to a RH of 25 %, the rate of evaporation in the plain cement concrete specimens was slightly less than in the fly ash cement concrete specimens. This difference, however, became more distinct in the specimens exposed to a RH of 95 %. In the specimens exposed to a RH of 95 %, the rate of evaporation in the plain cement concrete specimens was nearly 0.02 kg/m^2.h and it was 0.16 kg/m^2.h in the 30 % fly ash cement concrete specimens. The rate of water evaporation decreased by nearly 0.3 kg/m^2.h when the RH increased from 25 % to 95 % in all the concrete specimens.

Figure 4.32 shows the effect of relative humidity on the rate of water evaporation

in the silica fume cement concrete specimens. In the specimens exposed to a RH of 25 %, the rate of water evaporation was nearly the same in all the mixes. However, in the specimens exposed to a RH of 95 % the rate of water evaporation increased with an increase in the quantity of silica fume. In the specimens exposed to a RH of 25 %, the rate of water evaporation was in the range of 0.38 to 0.42 kg/m^2.h., while in the specimens exposed to a RH of 95 % the rate of water evaporation in the plain cement concrete specimen was 0.02 kg/m^2.h and it was 0.16 kg/m^2.h in the 15 % silica fume cement concrete specimens. The rate of water evaporation decreased by approximately 0.3 kg/m^2.h when the RH increased from 25 to 95 % in almost all the concrete mixes.

Figures 4.33 through 4.35 show the effect of different exposure conditions on the rate of water evaporation in the blended cement concrete specimens.

Figure 4.33 shows the effect of relative humidity on the rate of water evaporation in the blended cement concretes. These specimens were exposed to an ambient temperature of 45 °C. The relative humidity significantly affected the rate of water evaporation in the plain, silica fume and BFS cement concrete specimens, the rate of evaporation decreasing with increasing relative humidity. The increase in the rate of evaporation, with increasing humidity, was, however, not significant. The rate of evaporation decreased by nearly 0.11 kg/m^2.h from 0.36 kg/m^2.h to 0.25 kg/m^2.h in the silica fume concrete, whereas in the fly ash cement concrete it decreased by only 0.03 kg/m^2.h from 0.39 kg/m^2.h to 0.36 kg/m^2.h.

Figure 4.34 shows the effect of temperature on the rate of water evaporation in the plain and blended cement concrete specimens. These specimens were exposed to a RH of 25 %. The rise in temperature from 35 to 45 °C did not affect the rate of water evaporation. The rate of evaporation decreased by nearly 0.07 to 0.12 $kg/m^2.h$ in all the mixes due to elevation in the exposure temperature. These data clearly indicate that temperature alone cannot be a decisive factor in controlling the rate of water evaporation when compared to relative humidity.

Figure 4.35 shows the effect of wind velocity on the rate of water evaporation in the plain and blended cement concrete specimens. These specimens were exposed to an ambient temperature of 45 °C. The effect of wind was observed to be very minimal on the rate of water evaporation in the silica fume and BFS cement concrete specimens, while it increased with the wind velocity in the plain and the fly ash cement concrete specimens. The rate of water evaporation increased by only 0.01 $kg/m^2.h$ in the silica fume and BFS cement concrete specimens, whereas it increased by 0.05 $kg/m^2.h$ in the plain and fly ash cement concrete specimens. The rate of water evaporation was in the range of 0.3 to 0.45 $kg/m^2.h$ in all the concrete specimens exposed to both the conditions.

Figure 4.36 shows the effect of different exposure conditions on the rate of evaporation in the big concrete specimens. These specimens were made with a cement content of 350 kg/m^3 and a water-cement ratio of 0.40. In the concrete specimens exposed to a RH of 25 % and a wind velocity of 15 kmph, the rate of water evapo-

ration increased by 0.15 kg/m^2.h when the temperature increased from 30 to 45 °C. The increase in the rate of evaporation in the specimens exposed to a RH of 50 % and no wind was 0.07 kg/m^2.h.

Figures 4.37 through 4.39 show the variation in the rate of water evaporation with time.

Figure 4.37 shows the effect of environmental conditions on the rate of water evaporation in the specimens exposed to an ambient temperature of 45 °C. These data indicate that wind tremendously affects the rate of water evaporation in the initial three to four hours after casting. In the specimens exposed to a wind of 25 kmph, the rate of water evaporation was nearly the same when the RH was 25 and 50 %. In these specimens the rate of water evaporation was initially very high, and decreased consistently during the first three hours, and it did not change with time thereafter. When there was no wind, the rate of water evaporation was affected by the relative humidity in the initial 3 hours, after which its effect became negligible. The initial rate of water evaporation was 1.1 kg/m^2.h in the specimens exposed to a wind velocity of 25 kmph and a RH of 25 %, and it was 0.3 kg/m^2.h in the specimens exposed to no wind and a relative humidity of 25 %. Similarly, the initial rate of water evaporation was 0.3 kg/m^2.h and 0.18 kg/m^2 in the specimens exposed to a RH of 25 and 50 % respectively, with no wind. Another important feature of the data in Figure 4.37 is that the rate of water evaporation in the specimens exposed to windy conditions decreased rapidly with time, whereas in the specimens exposed

to no wind it remained unchanged with time till the end of the experiment.

Figure 4.38 shows the effect of ambient temperature on the rate of water evaporation in the concrete specimens made with a cement content of 350 kg/m^3 and a water-cement ratio of 0.40 and exposed to a RH of 50 %. The rate of water evaporation increased with time and ambient temperature. The rate of water evaporation in the specimens exposed to an ambient temperature of 55 °C was in the range of 0.15 to 0.25 kg/m^2.h, whereas in the specimens exposed to 25 °C it was in the range of 0.02 to 0.12 kg/m^2.h.

Figure 4.39 compares the rate of water evaporation in the plain and blended cement concrete specimens. These specimens were made with a cementitious material content of 350 kg/m^3, a water-cementitious materials ratio of 0.40 and exposed to a RH of 25 % and ambient temperature of 45 °C. The rate of water evaporation decreased with time in both the plain and blended cement concrete specimens. It decreased rapidly in the first two hours and showed no change thereafter till the end of experiment. Further, the rate of water evaporation in the plain and blended cement concrete specimens was not different.

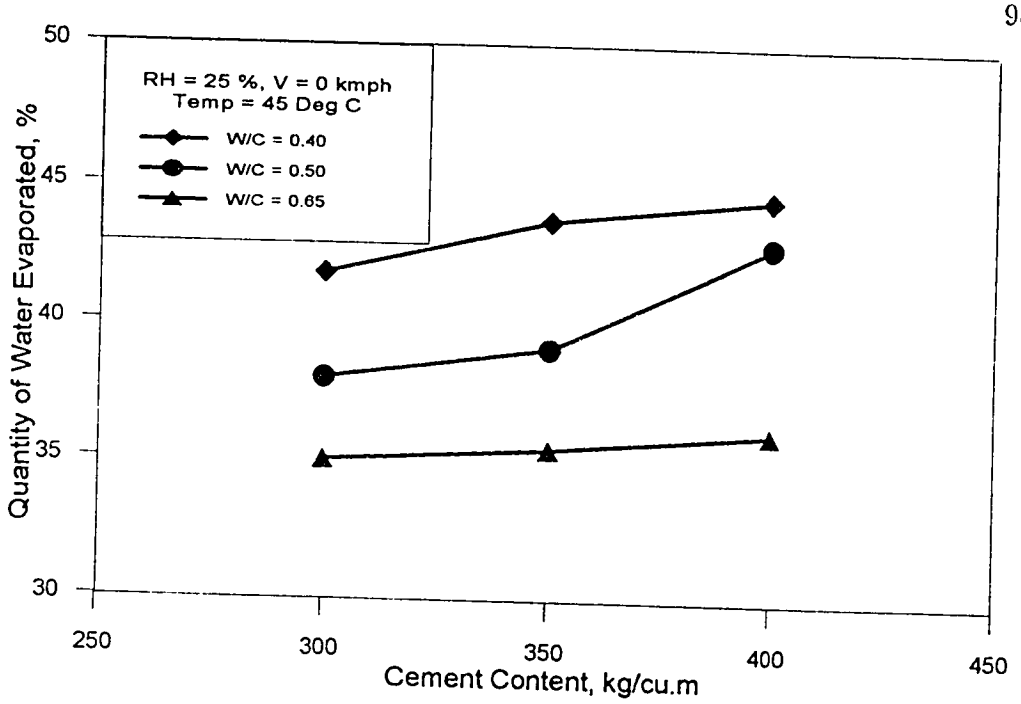

Figure 4.1: Effect of Cement Content on the Quantity of Water Evaporated (RH : 25% ; V : 0 kmph ; Temp : 45 °C)

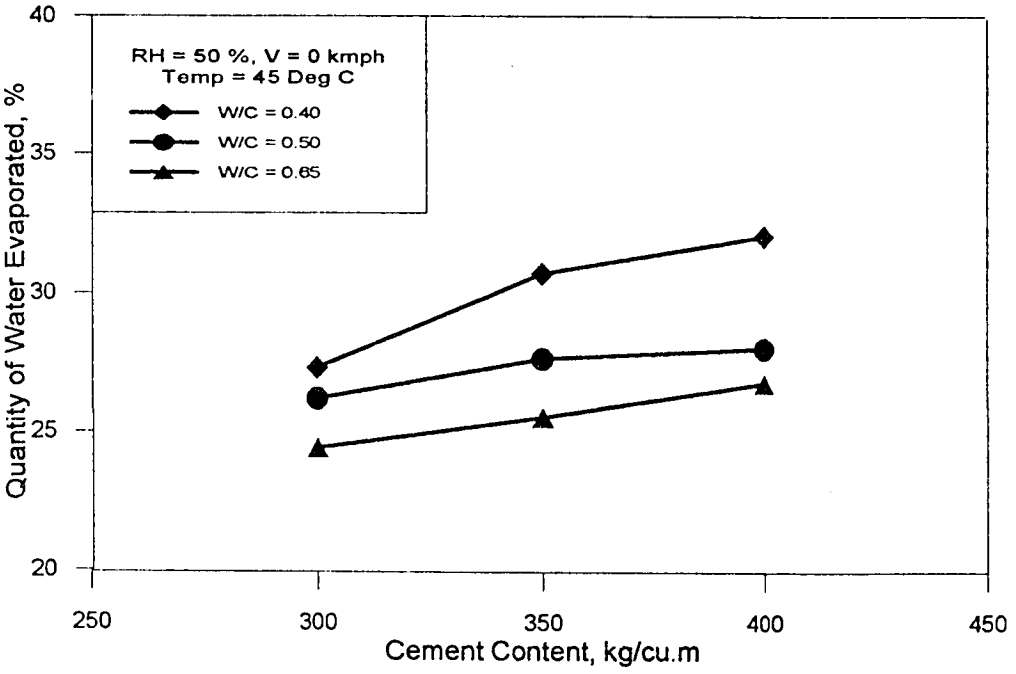

Figure 4.2: Effect of Cement Content on the Quantity of Water Evaporated (RH : 50% ; V : 0 kmph ; Temp : 45 °C)

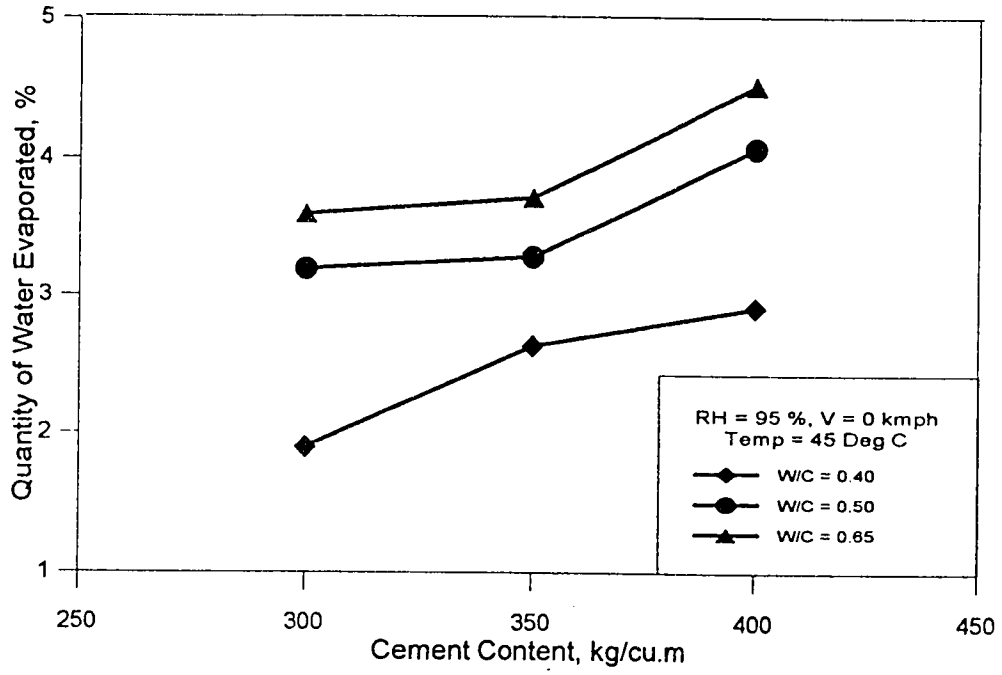

Figure 4.3: Effect of Cement Content on the Quantity of Water Evaporated (RH : 95% ; V : 0 kmph ; Temp : 45 °C)

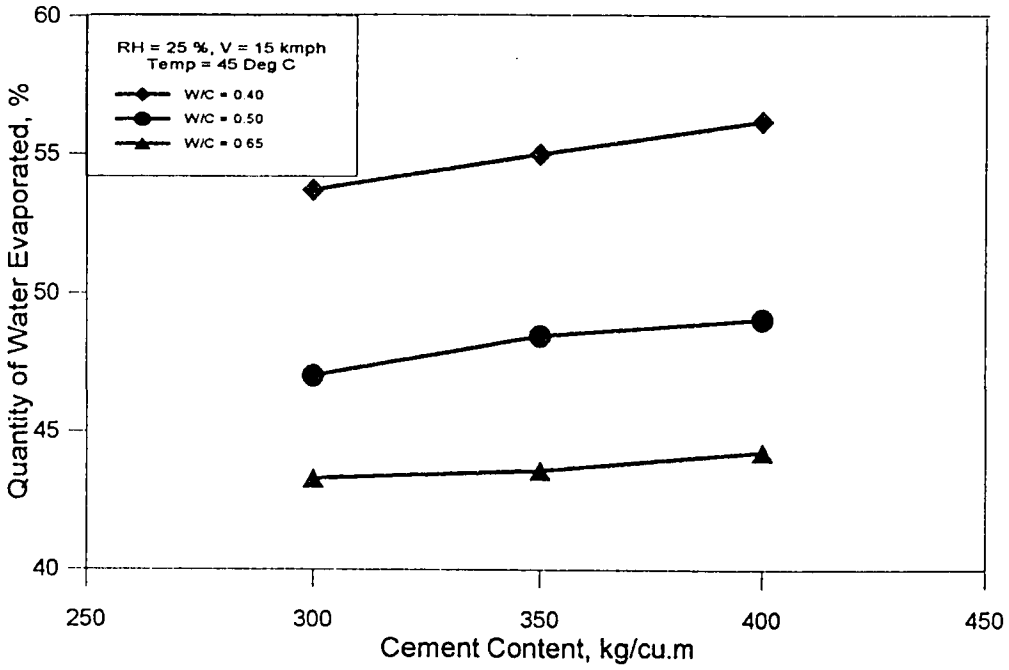

Figure 4.4: Effect of Cement Content on the Quantity of Water Evaporated (RH : 25% ; V : 15 kmph ; Temp : 45 °C)

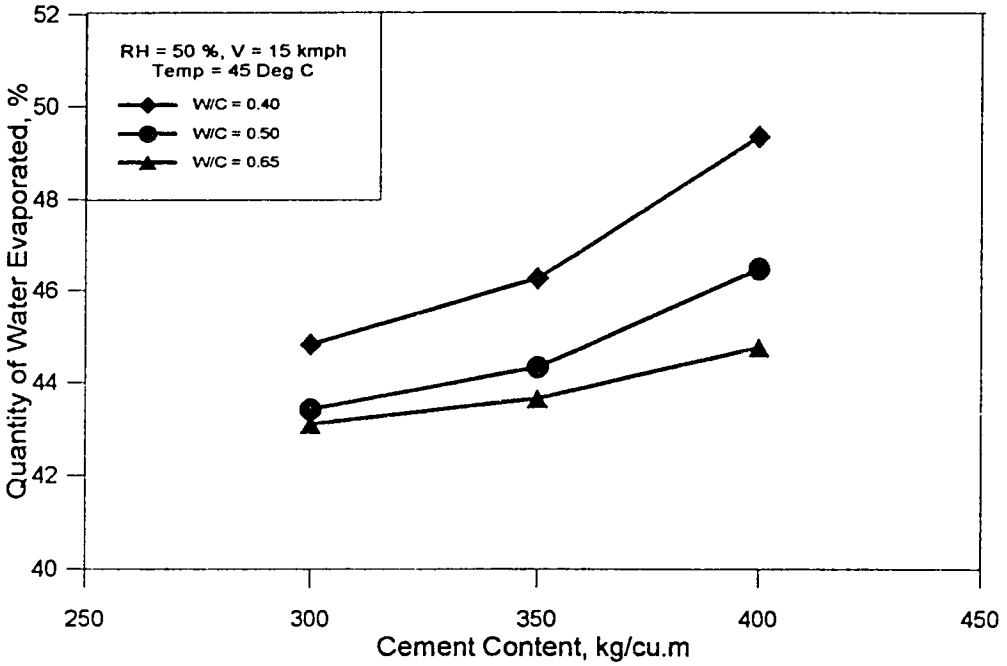

Figure 4.5: Effect of Cement Content on the Quantity of Water Evaporated (RH : 50% ; V : 15 kmph ; Temp : 45 °C)

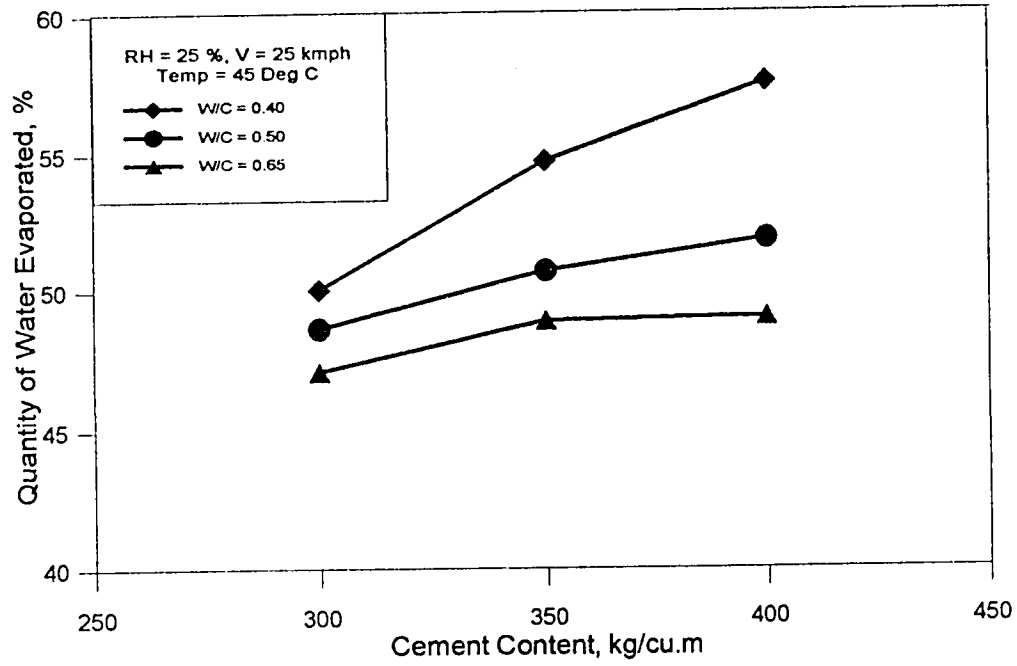

Figure 4.6: Effect of Cement Content on the Quantity of Water Evaporated (RH : 25% ; V : 25 kmph ; Temp : 45 °C)

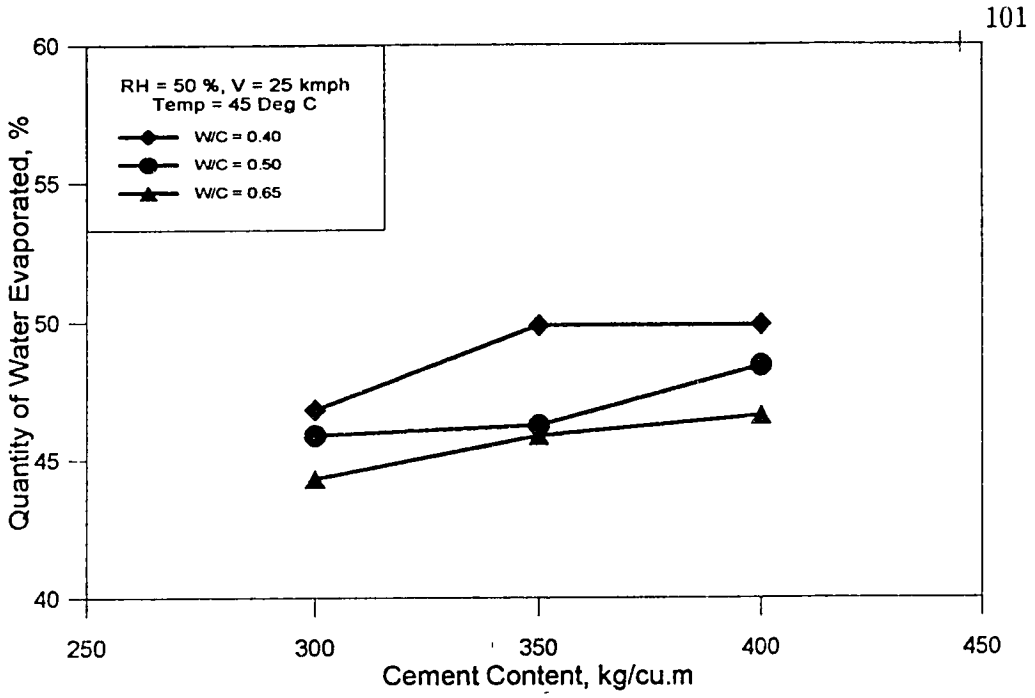

Figure 4.7: Effect of Cement Content on the Quantity of Water Evaporated (RH : 50% ; V : 25 kmph ; Temp : 45 °C)

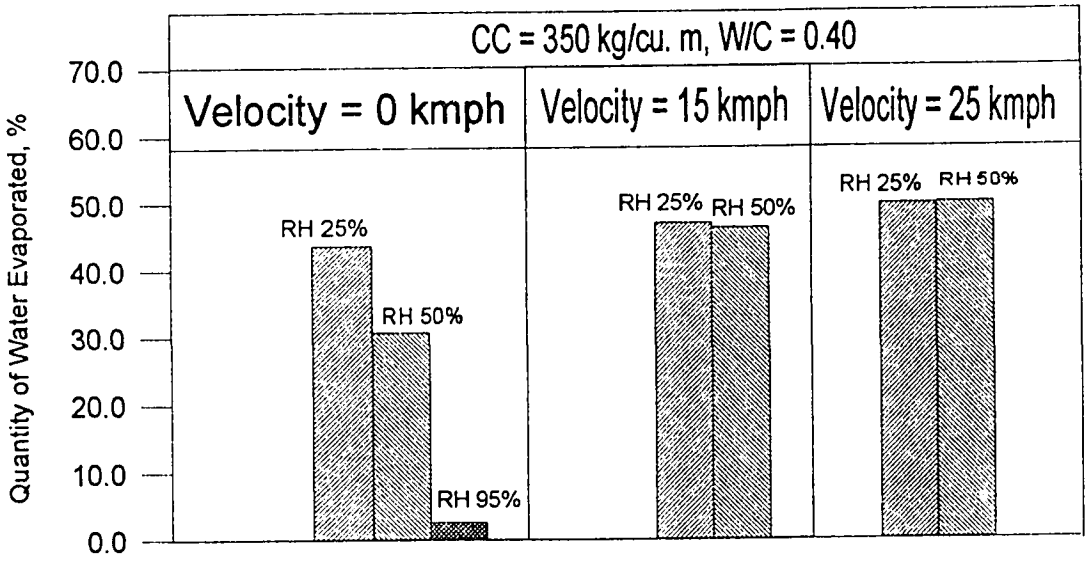

Figure 4.8: Effect of Relative Humidity and Wind Velocity on the Quantity of Water Evaporated (Temp : 45 °C ; CC : 350 kg/m^3 ; W/C : 0.40)

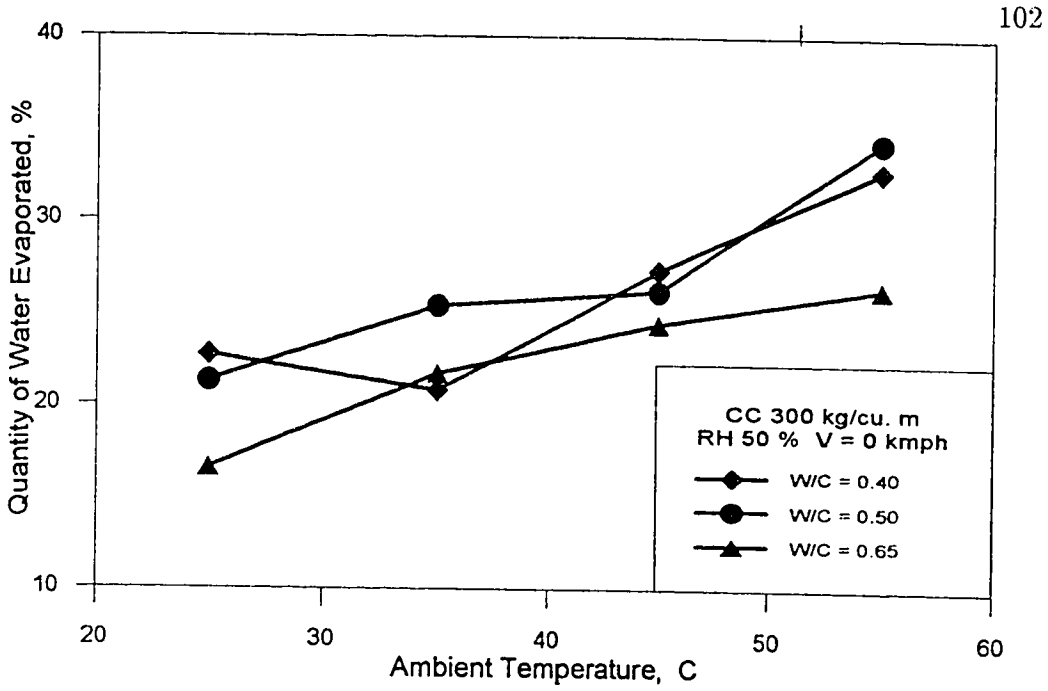

Figure 4.9: Effect of Ambient Temperature on the Quantity of Water Evaporated (RH : 50% ; V : 0 kmph ; CC : 300 kg/m^3)

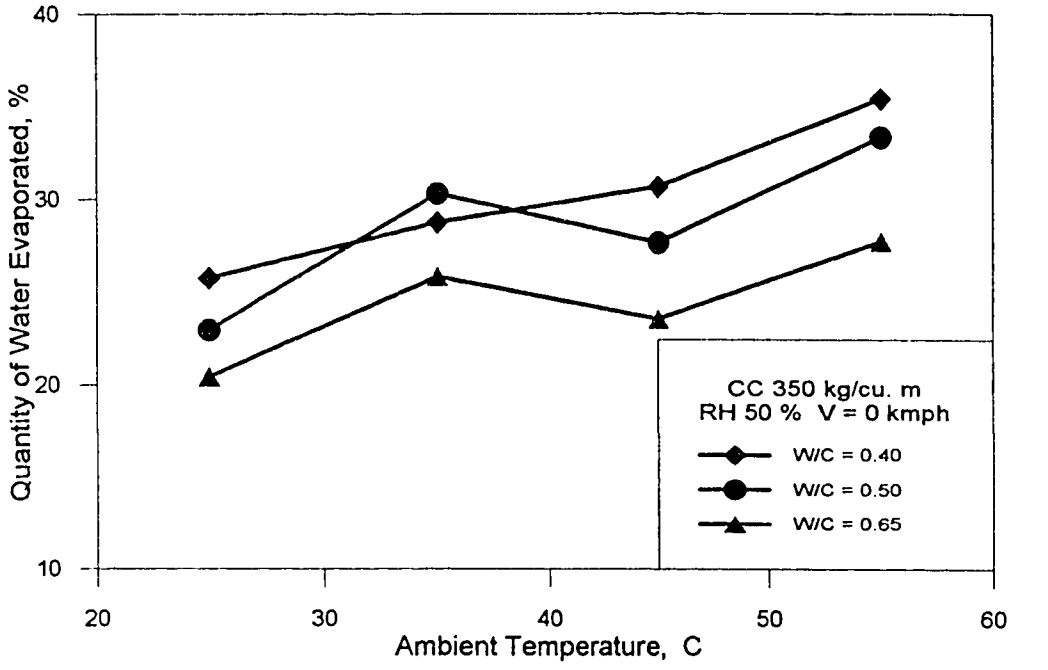

Figure 4.10: Effect of Ambient Temperature on the Quantity of Water Evaporated (RH : 50% ; V : 0 kmph ; CC : 350 kg/m^3)

Table 4.1: Efficient Concrete Mix for Various Environmental Conditions based on the Quantity of Water Evaporated

Exposure Conditions	Efficient Concrete Mix	
	Cement Content (kg/m^3)	W/C Ratio
Normal T : 45°C ; RH : 50% ;	300	0.65
Hot-Dry T : 45°C ; RH : 25% ;	300	0.65
Hot-Normal T : 45°C ; RH : 50% ;	300	0.65
Hot-Humid T : 45°C ; RH : 95% ;	300	0.40
Hot-Dry Windy T : 45°C ; RH : 25% ; V : 25 km/h ;	300	0.65
Hot-Normal Windy T : 45°C ; RH : 50% ; V : 25 km/h ;	300	0.65

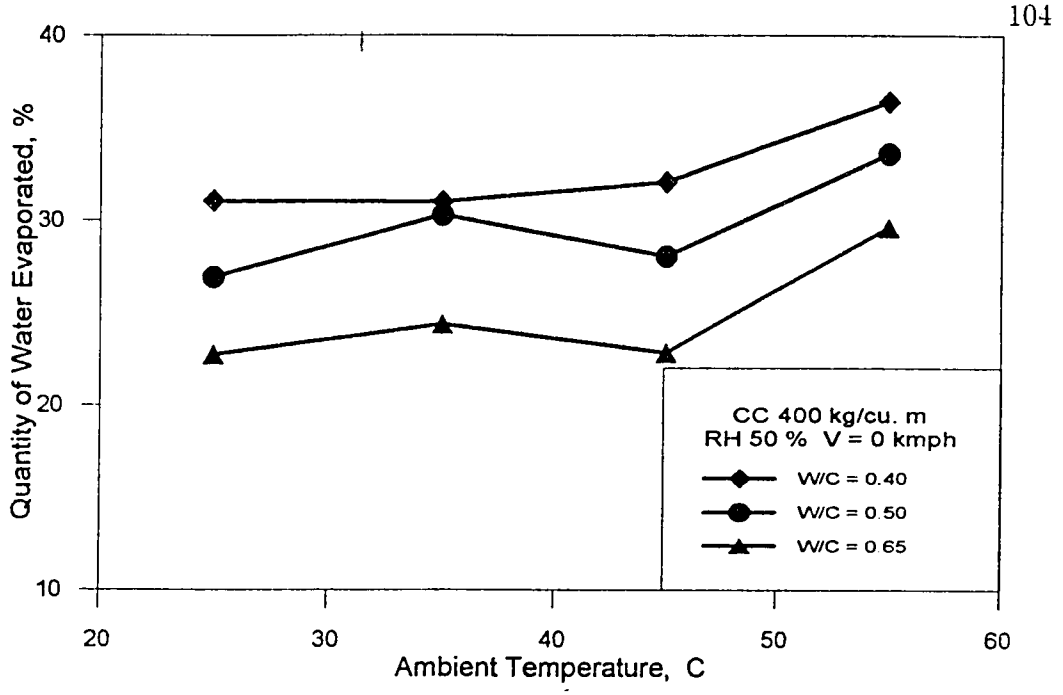

Figure 4.11: Effect of Ambient Temperature on the Quantity of Water Evaporated (RH : 50% ; V : 0 kmph ; CC : 400 kg/m^3)

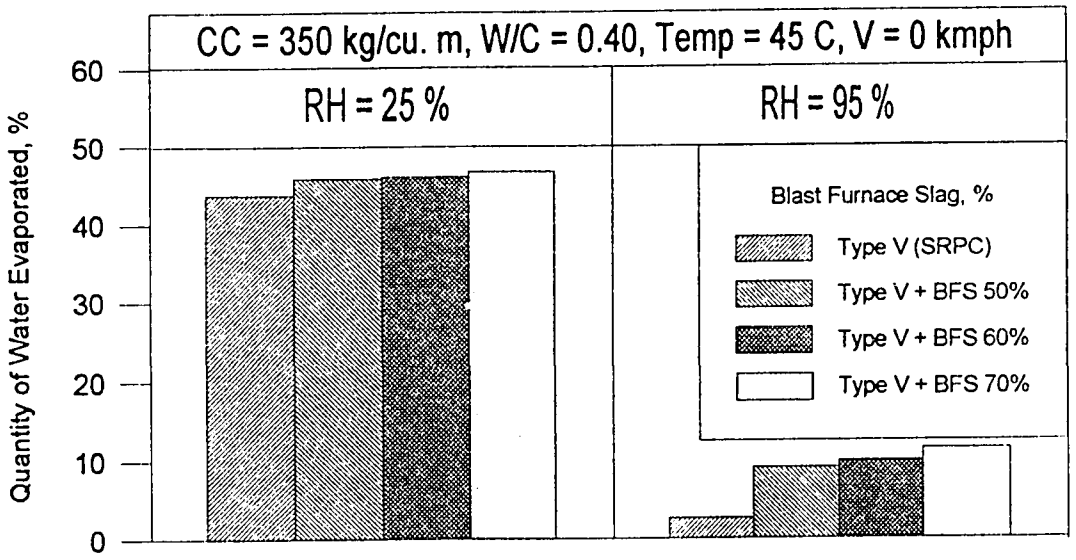

Figure 4.12: Quantity of Water Evaporated in the Blast Furnace Slag Cement Concrete (Temp : 45 °C ; V : 0 kmph ; CC : 350 kg/m^3 ; W/C : 0.40)

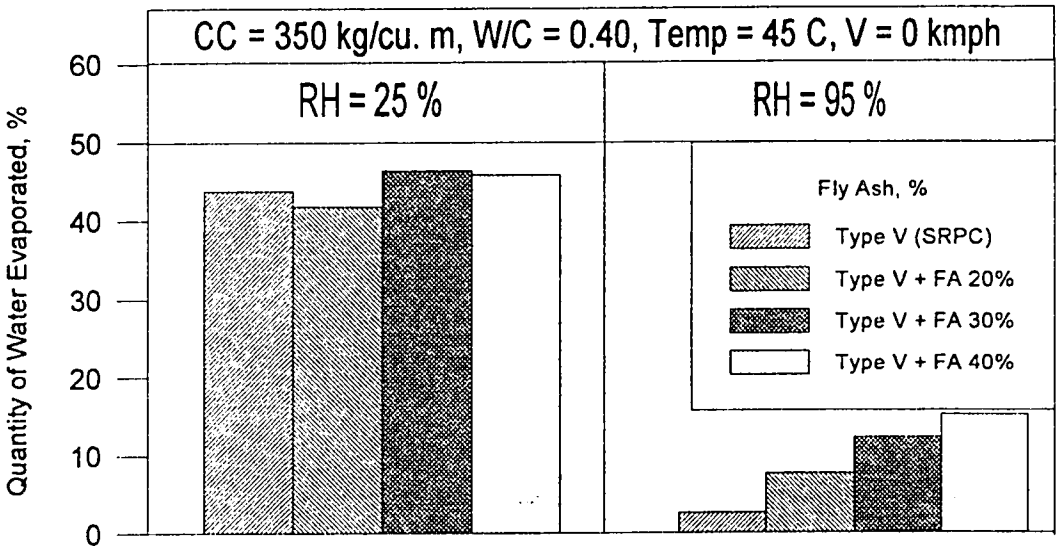

Figure 4.13: Quantity of Water Evaporated in the Fly Ash Cement Concrete (Temp: 45 °C ; V : 0 kmph ; CC : 350 kg/m^3 ; W/C : 0.40)

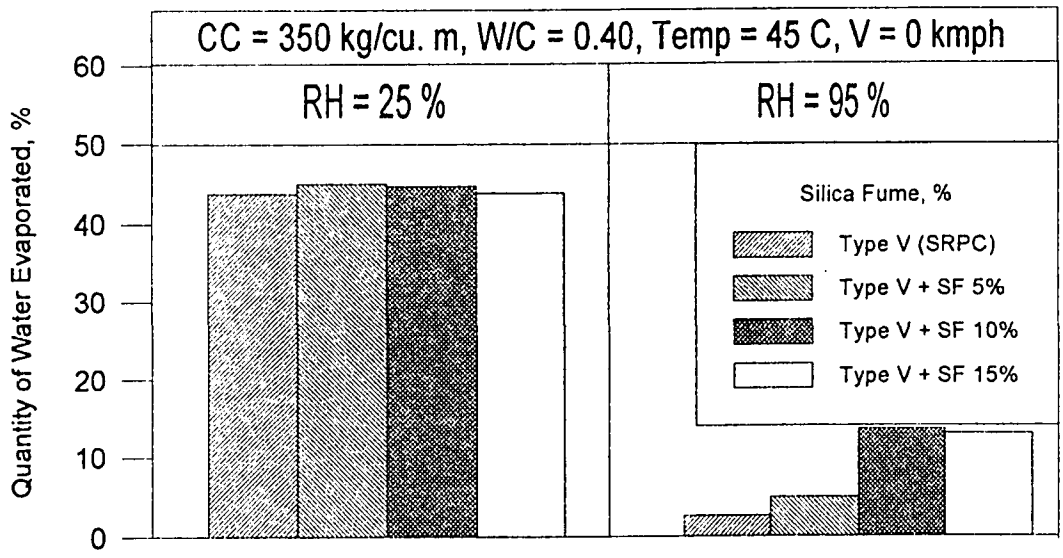

Figure 4.14: Quantity of Water Evaporated in the Silica Fume Cement Concrete (Temp : 45 °C ; V : 0 kmph ; CC : 350 kg/m^3 ; W/C : 0.40)

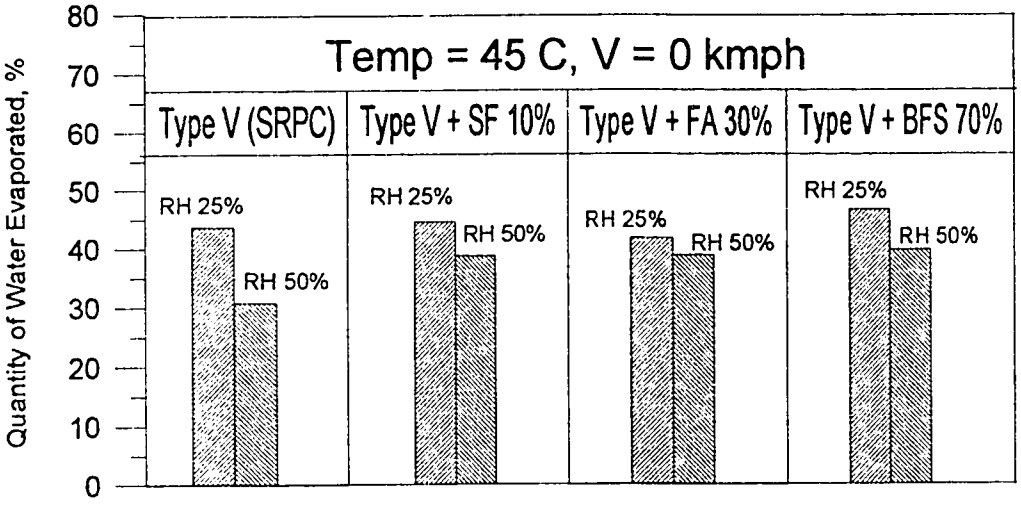

Figure 4.15: Effect of Relative Humidity on the Quantity of Water Evaporated in the Plain and Blended Cement Concretes (Temp : 45 °C ; V : 0 kmph ; CC : 350 kg/m^3 ; W/C : 0.40)

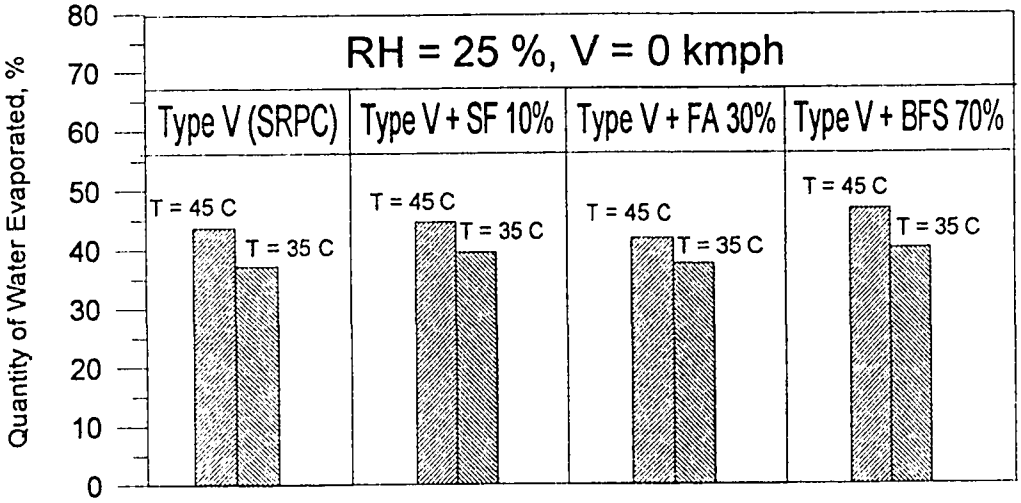

Figure 4.16: Effect of Ambient Temperature on the Quantity of Water Evaporated in Plain and Blended Cement Concretes (RH : 25% ; V : 0 kmph ; CC : 350 kg/m^3 ; W/C : 0.40)

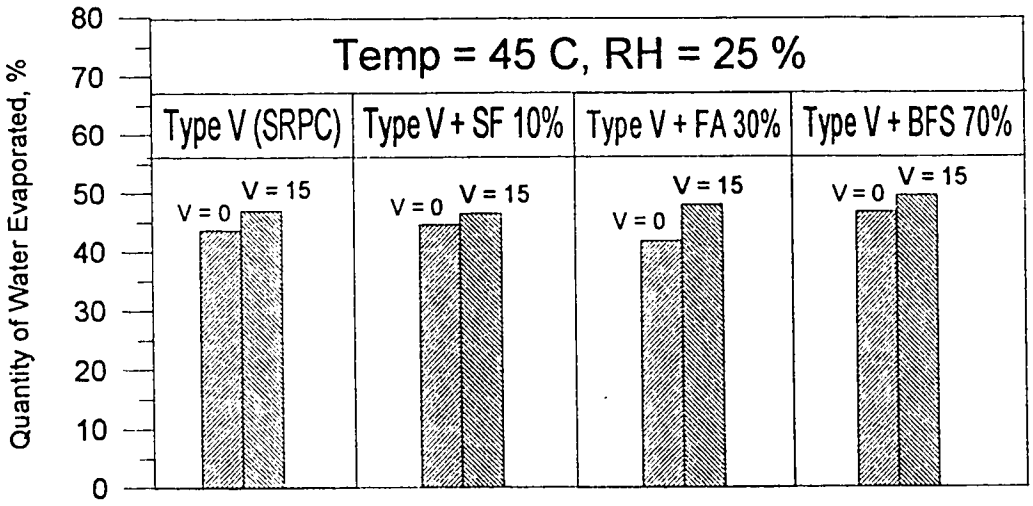

Figure 4.17: Effect of Wind Velocity on the Quantity of Water Evaporated in Plain and Blended Cement Concretes (Temp : 45 °C ; RH : 25% ; CC : 350 kg/m^3 ; W/C : 0.40)

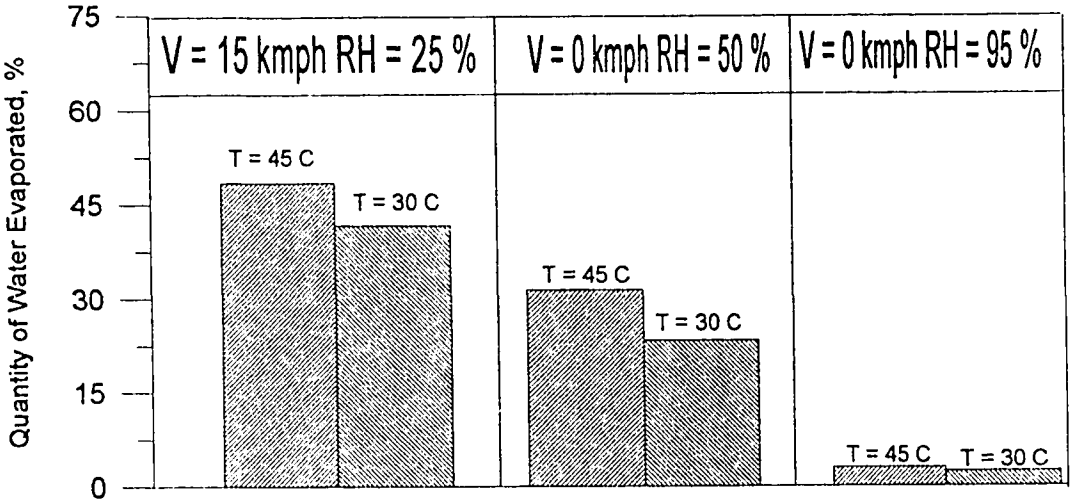

Figure 4.18: Effect of Ambient Temperature, Relative Humidity and Wind Velocity on the Quantity of Water Evaporated in the Big Concrete Specimens (CC : 350 kg/m^3 ; W/C : 0.40)

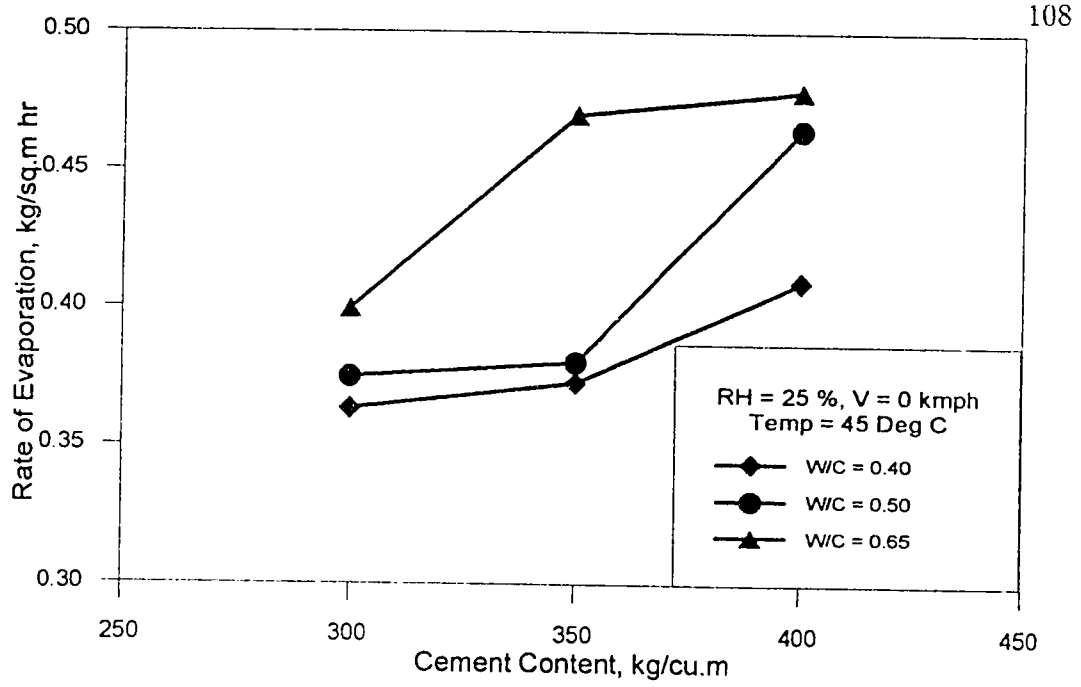

Figure 4.19: Effect of Cement Content on the Rate of Evaporation (RH : 25% ; V : 0 kmph ; Temp : 45 °C)

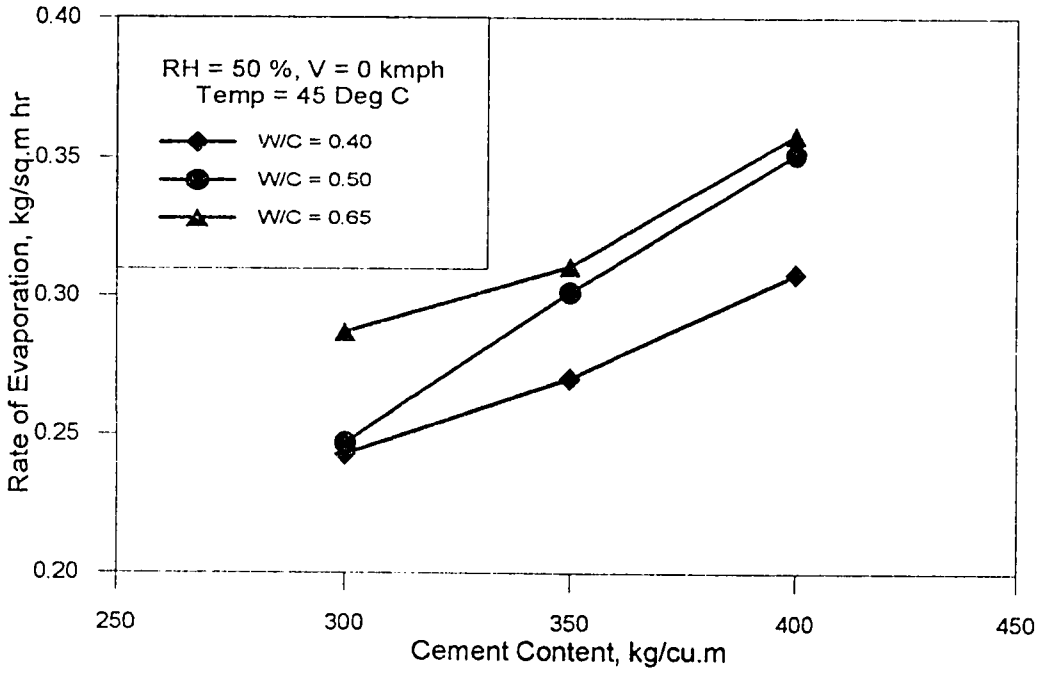

Figure 4.20: Effect of Cement Content on the Rate of Evaporation (RH : 50% ; V : 0 kmph ; Temp : 45 °C)

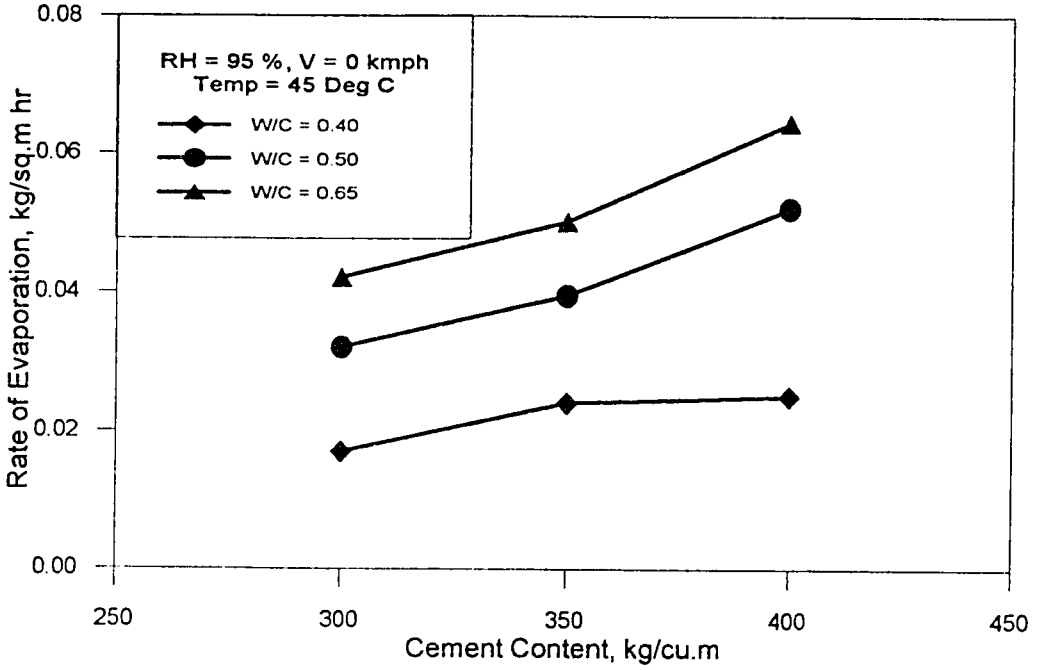

Figure 4.21: Effect of Cement Content on the Rate of Evaporation (RH : 95% ; V : 0 kmph ; Temp : 45 °C)

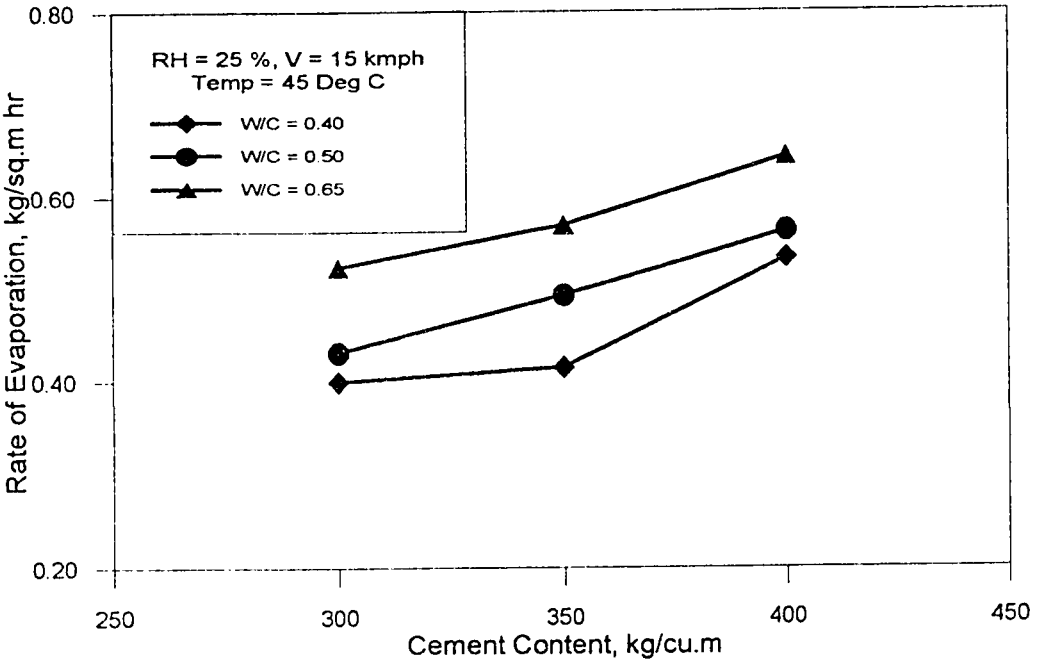

Figure 4.22: Effect of Cement Content on the Rate of Evaporation (RH : 25% ; V : 15 kmph ; Temp : 45 °C)

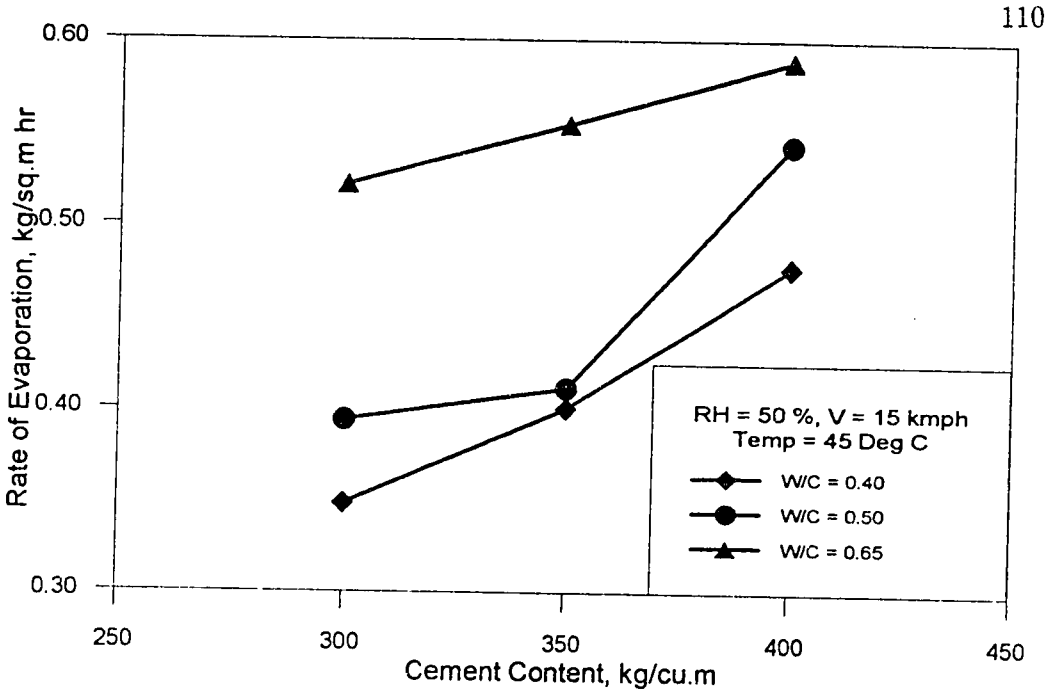

Figure 4.23: Effect of Cement Content on the Rate of Evaporation (RH : 50% ; V : 15 kmph ; Temp : 45 °C)

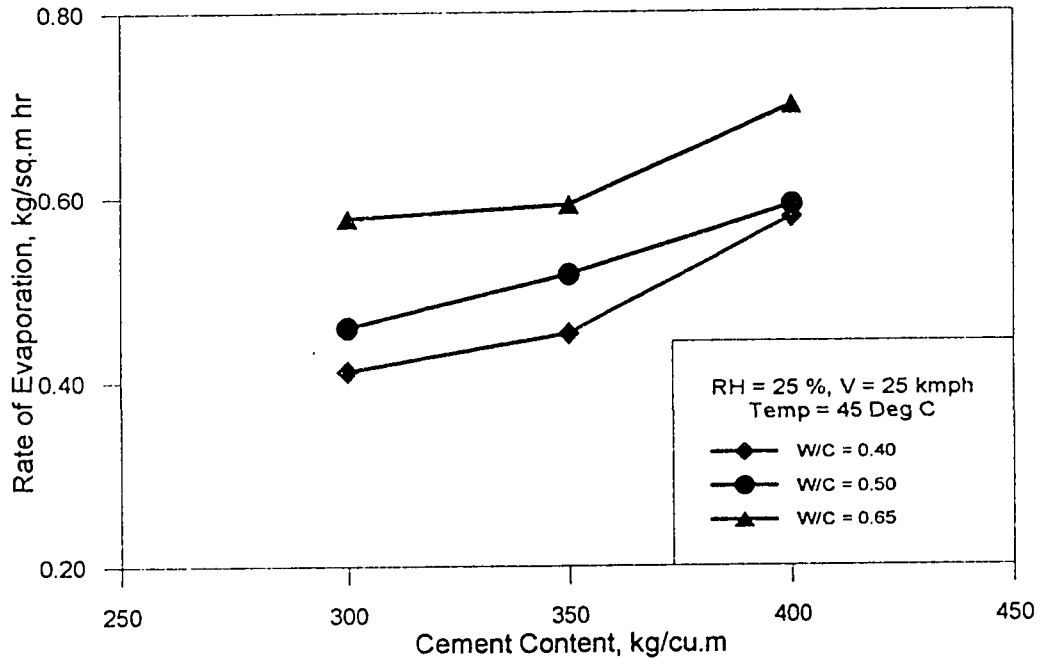

Figure 4.24: Effect of Cement Content on the Rate of Evaporation (RH : 25% ; V : 25 kmph ; Temp : 45 °C)

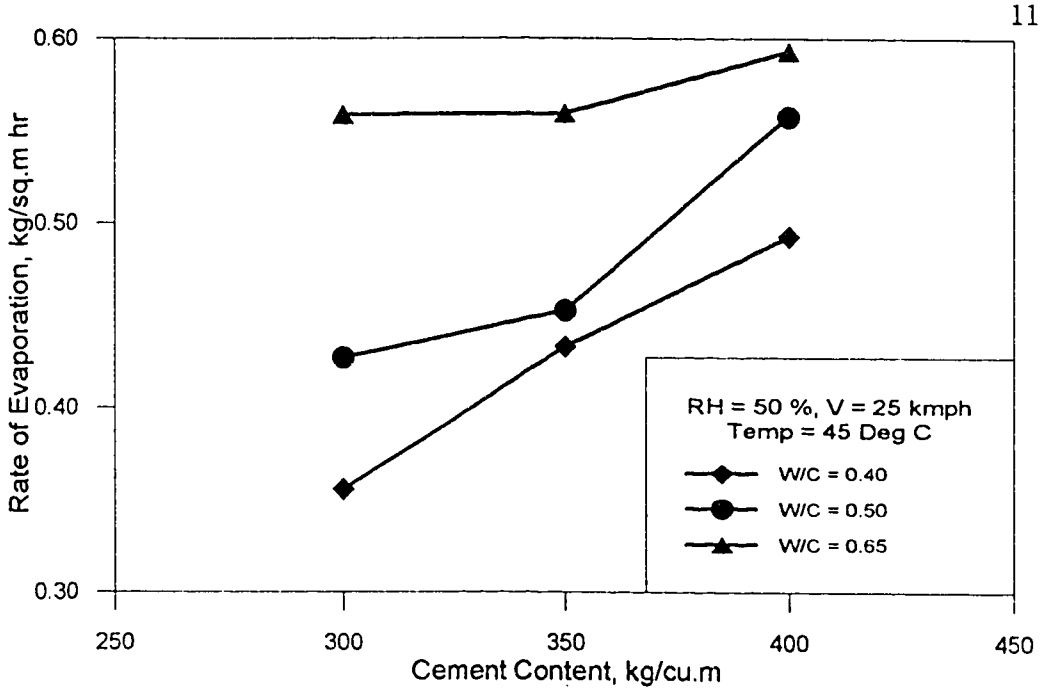

Figure 4.25: Effect of Cement Content on the Rate of Evaporation (RH : 50% ; V : 25 kmph ; Temp : 45 °C)

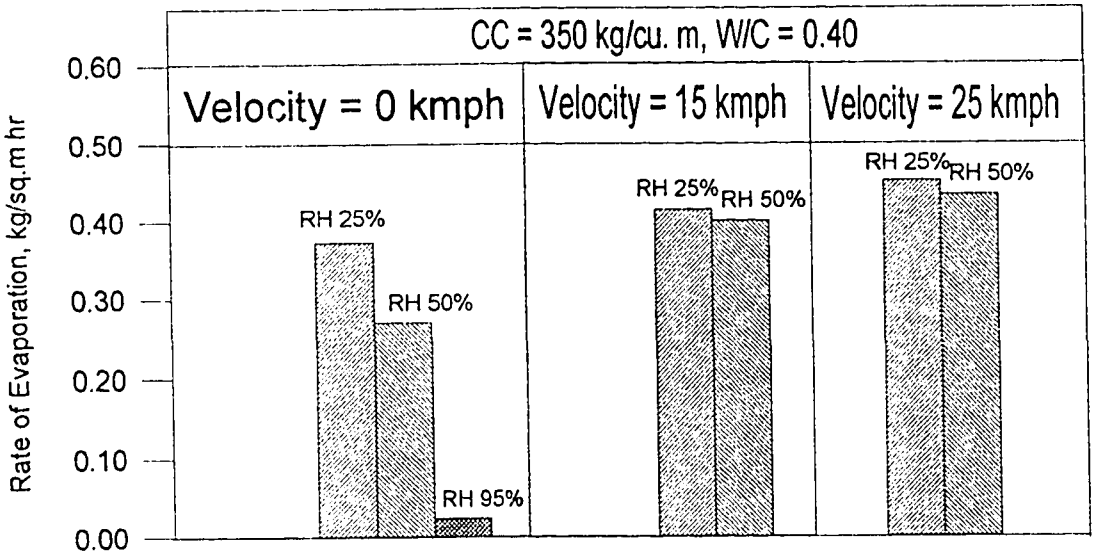

Figure 4.26: Effect of Relative Humidity and Wind Velocity on the Rate of Evaporation (Temp : 45 °C ; CC : 350 kg/m^3 ; W/C : 0.40)

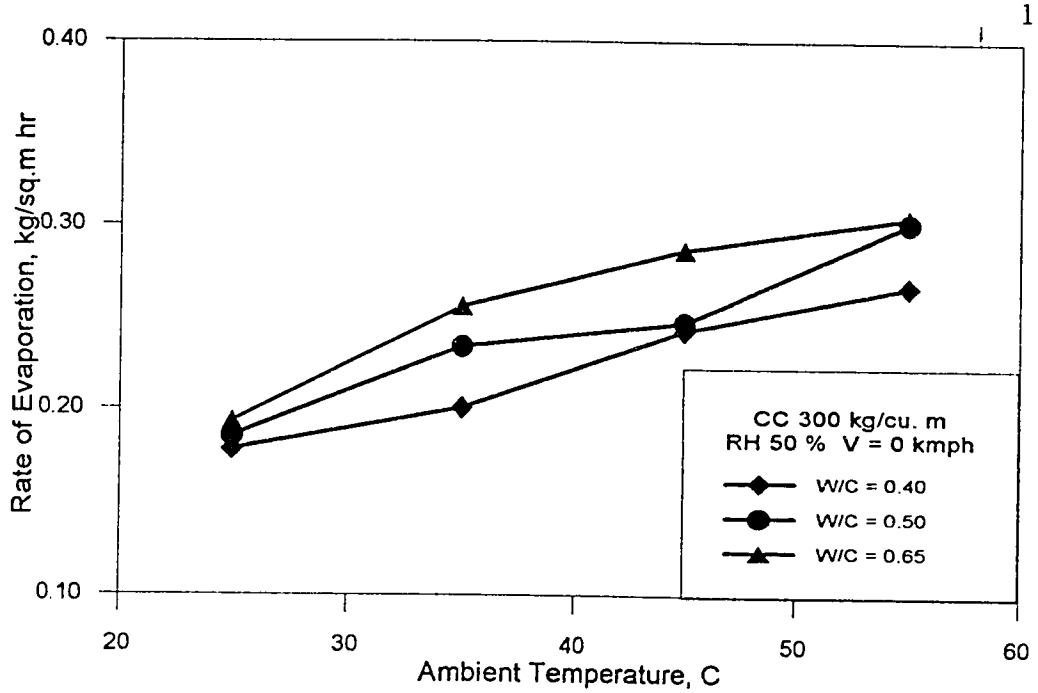

Figure 4.27: Effect of Ambient Temperature on the Rate of Evaporation (RH : 50%; V : 0 kmph ; CC : 300 kg/m^3)

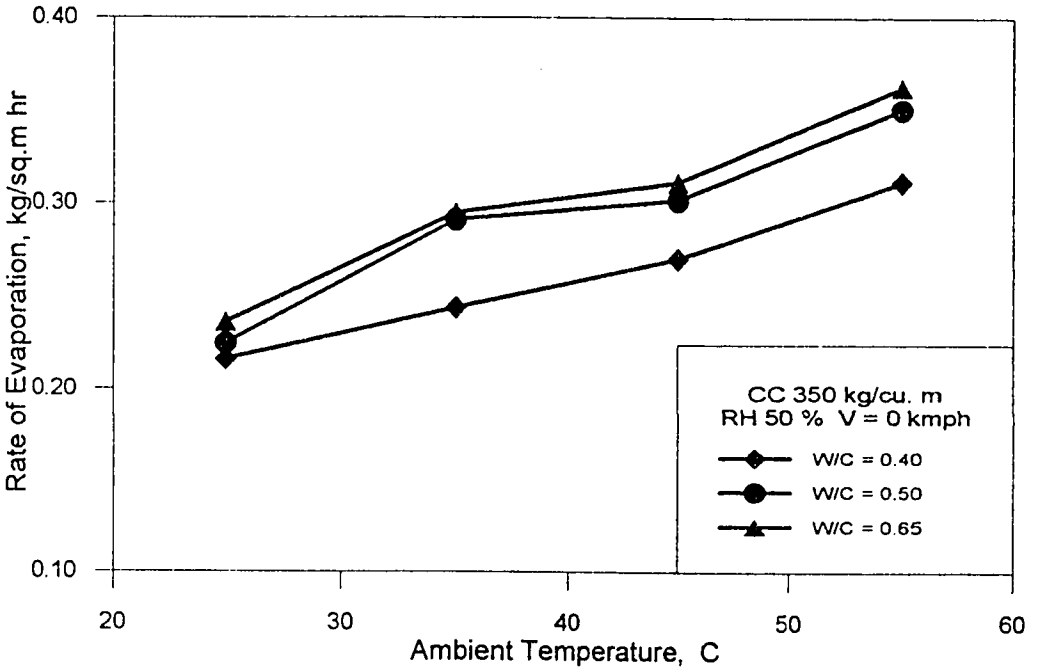

Figure 4.28: Effect of Ambient Temperature on the Rate of Evaporation (RH : 50%; V : 0 kmph ; CC : 350 kg/m^3)

Table 4.2: Comparison of the Rate of Evaporation Obtained Using the ACI Graphical Method and that Obtained in this Study

Exposure Conditions	Rate of Evaporation $kg/m^2.h$	
	ACI	Experimental
T : 25°C ; RH : 50% ;	0.2	0.124 - 0.213
T : 30°C ; RH : 25% ; V : 15 km/h ;	1.2	0.604
T : 30°C ; RH : 95% ;	0.1	0.188
T : 35°C ; RH : 25% ;	0.3	0.3
T : 35°C ; RH : 50% ;	0.25	0.141 - 0.232

Table 4.3: Efficient Concrete Mix for Various Environmental Conditions based on the Rate of Evaporation

Exposure Conditions	Efficient Concrete Mix	
	Cement Content (kg/m^3)	W/C Ratio
Normal T : 45°C ; RH : 50% ;	300	0.40
Hot-Dry T : 45°C ; RH : 25% ;	300	0.40
Hot-Normal T : 45°C ; RH : 50% ;	300	0.40
Hot-Humid T : 45°C ; RH : 95% ;	300	0.40
Hot-Dry Windy T : 45°C ; RH : 25% ; V : 25 km/h ;	300	0.40
Hot-Normal Windy T : 45°C ; RH : 50% ; V : 25 km/h ;	300	0.40

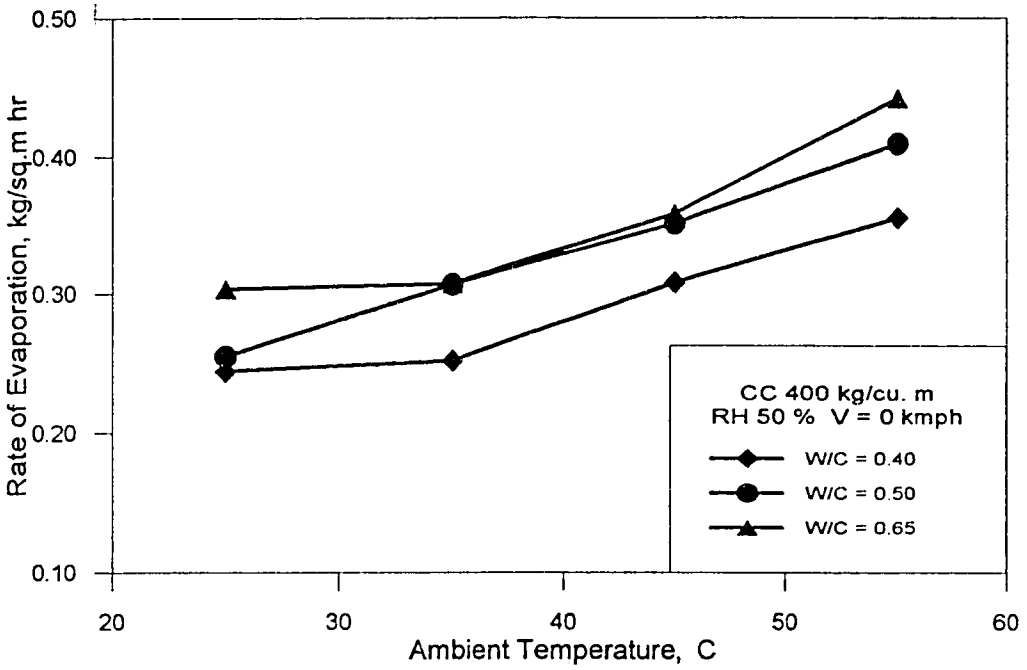

Figure 4.29: Effect of Ambient Temperature on the Rate of Evaporation (RH : 50%; V : 0 kmph ; CC : 400 kg/m^3)

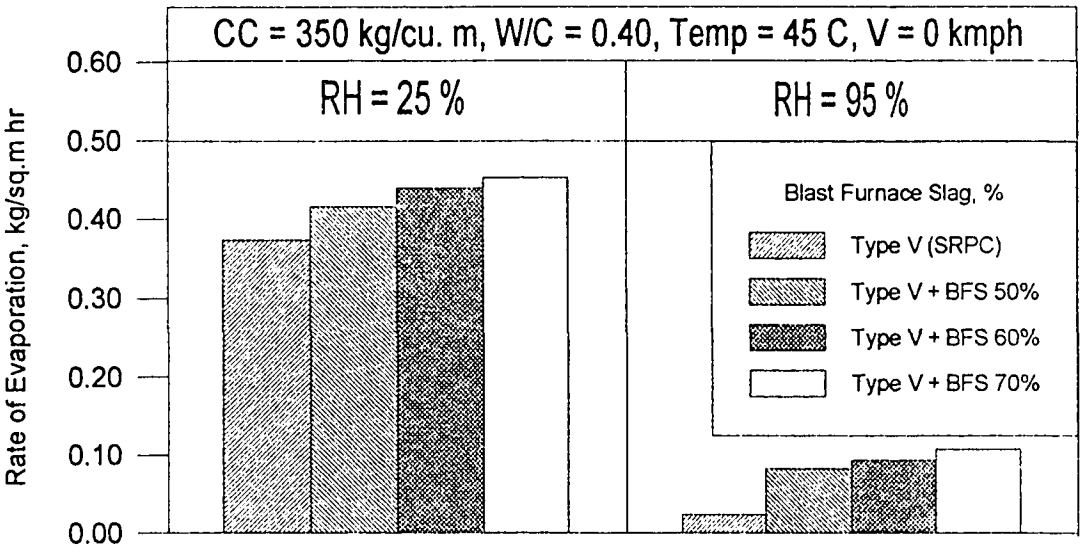

Figure 4.30: Rate of Evaporation in the Blast Furnace Slag Cement Concrete (Temp: 45 °C ; V : 0 kmph ; CC : 350 kg/m^3 ; W/C : 0.40)

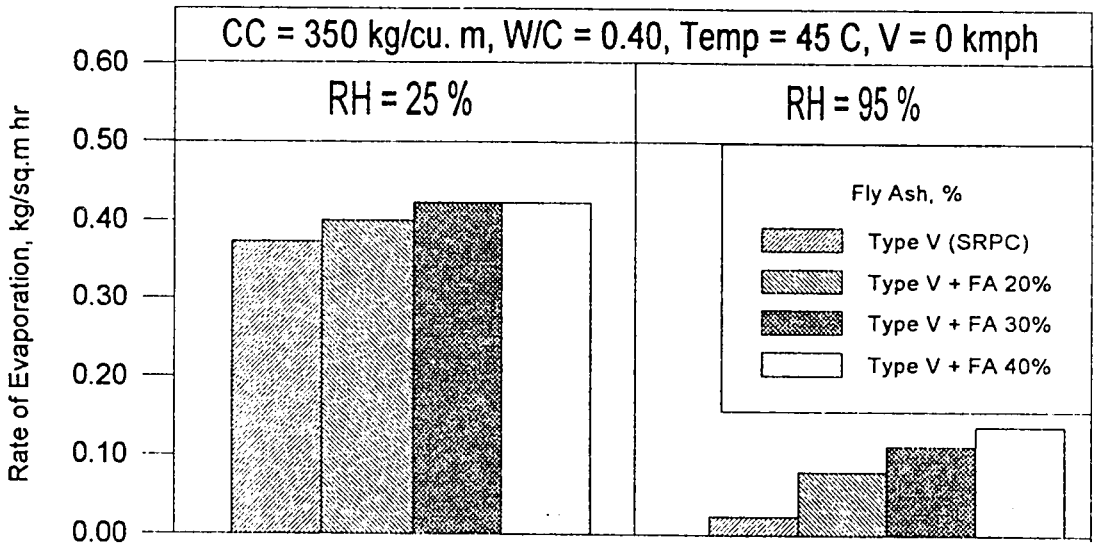

Figure 4.31: Rate of Evaporation in the Fly Ash Cement Concrete (Temp : 45 °C ; V : 0 kmph ; CC : 350 kg/m^3 ; W/C : 0.40)

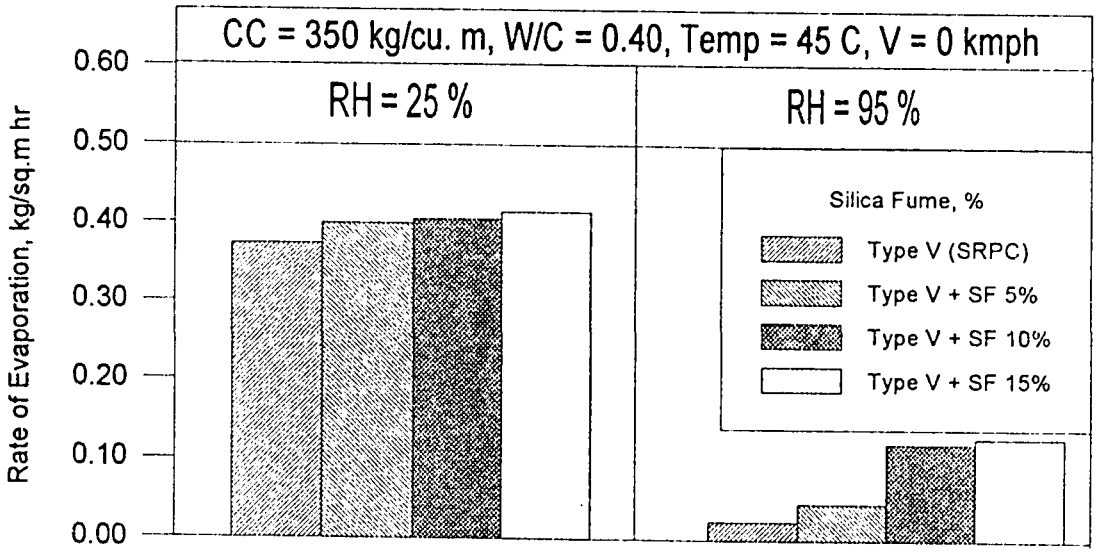

Figure 4.32: Rate of Evaporation in the Silica Fume Cement Concrete (Temp : 45 °C ; V : 0 kmph ; CC : 350 kg/m^3 ; W/C : 0.40)

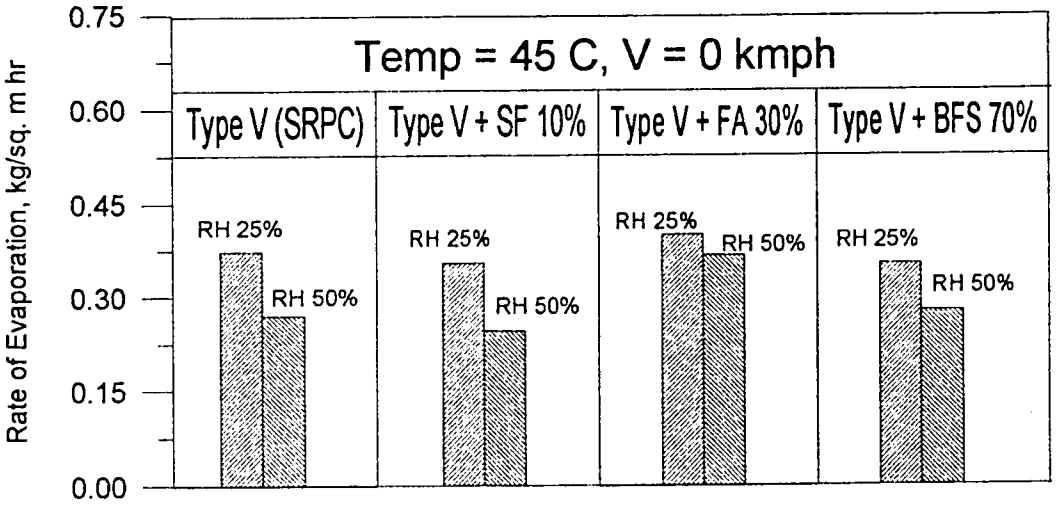

Figure 4.33: Effect of Relative Humidity on the Rate of Evaporation in the Plain and Blended Cement Concretes (Temp : 45 °C ; V : 0 kmph ; CC : 350 kg/m^3 ; W/C : 0.40)

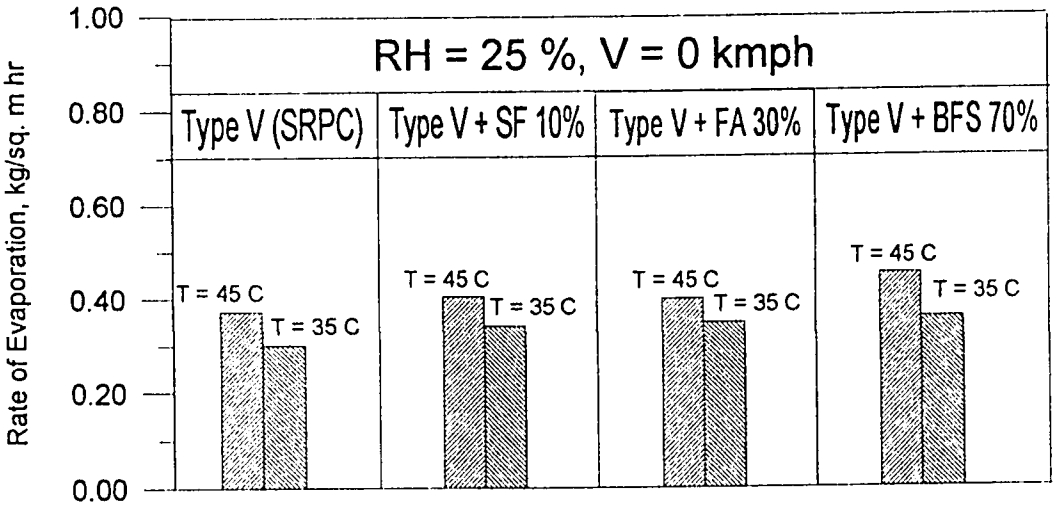

Figure 4.34: Effect of Ambient Temperature on the Rate of Evaporation in Plain and Blended Cement Concrete (RH : 25% ; V : 0 kmph ; CC : 350 kg/m^3 ; W/C : 0.40)

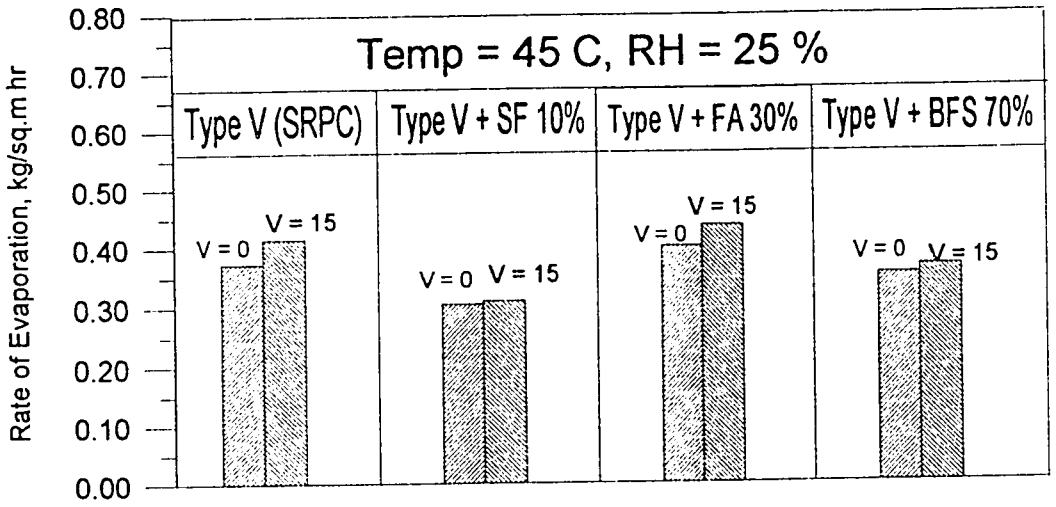

Figure 4.35: Effect of Wind Velocity on the Rate of Evaporation in Plain and Blended Cement Concrete (Temp : 45 °C ; RH : 25% ; CC : 350 kg/m^3 ; W/C : 0.40)

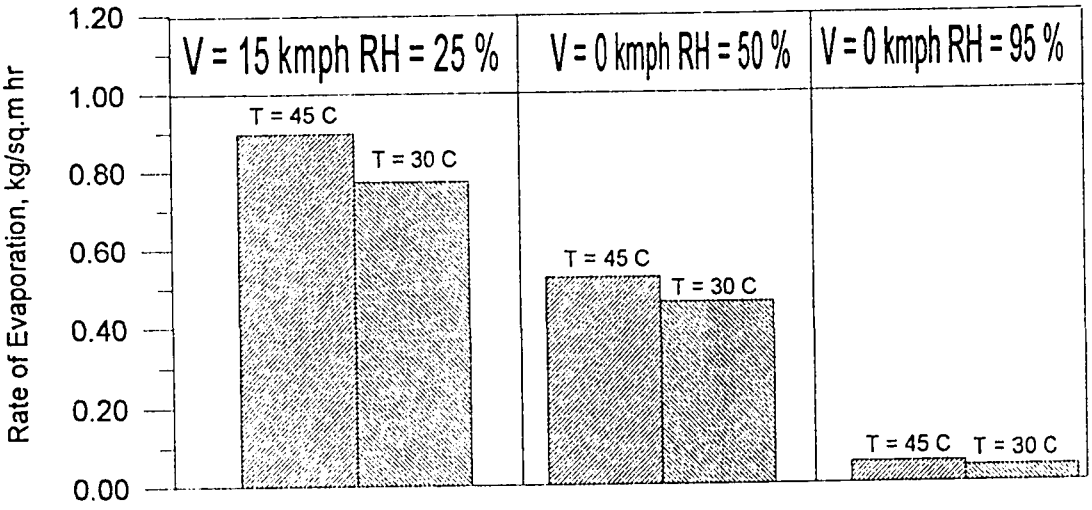

Figure 4.36: Effect of Ambient Temperature, Relative Humidity and Wind Velocity on the Rate of Evaporation in the Big Concrete Specimens (CC : 350 kg/m^3 ; W/C : 0.40)

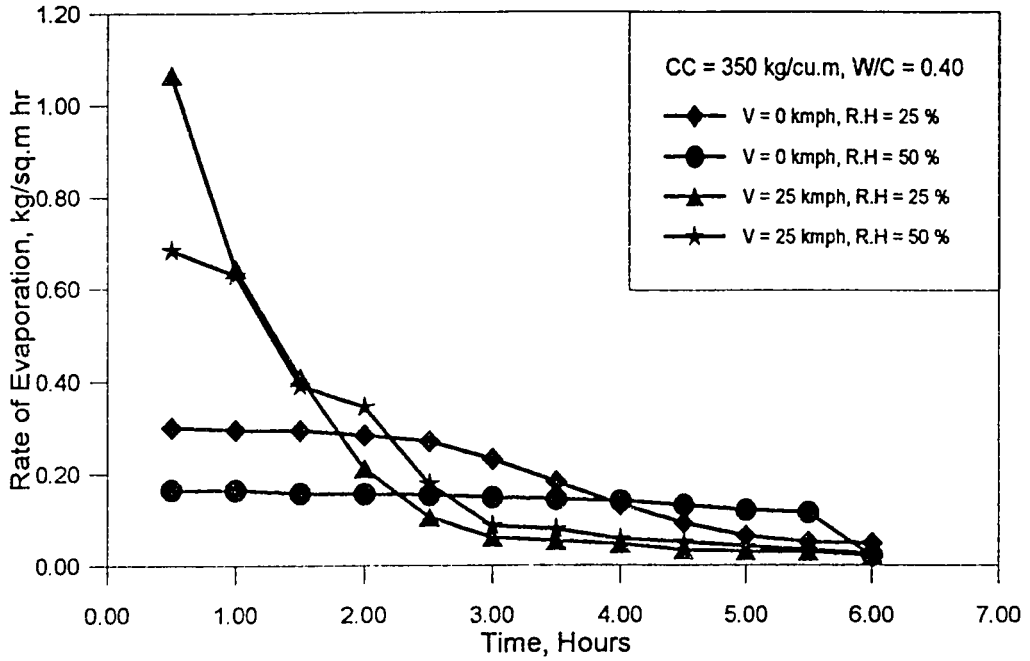

Figure 4.37: Effect of Relative Humidity and Wind Velocity on the Rate of Evaporation with Time (CC : 350 kg/m^3 ; W/C : 0.40 ; Temp : 45 °C)

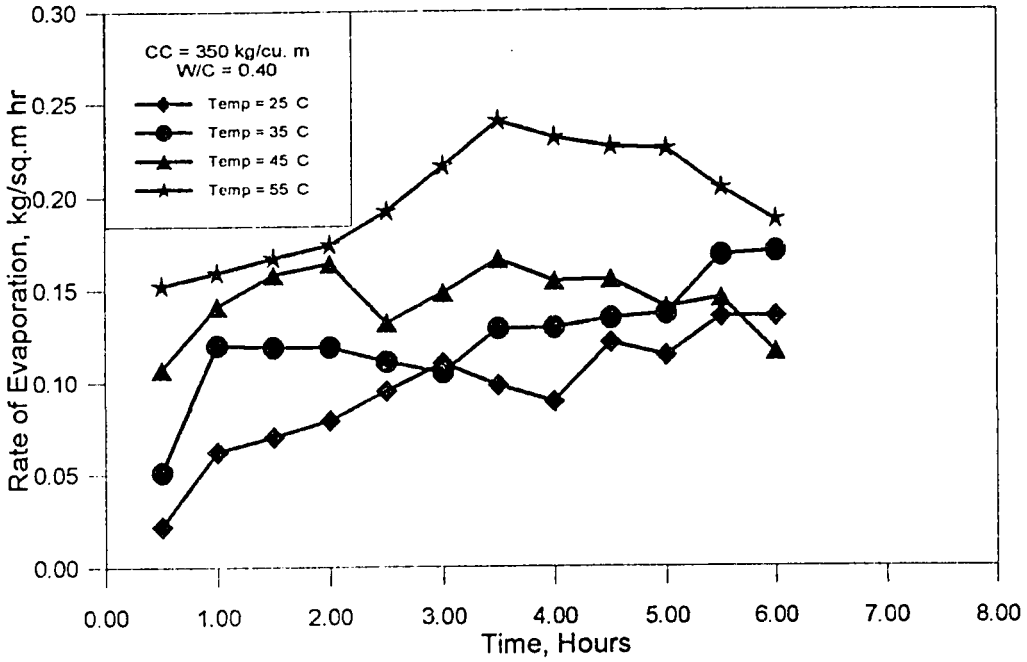

Figure 4.38: Effect of Ambient Temperature on the Rate of Evaporation With Time (CC : 350 kg/m^3 ; W/C : 0.40 ; RH : 50% ; V : 0 kmph)

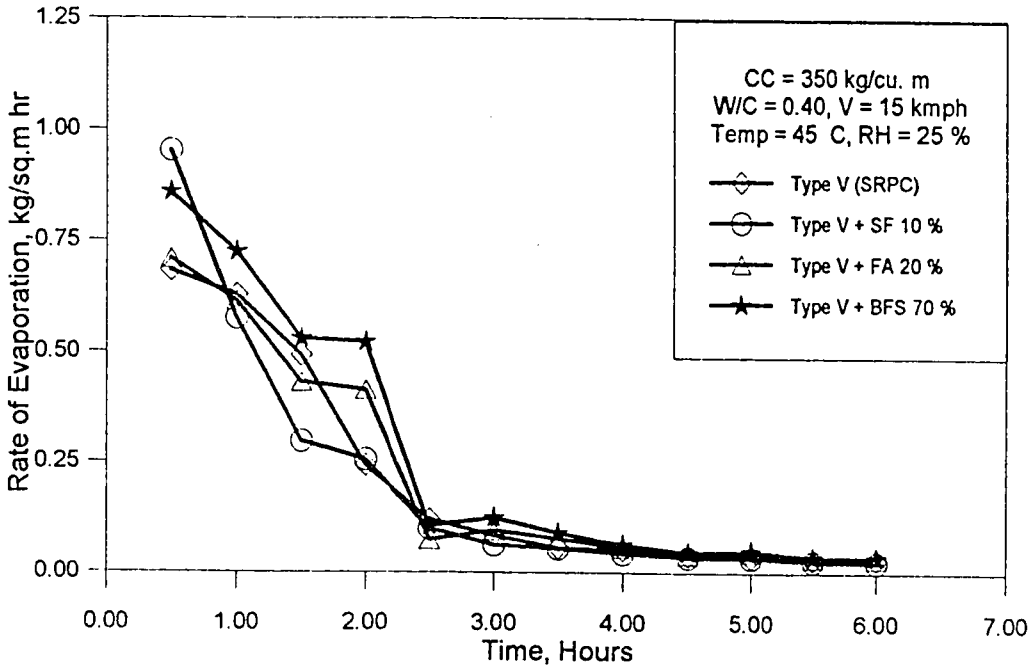

Figure 4.39: Rate of Evaporation in the Plain and Blended Cement Concretes (CC: 350 kg/m^3 ; W/C : 0.40 ; Temp : 45 °C ; V : 0 kmph ; RH : 25%)

4.2 PLASTIC SHRINKAGE CRACKING

Plastic shrinkage cracking was investigated by noting the time for appearance of first crack and the total cracked area, which was calculated as percentage of the total surface area of the concrete surface. The crack patterns in some selected specimens are shown in Figures 4.40 through 4.51.

4.2.1 Time to Cracking

Figures 4.52 through 4.57 show the effect of cement content and water-cement ratio on time to cracking in the concrete specimens exposed to varying environmental conditions.

Figure 4.52 shows the effect of mix proportions on the time to cracking in the concrete specimens exposed to a relative humidity of 25 % and an ambient temperature of 45 °C. The time to cracking increased linearly with both cement content and water-cement ratio. In the concrete mixes made with a cement content of 300 kg/m^3 and a water-cement ratio of 0.40, cracks were observed after three hours, while they were observed after four hours in the specimens made with a cement content of 400 kg/m^3, the water-cement ratio being the same. Cracks were observed after five hours in the concrete mixes made with a water-cement ratio of 0.65 and a cement content of 300 kg/m^3. A similar trend was observed in the specimens exposed to other environmental conditions, as shown in Figures 4.53 through 4.57. However, no

cracks were observed in the specimens exposed to a RH of 95 %, and a temperature of 45 °C.

From the data in Figures 4.52 through 4.57, it can be inferred that stiff mixes crack earlier than semi-plastic or plastic mixes. Similarly, lean mixes crack earlier than rich mixes. The delay in cracking due to an increase in the cement content and water-cement ratio may be attributed to the following :

(i) increased bleeding, and

(ii) increased early tensile strength.

Figure 4.58 summarizes the effect of relative humidity and wind velocity on the time to cracking in a concrete mix with a cement content of 350 kg/m^3, water-cement ratio of 0.40 and exposed to an ambient temperature of 45 °C. The time to cracking increased with increasing relative humidity in all the specimens. Cracks were observed after 3.5, 4.5 and 6 hours in the specimens exposed to a RH of 25, 50 and 95 %, respectively. In windy conditions, concrete specimens under similar relative humidity cracked earlier than the specimens exposed to non-windy conditions. Cracks were observed after 3.5 and 2 hours in the specimens exposed to a wind velocity of 0 and 25 kmph, respectively, the RH being 25 %. When the RH was 50 %, the time to cracking was 4.5 and 3 hours when the wind velocity was 0 and 25 kmph, respectively.

Figures 4.59 through 4.61 show the effect of ambient temperature on the time to

123

cracking in the concrete specimens with varying composition.

Figure 4.59 shows the effect of ambient temperature and water-cement ratio on the time to cracking in the concrete specimens made with a cement content of 300 kg/m^3 and exposed to a RH of 50 %. The time to cracking decreased with increasing temperature and increasing water-cement ratio. Cracks were observed after 5 and 3 hours in the concrete specimens made with a water-cement ratio of 0.40 and exposed to 35 and 55 °C, respectively. However, the cracking time increased to 5.5 hours when the water-cement ratio was increased from 0.40 to 0.65 in the specimens exposed to a constant temperature of 35 °C. A similar trend was observed in the concrete specimens made with a cement content of 350 (Figure 4.60) and 400 kg/m^3 (Figure 4.61). However, cracks were not observed in the majority of the mixes which were exposed to a temperature of 25 °C.

Figures 4.62 through 4.64 compare the time to cracking in the plain and blended cement concrete specimens.

Figure 4.62 shows the time to cracking in the plain and BFS cement concrete specimens. These specimens were made with a cementitious materials content of 350 kg/m^3, water-cementitious materials ratio of 0.40 and were exposed to a RH of 25 % and an ambient temperature of 45 °C. The time to cracking, in these specimens increased with increasing quantity of BFS. Cracks were observed in the plain cement concrete after 3.5 hours, while they were observed after 4.5 hours in the 70 % BFS cement concrete specimens.

Figure 4.63 shows the time to cracking in the plain and fly ash cement concrete specimens. These specimens were made with a cementitious materials content of 350 kg/m^3 and a water-cementitious materials ratio of 0.40 and exposed to a RH of 25 % and an ambient temperature of 45 °C. Again, the time to cracking increased with the percentage of fly ash. The time to cracking in the plain cement concrete specimen was 3.5 hours, while it was 4.5 hours in the of 40 % fly ash cement concrete specimens.

Figure 4.64 shows the time to cracking in the plain and silica fume cement concrete specimens. These concrete specimens were made with a cementitious materials content of 350 kg/m^3 and a water-cementitious materials ratio of 0.40 and exposed to a RH of 25 % and ambient temperature of 45 °C. Cracking was observed after 3.5 hours in all the specimens except in the 15 % silica fume cement concrete specimens in which cracking was observed after 4 hours.

Figures 4.65 and 4.66 show the effect of relative humidity and wind velocity on the time to cracking in the plain and blended cement concrete specimens.

Figure 4.65 shows the effect of relative humidity on the time to cracking in the plain and blended cement concrete specimens. These specimens were made with a cementitious materials content of 350 kg/m^3 and a water-cementitious materials ratio of 0.40 and were exposed to an ambient temperature of 45 °C. The time to cracking increased with increasing relative humidity, in both plain and blended cement concrete specimens. The time to cracking time increased from 3.5 to 4.5

hours, when the relative humidity was increased from 25 to 50 % in the plain cement concrete mixes, whereas in all the other mixes the increase was 0.5 hours.

Figure 4.66 shows the effect of wind velocity on the time to cracking in the plain and blended cement concrete specimens. The time to cracking in the specimens exposed to a wind of 15 kmph was more than that in the specimens which were exposed to no wind. The time to cracking decreased by 1, 1.5, 2 and 0.5 hours in the plain, fly ash, BFS and silica fume cement concrete specimens, respectively. These data indicate that the time to cracking in the plain and blended cements is not very significant.

Figure 4.67 shows the effect of different exposure conditions on time to cracking in big concrete specimens. These specimens were made with a cement content of 350 kg/m^3 and a water-cement ratio of 0.40. The time to cracking decreased with increasing temperature in the specimens exposed to a wind velocity of 15 kmph and a relative humidity if 25 %. In the specimens exposed to a relative humidity of 50 % and no wind, the time to cracking was similar in the specimens exposed to temperatures of 30 and 45 °C. No Cracking was observed in the specimens exposed to a relative humidity of 95 % and a temperature of 30 °C, while it was five hours in the specimens exposed to 45 °C and a RH of 95 %. No cracking was observed in the specimens exposed to a Rh of 95 % and no wind.

4.2.2 Crack Length

Figures 4.68 through 4.70 show the effect of relative humidity, wind velocity and ambient temperature on crack length in the plain and blended cement concrete specimens.

Figure 4.68 shows the effect of relative humidity and wind velocity on the crack length in the concrete specimens made with a cement content of 350 kg/m^3, water-cement ratio of 0.40 and exposed to 45 °C. The crack length increased with time in all the concrete specimens. Both the initial cracking time and the crack length were affected by the wind velocity and relative humidity. In windy conditions, an increase in the RH from 25 to 50 % increased the time to cracking by 1 hour. The crack length in the specimens exposed to both the conditions, however, was nearly the same. However, when there was no wind, the relative humidity not only affected the cracking time but also the length of cracks. In the specimens exposed to a wind velocity of 25 kmph and a RH of 25 %, cracks were observed after 2.5 hours of casting and the total crack length, after 6 hours, was 1050 mm. In the specimens exposed to no wind and a relative humidity of 25 %, cracks were visible after 4 hours and the crack length was 450 mm, while in the specimens exposed to a RH of 50 % and no wind cracks initiated after 5 hours after casting and the crack length after 6 hours was 200 mm. These data indicate that in windy conditions, an increase in the relative humidity delays the time to cracking, but the overall crack intensity is not

significantly affected. When there is no wind, however, an increase in the relative humidity not only delays cracking but also reduces the intensity of cracks.

Figure 4.69 shows the effect of ambient temperature on development of cracks in a concrete mix with a cement content of 350 kg/m^3, water-cement ratio of 0.40 and exposed to a RH of 50 %. These data indicate that the ambient temperature significantly affects the time to cracking as well as the length of cracks. In the specimens exposed to 55 °C, cracks were observed after 3.5 hours and the total crack length was nearly 450 mm. In the specimens exposed to 45 °C, these values were 4.5 hours and 350 mm, respectively. No cracks were observed in the specimens exposed to 25 °C.

Figure 4.70 shows the development of cracks in the plain and blended cement concrete specimens. These specimens were made with a cementitious materials content of 350 kg/m^3, water-cementitious materials ratio of 0.40 and exposed to a RH of 25 % and ambient temperature of 45 °C. In all the concrete specimens, cracks were observed after 3 hours of casting. However, the crack length was the highest in the silica fume cement concrete specimens, followed by fly ash and BFS cement concrete specimens. Least crack length was observed in the plain cement concrete specimens. The crack length in the silica fume cement concrete specimen was 1100 mm compared to 850 mm in the plain cement concrete specimens. This indicates that the addition of supplementary cementitious materials to plain concrete does not affect the time to cracking but increases the intensity of cracks.

4.2.3 Total Cracked Area

Figures 4.71 through 4.76 show the effect of cement content on the total area of cracks in concrete specimens exposed to varying environmental conditions.

Figure 4.71 shows the effect of mix proportions on the total area of cracks in the concrete specimens exposed to a RH of 25 % and an ambient temperature of 45 °C. The cracked area increased with both the cement content and the water-cement ratio. In the specimens made with a cement content of 300 kg/m^3 and a water-cement ratio of 0.40, the total cracked area was 0.01 %, and it increased to 0.03 % in the concrete specimens made with a cement content of 400 kg/m^3 and a similar water-cement ratio. The cracked area increased to 0.06 % when the water-cement ratio was increased to 0.65, the cement content remaining the same at 300 kg/m^3. A similar trend was observed in the concrete specimens exposed to the other environmental conditions, as shown in Figures 4.72 through 4.76. No cracks were observed in the concrete specimens exposed to a RH of 95 % and temperature of 45 °C.

The increase in the cracked area with an increase in the water-cement ratio may be attributed to a decrease in the tensile strength, due to such modification in the concrete constituents.

Figure 4.77 summarizes the effect of relative humidity and wind velocity on the cracked area in a typical concrete mix made with a cement content of 350 kg/m^3,

water-cement ratio of 0.40 and exposed to an ambient temperature of 45 °C. The cracked area decreased with increasing relative humidity. In the specimens exposed to no wind, the total cracked area was 0.04, 0.02 and 0.005 %, when the RH was 25, 50 and 95 %, respectively. The total cracked area also increased with increasing wind velocity. It increased from 0.04 % to 0.09 % when the wind velocity was increased from 0 to 25 kmph, for a RH of 25 %. In the specimens exposed to a RH of 50 %, the total cracked area increased from 0.02 to 0.08 % as the wind velocity was increased from 0 to 25 kmph.

Figures 4.78 through 4.80 show the effect of ambient temperature on total cracked area in the concrete specimens with varying composition .

Figure 4.78 shows the effect of ambient temperature and water-cement ratio on the cracked area in the concrete specimens with a cement content of 300 kg/m^3 and exposed to a RH of 50 %. The cracked area increased with both the temperature and the water-cement ratio. In the specimens with a water-cement ratio of 0.40 and exposed to 35 °C, the total cracked area was 0.005 % and increased to 0.013 % in the specimens exposed to 55 °C. The total cracked area increased to 0.025 % when the water-cement ratio was increased to 0.65, the temperature being constant at 35 °C. A similar trend was observed in the concrete specimens made with a cement content of 350 kg/m^3 (Figure 4.79) and 400 kg/m^3 (Figure 4.80).

The most efficient concrete mixes for various exposure conditions, based on cracking intensity, are shown in Table 4.4. The most efficient mix, based on total cracked

area, is a lean stiff mix having a cement content of 300 kg/m^3 and a water-cement ratio 0.40 for all the conditions. From the experimental results, it was noted that lean stiff mixes crack earlier than rich plastic mixes, but the cracking intensity is much less in the former.

Figure 4.81 shows the total cracked area in plain and the BFS cement concrete specimens. The concrete specimens were made with a cementitious materials content of 350 kg/m^3 and a water-cementitious materials ratio of 0.40, and exposed to a RH of 25 % and an ambient temperature of 45 °C. The total cracked area in the BFS cement concrete specimens was more than that in the plain cement concrete specimens. The total cracked area in the 0, 50, 60 and 70 % BFS cement concretes was 0.035, 0.04, 0.038 and 0.036 %, respectively. The increase in the crack area with the addition of BFS may be attributed to the low tensile strength of BFS compared to plain cements, particularly at early ages.

Figure 4.82 shows the total cracked area in the plain and fly ash cement concrete specimens. These specimens were made with a cementitious materials content of 350 kg/m^3, water-cementitious materials ratio of 0.40 and exposed to a RH of 25 % and an ambient temperature of 45 °C. The total cracked area in the fly ash cement concrete specimens was more than that in the plain cement concrete specimens. The total cracked area in the 0, 20, 30, 40 % fly ash cement concrete specimens was 0.035, 0.052, 0.050 and 0.048 %, respectively.

Figure 4.83 shows the total cracked area in the plain and silica fume cement

concrete specimens. These concrete specimens were made with a cementitious materials content of 350 kg/m^3, water-cementitious materials ratio of 0.40 and exposed to a RH of 25 % and an ambient temperature of 45 °C. The total cracked area in the silica fume cement concrete specimens was more than that in the plain cement concrete specimens. The total cracked area in the 0, 5, 10 and 15 % silica fume concrete specimens was 0.035, 0.08, 0.07 and 0.05 %, respectively.

Figure 4.84 shows the effect of relative humidity on the total cracked area in the plain and blended cement concrete specimens. These concrete mixes were made with a cementitious materials content of 350 kg/m^3, water-cementitious materials ratio of 0.40 and exposed to an ambient temperature of 45 °C. The total cracked area in the specimens exposed to a RH of 25 % was more than that in those exposed to a RH of 50 %. This trend was indicated in both plain and blended cements, except in the silica fume cement concrete specimens, in which the total cracked area was the same irrespective of the exposure conditions. Another point to be noted is that the total cracked area in the silica fume and fly ash cement concrete specimens was more than that in the plain and BFS cement concrete specimens. In the plain and BFS cement concrete specimens, the total cracked area was more or less the same.

Figure 4.85 shows the effect of wind velocity on the total cracked area in the plain and blended cement concrete specimens. These concrete mixes were made with a cementitious materials content of 350 kg/m^3, water-cementitious materials ratio of 0.40 and exposed to an ambient temperature of 45 °C. The total area of

cracks increased with increasing wind velocity. Again, the total cracked area in the silica fume and fly ash cement concrete was more than that in the plain and BFS cement concrete specimens.

Figure 4.86 shows the effect of different exposure conditions on the total cracked area in the big concrete specimens. These specimens were made with a cement content of 350 kg/m^3 and a water-cement ratio of 0.40. The total cracked area increased with increasing exposure temperature in the specimens exposed to a wind velocity of 15 kmph and RH of 25 %. A similar trend was observed in the specimens exposed to a RH of 50 %. However, no cracks were observed in the specimens exposed to a temperature of 30 °C and a RH of 95 %. The total cracked area decreased from 0.13 to 0.02 % when the RH was increased from 50 to 95 %. As in the small specimens, the relative humidity was observed to affect the extent of cracking in the big specimens also.

Figure 4.40: Typical Plastic Shrinkage Cracks in the Concrete Specimens Exposed to a RH of 25 % and Temperature of 45 °C

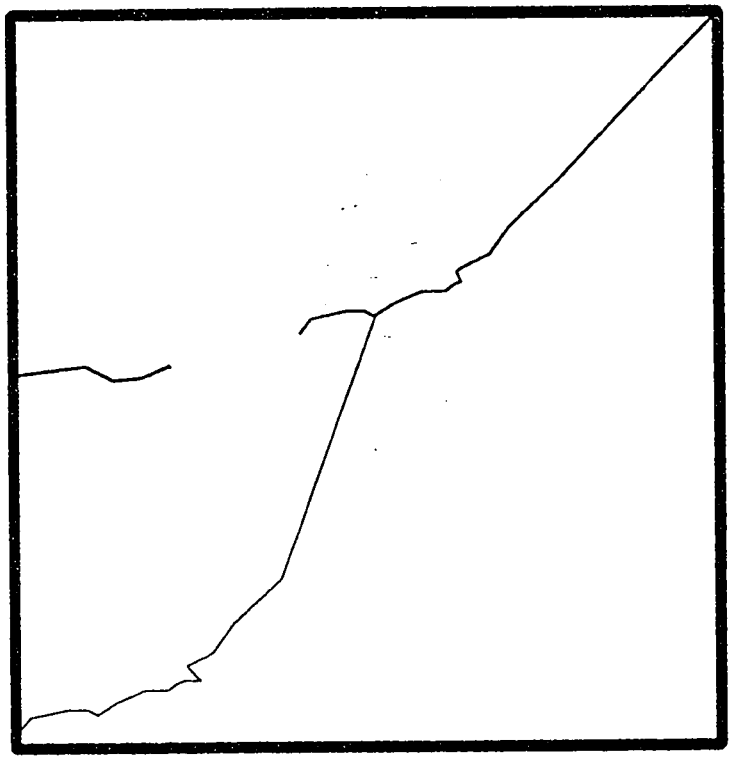

Figure 4.41: Typical Plastic Shrinkage Cracks in the Concrete Specimens Exposed to a RH of 50 % and Temperature of 45 °C

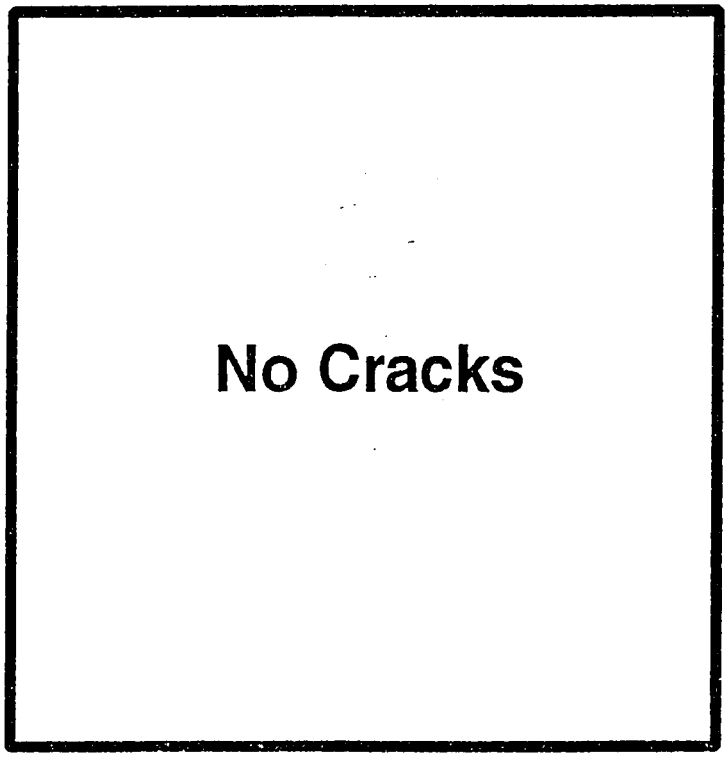

Figure 4.42: Typical Plastic Shrinkage Cracks in the Concrete Specimens Exposed to a RH of 95 % and Temperature of 45 °C

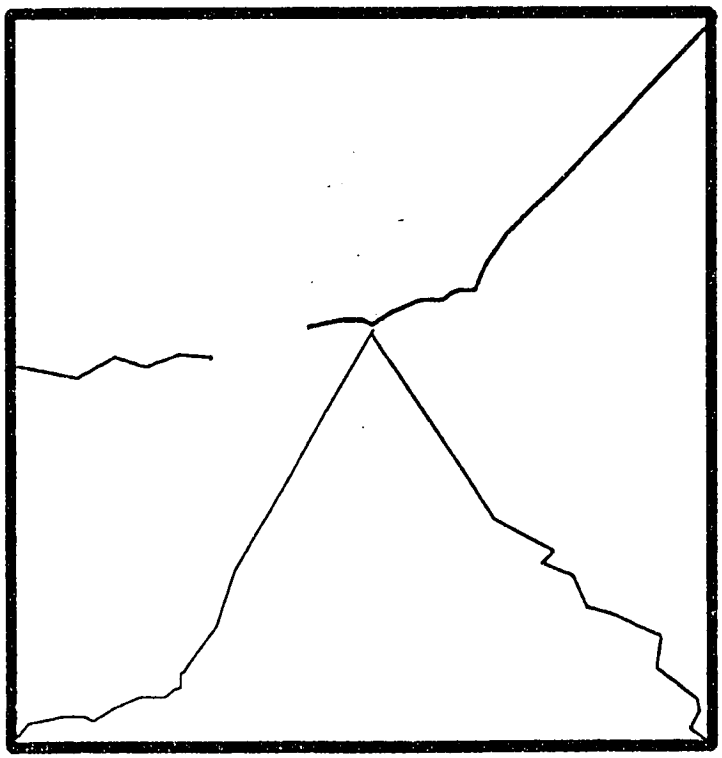

Figure 4.43: Typical Plastic Shrinkage Cracks in the Concrete Specimens Exposed to a RH of 25 %, Temperature of 45 °C and a Wind Velocity of 25 kmph

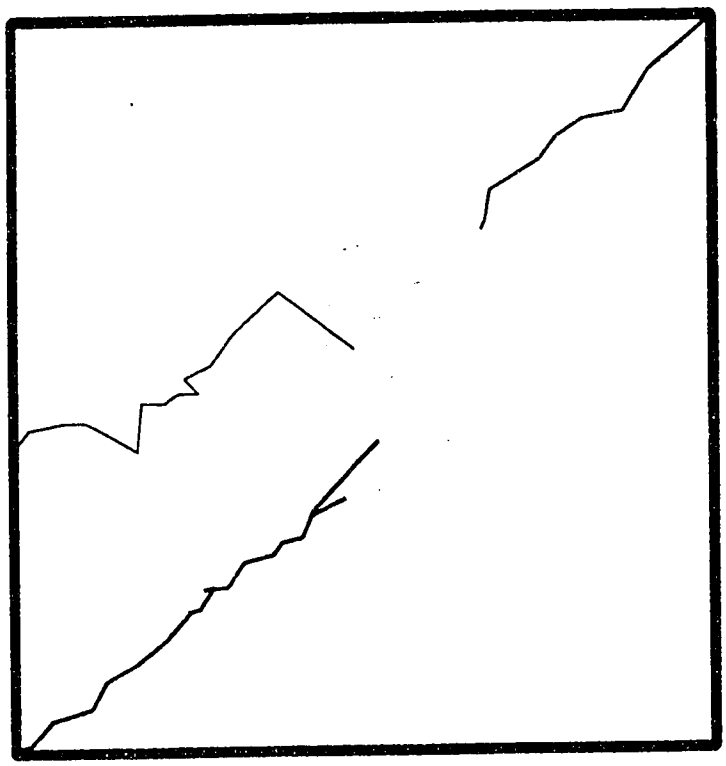

Figure 4.44: Typical Plastic Shrinkage Cracks in the Concrete Specimens Exposed to a RH of 50 %, Temperature of 45 °C and a Wind Velocity of 25 kmph

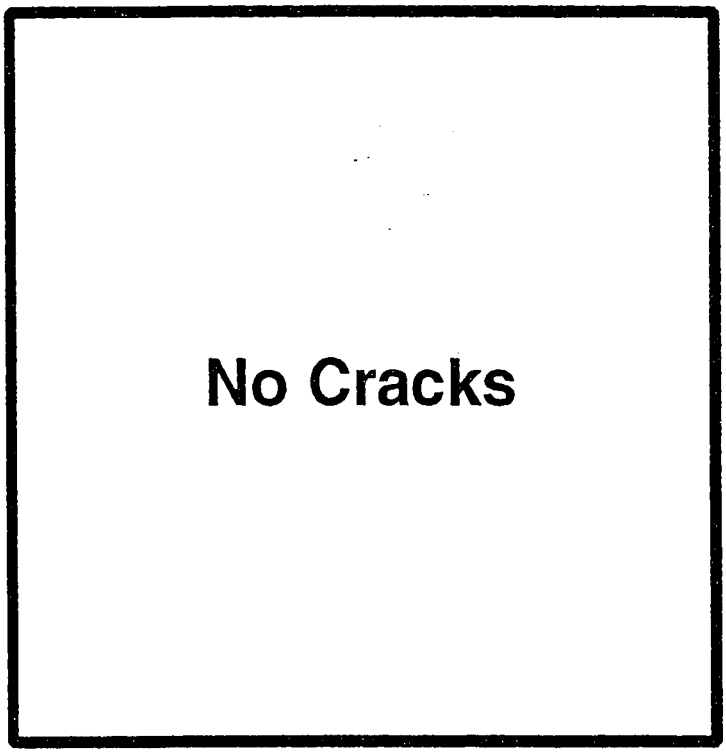

Figure 4.45: Typical Plastic Shrinkage Cracks in the Concrete Specimens Exposed to a RH of 50 % and Temperature of 25 °C

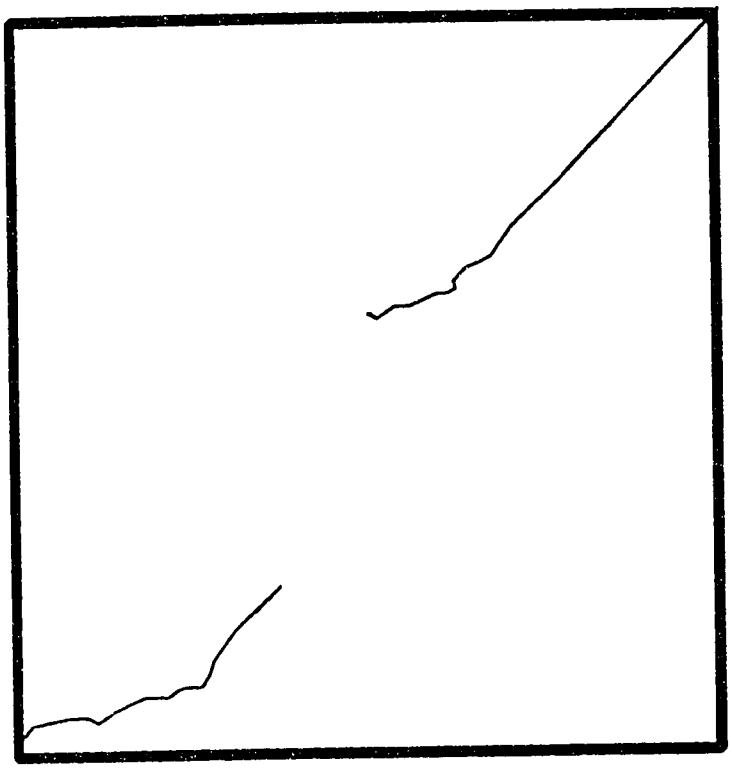

Figure 4.46: Typical Plastic Shrinkage Cracks in the Concrete Specimens Exposed to a RH of 50 % and Temperature of 35 °C

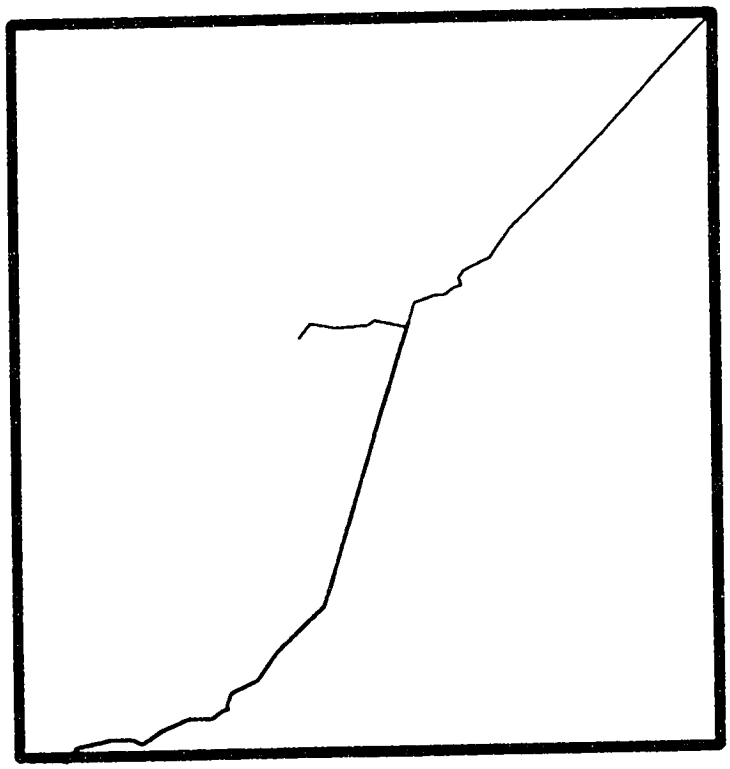

Figure 4.47: Typical Plastic Shrinkage Cracks in the Concrete Specimens Exposed to a RH of 50 % and Temperature of 55 °C

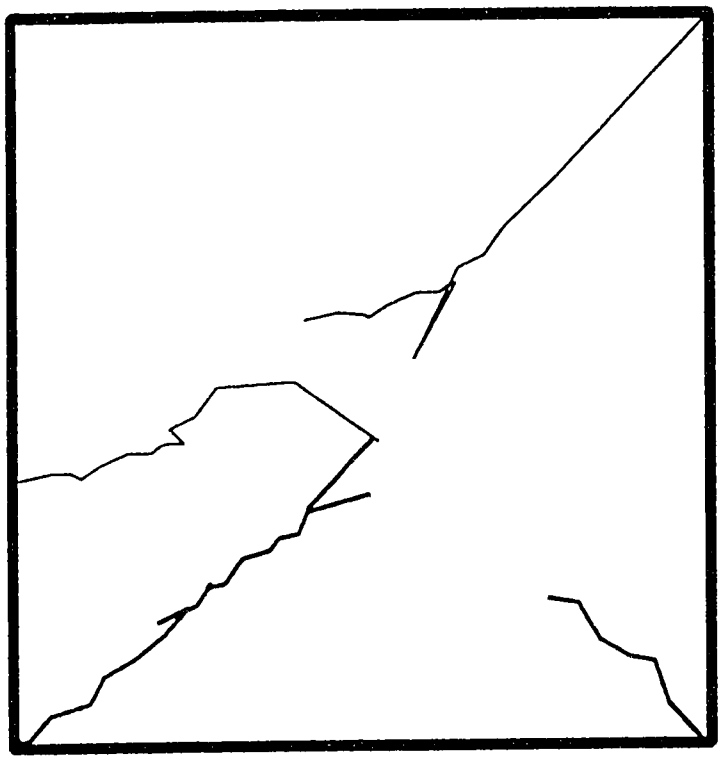

Figure 4.48: Typical Plastic Shrinkage Cracks in the Concrete Specimens Exposed to a RH of 25 %, Temperature of 45 °C and a Wind Velocity of 15 kmph

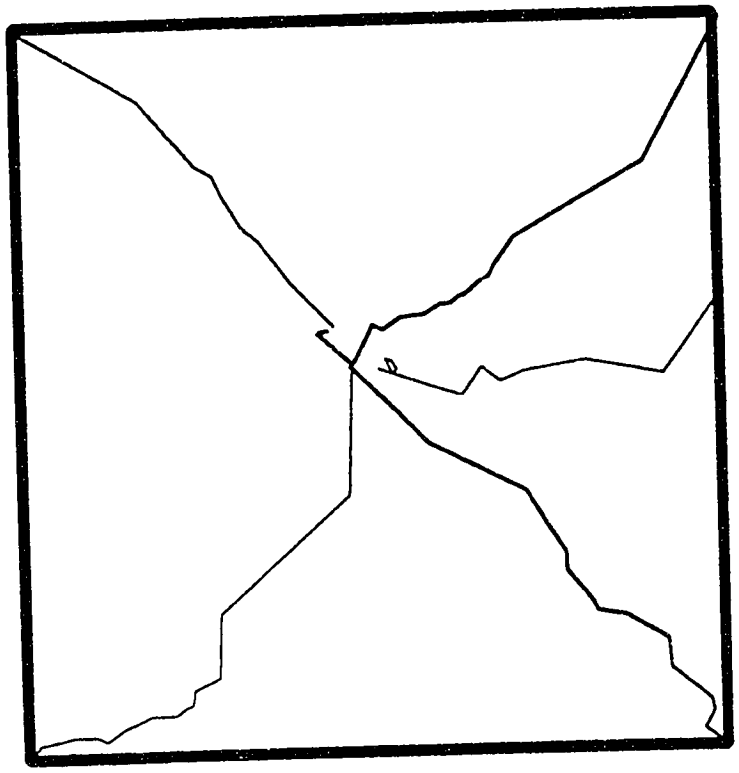

Figure 4.49: Typical Plastic Shrinkage Cracks in 70 % Blast Furnace Slag Cement Concrete Specimens Exposed to a RH of 25 %, Temperature of 45 °C and a Wind Velocity of 15 kmph

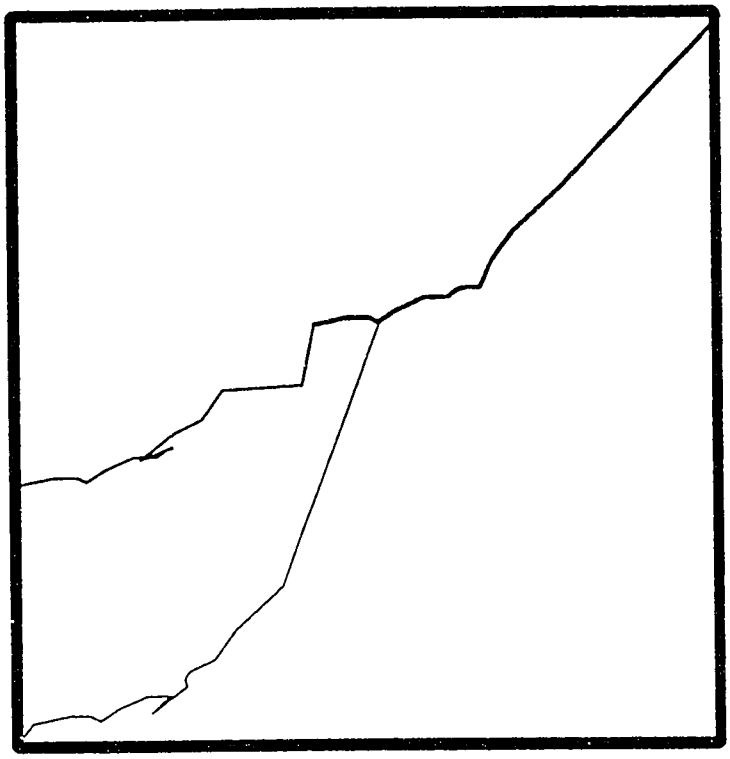

Figure 4.50: Typical Plastic Shrinkage Cracks in 30 % Fly Ash Cement Concrete Specimens Exposed to a RH of 25 %, Temperature of 45 °C and a Wind Velocity of 15 kmph

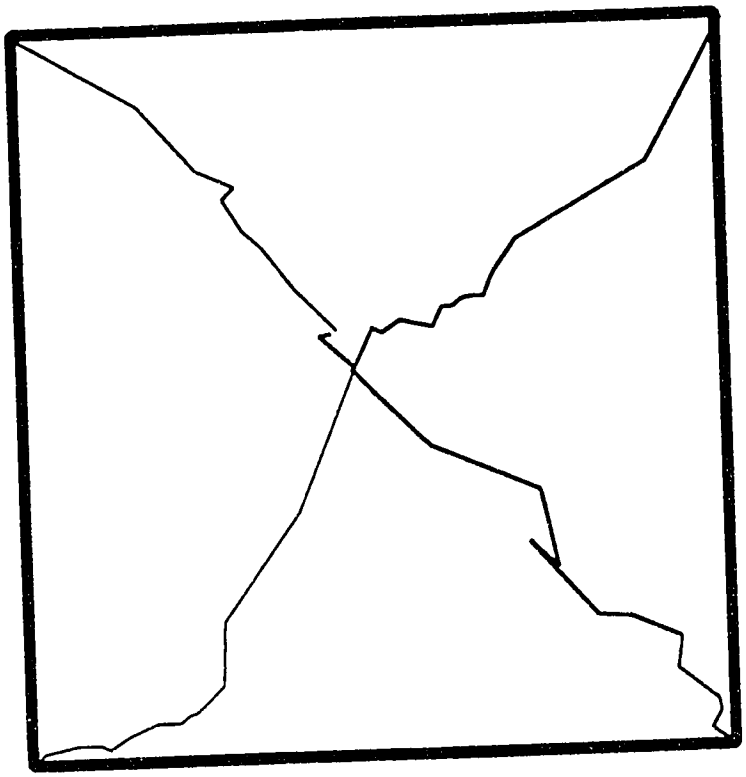

Figure 4.51: Typical Plastic Shrinkage Cracks in 10 % Silica Fume Cement Concrete Specimens Exposed to a RH of 25 %, Temperature of 45 °C and a Wind Velocity of 15 kmph

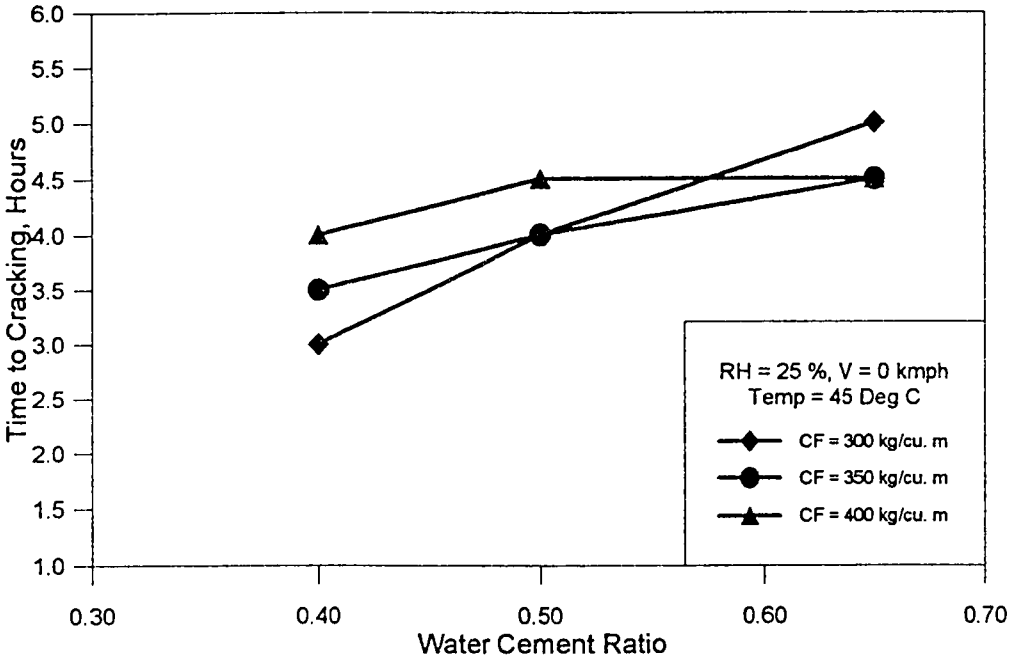

Figure 4.52: Effect of Water-Cement Ratio on Cracking Time (RH : 25% ; V : 0 kmph ; Temp : 45 °C)

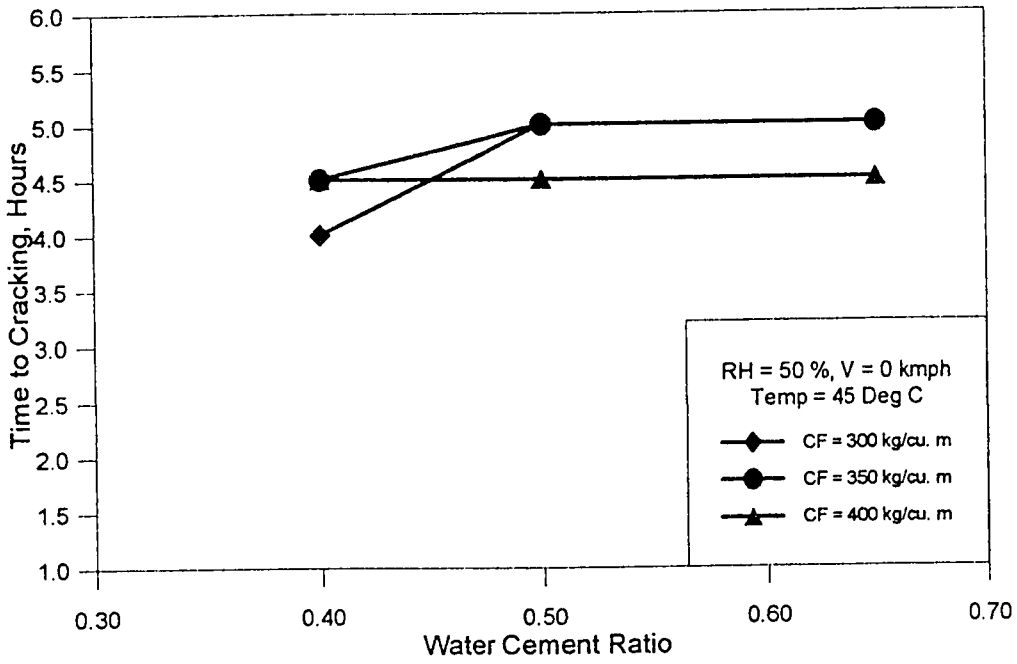

Figure 4.53: Effect of Water-Cement Ratio on Cracking Time (RH : 50% ; V : 0 kmph ; Temp : 45 °C)

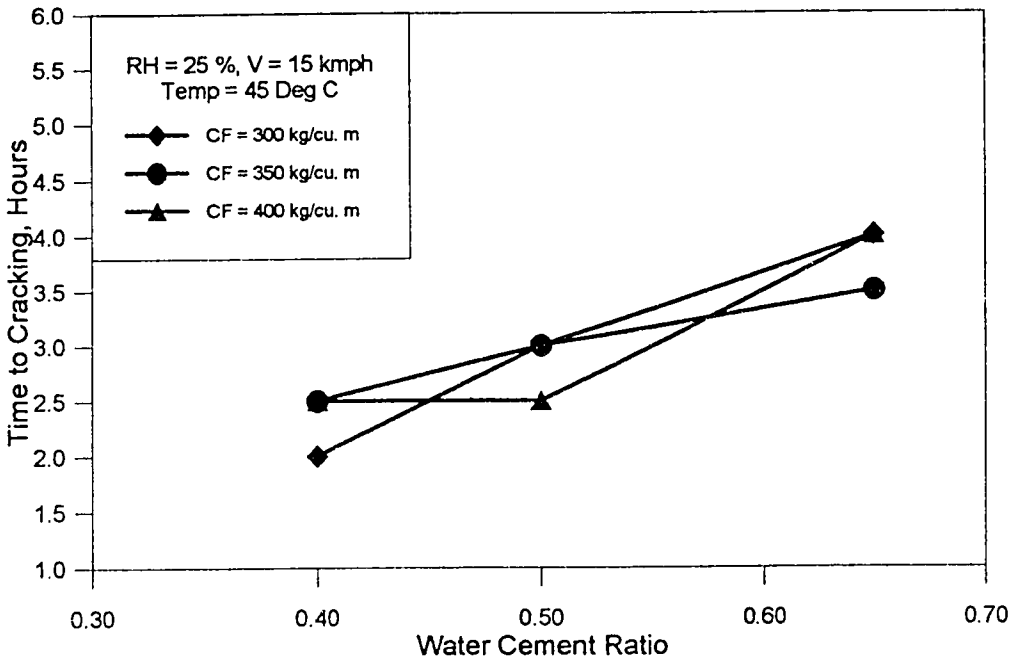

Figure 4.54: Effect of Water-Cement Ratio on Cracking Time (RH : 25% ; V : 15 kmph ; Temp : 45 °C)

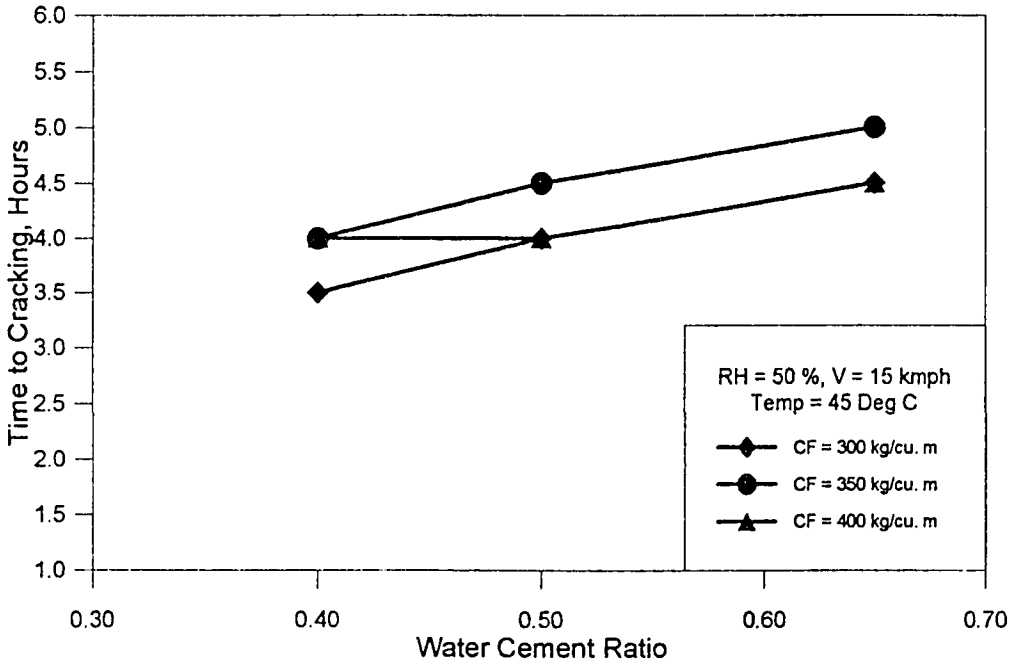

Figure 4.55: Effect of Water-Cement Ratio on Cracking Time (RH : 50% ; V : 15 kmph : Temp : 45 °C)

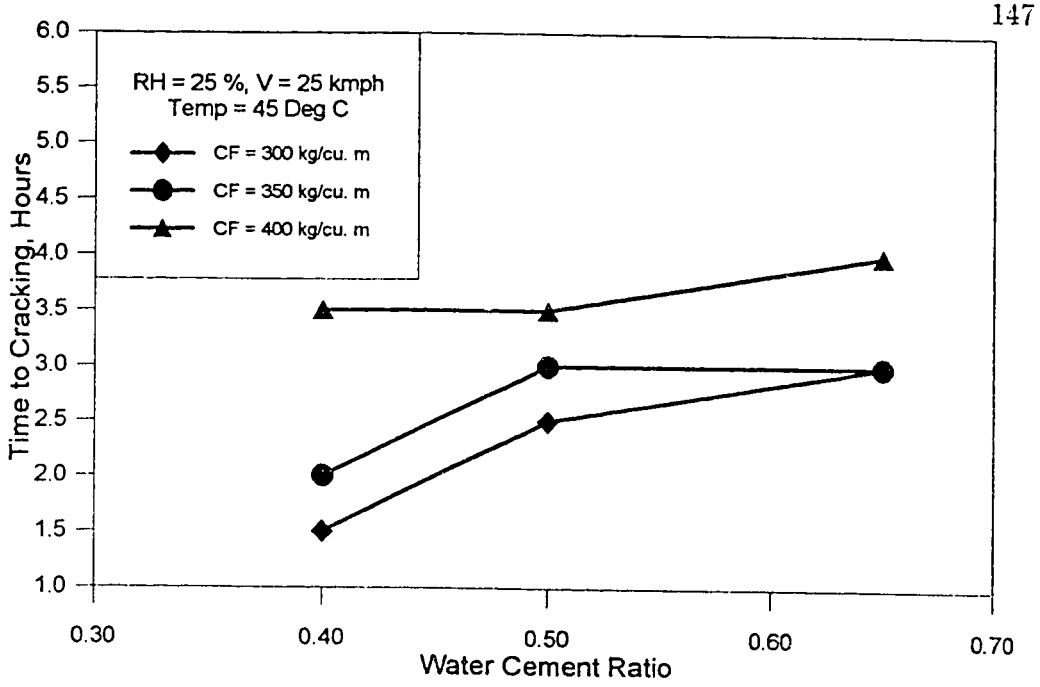

Figure 4.56: Effect of Water-Cement Ratio on Cracking Time (RH : 25% ; V : 25 kmph ; Temp : 45 °C)

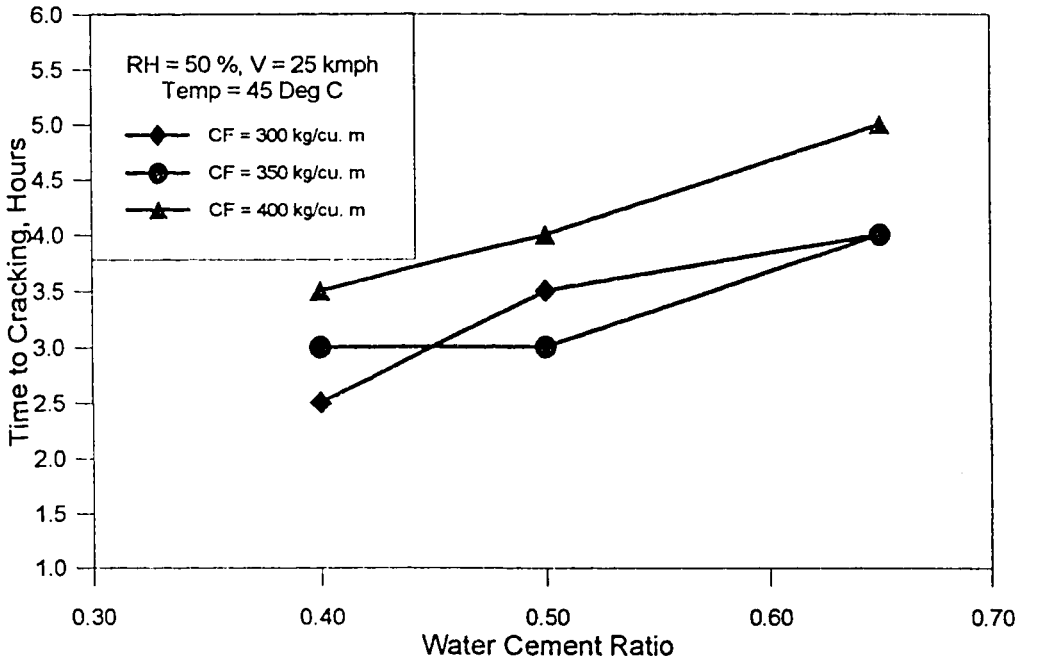

Figure 4.57: Effect of Water-Cement Ratio on Cracking Time (RH : 50% ; V : 25 kmph ; Temp : 45 °C)

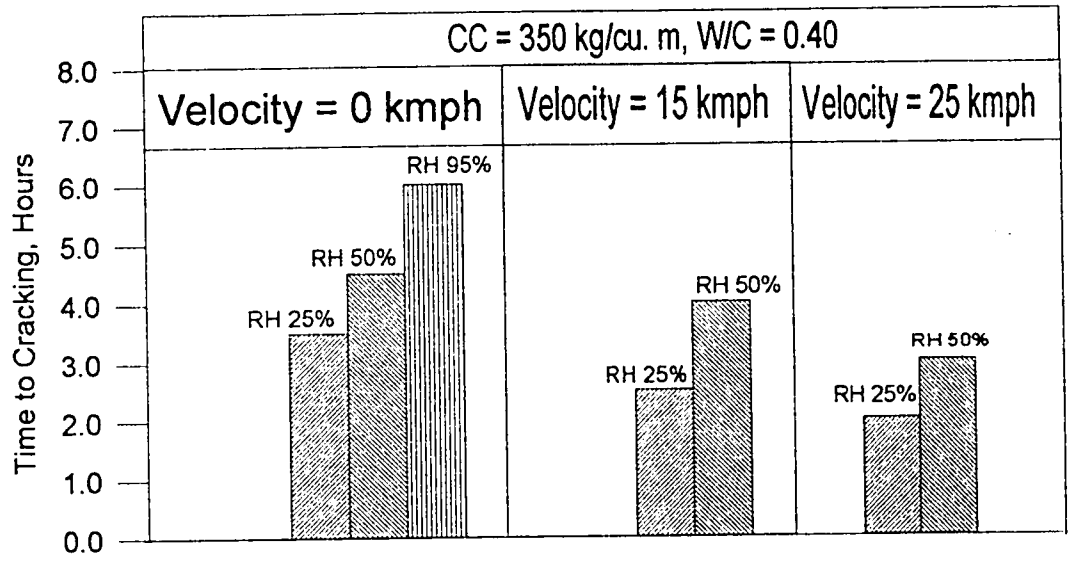

Figure 4.58: Effect of Relative Humidity and Wind Velocity on Cracking Time (CC: 350 kg/m^3 ; W/C : 0.40 ; Temp : 45 °C)

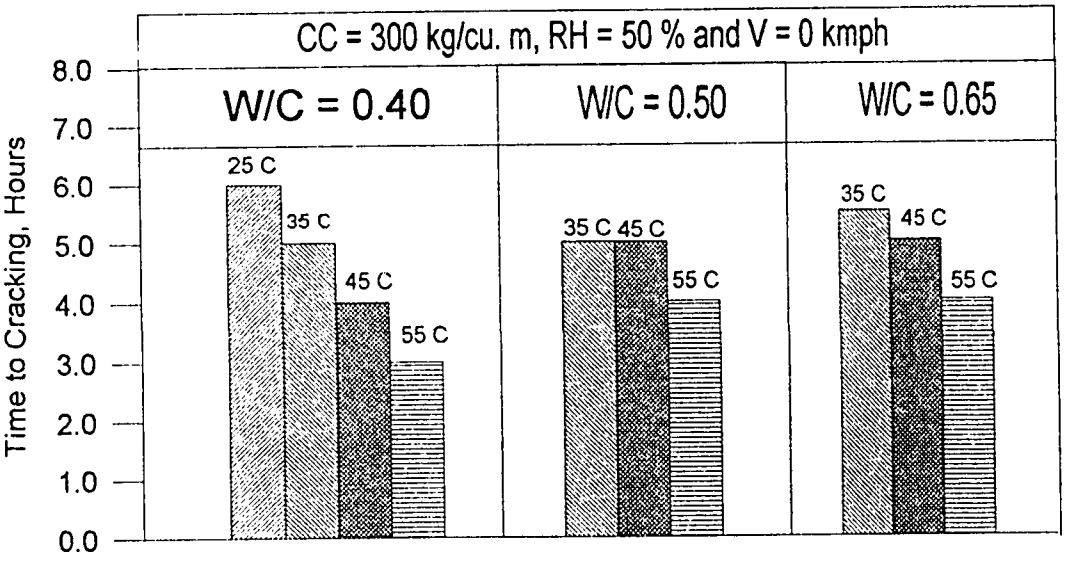

Figure 4.59: Effect of Ambient Temperature and Water-Cement Ratio on Cracking Time (RH : 50% ; V : 0 kmph ; CC : 300 kg/m^3)

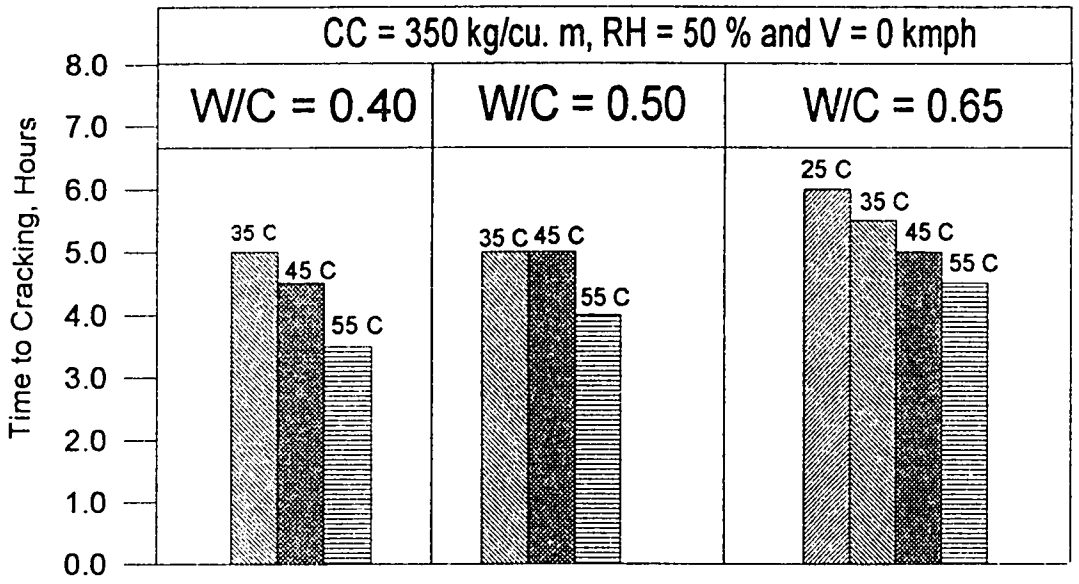

Figure 4.60: Effect of Ambient Temperature and Water-Cement Ratio on Cracking Time (RH : 50% ; V : 0 kmph ; CC : 350 kg/m^3)

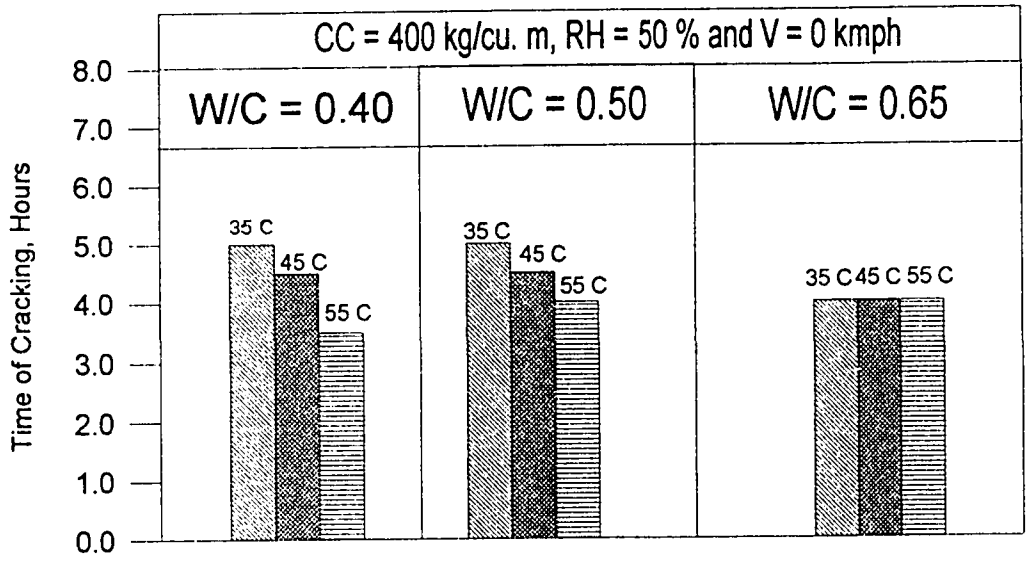

Figure 4.61: Effect of Ambient Temperature and Water-Cement Ratio on Cracking Time (RH : 50% ; V : 0 kmph ; CC : 400 kg/m^3)

Table 4.4: Efficient Concrete Mix for Various Environmental Conditions based on Cracking Intensity

Exposure Conditions	Most Efficient Mix	
	Cement Content (kg/m^3)	W/C Ratio
Normal T : 45°C ; RH : 50% ;	300 - 400	0.40 - 0.65
Hot-Dry T : 45°C ; RH : 25% ;	300	0.40
Hot-Normal T : 45°C ; RH : 50% ;	300	0.40
Hot-Humid T : 45°C ; RH : 95% ;	300	0.40
Hot-Dry Windy T : 45°C ; RH : 25% ; V : 25 km/h ;	300	0.40
Hot-Normal Windy T : 45°C ; RH : 50% ; V : 25 km/h ;	300	0.40

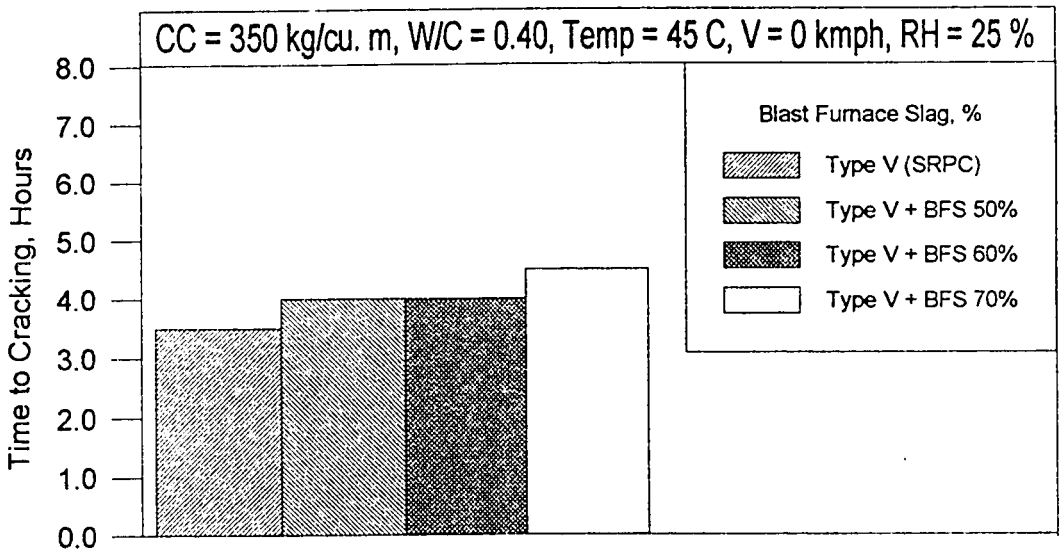

Figure 4.62: Cracking Time in the Blast Furnace Slag Cement Concrete (Temp : 45 °C ; V : 0 kmph ; CC : 350 kg/m^3 ; W/C : 0.40)

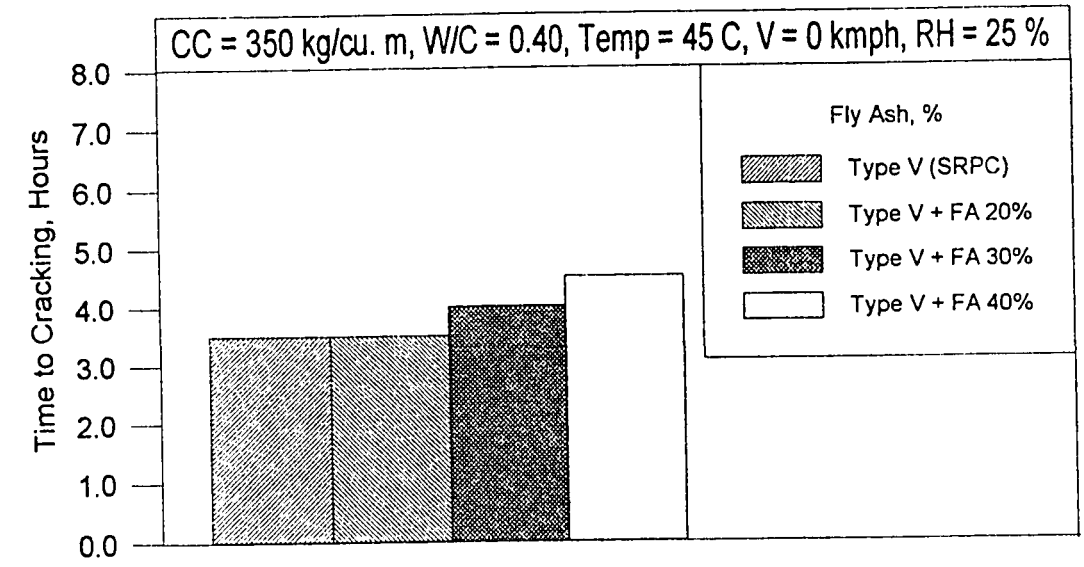

Figure 4.63: Cracking Time in the Fly Ash Cement Concrete (Temp : 45 °C ; V : 0 kmph ; CC : 350 kg/m^3 ; W/C : 0.40)

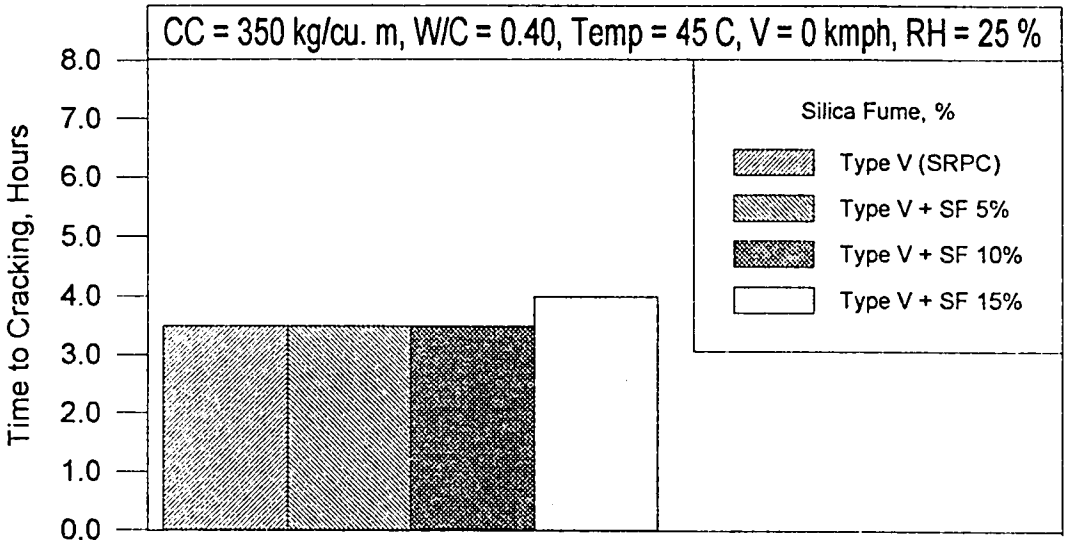

Figure 4.64: Cracking Time in the Silica Fume Cement Concrete (Temp : 45 °C ; V : 0 kmph ; CC : 350 kg/m^3 ; W/C : 0.40)

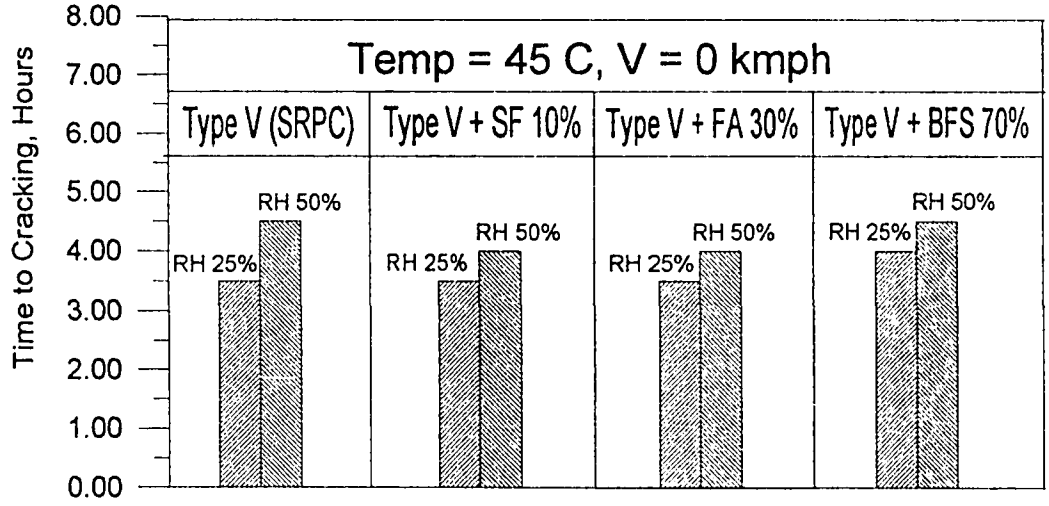

Figure 4.65: Effect of Relative Humidity on Cracking Time in Plain and Blended Cement Concretes (Temp : 45 °C ; V : 0 kmph ; CC : 350 kg/m^3 ; W/C : 0.40)

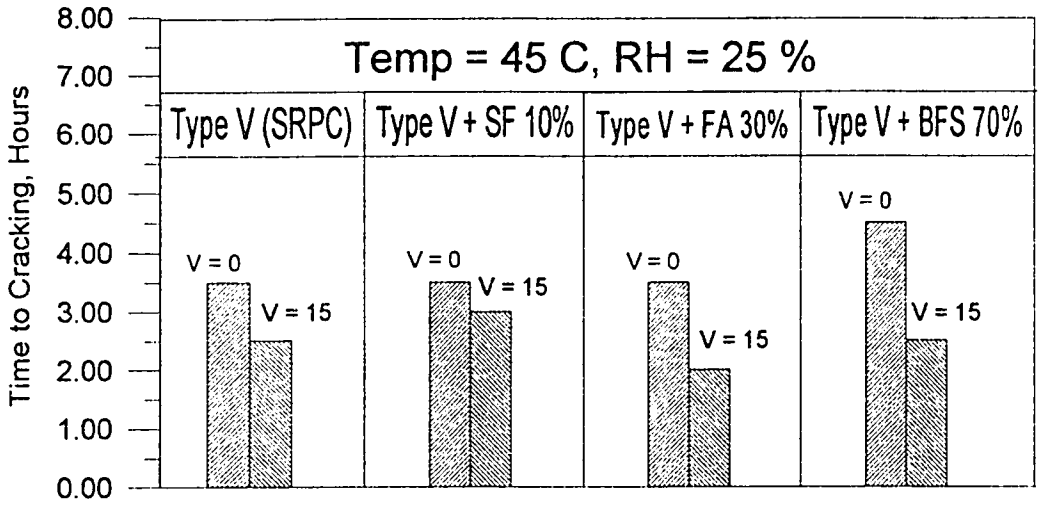

Figure 4.66: Effect of Wind Velocity on Cracking Time in Plain and Blended Cement Concretes (Temp : 45 °C ; RH : 25% ; CC : 350 kg/m^3 ; W/C : 0.40)

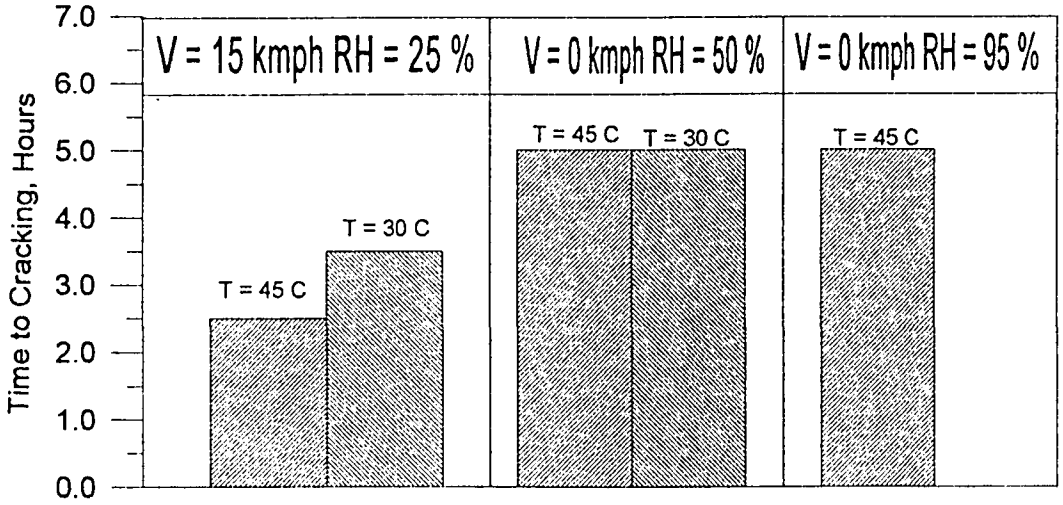

Figure 4.67: Effect of Ambient Temperature, Relative Humidity and Wind Velocity on Cracking Time in the Big Concrete Specimens (CC : 350 kg/m^3 ; W/C : 0.40)

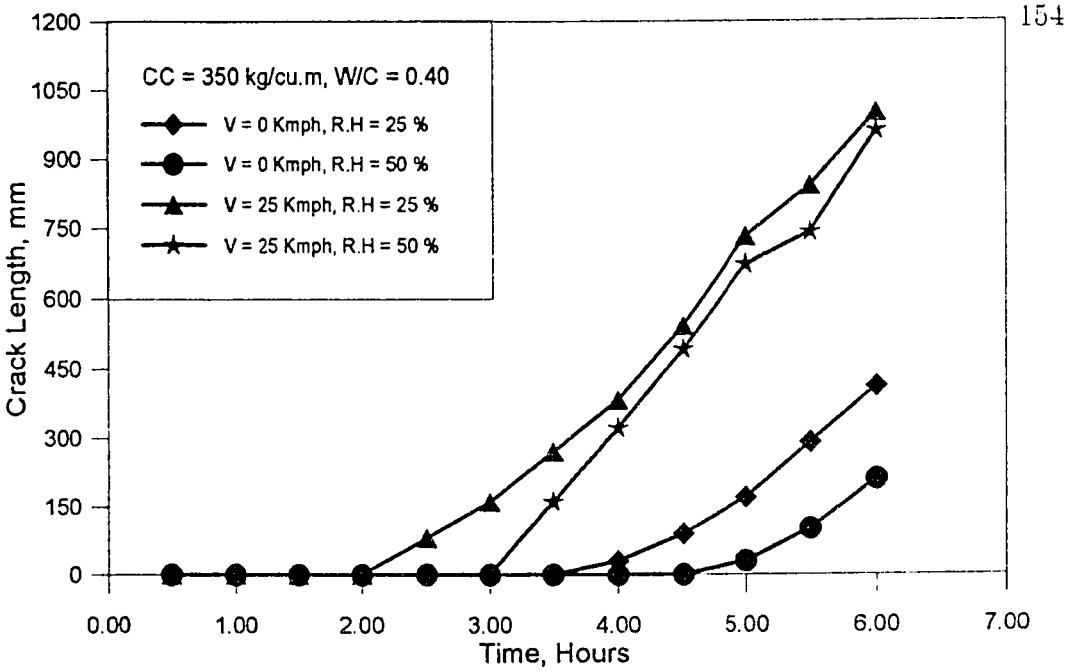

Figure 4.68: Effect of Relative Humidity and Wind Velocity on Development of Cracks (CC : 350 kg/m^3 ; W/C : 0.40 ; Temp : 45 °C)

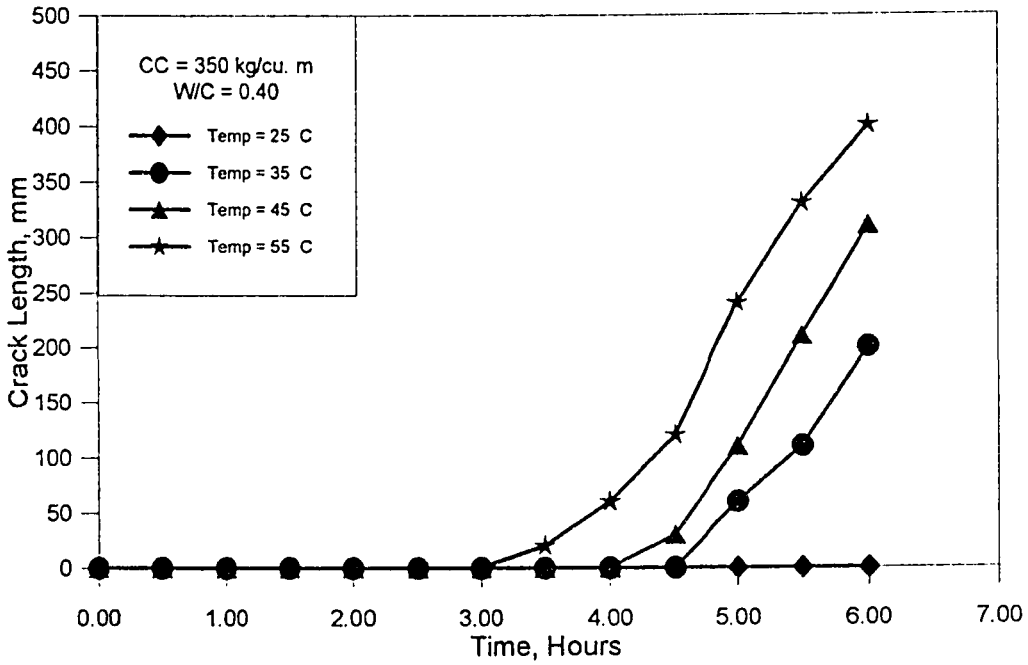

Figure 4.69: Effect of Ambient Temperature on Development of Cracks (CC : 350 kg/m^3 ; W/C : 0.40 ; RH : 50% ; V : 0 kmph)

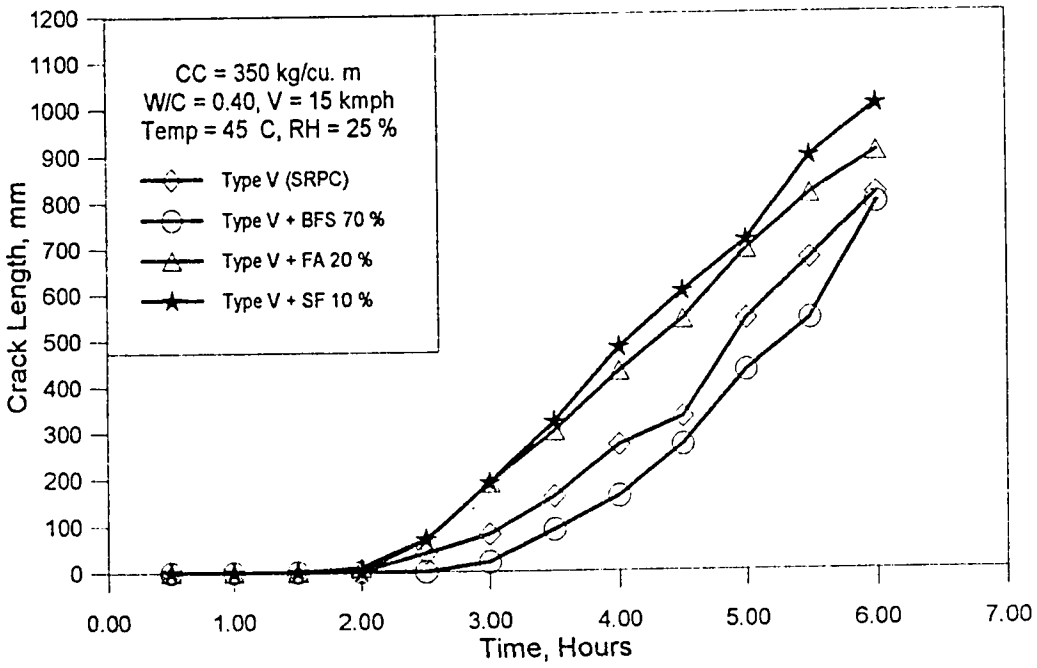

Figure 4.70: Development of Cracks in the Plain and Blended Cement Concretes (CC : 350 kg/m^3 ; W/C : 0.40 ; Temp : 45 °C ; V : 0 kmph ; RH : 25%)

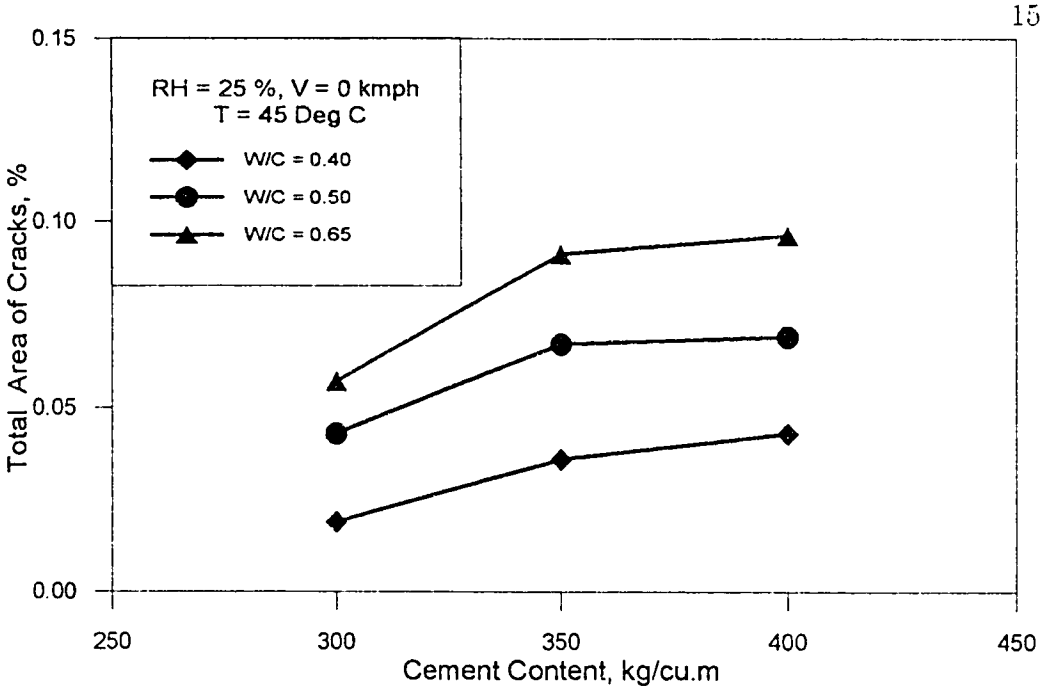

Figure 4.71: Effect of Cement Content on the Total Area of Cracks (RH : 25% ; V : 0 kmph ; Temp : 45 °C)

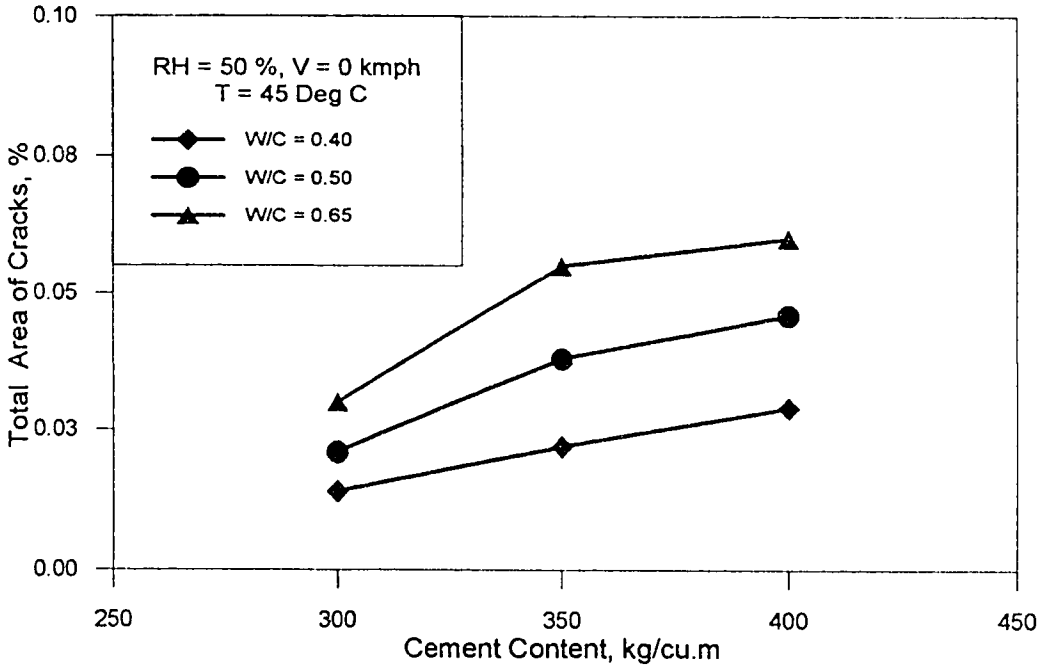

Figure 4.72: Effect of Cement Content on the Total Area of Cracks (RH : 50% ; V : 0 kmph ; Temp : 45 °C)

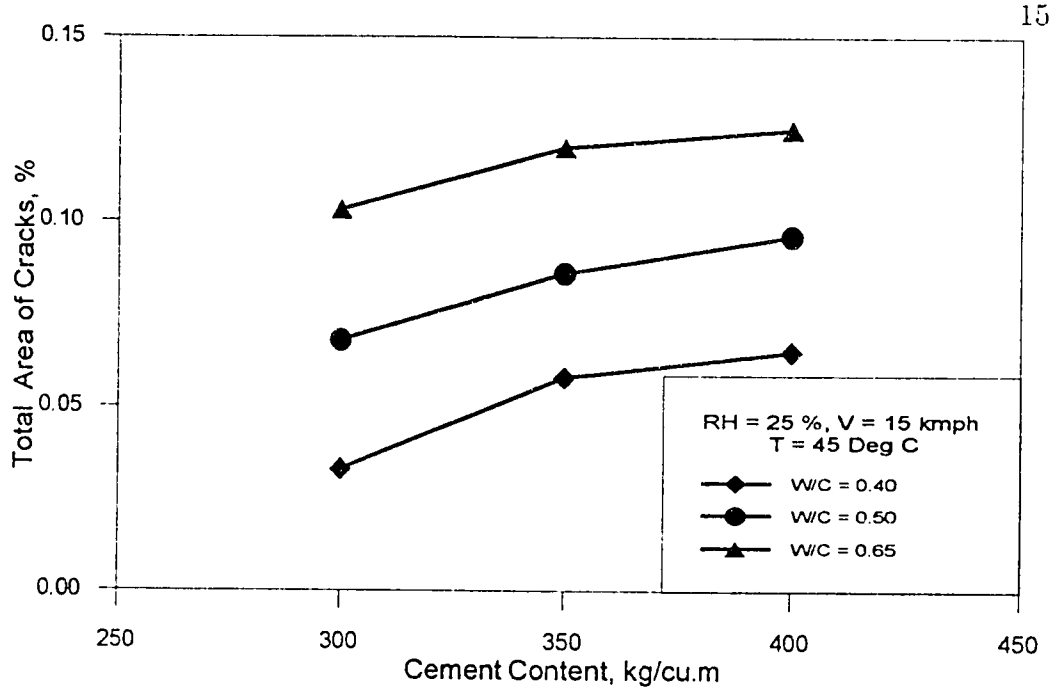

Figure 4.73: Effect of Cement Content on the Total Area of Cracks (RH : 25% ; V : 15 kmph ; Temp : 45 °C)

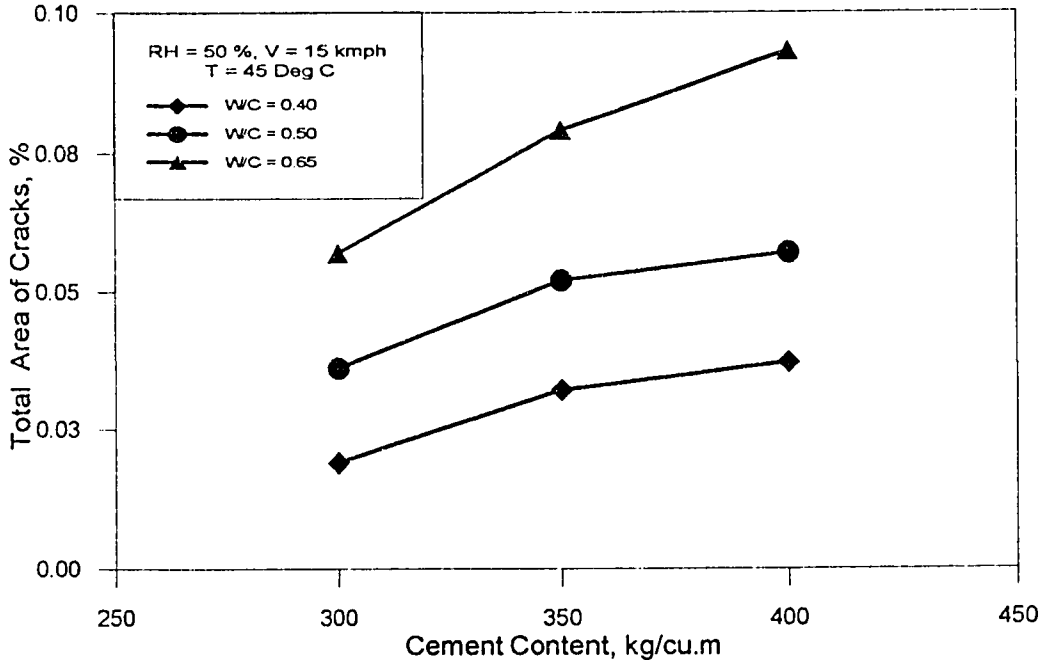

Figure 4.74: Effect of Cement Content on the Total Area of Cracks (RH : 50% ; V : 15 kmph ; Temp : 45 °C)

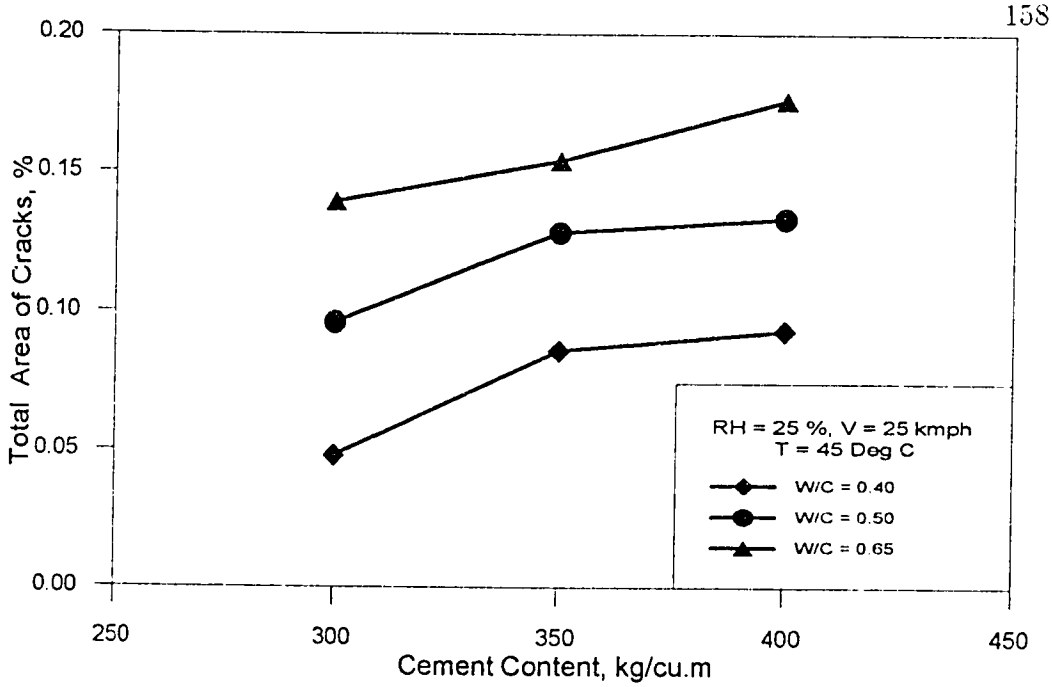

Figure 4.75: Effect of Cement Content on the Total Area of Cracks (RH : 25% ; V : 25 kmph ; Temp : 45 °C)

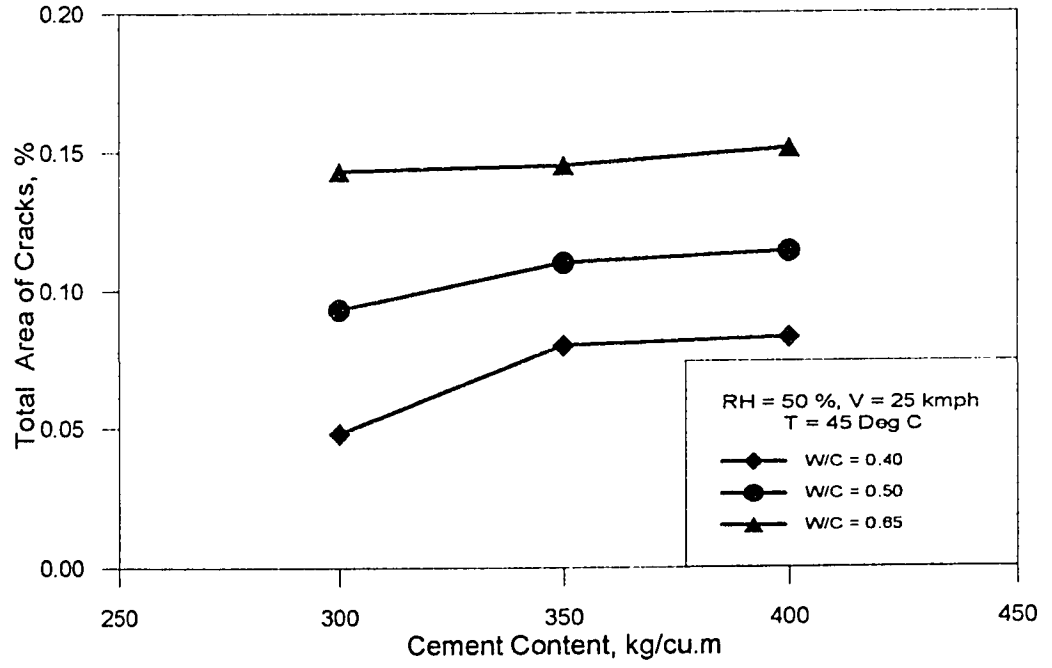

Figure 4.76: Effect of Cement Content on the Total Area of Cracks (RH : 50% ; V : 25 kmph ; Temp : 45 °C)

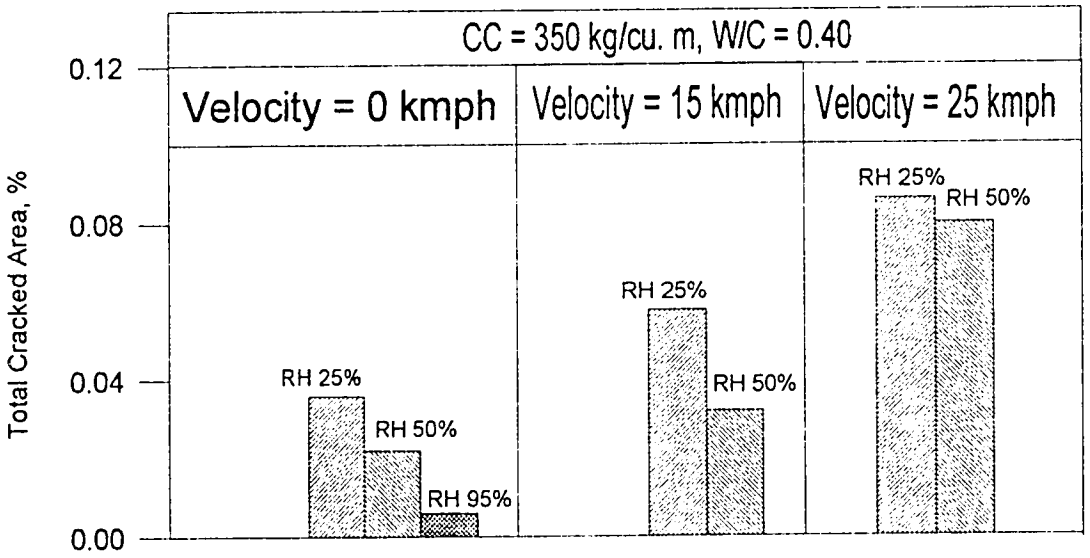

Figure 4.77: Effect of Relative Humidity and Wind Velocity on the Total Area of Cracks (CC : 350 kg/m^3 ; W/C : 0.40 ; Temp : 45 °C)

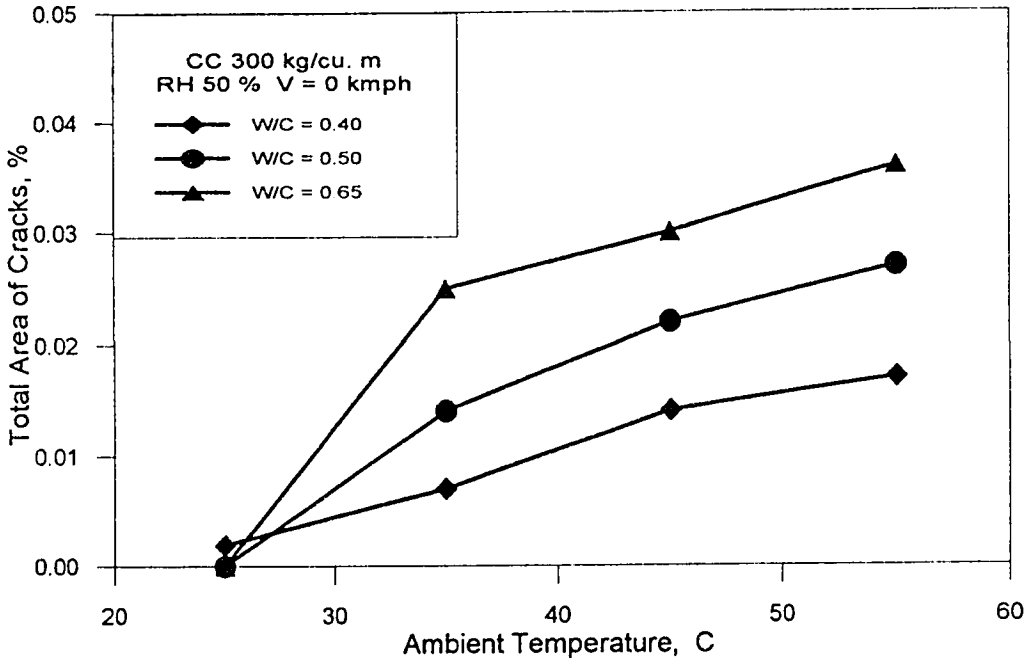

Figure 4.78: Effect of Ambient Temperature on the Total Area of Cracks (RH : 50%; V : 0 kmph ; CC : 300 kg/m^3)

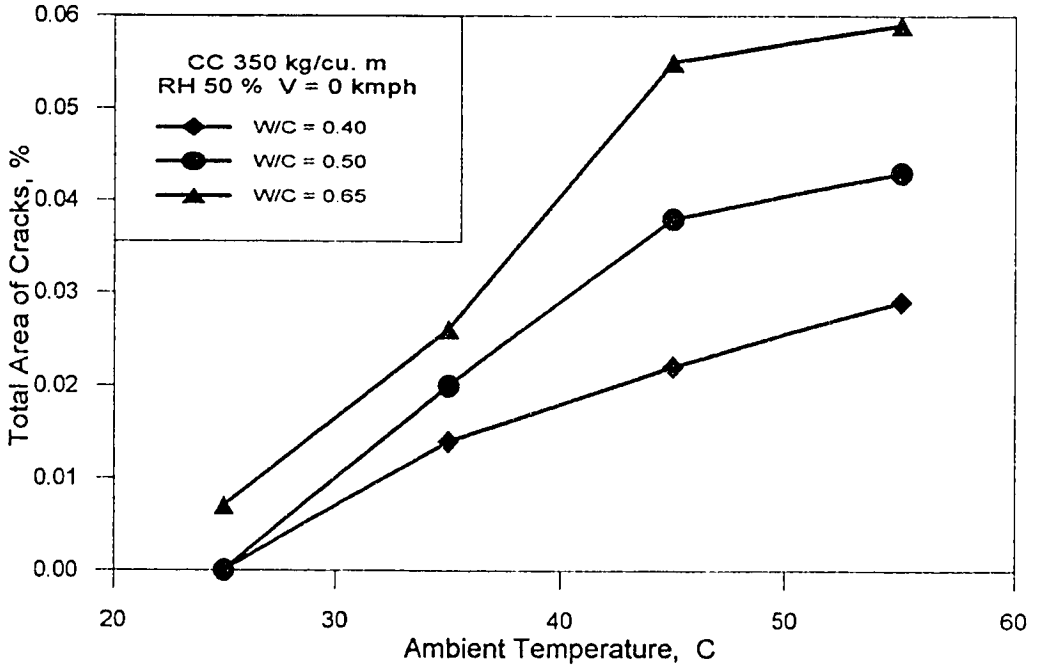

Figure 4.79: Effect of Ambient Temperature on the Total Area of Cracks (RH : 50%; V : 0 kmph ; CC : 350 kg/m^3)

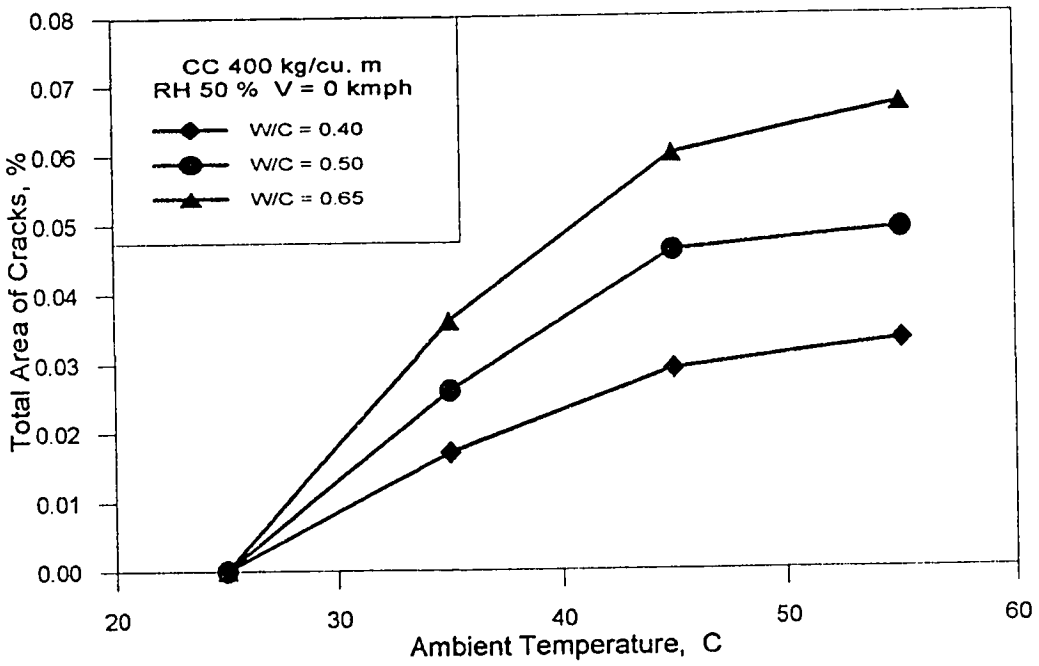

Figure 4.80: Effect of Ambient Temperature on the Total Area of Cracks (RH : 50%; V : 0 kmph ; CC : 400 kg/m^3)

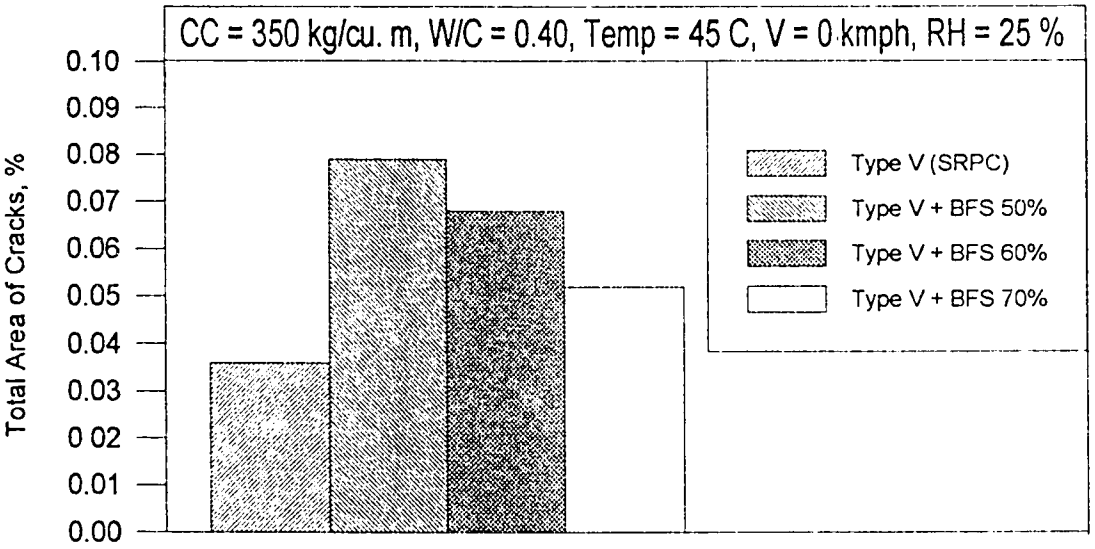

Figure 4.81: Total Area of Cracks in the Blast Furnace Slag Cement Concrete (Temp : 45 °C ; V : 0 kmph ; CC : 350 kg/m^3 ; W/C : 0.40)

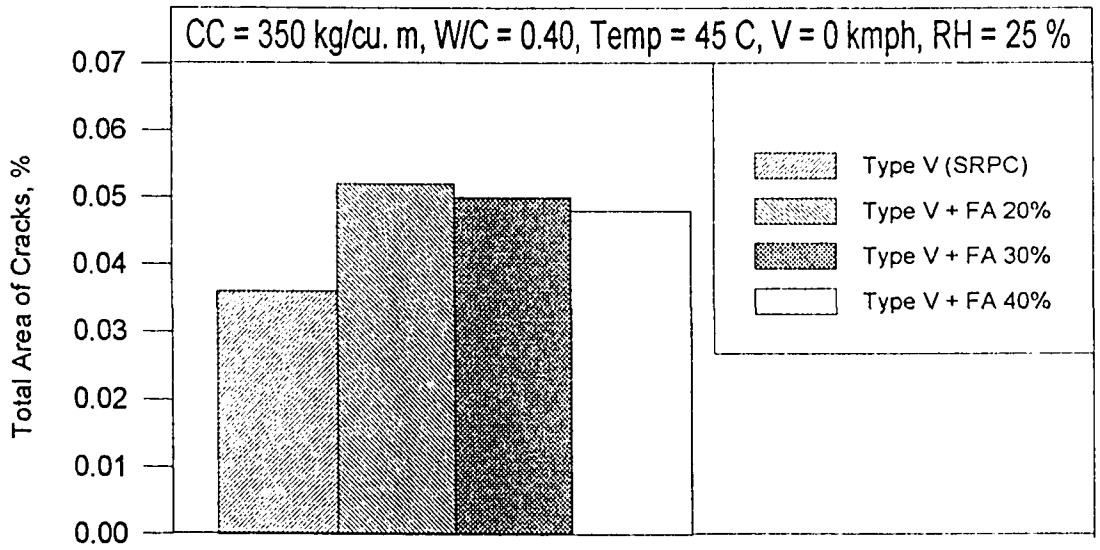

Figure 4.82: Total Area of Cracks in the Fly Ash Cement Concrete (Temp : 45 °C; V : 0 kmph ; CC : 350 kg/m^3 ; W/C : 0.40)

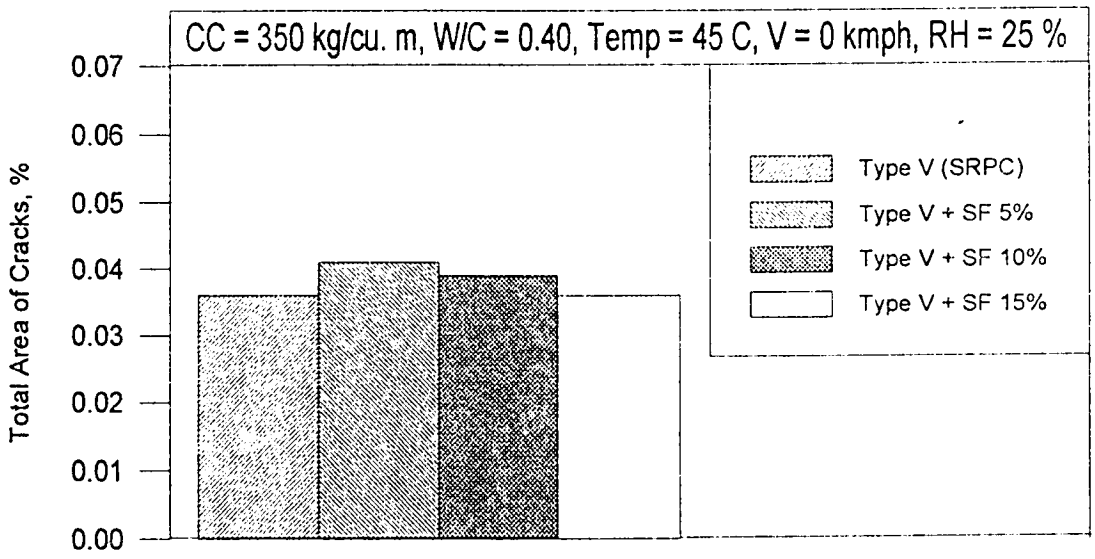

Figure 4.83: Total Area of Cracks in the Silica Fume Cement Concrete (Temp : 45 °C ; V : 0 kmph ; CC : 350 kg/m^3 ; W/C : 0.40)

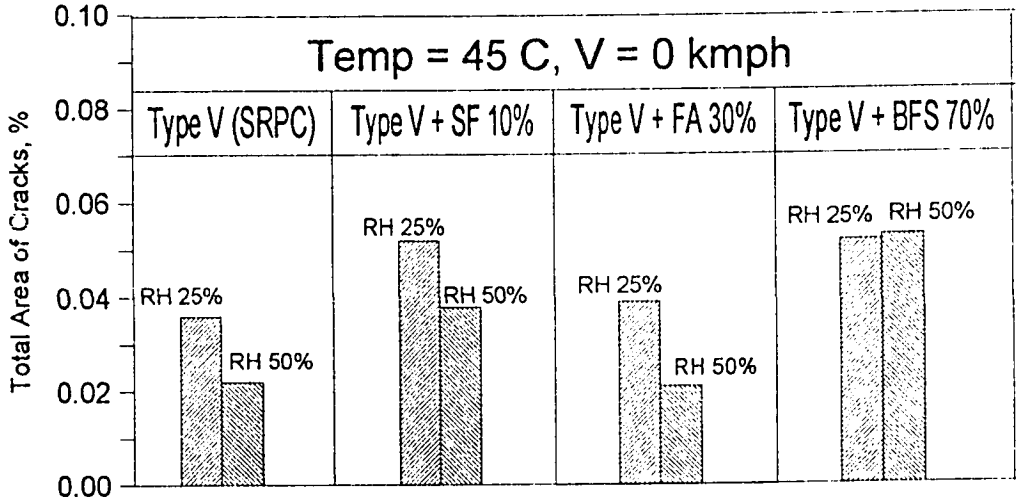

Figure 4.84: Effect of Relative Humidity on the Total Area of Cracks in Plain and Blended Cement Concretes (Temp : 45 °C ; V : 0 kmph ; CC : 350 kg/m^3 ; W/C : 0.40)

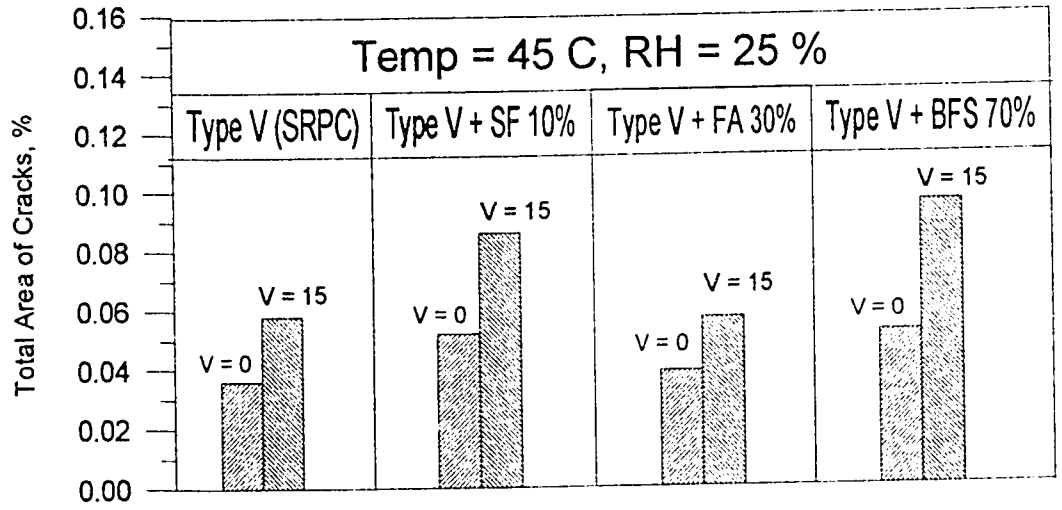

Figure 4.85: Effect of Wind Velocity on the Total Area of Cracks in Plain and Blended Cement Concretes (Temp : 45 °C ; RH : 25% ; CC : 350 kg/m^3 ; W/C : 0.40)

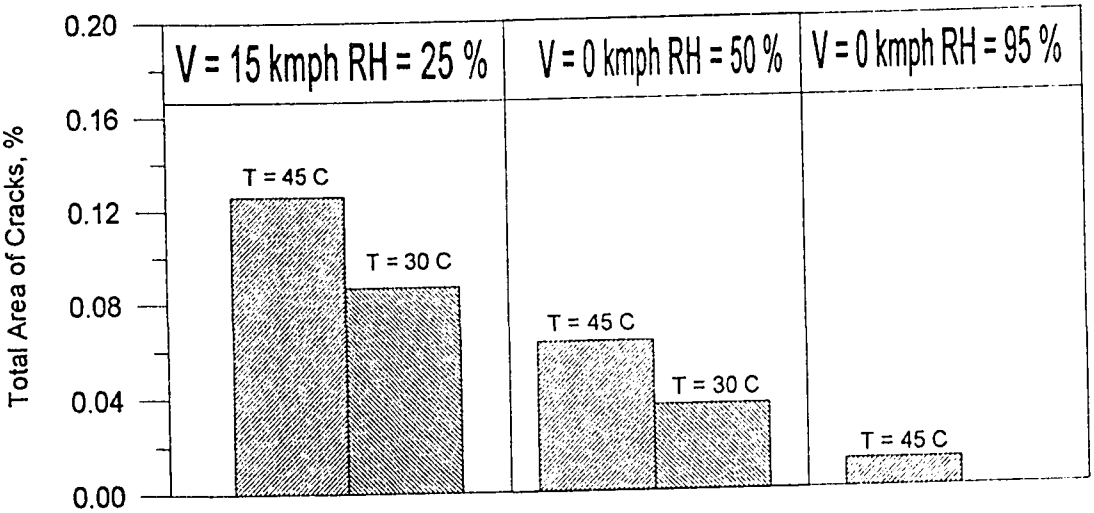

Figure 4.86: Effect of Ambient Temperature, Relative Humidity and Wind Velocity on the Total Area of Cracks in the Big Concrete Specimens (CC : 350 kg/m^3 ; W/C : 0.40)

4.3 RELATIONSHIP BETWEEN RATE OF EVAPORATION AND PLASTIC SHRINKAGE CRACKING

Figure 4.87 depicts the relationship between the rate of evaporation and cracking time in all the concrete mixtures and exposure conditions investigated in this study. As seen from the figure there is no relationship between the rate of evaporation and the cracking time.

Figure 4.88 shows the relationship between the rate of evaporation and the total cracked area in all the concrete mixtures and exposure conditions investigated in this study. As seen from the figure, there exists a definite relationship between the rate of evaporation and total cracked area. This result was also noted in Tables 4.3 and 4.4 which show that the efficient mixes for all the conditions based on the rate of evaporation and the total cracked area were similar.

4.4 EFFECT OF EXPOSURE CONDITIONS ON CONCRETE SURFACE TEMPERATURE

Figure 4.89 shows the effect of relative humidity and wind velocity on the concrete surface temperature in a typical concrete mix made with a cement content of 350 kg/m^3, water-cement ratio of 0.40 and exposed to an ambient temperature of 45 °C. The surface temperature in the concrete specimens exposed to a wind velocity of 25 kmph was higher than that in the specimens exposed to no wind. The surface temperature was, however, nearly the same in the concrete specimens exposed to a RH of 25 and 50 %, irrespective of the wind velocity. The surface temperature was 47 °C in the specimens exposed to windy conditions, whereas it was 37 °C when there was no wind. Another important feature to be noticed from these data is that the surface temperature in the specimens exposed to windy conditions increased rapidly from around 30 to 47 °C in three hours and was constant thereafter, whereas in the specimens exposed to no wind it was nearly constant at 35 °C till the end of the experiment. The higher surface temperature noted in the specimens exposed to windy conditions may be attributed to the increased rate of evaporation.

Figure 4.90 shows the effect of ambient temperature on the concrete surface temperature in a typical concrete mix with a cement content of 350 kg/m^3, water-

cement ratio of 0.40 and exposed to a RH of 50 %. The surface temperature increased with increasing ambient temperature. In the specimens exposed to 25 and 35 °C, the surface temperature remains more or less similar at 28 and 30 °C. However, in the specimens exposed to 45 and 55 °C, the surface temperature increased with time. After six hours, the surface temperature in these specimens was 38 and 43 °C, respectively.

The concrete surface temperature in the plain and blended cement concrete specimens is shown in Figure 4.91. These specimens were made with a cementitious materials content of 350 kg/m^3, water-cementitious materials ratio of 0.40 and exposed to a RH of 25 % and ambient temperature of 45 °C. The surface temperature in both the plain and blended cement concrete specimens increased with time. After six hours, the concrete surface temperature was 45 °C in all the specimens.

4.5 EFFECT OF CONCRETE COMPOSITION ON BLEEDING

Figures 4.92 through 4.94 show the effect of water-cement ratio on bleeding in the concrete specimens with varying cement content. Figures 4.95 and 4.96 show the percentage of bleed water in the plain and blended cement concretes.

Figure 4.92 shows the effect of water-cement ratio on the cumulative bleed water in concrete mixes made with a cement content of 300 kg/m^3. Bleeding was influenced

by the water-cement ratio, increasing with increasing water-cement ratio. Bleeding in concrete mixes with a water-cement ratio of 0.40 and 0.50 stopped after 1 hour whereas in the mix with a water-cement ratio of 0.65 it ceased after 3.5 hours. The cumulative bleed water in the concrete with a water-cement ratio of 0.40 was 0.20 kg/m^2, whereas it was 1.6 kg/m^2 in the concrete with a water-cement ratio of 0.50. In the concrete mixes with a water-cement ratio of 0.65, the cumulative bleed water was as high as 4 kg/m^2. A similar trend was observed in the concrete mixes with a cement content of 350 kg/m^3 (Figure 4.93) and 400 kg/m^3 (Figure 4.94).

Figure 4.95 shows the effect of mix proportions on the total bleed water in the plain cement concrete mixes. The total bleed water increased with increasing water-cement ratio and cement content, but it was affected more by the former than the latter. A significant increase in the bleed water was noted when the cement content was increased from 300 to 350 kg/m^3. However, quantity of bleed water in the concrete with a cement content of 400 kg/m^3 was not significantly different than those made with a cement content of 350 kg/m^3. In the concrete mixes made with a cement content of 350 kg/m^3 and a water-cement ratio of 0.40 the bleed water was 0.5 % and it increased to 3 % in the concrete with a cement content of 400 kg/m^3, water-cement ratio being the same. But the percentage of bleed water increased to 7 % when the water-cement ratio was increased to 0.65 with the cement content being constant at 300 kg/m^3. From this it can be inferred that bleeding increases both with the water-cement ratio and the cement content. The reason for an increase in

bleed water may be the increase in the volume of water added to the mix.

Figure 4.96 shows the cumulative bleed water in the plain and blended cement concrete specimens. These concrete mixes were made with a cementitious material content of 350 kg/m^3 and a water-cementitious materials ratio of 0.40. Maximum bleeding was measured in the plain cement concrete mixes, and minimum bleeding was observed in the 5 % silica fume cement concrete. Bleeding in the fly ash and BFS cement concrete specimens was also lower than that in the plain cement concrete specimens. In the silica fume cement concrete specimens bleeding was in the range of 0.9 to 1.5 %, while in the fly ash and BFS cement concrete it was in the range from 1.2 to 1.7 % and 1.5 to 1.8 %, respectively. In the plain cement concrete it was 1.85 %.

4.6 RELATIONSHIP BETWEEN BLEEDING, RATE OF EVAPORATION AND PLASTIC SHRINKAGE CRACKING

The experimental data indicates that the rate of evaporation is greater than the rate of bleeding in nearly all the exposure conditions and for all the mixes. The bleeding in most of the mixes ceased after 1 to 3 hours, whereas the rate of evaporation continues upto nearly 6 hours. Initially the bleeding was greater than the rate of

evaporation but with time either the bleeding reduced or stopped whereas the rate of evaporation remained nearly constant. One more interesting point observed was the occurrence of cracks earlier in the lean-stiff mixes, where the bleeding was very low and continues upto only one hour after casting. In the rich plastic concrete mixes, bleeding was high and continued upto nearly five hours after casting. From this observations it can be inferred that whenever the bleeding stops or the rate of evaporation exceeds the bleeding rate, plastic shrinkage cracking can occur.

4.7 EFFECT OF EXPOSURE CONDITIONS ON PLASTIC SHRINKAGE STRAIN

Figure 4.97 shows the effect of ambient temperature on the plastic shrinkage strain in a typical concrete mix with a cement content of 350 kg/m^3, water-cement ratio of 0.40, and exposed to a RH of 25 % and a wind of 15 kmph. Plastic shrinkage strain increased with the ambient temperature. After 24 hours of casting, the plastic shrinkage strain was 7000 micro strain in the specimens exposed to 45 °C, while it was 3500 micro strain in those exposed to 30 °C. A similar trend was observed in the specimens exposed to a RH of 50 % (Figure 4.98) and a RH of 95 % (Figure 4.99).

Figure 4.100 summarizes the effect of exposure conditions on plastic shrinkage strain in the big concrete specimens. These specimens were made with a cement

content of 350 kg/m^3 and a water-cement ratio of 0.40. In these specimens also plastic shrinkage strain increased with the exposure temperature, and decreased with increasing relative humidity. The decrease in plastic shrinkage strain was in the range of 1000 micro strain when the RH was increased from 50 to 95 %.

4.8 EFFECT OF SPECIMEN SIZE ON PLASTIC SHRINKAGE

The effect of specimen size on water evaporation and plastic shrinkage cracking is shown in Figure 4.101. The big specimen were 3 x 3 feet and 2 inch thick, whereas the small small specimen were 1.5 x 1.5 feet and 3/4 inch thick. The cement content and water-cement ratio in these specimens was 350 kg/m^3 and 0.40 and they were exposed to a RH of 25 %, temperature of 45 °C and wind velocity of 15 kmph. The rate of evaporation was nearly twice in the small specimens compared to big specimens. However, the percentage water evaporated and time to cracking were nearly the same in both the types of specimens. The total cracked area in the big specimens was twice that in the small specimens. Further, the rate of evaporation decreases and cracking intensity increases with increasing size of the specimen.

4.9 EFFECT OF EXPOSURE CONDITIONS ON THE PROPERTIES OF HARDENED CONCRETE

In this part of the study, the effect of different exposure conditions on the compressive strength and microstructure of concrete was evaluated. The microstructure of hardened concrete was studied by measuring the ultrasonic pulse velocity and the pore size distribution.

4.9.1 Compressive Strength

The effect of different exposure conditions on the compressive strength of concrete specimens is shown in Figure 4.102. These specimens were prepared with a cement content of 350 kg/m^3 and a water-cement ratio of 0.40. The compressive strength in the specimens exposed to 30 °C was more than those exposed to 45 °C. An average change of 5 MPa was measured in the specimens exposed to all the exposure conditions. The effect of varying the wind velocity and the relative humidity on the compressive strength was, however, insignificant.

4.9.2 Pulse Velocity

The effect of exposure conditions on the pulse velocity of concrete specimens is shown in Figure 4.103. The trend of these data was more or less similar to that of the compressive strength. The concrete specimens exposed to 30 °C were more dense than those exposed to 45 °C. The pulse velocity in the specimens exposed to 30 °C was 1000 m/s more than that of those exposed to 45 °C. The relative humidity and wind velocity had an insignificant effect on the pulse velocity.

4.9.3 Porosity

Figures 4.104 through 4.106 show the pore size distribution in the concrete specimens exposed to varying environmental conditions. Figure 4.107 shows the effect of exposure conditions on the cumulative pore volume.

Figure 4.104 shows the effect of ambient temperature on the pore size distribution in a typical concrete mix made with a cement content of 350 kg/m^3, water-cement ratio of 0.40 and exposed to a RH of 25 % and a wind velocity of 15 kmph. The volume of coarse pores in the specimens exposed to 45 °C was more than those exposed to 30 °C. The cumulative pore volume in the specimens exposed to 45 °C was 55 mm^3/gm, whereas it was 23 mm^3/gm in those exposed to 30 °C. A similar trend was observed in the specimens exposed to a RH of 50 and 95 %, as shown in Figures 4.105 and 4.106, respectively.

The data in Figures 4.104 through 4.106, indicate that the cumulative pore volume increases with increasing exposure temperature. This may be attributed to the fact that, at low temperatures, the hydration products have sufficient time to diffuse throughout the cement paste matrix thereby precipitating uniformly. However, at higher temperature, the rate of hydration reactions is much faster than the rate of diffusion, due to which the hydration products remains near the cement grains, leaving the interstitial space relatively open. The results also show that the temperature has a greater effect on the finer pores. It can thus be concluded that high exposure temperatures have detrimental effect on the pore volume and hence the porosity.

Figure 4.107 summarizes the effect of exposure conditions on the cumulative pore volume. These specimens were made with a cement content of 350 kg/m^3 and a water-cement ratio of 0.40. As discussed earlier, the cumulative pore volume in the specimens exposed to 45 °C was more than those exposed to 30 °C. In the specimens exposed to no wind, the increase in the cumulative pore volume was more prominent in the specimens exposed to a RH of 50 % than those exposed to a RH of 95 %. This increase in the pore volume may be attributed to the reduced humidity which may lead to increased evaporation, thus retarding the cement hydration.

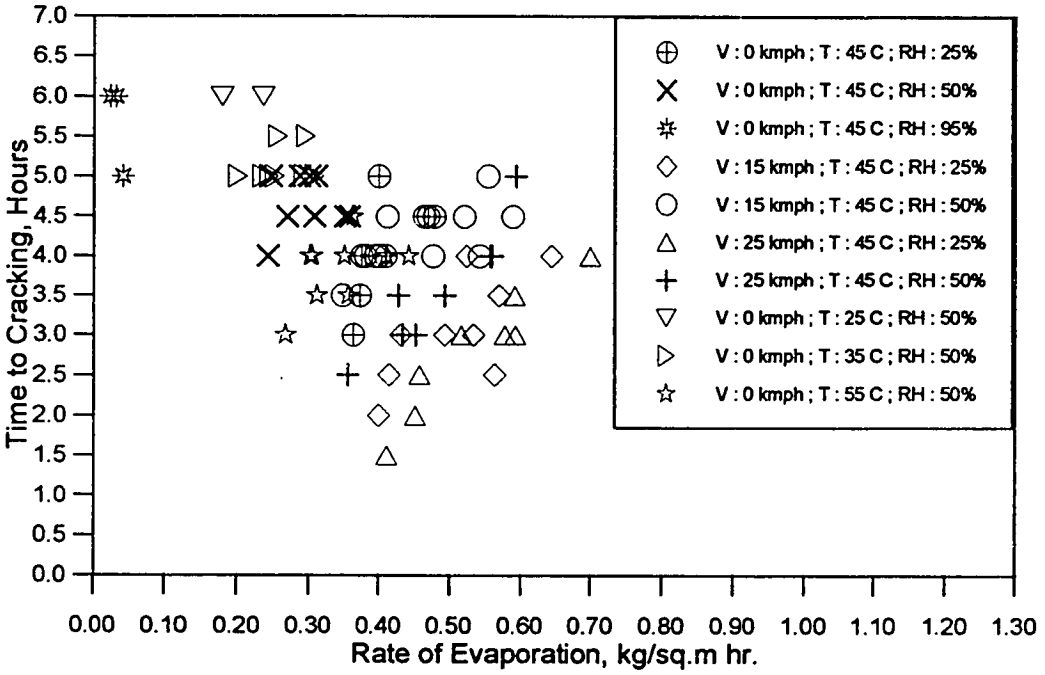

Figure 4.87: Relationship Between Rate of Evaporation and Cracking Time

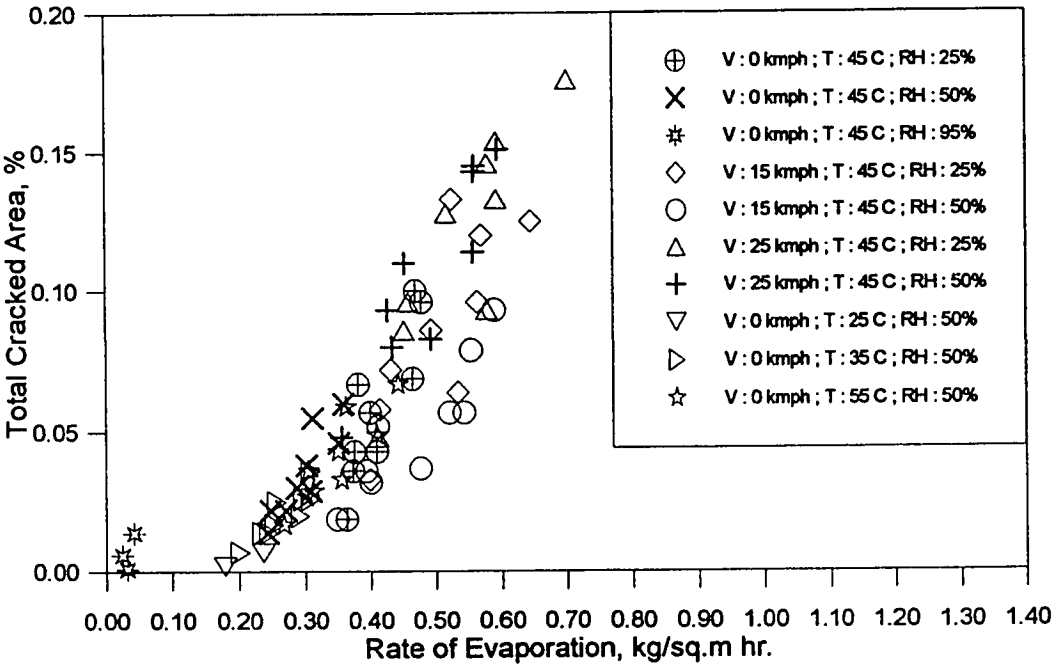

Figure 4.88: Relationship Between Rate of Evaporation and the Total Cracked Area

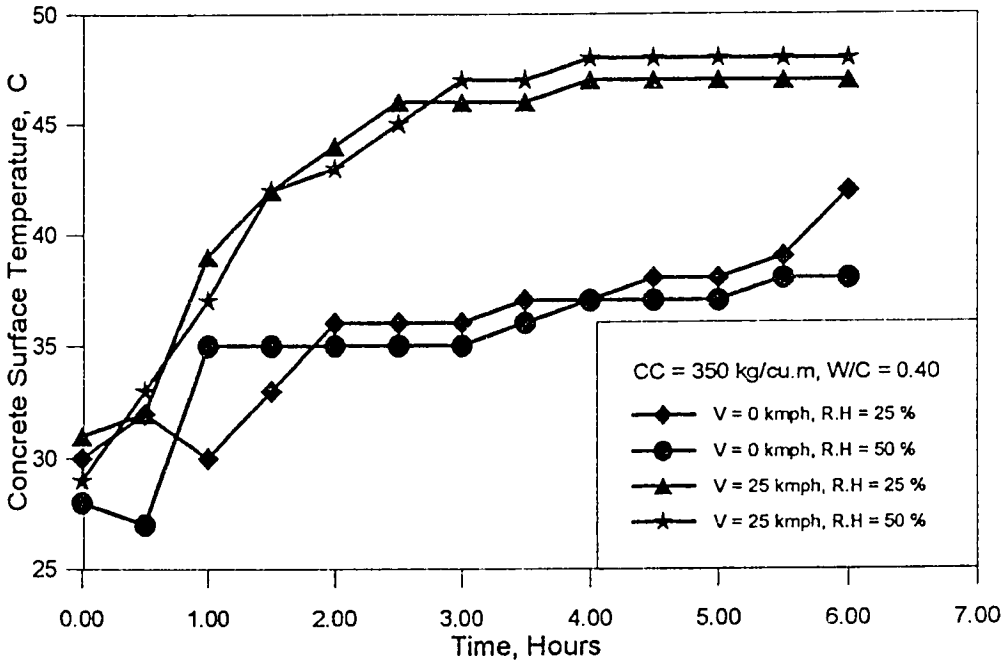

Figure 4.89: Effect of Relative Humidity and Wind Velocity on Concrete Temperature (CC : 350 kg/m^3 ; W/C : 0.40 ; Temp : 45 °C)

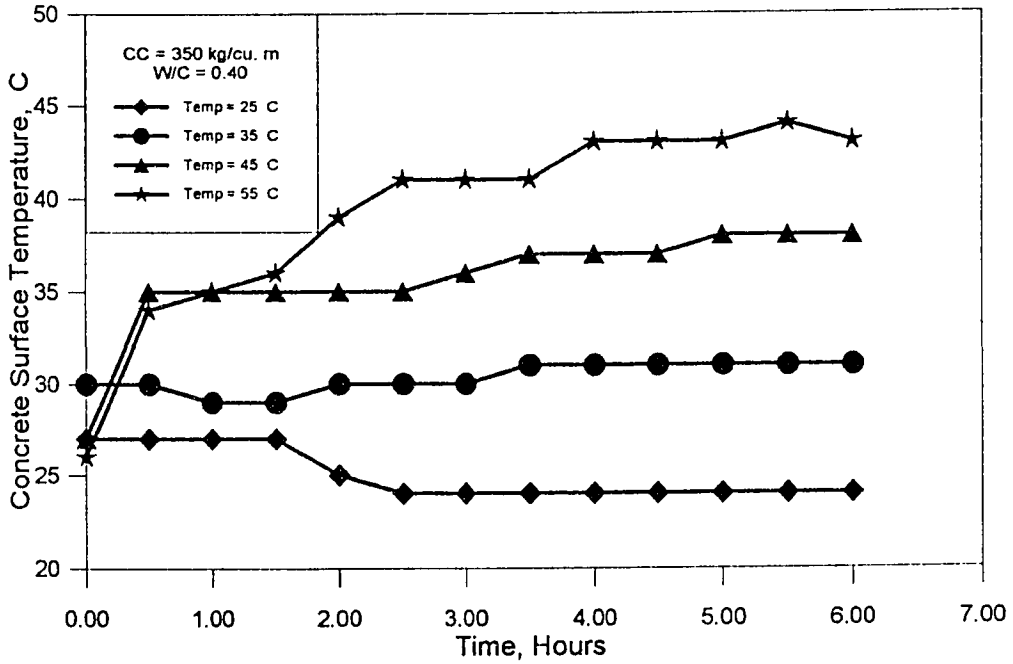

Figure 4.90: Effect of Ambient Temperature on Concrete Temperature (CC : 350 kg/m^3 ; W/C : 0.40 ; RH : 50% ; V : 0 kmph)

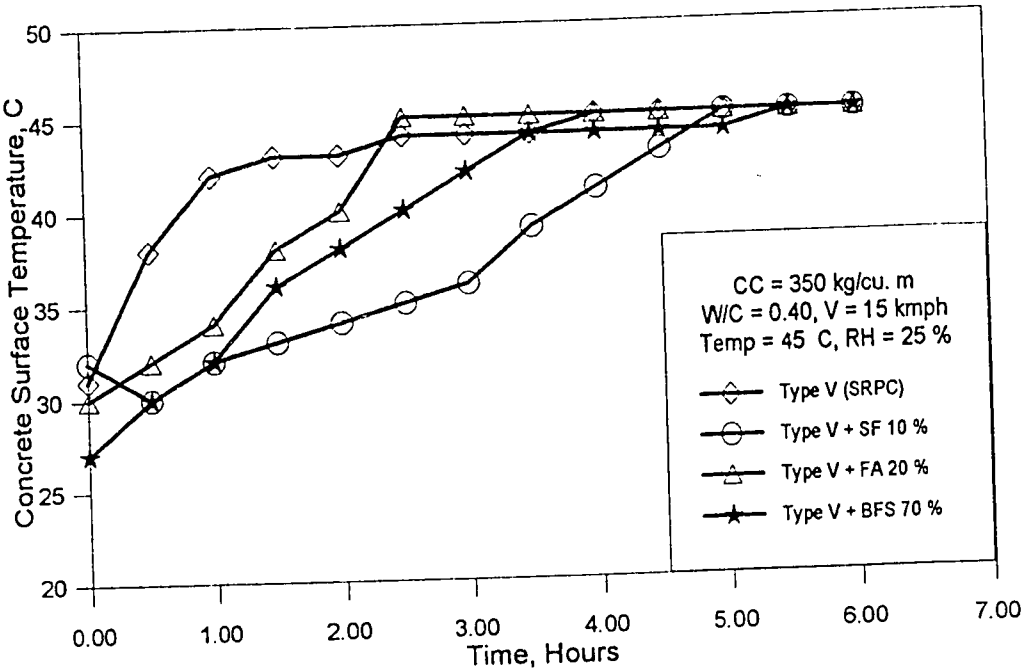

Figure 4.91: Variation of Concrete Temperature With Time in the Plain and Blended Cements (CC : 350 kg/m^3 ; W/C : 0.40 ; Temp : 45 °C ; V : 0 kmph ; RH : 25%)

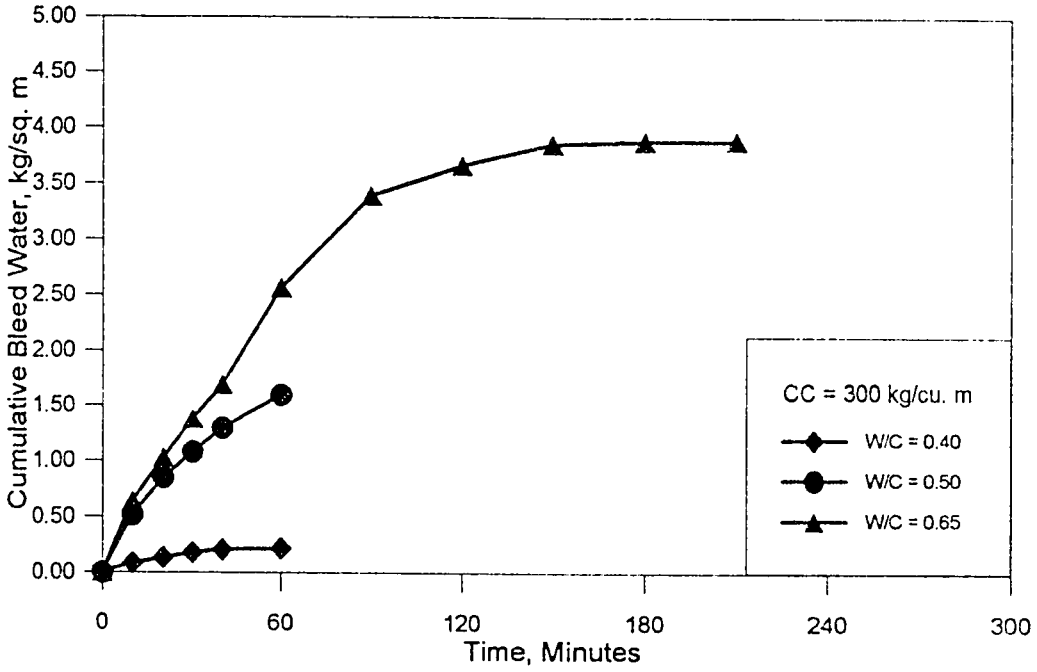

Figure 4.92: Effect of Water-Cement Ratio on Bleeding (CC : 300 kg/m^3)

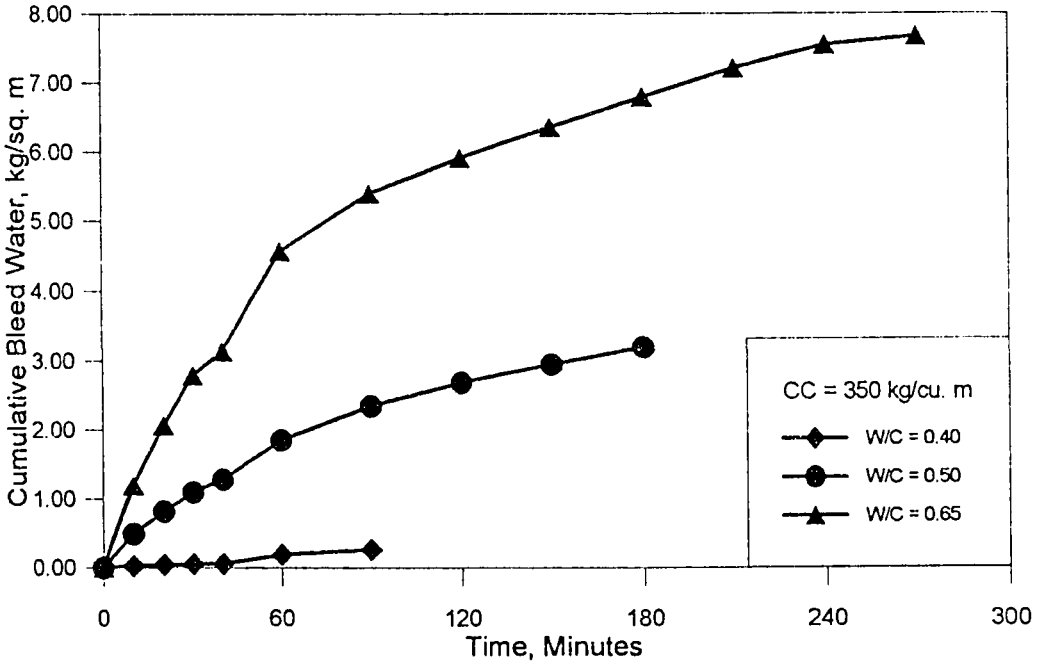

Figure 4.93: Effect of Water-Cement Ratio on Bleeding (CC : 350 kg/m^3)

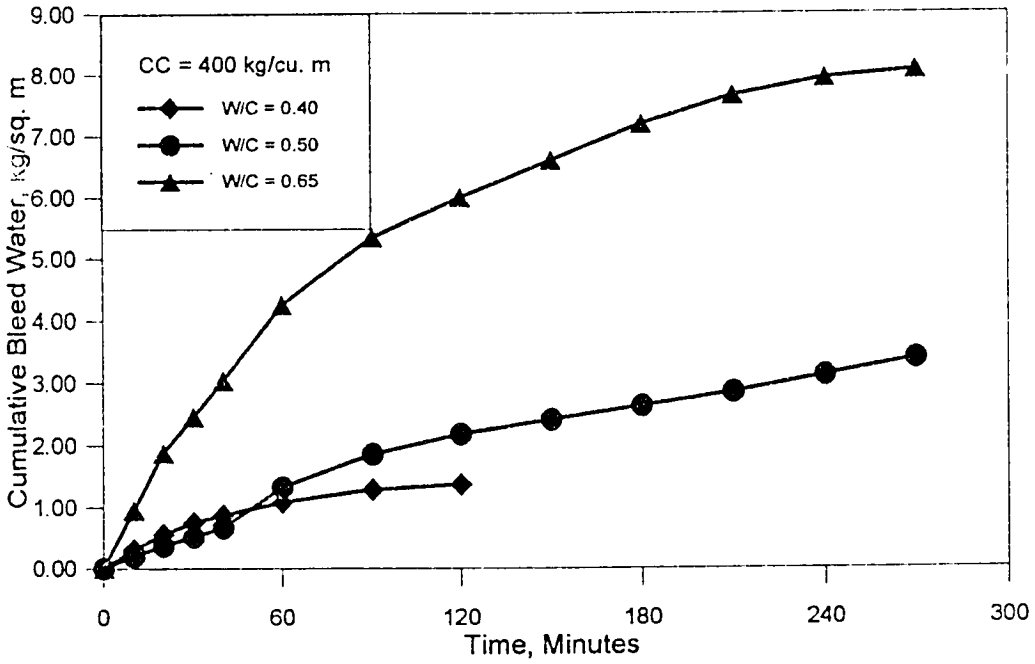

Figure 4.94: Effect of Water-Cement Ratio on Bleeding (CC : 400 kg/m^3)

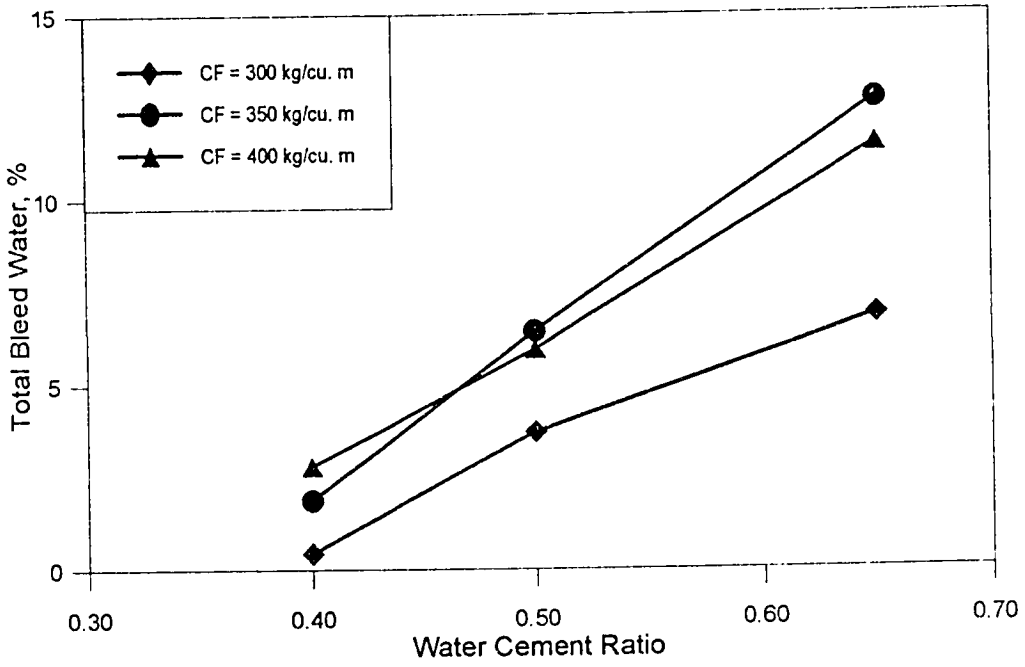

Figure 4.95: Effect of Water-Cement Ratio and Cement Content on Bleeding

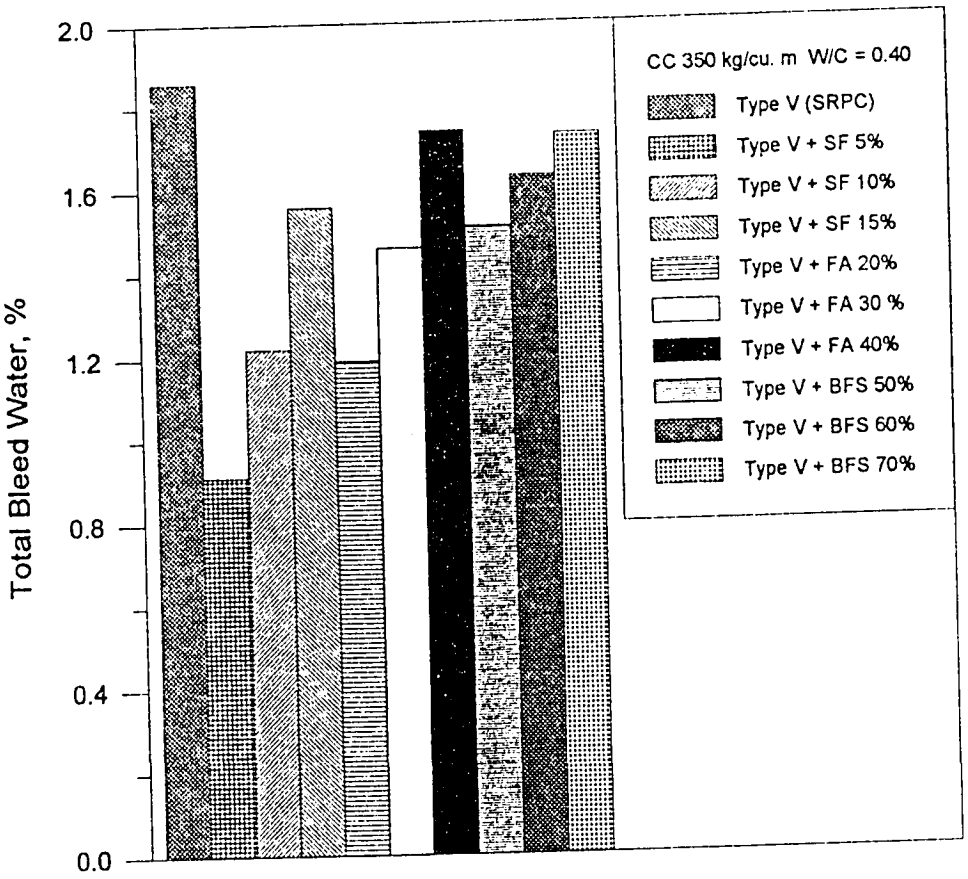

Figure 4.96: Bleeding in Plain and Blended Cements

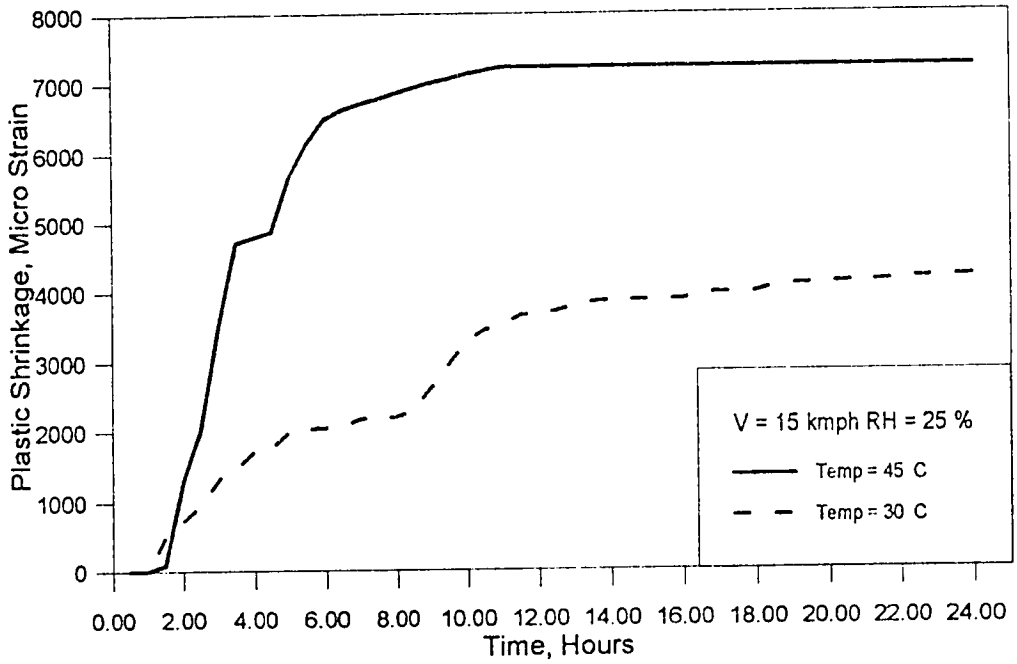

Figure 4.97: Variation of Plastic Shrinkage Strain With Time (V : 15 kmph ; RH : 25% ; CC : 350 kg/m^3 ; W/C : 0.40)

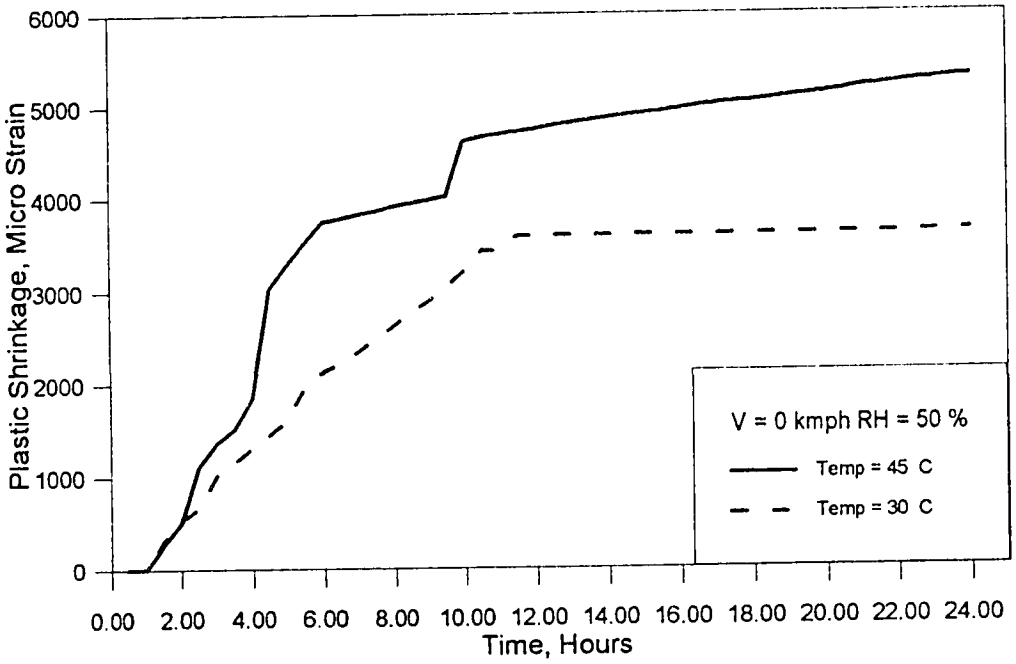

Figure 4.98: Variation of Plastic Shrinkage Strain With Time (V : 0 kmph ; RH : 50% ; CC : 350 kg/m^3 ; W/C : 0.40)

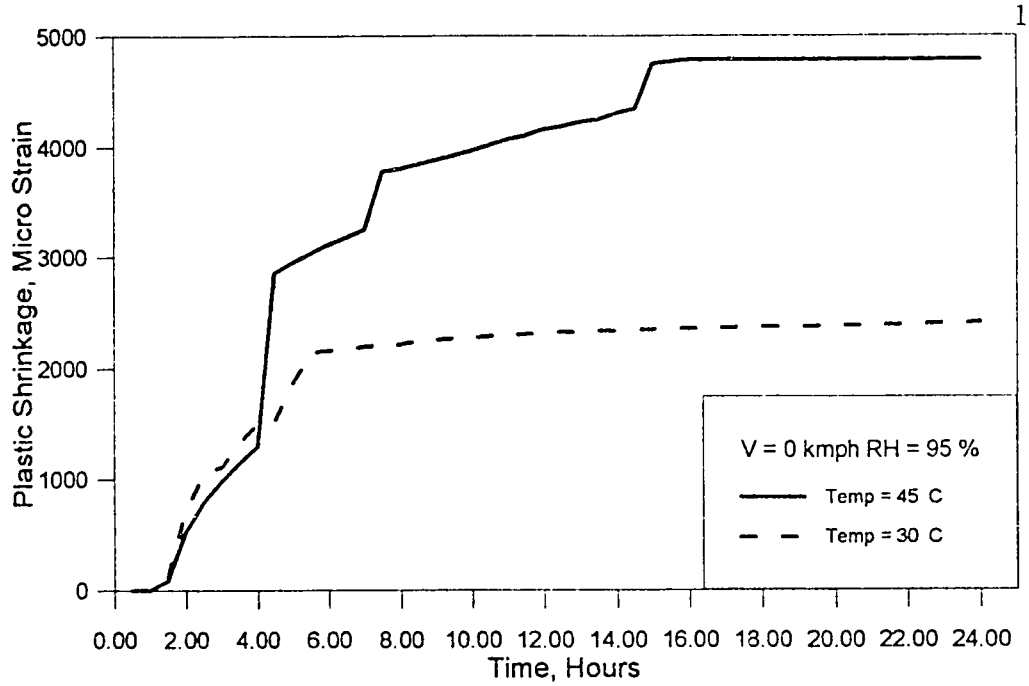

Figure 4.99: Variation of Plastic Shrinkage Strain With Time (V : 0 kmph ; RH : 95% ; CC : 350 kg/m^3 ; W/C : 0.40)

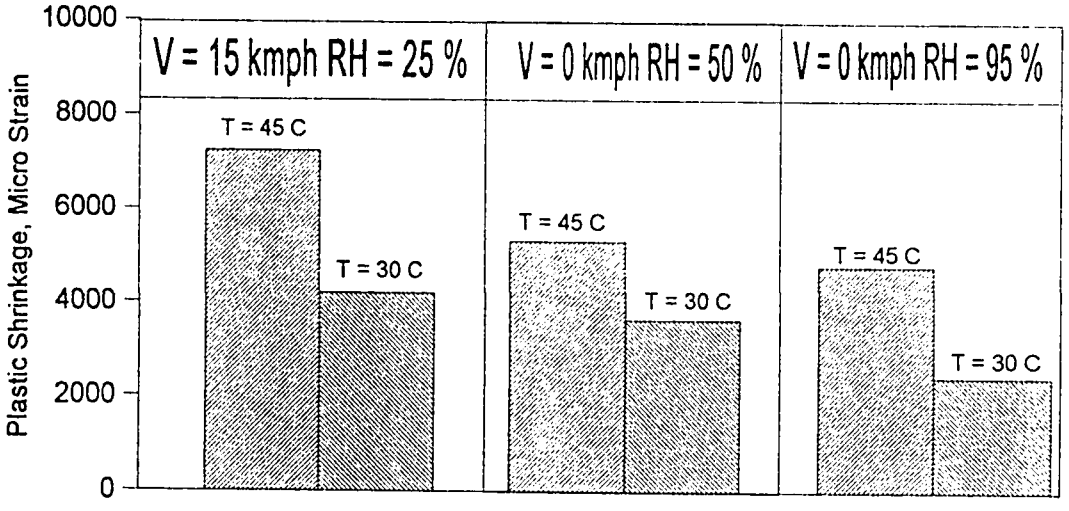

Figure 4.100: Effect of Ambient Temperature, Relative Humidity and Wind Velocity on Plastic Shrinkage Strain in the Big Concrete Specimens (CC : 350 kg/m^3 ; W/C : 0.40)

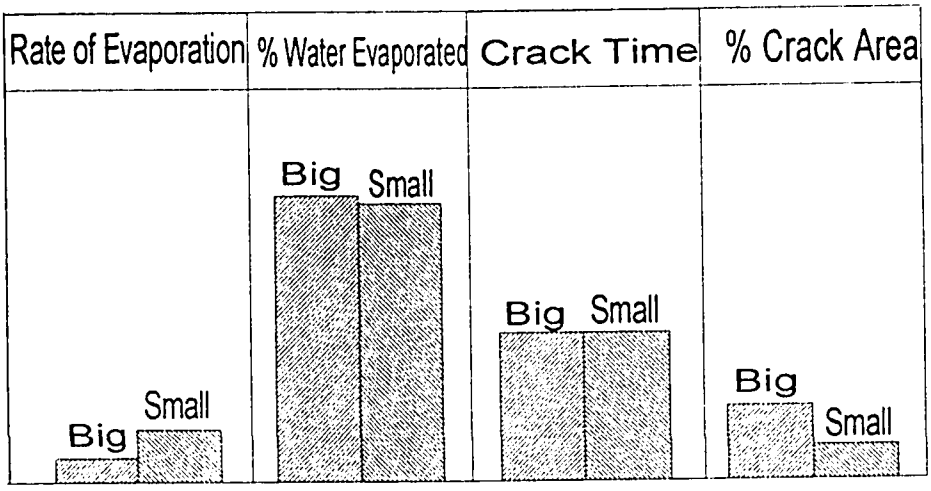

Figure 4.101: Effect of Specimen Size on Water Evaporation and Plastic Shrinkage Cracking (CC : 350 kg/m^3 ; W/C : 0.40)

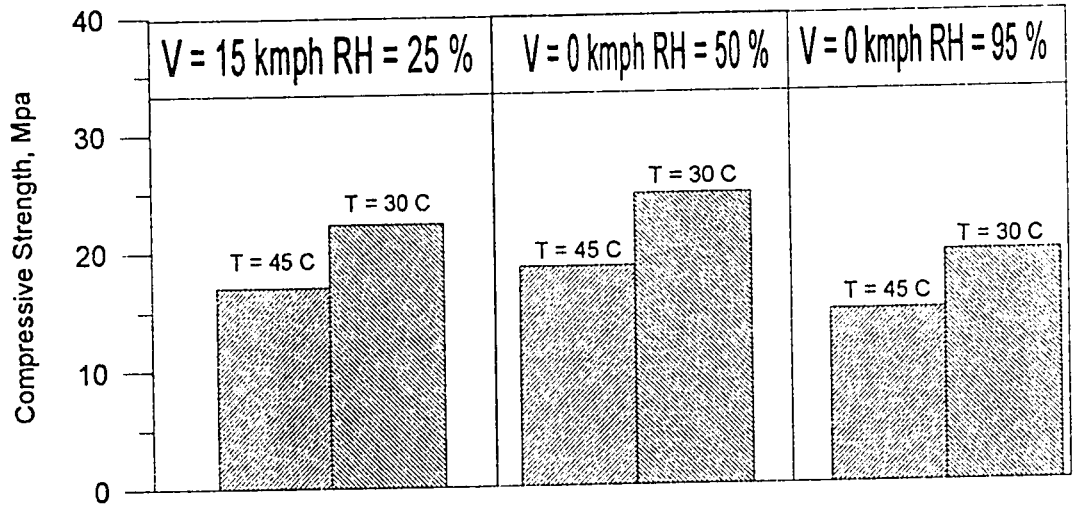

Figure 4.102: Effect of Ambient Temperature, Relative Humidity and Wind Velocity on the Compressive Strength of Big Concrete Specimens (CC : 350 kg/m^3 ; W/C : 0.40)

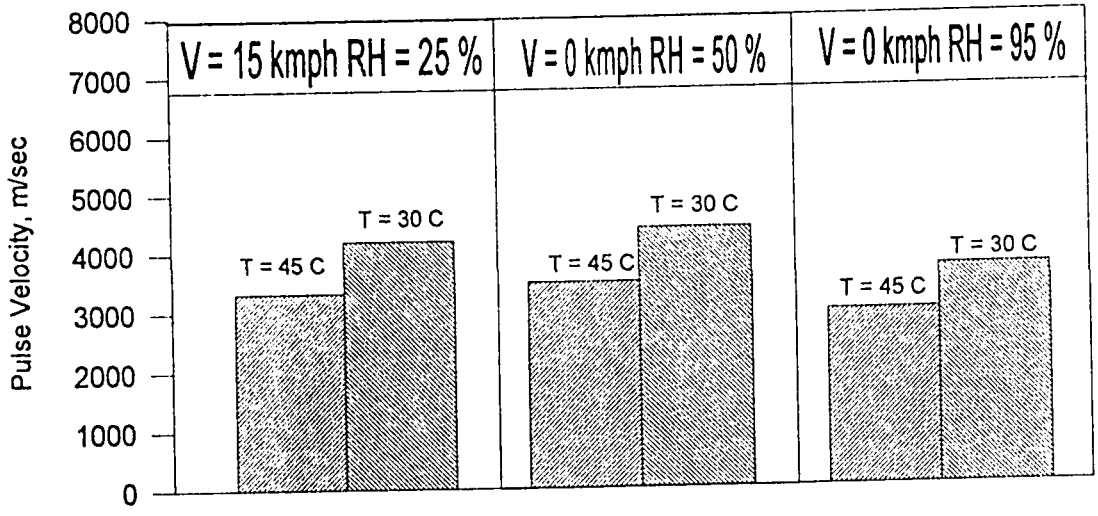

Figure 4.103: Effect of Ambient Temperature, Relative Humidity and Wind Velocity on the Pulse Velocity in the Big Concrete Specimens (CC : 350 kg/m^3; W/C : 0.40)

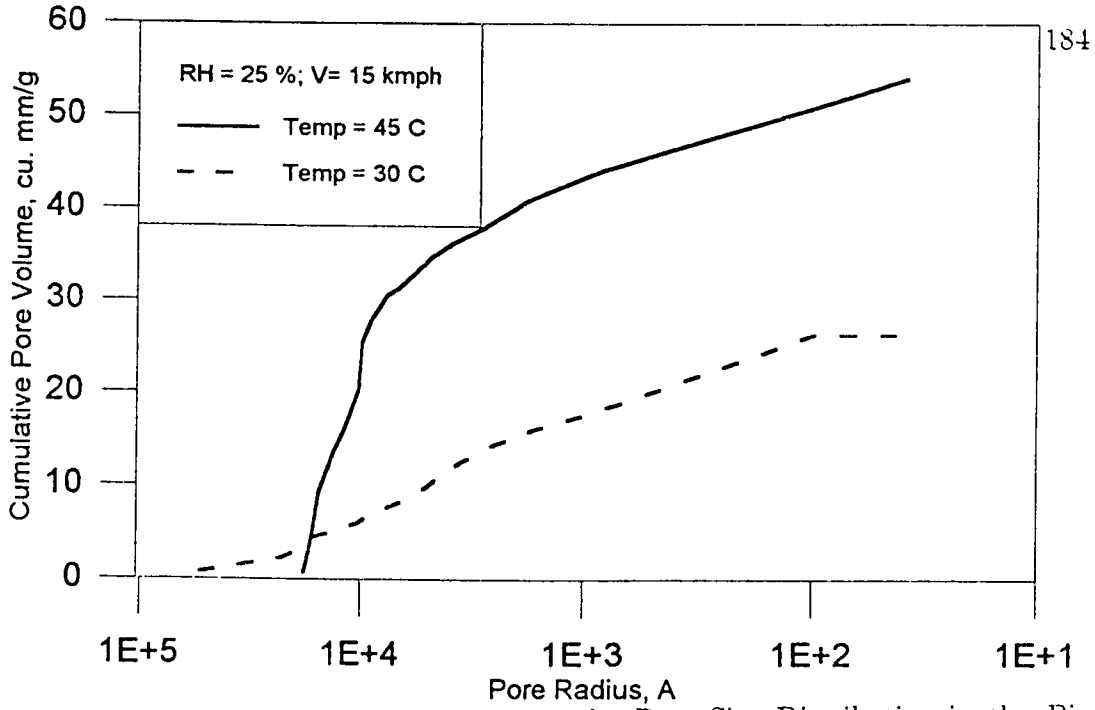

Figure 4.104: Effect of Temperature on the Pore Size Distribution in the Big Concrete Specimens (V : 15 kmph ; RH : 25% ; CC : 350 kg/m^3 ; W/C : 0.40)

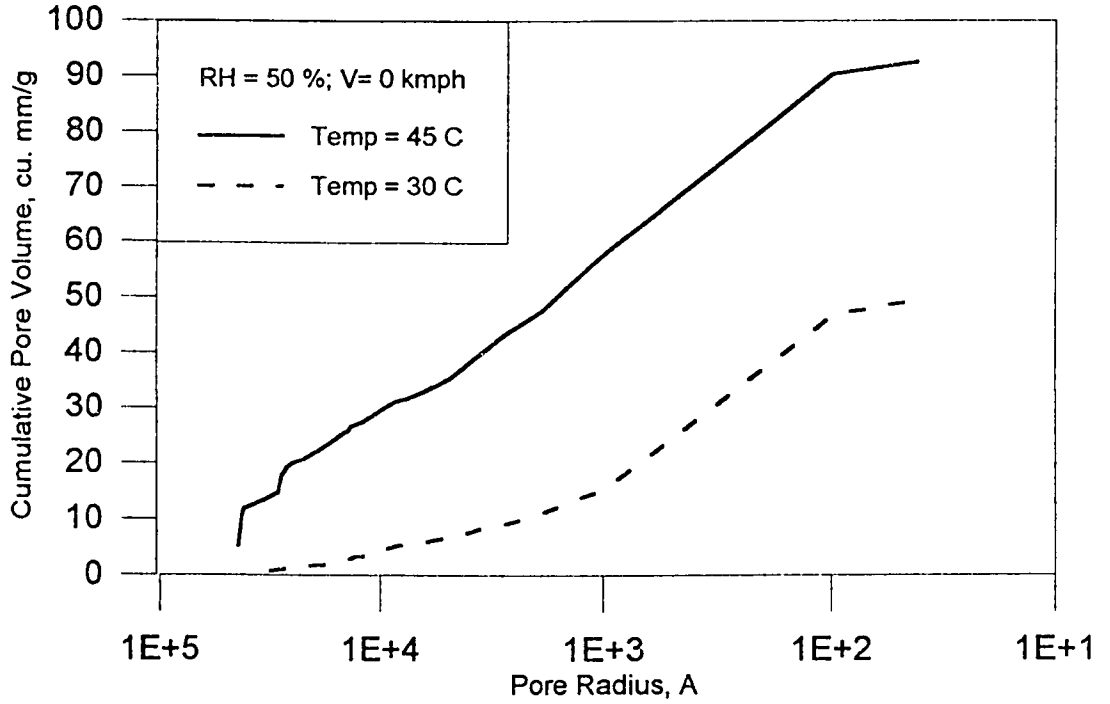

Figure 4.105: Effect of Temperature on the Pore Size Distribution in the Big Concrete Specimens (V : 0 kmph ; RH : 50% ; CC : 350 kg/m^3 ; W/C : 0.40)

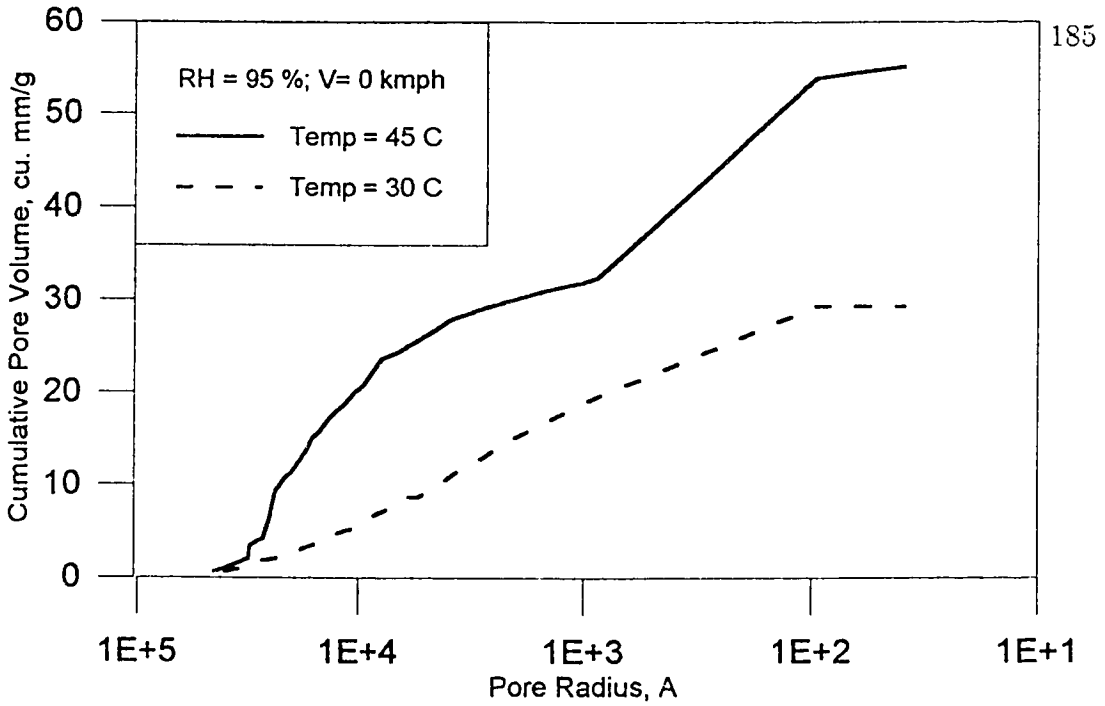

Figure 4.106: Effect of Temperature on the Pore Size Distribution in the Big Concrete Specimens (V : 0 kmph ; RH : 95% ; CC : 350 kg/m^3 ; W/C : 0.40)

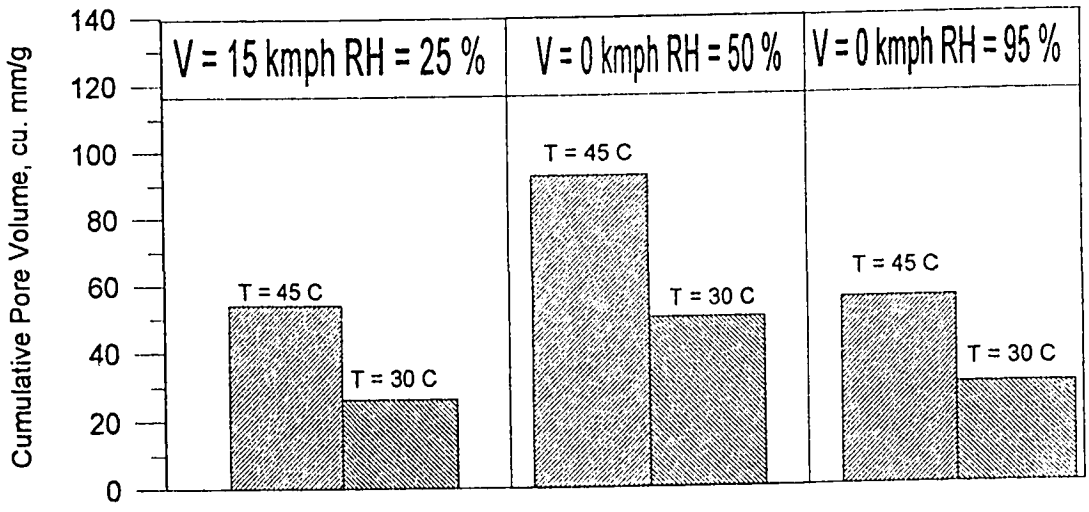

Figure 4.107: Effect of Ambient Temperature, Relative Humidity and Wind Velocity on Cumulative Pore Volume in the Big Concrete Specimens (CC : 350 kg/m^3 ; W/C : 0.40)

Chapter 5

CONCLUSIONS AND RECOMMENDATIONS

5.1 CONCLUSIONS

5.1.1 Effect of Environmental Conditions on Plastic Shrinkage Cracking

5.1.1.1 Relative Humidity

The time to cracking in the concrete specimens exposed to high relative humidity was more than those exposed to a lower humidity. However, the effect of relative humidity on the time to cracking was minimal in the blended cements.

When there is no wind, an increase in the relative humidity decreases the quantity

of water evaporated in almost all the mixes. However, in the windy conditions, increasing relative humidity had no significant effect on the evaporation. The rate of evaporation decreases when the relative humidity is high. Again, the effect of humidity on the rate of evaporation is not significant in the windy conditions. An increase in the relative humidity reduces the crack length and crack area, except in windy conditions.

An increase in the relative humidity does not affect the concrete surface temperature.

5.1.1.2 Wind Velocity

An increase in the wind velocity increases :

(i) the quantity of water evaporated from the concrete,

(ii) the rate of evaporation,

(iii) the crack length,

(iv) the crack area, and

(ii) the concrete surface temperature.

However, an increase in the wind velocity decreases the time to cracking.

5.1.1.3 Ambient Temperature

An increase in the ambient temperature increases :

(i) the quantity of water evaporated from the concrete,

(ii) the rate of evaporation,

(iii) the crack length,

(iv) the crack area,

(v) the concrete surface temperature,

(vi) the plastic shrinkage strain, and

(vii) the cumulative pore volume.

An increase in the ambient temperature decreases :

(i) the time of cracking,

(ii) the 28 day compressive strength, and

(iii) the 28 day pulse velocity.

However, no cracks were observed in the concrete specimens cast at a temperature of less than 35 °C.

5.1.2 Effect of Mix Proportions on Plastic Shrinkage

5.1.2.1 Cement Content

An increase in the cement content increases :

(i) the quantity of water evaporated from the concrete mix,

(ii) the rate of evaporation,

(iii) the cracking time,

(iv) the crack area, and

(v) the bleeding.

5.1.2.2 Water-Cement Ratio

An increase in the water-cement ratio increases :

(i) the rate of evaporation,

(ii) the crack time,

(iii) the crack area, and

(iv) the bleeding.

However, an increase in the water-cement ratio reduces the quantity of water evaporated from the concrete mix.

5.1.2.3 Blended Cements

An increase in the quantity of blending materials (i.e fly ash, silica fume and BFS) increases :

(i) the quantity of water evaporated, except in silica fume cement concrete in which the quantity of water evaporated decreases,

(ii) the rate of evaporation,

(iii) the crack time, and

(iv) the bleeding.

However, in the plain cements, bleeding is more than that in the blended cements. The cracked area decreases with the quantity of the blending material. The cracked area, in the blended cements, is however more than that in the plain cements.

5.1.2.4 Specimen Size

An increase in the specimen size increases

(i) the crack area, and

(ii) the bleeding.

The rate of evaporation decreases with the specimen size. An increase in the specimen size has no effect on :

(i) the quantity of water evaporated from the concrete mix, and

(ii) the crack time.

5.1.3 Selection of Concrete Composition

The data developed in this investigation indicate that the concrete mix composition significantly affects the parameters influencing plastic shrinkage. Therefore, the negative effect of environmental conditions on plastic shrinkage can be minimized to a great extent by choosing appropriate concrete mix.

5.1.3.1 Quantity of Water Evaporated

The quantity of water evaporated was the least in a lean plastic mix with a cement content of 300 kg/m^3 and a water-cement ratio of 0.65, in nearly all the exposure conditions. However, in the hot-humid environment (45 °C, RH : 95 %), it was the least in a lean stiff mix with a cement content of 300 kg/m^3 and a water-cement ratio of 0.40.

5.1.3.2 Rate of Evaporation

The rate of evaporation was the least in a lean stiff mix, with a cement content of 300 kg/m^3 and a water-cement ratio of 0.40 in all the exposure conditions.

5.1.3.3 Time to Cracking

Cracks were not observed in the concrete specimens exposed to normal (25 °C, RH : 50 %) conditions. However, they were observed in the specimens cast at temperatures of more than 25 °C. Cracking was delayed in the rich-plastic concrete specimens.

5.1.3.4 Cracked Area

Although the lean-stiff mixes cracked earlier than rich-plastic mixes, the intensity of the cracks in the former was less than that in the latter. The intensity of cracks in the concrete mixes with a cement content of 300 kg/m^3 and a water-cement ratio of 0.40 was the least, in all the exposure conditions.

5.1.3.5 Bleeding

Bleeding was very low in the lean-stiff mixes continuing only upto one hour, whereas it continued upto four to five hours in the rich-plastic mixes.

5.1.4 Specific Conclusions

Some specific findings of this research are :

(1) ACI 305 graphical method can only be used to determine the rate of evaporation and not plastic shrinkage cracking. Further, this method is not very useful in the Arabian Gulf, particularly in summer, as it is formulated for

temperatures of up to 38 °C.

(2) Cracking was observed at evaporation rates ranging from 0.2 to 0.7 kg/m^2.h, as against a value of 1 kg/m^2.h, recommended by ACI 305.

(3) The quantity of water evaporated in the lean-plastic mixes was less than that in the rich-stiff mixes.

(4) The rate of evaporation in the lean-stiff mixes was less than that in the rich-plastic mixes.

(5) The time to cracking in the rich-plastic mixes was more than that in the lean-stiff mixes.

(6) The intensity of cracks in the lean-stiff mixes was less than that in the rich-plastic mixes.

(7) Bleeding was the least in the lean-stiff mixes and blended cement concretes.

(8) The specimen thickness and size, both influence the rate of evaporation and crack intensity. The rate of evaporation decreased from 0.9 kg/m^2.h in 1x1 feet specimens to 0.42 kg/m^2.h in 1.5x1.5 feet specimen. However, the cracking intensity increased from 0.06 % in 1.5x1.5 feet specimens to 0.13 % in 3x3 feet specimens.

(9) In a given environment, bleeding, water evaporation and plastic shrinkage cracking are controlled by the mix constituents, water-cement ratio and the

type and quantity of cement, in particular.

(10) The environmental conditions also influence the water evaporation, plastic shrinkage cracking and plastic shrinkage strain.

(11) Exposure conditions at the time of casting, influence the properties of hardened cement concrete such as compressive strength, soundness, porosity and microstructure. An increase in temperature from 30 to 45 °C at a RH of 50 %, reduced the compressive strength from 25 to 18 MPa, pulse velocity from 4500 to 3200 m/s and increased the cumulative pore volume from 50 to 95 mm^3/g. An increase in the relative humidity from 50 to 95 % at a temperature of 30 °C reduced the compressive strength from 25 to 20 MPa, pulse velocity from 4500 to 3500 m/s and the cumulative pore volume from 50 to 30 mm^3/g.

(12) Plastic shrinkage cracking in the blended cement concretes was more than that in the plain cement concretes.

(13) No relation was found between the rate of evaporation and the time to cracking. However, the total cracked area increased almost linearly with the rate of evaporation.

(14) The data generated on rate of evaporation is in excellent agreement with that calculated from the ACI 305 graphical method in most of the exposure conditions. This suggests that the constructed controlled temperature humid-

ity chamber and the adopted test procedure were appropriate for generating the desired exposure conditions. Hence, this controlled temperature-humidity chamber can be utilized in further research.

5.2 RECOMMENDATIONS

The following recommendations can be drawn from this study.

(1) ACI 305 graphical method should be used to determine the rate of evaporation. However, it may not provide any indication of plastic shrinkage cracking.

(2) The data developed in this study indicate that plastic shrinkage cracks occur at a much lower rate of evaporation compared to the value recommended by ACI 305. Hence, extreme precaution should be taken to reduce the rate of evaporation.

(3) Concrete mixes with low cement content and low water-cement ratio should be used to avoid plastic shrinkage cracking. Superplasticizers may be used to increase the workability. However, the effect of low cement content on durability of concrete should also be considered.

(4) It was observed that concrete mixes with low cement contents exhibited less cracking than mixes with high cement contents but cracks were observed earlier in the former than the latter. Therefore, initial cracking should be prevented

by suitable means.

(5) The data developed in this study indicated that wind velocity significantly influences plastic shrinkage cracking. Use of wind barriers may be appropriate in windy conditions.

(6) High ambient temperature reduces the relative humidity and creates a hot-dry environment which promotes plastic shrinkage cracking. Therefore concrete should be placed in the evening or night, particularly in summers to avoid plastic shrinkage cracking.

(7) The results of this investigation indicate that plastic shrinkage cracking is enhanced in blended cements, in hot weather conditions. Therefore, appropriate measures should be implemented when using these cements.

(8) Suitable precautions should be taken while curing concrete in hot-dry environment as the exposure conditions at the time of casting influence the properties of hardened concrete.

5.3 FUTURE STUDY

Further research is recommended in the following areas :

(1) Influence of cement type on plastic shrinkage.

(2) Influence of superplasticizers on plastic shrinkage.

(3) Influence of types and dosages of fibers on plastic shrinkage.

(4) The influence of commercially available curing compounds on plastic shrinkage.

(5) The influence of shrinkage compensating cement on plastic shrinkage.

(6) Plastic shrinkage in high strength concrete.

(7) The durability performance of low cement content and low water-cement ratio concretes.

Bibliography

[1] Fooks P.G and L. Collins, "*Problems in the Middle East Concrete* ", Cement and Concrete Association, 1975.

[2] "*The CIRIA Guide to Concnrete Construction in the Gulf Region* ", 1984.

[3] Rasheeduzzafar and F.H. Dakhil, "Field Studies on the Durability of Construction in a High Chloride-Sulphate Environment ", *International Journal of Housing Science*, No. 4, 1980. pp. 203-232.

[4] Maslehuddin M. "Optimization of Concrete Mix Design for Durability in the Eastern Province of Saudi Arabia ". MS thesis, Department of Civil Engineering, King Fahd University of Petroleum and Minerals, Dhahran, Saudi Arabia, 1981.

[5] Al-Saadoun. S.S, Rasheeduzzafar., and A.S. Al-Gahtani, "Mix Design Considerations of Durable Concrete in the Gulf Environment ", *The Arabian Journal of Science and Engineering*, Vol. 17, No. 1, Jan. 1992. pp. 17-33.

[6] Hsu T.T.C., "Mathematical Analysis of Shrinkage Stresses in a Model of Hardened Concrete ", *ACI Journal Proceedings*, Vol. 60, No. 3, Mar. 1963. pp. 371-390.

[7] Slate F.O. and R.E. Matheus, "Volume Changes upon Setting and Curing of Cement Paste and Concrete from Time Zero to Seven Days ", *ACI Journal Proceedings*, Vol. 64, No. 1, Jan. 1967. pp. 34-39.

[8] Emery K.O., "Sediments and Water of Persian Gulf ", *Bull. American Association of Petroleum Geologists*, Vol. 40, 1956. p. 2354.

[9] Rasheeduzzafar, F.H. Dakhil, and A.S. Al-Gahtani, "The Deterioration of Concrete Structures in the Environment of the Middle East ", *ACI Journal*, Vol. 81, No. 1, 1984. pp. 13-20.

[10] Rasheeduzzafar, F.H. Dakhil, and A.S. Al-Gahtani, "Corrosion of Reinforcement in Concrete Structures in the Middle East ", *Concrete International*, Vol. 9, No. 7, 1985. pp. 48-55.

[11] Maslehuddin M., "*The Influence of Arabian Gulf Environment on Mechanism of Reinforcement Corrosion* ", PhD thesis, University of Aston, Birmingham, U.K., 1994.

[12] Wittman F.H., "On the Action of Capillary Pressure in Fresh Concrete", *Cement and Concrete Research*, Vol. 6, No. 1, 1976. pp. 49-56.

[13] Berhane Z., "Evaporation of Water from Fresh Mortar and Concrete at Different Environmental Conditions", *ACI Journal Proceedings*, Vol. 81, Nov.-Dec. 1984. pp. 560-565.

[14] Hasanain G.S., T.A. Khallaf, and K. Mahmood, "Water Evaporation from Freshly Placed Concrete Surfaces in Hot Weather", *Cement and Concrete Research*, Vol. 19, No. 3, 1989. pp. 465-475.

[15] American Concrete Institute, "ACI Manual of Concrete Practice ", Technical report.

[16] Jaegermann C.H., D. Ravina, and B. Pundak, "Accelerated Curing of Concrete by Solar Radiation ", *Proceedings, RILEM International Symposium on Concrete and Reinforced Concrete in Hot Countries, Technion.* Israel Institute of Technology, Haifa. 1971, pp. 339-362.

[17] "Development of Building and Construction Materials Using Available Resources in Saudi Arabia ", Technical report, SANCST Project AR-4.

[18] Basham Kim D., "Hot Weather Affects Fresh Concrete ", *Concrete Construction*, July 1992. pp. 523-524.

[19] "Making Good Concrete in Hot Weather ". *Concrete International*, April 1992. pp. 55-57.

[20] "*Concrete in Hot Climates* ", STUVO, FIP, 1986.

[21] Gebler S., "Predict Evaporation Rate and Reduce Plastic Shrinkage Cracks ", *Concrete International*, Vol. 36, April 1983. pp. 19-22.

[22] "Prevention of Plastic Cracking in Concrete ", Technical report, Concrete Information Sheet, Structural and Railways Bureau, Portland Cement Association, Chicago. 1955.

[23] Soroka I., "*Concrete in Hot Climates*", E and FN SPON, London, 1993.

[24] Hover K.C., "Evaporation of Surface Moisture: A Problem in Concrete Technology and Human Physiology ", *Concrete in Hot Climates, Proceedings of The Third International RILEM Conference, England.* Sept. 1992, pp. 13-24.

123

[25] Cebeci O.Z. and A.M. Saatci, "Estimation of Evaporation from Concrete Surfaces ", *Concrete in Hot Climates, Proceedings of The Third International RILEM Conference, England.* Sept. 1992, pp. 25-31.

[26] Ravina D. and R. Shalon, "Tensile Stress and Strength of Fresh Mortar Subjected to Evaporation", *Proceedings, RILEM International Symposium on Concrete and Reinforced Concrete in Hot Countries.Technion.* Israel Institute of Technology, Haifa. 1971, pp. 275-296.

[27] Bloem D., "Plastic Cracking of Concrete ", Technical report, Engineering Information, National Ready Mixed Concrete Association. 1960.

[28] ACI Committee 305, "Hot Weather Concreting (ACI 305R-77) ", Technical report, ACI Manual of Concrete Practice, Part 2.

[29] Freedman S., "Hot Weather Concreting ", *Modern Concrete*, May 1969. pp. 31-38.

[30] Malisch W.R., "Hot Weather Concreting Tips", *Concrete Construction.* June 1990. pp. 541-544.

[31] Mowery W.A., "Hazards of Hot Weather Concreting ", *Civil Engineering, ASCE*, Vol. 36, No. 8, Aug. 1966. pp. 56-57.

[32] Shalon R., "Report on Behaviour of Concrete in Hot Climates ", *Materials and Structures*, Vol. 11, No. 62, Mar.-April 1978. pp. 127-131.

[33] Newlon H.H., "Random Cracking of Bridge Decks Caused by Plastic Shrinkage ", Technical report, Special Report 106, Highway Research Board. 1970, pp. 57-61.

[34] Chatterji S., " Probable Mechanisms of Crack Formation at Early Ages of Concrete : A Literature Survey ", *Cement and Concrete Research*, Vol. 12, No. 3, 1982. pp. 371-376.

[35] Kasai Y., I. Matsui, and K. Yokohama, "Shrinkage and Cracking of Concrete at Early Ages ", *International Conference on Concrete of Early Ages, Paris.* Apr. 1982, pp. 45-50.

[36] Concrete Society Working Party, "Non-structural Cracks in Concrete ", Technical report, The Concrete Society, Dec. 1982.

[37] Lerch W., "Plastic Shrinkage ", *ACI Journal Proceedings*, Vol. 53, No. 8, Feb. 1957. pp. 797-802.

[38] Shalon R. and D. Ravina, "Studies in Concreting in Hot Countries", *RILEM International Symposium on Concrete and Reinforced Concrete in Hot Countries*. Haifa 1960. pp. 1-46.

[39] Jaegermann C.H. and J. Glucklich, "Effect of Plastic Shrinkage on Subsequent Shrinkage and Swelling of the Hardened Concrete", *Proceedings, International Colloquium on the Shrinkage of Hydraulic Concretes*. Madrid 1968. pp. 1-26.

[40] Shalon R. and D. Ravina, "Shrinkage of Fresh Mortars Cast Under and Exposed to Hot Dry Climate Conditions", *RILEM-CEMBUREAU Colloquium on the Shrinkage of Hydraulic Concretes*. Madrid 1968. pp. 1-19.

[41] Shalon R. and D. Ravina, "Plastic Shrinkage Cracking", *ACI Journal Proceedings*, Vol. 65, No. 4. April 1968. pp. 282-291.

[42] Dutt A.J., S.K. Roy, and M.Y.L. Chew, "Effects of Wind Flow on Freshly Poured Concrete", *Journal of Wind Engineering and Industrial Aerodynamics*. (41-44, 1992. pp. 2629-2630.

[43] Franklin R.E., "The Effect of Weather Conditions on Early Strains in Concrete Slabs", Technical report, RRL Report LR 266, Road Research Laboratory, Berkshire. 1969.

[44] Senbetta E. and M.A. Bury, "Control of Plastic Shrinkage Cracking in Cold Weather", *Concrete International*, Mar. 1991. pp. 49-53.

[45] Kral S. and J. Gabauer, "Shrinkage and Cracking of Concrete at Early Ages", *Proceedings, Conference Internationale sue le Dallas en Beton*. Dundee, Apr. 1979. pp. 412-420.

[46] Cebeci O.Z., A.M. Saatci, and B. Mather, "Discussion on Paper by Berhane", *ACI Journal*, Nov.-Dec. 1985. pp. 930-933.

[47] Abdun-Nur E.A., F.D. Beresford, F.A. Blakey, M. Spindel, L.H. Tuthill, and W. Lerch, "Discussion on Paper by Lerch", *ACI Journal Proceedings*, Part 2, Dec. 1957. pp. 1341-1345.

[48] Brull L., K. Komlos, and B. Majzlan, "Early Shrinkage of Cement Pastes, Mortars and Concretes", *Materials and Structures*, Vol. 13, No. 73, 1980. pp. 41-45.

[49] Brull L. and K. Komlos, "Early Shrinkage of Hardening Cement Pastes", *Fundamental Research on Creep and Shrinkage of Concrete*. Martinus Nijhoff Publishers. 1982. pp. 239-248.

123

[50] Carlson R.W., D.L. Houghton, and M. Polivka, "Causes and Control of Cracking in Unreinforced Mass Concrete", *ACI Journal Proceedings*, July 1979. pp. 821-837.

[51] Bloom R. and A. Bentur, "Free and Restrained Shrinkage of Normal and High Strength Concretes", *ACI Materials Journal*, Vol. 92, No. 2, Mar.-Apr. 1995. pp. 211-217.

[52] Guo C., "Early Age Behaviour of Portland Cement Paste", *ACI Materials Journal*, Vol. 91, No. 1, Jan.-Feb. 1994. pp. 13-25.

[53] Shaeles C.A. and K.C. Hover, "Influence of Mix Proportions on Plastic Shrinkage Cracking in Thin Slabs", *ACI Materials Journal*, Vol. 85, Nov.-Dec. 1988. pp. 495-504.

[54] Kraai P.P., "A Proposed Test to Determine the Cracking Potential due to Drying Shrinkage of Concrete ", *Concrete Construction*, Sept. 1985. pp. 775-778.

[55] Turton C.D., "Discussion on Paper by Shaeles and Hover", *ACI Materials Journal*, Sept.-Oct. 1989. pp. 531-532.

[56] Cohen M.D., J. Olek, and W.C. Dolch, "Mechanism of Plastic Shrinkage Cracking in Portland Cement-Silica Fume Paste and Mortar", *Cement and Concrete Research*, Vol. 20, No. 1, 1990. pp. 103-119.

[57] Troxell G.E., J.M. Raphael, and R.E. Davis, "Long-Time Creep and Shrinkage Tests of Plain and Reinforced Concrete ", *Proceedings ASTM*, Vol. 58, 1958. pp. 1101-1120.

[58] Richard T.E., "Creep and Drying Shrinkage of Lightweight and Normal Weight Concrete ", Technical report, Monograph 74, National Bureau of Standards, Washington D.C. 1964. 30 pp.

[59] Powers T.C., "Causes and Control of Volume Change ", *Portland Cement Association Research and Development Laboratories*, , No. 1, Jan. 1959. pp. 29-39.

[60] Zollo R.F., J.A. Liter, and G.B Bouchacourt, "Plastic and Drying Shrinkage in Concrete Containing Collated Fibrillated Polypropylene Fibre ", *Development in Fibre Reinforced Cement and Concrete, RILEM Symposium*. Vol. 1, Jul. 1986.

[61] P.S. Mangat and M.M. Azari, "Plastic Shrinkage of Steel Fibre Reinforced Concrete", *Materials and Structures*, Vol. 23, 1990. pp. 186-195.

[62] Krencheil H. and S. Shah, "Restrained Shrinkage Tests with PP-Fiber Reinforced Concrete", *Fiber Reinforced Concrete Properties and Applications, SP-105.* American Concrete Institute, Detroit. 1987, pp. 141-158.

[63] Paillene A.M., M. Buil, and J.J. Sevrano, "Effect of Fiber Addition on the Autogenous Shrinkage of Silica Fume Concrete", *ACI Materials Journal, Proceedings,* Vol. 86, No. 2, 1989. pp. 139-144.

[64] Balaguru P., "Contribution of Fiber to Crack Reduction of Concrete Composites During the Initial and Final Setting Period", *ACI Materials Journal,* Vol. 91, No. 3, 1994. pp. 280-288.

[65] Komlos K. and L. Brull, "Early Age Shrinkage and Cracking Tendency of Fibre Reinforced Cements and Mortars", *Proceedings of International Symposium on Fibre Reinforced Concrete, Madras.* Vol. 2, Dec. 1987. pp. 4.41-4.51.

[66] Swamy R.N. and H. Stavides, "Influence of Fiber Reinforcement on Restrained Shrinkage and Cracking", *ACI Journal,* Vol. 76, No. 3, Mar. 1979. pp. 443-460.

[67] Grzybowski M. and S.P. Shah, "Shrinkage Cracking of Fiber Reinforced Concrete", *ACI Materials Journal,* Vol. 87, No. 2, Mar.-Apr. 1990. pp. 138-148.

[68] Chern J. and C. Young, "Study of Factors Influencing Drying Shrinkage of Steel Fiber Reinforced Concrete", *ACI Materials Journal,* Vol. 87, 1989. pp. 123-129.

[69] Soroushian P. and Z. Byasi, "Fiber-Type Effect on the Performance of Steel Fiber Reinforced Concrete", *ACI Materials Journal,* Vol. 88, 1991. pp. 129-133.

[70] Al-Waleed A., Al-Ekrish and S.H. Al-Sayed, "Shrinkage of Fiber and Reinforced Fiber Concrete Beams in Hot-Dry Climate", *Cement and Concrete Composites,* Vol. 16, 1994. pp. 299-307.

[71] Reeves C.M., "The Use of Ground Granulated Blast Furnace Slag to Produce Durable Concrete", *How to Make Today's Concrete Durable for Tomorrow, Iceland, UK.* Thomas Telford, London. 1985, pp. 59-75.

[72] Cabrera J.G., "The Use of Pulverised Fly Ash to Produce Durable Concrete", *How to Make Today's Concrete Durable for Tomorrow, Iceland, UK.* Thomas Telford, London. 1985, pp. 29-57.

[73] Cabrera J.G. and S.O. Nwaubani, "Strength and Chloride Permeability of Pozzolonic Mortars and Concretes", *Magazine of Concrete Research,* 1992.

[74] Wainwright P.J., J.G. Cabrera, and N. Gowripalan, "Assesment of the Effeciency of Chemical Membranes to Cure Concrete", *International Conference on Protection of Concrete, Dundee, Scotland.* 1990, pp. 907-920.

[75] Cabrera J.G. and S.O. Nwaubani, "The Influence of High Temperature on Strength and Pore Structure of Concrete made with Natural Pozzolan", *Proceedings of The Third International RILEM Conference, Torquay, England.* Sept. 1992.

[76] Wainwright P.J., J.G. Cabrera, and A.M. Al-Amri, "Performance and Properties of Pozzolonic Mortars Cured in Hot Dry Environments", *Proceedings of The Third International RILEM Conference, Torquay, England.* Sept. 1992.

[77] Jaegarmann C.H. and D. Ravina, "Effect of Some Admixtures on Early Shrinkage and Other Properties of Prolonged-Mixed Concrete Subjected to High Evaporation", *RILEM Symposium on Admixtures for Mortar and Concrete.* Brussels. Vol. 4, 1967, pp. 321-350.

[78] Cabrera J.G., A.R. Cusens, and Y. Brookes-Wang, "Effect of Superplasticizers on the Plastic Shrinkage of Concrete", *Magazine of Concrete Research*, Vol. 44, No. 160, Sept. 1992, pp. 149-155.

[79] Yamamoto Y. and S. Kabayashi, "Effect of Temperature on the Properties of Superplasticized Concrete", *ACI Journal*, Jan.-Feb. 1986, pp. 80-87.

[80] Berhane Z., "Effect of Water from Fresh Concrete in Hot Climates on the Properties of Concrete", *Concrete in Hot Climates, Proceedings of The Third International RILEM Conference, England.* Sept. 1992, pp. 81-88.

[81] King J.W.H. and J. Timusk, "The Design and Construction of a Chamber with Controlled Temperature and Humidity", *Magazine of Concrete Research*, Vol. 17, No. 51, June 1965, pp. 101-102.

[82] Campbell R.H., W. Harding, E. Misenhimer, L.P. Nicholson, and J. Sisk, "Job Conditions Affect Cracking and Strength of Concrete In-Place", *ACI Journal Proceedings*, Vol. 73, No. 1, Jan. 1976, pp. 10-13.

VITA

- Mohammed Abdul Waris
- Born in 1969 at Hyderabad, India.
- Permanent Address :

  H.No. 33/2RT,

  Muncipal Colony,

  Malakpet,

  Hyderabad 500036, INDIA.

- Received Bachelor of Engineering (**B.E.**) degree in Civil Engineering from Osmania University, Hyderabad, India in August 1991.
- Received Master of Science (**M.S.**) degree in Civil Engineering with specialization in Structures from KFUPM, in April 1996.